

Changes in Spatial Summation in
Response to Intraocular
Pressure-lowering Treatment in
Glaucoma: Evidence of Neural
Remodeling?

Doctor of Philosophy (PhD)
(November 2017)

Shindy Je
Bsc Optom

Thesis abstract

Recent studies of experimental glaucoma have suggested that retinal ganglion cells (RGCs) undergo a period of pre-morbid dysfunction, and there is some evidence that this may also occur in humans with glaucoma. A conceptual model by Porciatti & Ventura (2012) illustrates that reduced visual function owing to pre-morbid changes in RGCs may be recoverable in early disease with timely intraocular pressure-lowering treatment. In this thesis, pre-morbid dysfunction is investigated in glaucoma patients before, and 6 months after, trabeculectomy treatment with measures of spatial summation (specifically, Ricco's area, previously found to be larger in glaucoma patients than in healthy controls in visual field regions with very early damage). Controls were a cohort of patients with stable glaucoma, and age-similar healthy individuals. The hypothesis was that an already-enlarged Ricco's area would shrink in response to IOP-lowering treatment, while no between-visit change would be observable in the stable glaucoma and healthy control groups. A slight overall reduction in Ricco's area was found in those test locations with least baseline damage, but an overall enlargement was found in those with more moderate-advanced baseline damage. An initial study of Ricco's area in amblyopia, a condition in which the retinal receptive fields are understood to be normal, found that Ricco's area was larger than normal when measured through the amblyopic eye, and smaller than normal when measured through the non-amblyopic eye. This finding, together with findings described in published literature suggest a cortical origin for Ricco's area. Thus, it may be that in regions with early damage, recovery from dysfunction was observed, while in those with moderate-advanced damage, a cortical adaptation to cell death was observed. Finally, permutation of between-visit differences in Ricco's area and sensitivity to a Goldmann III stimulus indicates that the former has a relatively higher signal-to-noise ratio (SNR) for identifying change over time.

Table of Contents

THESIS ABSTRACT	I
LIST OF FIGURES.....	V
LIST OF TABLES.....	IX
DECLARATIONS.....	XI
TERMS AND ABBREVIATIONS	XIV
CHAPTER 1: GLAUCOMA AND SPATIAL SUMMATION	1
1.1. INTRODUCTION.....	1
1.2. PATHOPHYSIOLOGY OF GLAUCOMA	2
1.2.1. <i>Mechanical changes in the optic nerve head</i>	4
1.2.2. <i>Ischaemic theory in glaucoma</i>	5
1.2.3. <i>Neurotoxicity theory in glaucoma</i>	5
1.3. TESTS FOR DIAGNOSIS AND ASSESSMENT OF GLAUCOMA	7
1.3.1. <i>Tests of neural structure in glaucoma</i>	7
1.3.2. <i>Tests of visual function in glaucoma</i>	9
1.3.3. <i>Measurement of Intraocular Pressure (IOP)</i>	16
1.4. RETINAL GANGLION CELL DYSFUNCTION.....	17
1.5. SPATIAL SUMMATION AND RICCO'S AREA	27
1.5.1. <i>Introduction</i>	27
1.5.2. <i>Statistical fitting of spatial summation functions</i>	32
1.5.3. <i>Ricco's area in glaucoma</i>	35
1.6. AIMS AND OBJECTIVES OF THE PHD	38
CHAPTER 2: PRELIMINARY STUDIES AND OPTIMISATION OF EXPERIMENTAL METHODS.....	39
2.1. INTRODUCTION	39
2.1.1. <i>Experimental apparatus</i>	39
2.1.2. <i>Choosing a thresholding algorithm</i>	42
2.2. <i>Optimisation of thresholding algorithm and test time</i>	47
2.2.1. Method for experiment 1	49
2.2.1.1. Subjects.....	49
2.2.1.2. Apparatus and Stimuli.....	49
2.2.1.3. Procedure	49
2.2.2. <i>Results for experiment 1</i>	51
2.2.3. <i>Discussion for experiment 1</i>	56
2.2.4. <i>Methods for experiment 2</i>	58
2.2.4.1. Procedure	58
2.2.5. <i>Results for experiment 2</i>	60
2.2.6. <i>Discussion for experiment 2</i>	62
2.3. LEARNING EFFECT AND VARIABILITY.....	63
2.3.2. <i>Methods</i>	66
2.3.2.1. Subjects.....	66
2.3.2.2. Apparatus and Stimuli.....	66
2.3.2.3. Procedure	67
2.3.2.4. Data analysis.....	68
2.3.3. <i>Results</i>	69
2.3.4. <i>Discussion</i>	72
2.4. CORNEAL WAVEFRONT ABERRATIONS.	74

2.4.1. Introduction	74
2.4.2. Methods.....	77
2.4.3. Results	80
2.4.3. Discussion	85
2.5. EFFECT OF LOCALISED DEFOCUS ON MEASUREMENTS OF RICCO'S AREA	86
2.5.2. Methods.....	88
2.5.2.1. Subjects.....	88
2.5.2.2. Apparatus and stimulus	88
2.5.2.3. Procedure	89
Total defocus.....	93
2.5.3. Results	96
2.5.4. Discussion	100
CHAPTER 3: ON THE PHYSIOLOGICAL BASIS FOR RICCO'S AREA: A STUDY OF AMBLYOPIA.....	105
3.1. INTRODUCTION.....	105
3.2. METHODS	109
3.3. RESULTS	114
3.4. DISCUSSION.....	123
CHAPTER 4: CHANGES IN RICCO'S AREA IN GLAUCOMA, IN RESPONSE TO IOP- LOWERING TREATMENT.....	130
4.1. INTRODUCTION.....	130
4.2. MEASURING RGC DYSFUNCTION	131
4.3. CHANGES IN SPATIAL SUMMATION AS A MEASURE OF RGC DYSFUNCTION?	132
4.4. MEASUREMENT OF CORNEAL WAVEFRONT ABERRATIONS	135
4.5. METHODS.....	139
4.5.1. Experiment 1	139
4.5.1.1. Participants.....	139
4.5.1.2. Apparatus and Stimuli.....	141
4.5.1.3. Procedure	142
4.5.1.4. Data analysis.....	143
4.5.2. Experiment 2	147
4.5.2.2. Apparatus and Stimuli.....	147
4.5.2.3. Procedure	148
4.5.2.4. Data analysis.....	148
4.6. RESULTS.....	151
4.6.1. Experiment 1	151
4.6.2. Experiment 2	170
4.7. DISCUSSION	177
CHAPTER 5: SIGNAL/NOISE ANALYSIS FOR COMPARISON OF METHODS OF MAPPING TO THE CHANGING SPATIAL SUMMATION CURVE IN GLAUCOMA.....	186
5.1. INTRODUCTION	186
5.2. METHODS.....	194
5.2.1. Participants.....	194
5.2.2. Apparatus and stimulus.....	195
5.2.3. Thresholding procedure	195
5.2.4. SNR procedure	196
5.2.5. Data analysis	199
5.3. RESULTS.....	200
5.4. DISCUSSION	202
CHAPTER 6: CONCLUSION AND FUTURE WORKS.....	205
APPENDICES	214

REFERENCES.....228

List of Figures

Figure	Subject	Page
Chapter 1		
1.1	Test-retest limits of standard automatic perimetry measured with SITA-Standard strategy	11
1.2	Confocal images of RGCs from primate retina	19
1.3	Pattern electroretinogram on patients before and after trabeculectomy procedure	21
1.4	Pattern electroretinogram recording on ocular-hypertensive participants with and without treatment	23
1.5	Cortical cells receiving input from different amount of retinal ganglion cells	36
Chapter 2		
2.1	Zippy Estimation by Sequential Testing thresholding procedure with pdf	45
2.2	54 test locations visual field pattern with Ricco's area estimates	53
2.3	30 test locations visual field pattern with Ricco's area estimates	54
2.4	16 test locations visual field pattern with Ricco's area estimates	55
2.5	Staircase method thresholding procedure	58
2.6	8 test locations visual field pattern with Ricco's area estimates	61
2.7	Illustration of possible improvement in Goldmann size threshold	64
2.8	8 visual field test locations in the experiment	67

2.9	Ricco's area estimates of naïve and experienced participants	70
2.10	Pyramids of Zernike term up to 5 th radial orders	75
2.11	Aberration coefficients for front surface cornea up to 6 th radial orders	80
2.12	Aberration coefficients for front surface cornea up to 6 th radial orders but excluding polynomials 0 and 4	81
2.13	Coefficient range for front surface corneal aberrations up to 6 th radial or	81
2.14	Aberration coefficients for front surface cornea up to 6 th radial orders	82
2.15	Aberration coefficients for front surface cornea up to 6 th radial orders but excluding polynomials 0, 1 and 4	83
2.16	Aberration coefficients for back surface cornea up to 6 th radial orders	84
2.17	6 visual field locations on the right eye	89
2.18	X and Y coordinates of Octopus 900 testing locations with schematic representations for target distance calculation	91
2.19	Right angle triangles for calculations of peripheral target distance	92
2.20	Target set up for peripheral refractive error measurement	93
2.21	Illustration of estimation of total defocus (the sum of optical and ocular blur)	94
2.22	Ricco's area estimates obtained at 3 eccentricities under 3 different levels of optical blurs	97
2.23	Ricco's area estimates at individual test eccentricities	98

2.24	Projected stimulus with and without any optical filtering falling onto one Ricco's area and its point spread function	102
2.18	Spatial summation curves with and without blurring lens	103
Chapter 3		
3.1	Visual field test locations	111
3.2	Ricco's area as a function of visual field eccentricity in both eyes of healthy and amblyopic participants	117
3.3	Ricco's area in strabismic and anisometropic groups as well as binocular and non-binocular groups	119
3.4	Mean Ricco's area as a function of eccentricity in amblyopic participants, separated by binocular and non-binocular status	120
3.5	Mean Ricco's area, measured binocularly, in amblyopic participants and healthy controls	122
Chapter 4		
4.1	Possible changes of Ricco's area in response to treatment (or more rigorous treatment)	133
4.2	Pyramids of Zernike term up to 5 th radial order	136
4.3	Visual field test location	142
4.4	Schematic timeline of tests for both visits	142
4.5	Graphical representation of mean deviation from first visit	153
4.6	Time difference between visits	157
4.7	Examples of typical spatial summation curves	158

4.8	Comparison of Ricco's area pool for all locations between visits	159
4.9	Comparison of Ricco's area between participant groups on 3 different levels of TD	161
4.10	Comparison of Ricco's area obtained per location between visits	162
4.11	Comparison of different in IOP with Ricco's area	166
4.12	Slope of second line as a function of total deviation in all participant groups on both visits	167
4.13	Ricco's area size obtained per location from different participants' age for different visits	169
4.14	Different in Zernike coefficients for 28 Zernike polynomials contained in 6 th radial orders in healthy group	171
4.15	Different in Zernike coefficients for 28 Zernike polynomials contained in 6 th radial orders in stable group	172
4.16	Different in Zernike coefficients for 28 Zernike polynomials contained in 6 th radial orders in trabeculectomy group	173
4.17	Graphical explanation of one of the study hypothesis	181
4.18	Hypothesis on possible cause of enlargement of Ricco's area in trabeculectomy group second visit	184
Chapter 5		
5.1	Conceptual model for RGC dysfunction and death by Porciatti and Ventura	187
5.2	Schematic of spatial summation curve measured in time	192
5.3	Signal to noise ratio protocol for Ricco's area calculation	198
5.4	Scatterplots with lines of equality for all participant groups	201

List of Tables

Tables	Subject	Page
Chapter 1		
1.1	Summary of mean IOP in untreated and treated eyes in different studies investigating retinal ganglion cells dysfunction	24
Chapter 2		
2.1	Average testing times for Goldmann I-V with ZEST	51
2.2	Average testing times for Goldmann I-V with staircase method	60
2.3	Threshold values of GI, III and V for 4 visits in experienced participants	71
2.4	Threshold values of GI, III and V for 5 visits in naïve participants	71
2.5	Peripheral refractive errors in all participants	96
2.6	Mean refractive errors at all test locations in all participants	96
Chapter 3		
3.1	Clinical characteristics of amblyopic participants	114
3.2	Clinical characteristics of control participants	115
3.3	Difference in mean Ricco's area between amblyopes and healthy controls	118
Chapter 4		
4.1	Preliminaries data from all participants	152

4.2	Time difference in days between first and second visit of participants in healthy group	154
4.3	Time difference in days between first and second visit of participants in stable group	155
4.4	Time difference in days between first and second visit of participants in trabeculectomy group, also with operation times	156
4.5	Median Ricco's and IQR area for different participant groups	159
4.6	Median Ricco's and IQR area for different participant groups divided into 3 strata	160
4.7	Sensitivity (dB) from all participant groups of both visits and their medians	164
4.8	Zernike coefficients of 6 th radial orders from front surface corneas of all participant groups of both visits	174
4.9	Zernike coefficients of 6 th radial orders from back surface corneas of all participant groups of both visits	175
Chapter 5		
5.1	Mean and standard deviation of signal, noise and signal-to-noise ratio of both Ricco's area and Goldmann III sensitivity methods	200

Acknowledgments

Firstly, I would like to express my sincere gratitude to my supervisor and friend Dr Tony Redmond for his unwavering support of my PhD study, for his patience, and also for the life and research advices.

I would also like to thank Prof. Morgan and Dr Maggie Woodhouse OBE for their insight and guidance throughout this PhD study.

My sincere thanks go to Mrs Sue Hobbs for her friendship and help with all the administrative aspects of this PhD. I am also grateful to Mrs Judith Colwill and Leanne Morrish for their patience.

I am deeply grateful to Prof. Andrew Quantock and Dr Rob Young for their companionship and helpful advice throughout my study.

I am grateful to Dr Fergal Ennis for his guidance on teaching.

I thank my fellow PhD mates Flors, Aysha, Nikki, Lindsay and Louise for all the fun we have had in the last few years, also I thank my friend and collaborator Dr Yan Hui Ma for her help in the programming, Dr James Ferguson for his help with instrument calibration, Mrs Rohie Khan for her help in recruitment of participants, Miss Julia Rose and Miss Anisha Chowlia for their help in data collection.

I would also like to thank my parents, Muslan and Ellien, my siblings David and Michael, my sister in law Felicia, my beloved nephew and niece Jarred and Jadey. All of you are my constant source of strength.

Lastly I would like to thank all of participants in this study. Even after they volunteered 7 hours of their time to sit in the dark with me, staring at spots of light, they still managed to smile brightly at the end of the experiment. Thank you for your effort and delightful conversations during break times.

Terms and Abbreviations

IOP	Intraocular pressure
OAG	Open angle glaucoma
ACG	Angle closure glaucoma
RGCs	Retinal ganglion cells
ONH	Optic nerve head
C/D ratio	Cup-to-disc ratio
OCT	Optical coherence tomography
VF	Visual field
SAP	Standard automatic perimetry
FDP	Frequency doubling perimetry
SWAP	Short wavelength automated perimetry
SITA	Swedish interactive threshold algorithm
PERG	Pattern electroretinogram
VA	Visual acuity
OPI	Open perimetry interface
ZEST	Zippy estimation by sequential testing
pdf	Probability density function
G	Goldmann

PSF	Point spread function
LGN	Lateral geniculate nucleus
OD	Ocular dominance
ΔI	Increment threshold
TD	Total deviation
Δ_{RA}	The difference in Ricco's area between visits
Δ_A	Between-visit differences in aberrations
PoPLR	Pointwise linear regression
SNR	Signal-to-noise ratio
MD	Mean deviation
SD	Standard deviation
Δ_{GIII}	The difference in Goldmann size III sensitivity between visits

Chapter 1: Glaucoma and Spatial Summation

1.1. Introduction

Glaucoma is a single term used to describe a group of degenerative eye conditions that cause optic nerve damage, with resultant loss of visual function (Quigley 2005). It is the second most prevalent cause of irreversible blindness worldwide, with an estimated 60 million people affected, predicted to increase to 111.8 million people by 2040 (Tham *et al.* 2014). Its prevalence increases with age and is more commonly reported in people over 40 years of age (Quigley & Vitale 1997).

There are two subdivisions of glaucoma types, open and close angle. Both can be subdivided into primary and secondary diseases. Primary refers to cases of glaucomatous optic neuropathy with normal or elevated intraocular pressure (IOP) with no other pathological causes present. Secondary refers to cases occurring secondary to trauma, as a side effect of medication or ocular pathology such as anterior uveitis, neovascularization, pigment dispersion and pseudoexfoliation syndrome. These conditions can elevate IOP either by loss of cellular tissue or pigment deposition in the trabecular meshwork (Casson *et al.* 2012; Foster *et al.* 2002).

Primary open angle glaucoma (OAG) is most commonly bilateral (not necessarily symmetrical) asymptomatic optic neuropathy, with or without elevated IOP. Previously, Primary OAG with IOP <21mmHg was called 'Normal Tension Glaucoma (NTG)', but this term has fallen out of favour, as we now know that disease progression can happen

at all IOP levels. The loss of visual function in POAG usually progresses slowly, beginning in the mid-periphery and expanding both toward the center and periphery (Foster *et al.* 2002; Quigley 2011).

Primary angle closure glaucoma has elevated IOP that caused by obstruction of aqueous humor outflow due to narrowing and closure of the anterior chamber angle. The anterior chamber angle closure can be caused by age-related enlargement of crystalline lens, pushing the peripheral iris to be in contact with posterior cornea, leading to obstruction of the trabecular meshwork for more than half of the 360° angle that is observable in gonioscopy. Unlike primary OAG in which the patient is usually asymptomatic until the moderate or advanced stage of the disease, Primary angle closure patients report pain and sudden decrease in vision due to the acute rise in IOP (Foster *et al.* 2002; Quigley 2011). Primary OAG is more common in the West African population than in Caucasian population, whilst primary angle closure glaucoma is more common in Asian populations (Foster *et al.* 1996; Foster *et al.* 2000; Racette *et al.* 2003).

1.2. Pathophysiology of glaucoma

In healthy eyes, the flow of aqueous humor against resistance result in a mean IOP of approximately 15mmHg, with 21mmHg taken as the threshold for IOP normality (Hollows & Graham 1966). For many years, the widely held hypothesis was that glaucoma is caused by elevated IOP to a pressure higher than 21mmHg due to disruption of the aqueous outflow. This has since been questioned by population studies (Buhrmann *et al.* 2000; Sommer *et al.* 1991; Quigley *et al.* 2001) showing individuals with IOP higher than ‘normal’ not developing glaucoma and individuals with ‘normal’

IOP diagnosed with glaucoma. Thus there must be other mechanisms involved in the pathogenesis of glaucoma.

Elevated IOP, although now not considered as the main cause of glaucoma, is now widely recognized as one of the treatable risk factors, with the greatest risk factor being age (Chauhan *et al.* 2008a; Klein *et al.* 1992; Quigley *et al.* 2001). It has been demonstrated that an IOP reduction of 20% slows down the rate of progression in glaucoma by 50% (AGIS-Investigators 2000; Heijl *et al.* 2002; Kass *et al.* 2002). IOP is balanced by the secretion of aqueous humor by the ciliary body and its drainage through the trabecular meshwork and the uveoscleral pathway. Elevated IOP can cause mechanical strain on the back surface of the eye, particularly on the lamina cribosa, the weakest point in the posterior eye surface. This causes compression and deformation of the lamina cribosa, giving rise to axonal damage and disruption of both orthograde and retrograde delivery of essential trophic factors. Therefore experimental models of glaucoma with elevated IOP should provide useful insights into the pathogenesis and pathophysiology of glaucoma. Indeed, experiments to study the nature of glaucoma are still done by observation of the histological changes in animal eyes (rodents and primates), with glaucoma that is induced by elevating the IOP experimentally or which occurs spontaneously in rodent models that have been manipulated genetically (Johnson & Tomarev 2010; Morrison *et al.* 2008)

Loss of retinal ganglion cells (RGCs) is responsible for visual field loss in glaucoma. The normal human retina contains approximately 1.07 million RGCs with 0.3-0.6% loss per year due to ageing (Harwerth *et al.* 2008; Mikelberg *et al.* 1989). This number increases to an average of 4.4% per year in glaucoma (Medeiros *et al.* 2012). The

primary mechanism of RGCs loss in glaucoma is not clear, but evidence has suggested that it occurs via apoptosis, a programmed cell death in the absence of inflammation, characterized by DNA fragmentation, chromosome clumping, cell shrinkage and membrane blebbing (Nickells 1999; Derick *et al.* 1994; Pease *et al.* 2000; Quigley 1999). Several hypotheses have been proposed to be responsible for RGCs loss and will be discussed in details in subsequent sections.

1.2.1. Mechanical changes in the optic nerve head

Studies in experimental glaucoma have provided extensive evidence for the optic nerve head (ONH) /optic disc as the site of initial damage. It has been observed in experimental glaucoma, that IOP elevation causes compression of the structural plates of the connective tissue of the ONH and outward rotation of the insertion of the lamellar plates into the sclera (Quigley, Davis & Anderson 1977; Quigley *et al.* 1983; Quigley 1995). One of the widely held hypotheses for the trigger of the RGCs death process in glaucoma is that these mechanical changes in ONH cause interruption to the axonal transport at the level of the lamina cribosa, blocking of anterograde and retrograde axoplasmic transport, leading to deficits in brain derived neurotrophic factor and neurotrophins 4/5 from the superior colliculus to RGC soma, which is necessary for RGC survival (Chen & Weber 2001; Di Polo *et al.* 1998; Johnson *et al.* 2000; Quigley 1999; Weber & Harman 2008). When neurotrophic factors such as nerve growth factor, ciliary neurotropic factor and brain derived neurotrophic factor were administered exogenously, there was evidence of in vitro and in vivo RGC protection (Johnson *et al.* 1986; Rabacchi *et al.* 1994). Racial and gender differences were observed despite similar IOP profiles, suggesting lack of perfect correlation between IOP and visual field loss (Foster *et al.* 1996; Vajaranant *et al.* 2010). It is possible that there are variations in

the biomechanical properties of tissues at ONH and sclera, contributing to variability of deformation of ONH (Downs 2015).

1.2.2. Ischaemic theory in glaucoma

Reduced ocular blood flow had been proposed to cause RGC death either by recurrent mild ischaemic injury, that leads to chronic oxidative stress and excitotoxicity, or by reducing RGC tolerance to secondary insults from glutamate, nitric oxide and phototoxicity causing mitochondrial dysfunction (Chrysostomou *et al.* 2013; Mozaffarieh & Flammer 2013; Osborne 2010). This theory is supported by increased prevalence of glaucoma with age, as mitochondrial function decreases with age and is more susceptible to insult caused by elevated IOP (Chrysostomou *et al.* 2010; Lascaratos *et al.* 2012). Positive association has been observed between glaucoma with peripheral vascular conditions (Wang *et al.* 1997) and migraine (Cursiefen *et al.* 2000).

1.2.3. Neurotoxicity theory in glaucoma

The toxic effect of glutamate, an excitatory neurotransmitter in the mammalian central nervous system in RGCs, was first observed when subcutaneous glutamate injections in mice caused severe degeneration of inner retinal layers, including the RGC layer (Lucas & Newhouse 1957). It was also observed to cause loss of the RGC layer in neonatal mice (Siliprandi *et al.* 1992) and rats (Dreyer *et al.* 1994). RGC death in glutamate toxicity was hypothesized to occur due to the production of matrix-metalloproteinases by astrocytes that leads to apoptosis of RGCs (Zhang *et al.* 2004). Glutamate toxicity has also been observed in other neurodegenerative conditions, such as Parkinson's and Huntington's disease (Choi 1988).

Nitric oxide synthase-2 has been suggested to produce neurotoxic effects upon RGCs, since its concentration rose proportionally with increase in IOP. Nitric oxide synthase-2 has been observed to increase in glaucomatous eyes, when compared to healthy eyes (Neufeld *et al.* 1997; Neufeld *et al.* 1999)

1.3. Tests for diagnosis and assessment of glaucoma

The progressive loss of RGCs in glaucoma is detected, monitored and evaluated with a combination of structural and functional tests. In clinical practice, a triad of tests is routinely used to diagnose glaucoma; optic nerve head assessment, IOP measurement and perimetry (EGS Guidelines 2017).

1.3.1. Tests of neural structure in glaucoma

RGCs are post-mitotic neurons, and thus are not replaced once lost. The loss of RGCs is usually manifest structurally as progressive thinning of nerve fibers in the retina that is observable clinically with direct ophthalmoscopy and indirect slit-lamp biomicroscopy as an enlargement of the optic nerve cupping in relation to constant disc size (cup-to-disc ratio [C/D ratio]) (Quigley 2011).

Traditionally, horizontal measurement of C/D ratio is used to assess the presence and monitor the progression of glaucoma (Armaly 1967). However, it was observed that the optic cup enlarged more vertically in glaucoma, possibly due to the lack of connective tissue support in upper and lower poles of the optic disc that in turn accelerates the axonal loss in the areas with resultant enlargement of vertical C/D ratio, contributing to greater interruption of axonal transport in the areas (Garway-Heath *et al.* 1998; Quigley & Addicks 1981; Quigley 1999). Thus vertical C/D ratio is thought to provide a better insight into progression of glaucoma. Subjective assessment of ONH with ophthalmoscopy and slit-lamp biomicroscopy suffers from inter- and intra- subject variability that impedes the judgment of the presence and progression of glaucoma

(Varma *et al.* 1992). The major problem with trying to assess glaucoma with this technique is that there is a wide range of C/D ratio in the normal population (up to 0.87), with big optic discs having bigger cup sizes and vice versa, making it a challenge to categorize an optic disc as normal or glaucomatous (Jonas *et al.* 1988a). Foster *et al.* (2002) in a population-based study suggested that a C/D ratio of 0.7 represents 97.5 percentile for limits of normality in most of the ethnic groups participating in the study. But it has to be noted that even though 0.7 is considered the threshold for normality, it is not a clear-cut point for all people. Hypermetropes generally have a smaller ONH with smaller optic cup and thus need to lose more of the neural tissue before the C/D ratio exceeds 'normal' range, and vice versa for myopes (Jonas *et al.* 1988b; Papastathopoulos *et al.* 1995).

There are other signs of glaucomatous optic nerve damage that, when taken into account with the C/D ratio, can help improve diagnosis accuracy of glaucoma. Glaucoma usually affects the eyes asymmetrically and thus can cause asymmetry in C/D ratio between two eyes; C/D ratio differences of more than 0.2 are considered suspicious (Sharma & Chaturvedi 1982). Other glaucomatous signs in the optic disc include stretching of the pores of lamina cribosa (Susanna 1983), focal notching due to localized nerve fiber layer loss, peri-papillary atrophy, optic disc pallor, arterial narrowing, overpass vessels, disc hemorrhages and uneven reflections from the nerve fibre layer (Hitchings 1978).

Objective techniques for imaging the optic nerve head and for quantifying the retinal nerve fibre layer have been developed in an attempt to more accurately identify changes in the neural retina in glaucoma. Confocal scanning laser ophthalmoscopy and optical

coherence tomography (OCT) have been used as adjuncts to subjective ONH assessment. Confocal scanning laser ophthalmoscopy uses a laser point light source to scan the retina, enabling retinal photographic imaging. The confocal pinhole aperture acts to minimize scattered and reflected light outside of the image focal-plane, increasing the lateral resolution when compared to fundus photography. However confocal scanning laser ophthalmoscopy does not work well when patients have small pupils or ocular opacities (Alexandrescu *et al.* 2010). OCT is a non-invasive optical imaging system that utilizes low-coherence interferometry to produce a two-dimensional cross sectional image of the retina. Spectral domain OCT has been used clinically to monitor longitudinal retinal nerve fiber layer changes in glaucoma. However OCT still cannot visualize RGCs due to their near transparent nature (Bussel *et al.* 2014).

1.3.2. Tests of visual function in glaucoma

Visual field (VF) measurement with white-on-white standard automatic perimetry (SAP) remains the most common measurement of visual function for detection and monitoring glaucoma progression in clinical practice. As the ‘gold standard’ functional measurement for assessing the effectiveness of glaucoma treatment, SAP is surprisingly variable (Artes *et al.* 2002; Bengtsson, Heijl & Olsson 1998; Heijl, Lindgren & Lindgren 1989; Spry *et al.* 2001). Artes *et al.* (2002) highlight the problem particularly well. They were looking at the variability of SAP thresholds and reported that SAP only performed relatively well in areas of visual field with high sensitivity. As can be seen from Figure 1.1, the test-retest variability increases with decreasing sensitivity. The variability then decreases again at near zero region because of the limited dynamic range of SAP, the so called “floor effect” (Artes *et al.* 2002). SAP has also been shown

to exhibit even larger amounts of variability in patients with glaucoma and in glaucoma suspects (Donovan *et al.* 1978; Flammer, Drance & Zulauf 1984; Werner *et al.* 1982). The variability in SAP causes difficulty in distinguishing whether the changes observed in the field are true glaucomatous VF loss, or just the variation in test results (Heijl *et al.* 2003; Keltner *et al.* 2006). Consequently, multiple measurements over a long period of time are needed to distinguish true glaucomatous field loss from long-term fluctuations. Chauhan *et al.* (2008b) performed statistical calculation to detect the rates of mean deviation change for a given number of presentations and reported that in order to detect a typical scenario with moderate glaucoma progression (-0.5dB/year loss), 13 years are needed, if one VF examination is performed per year; 6.4 and 4.3 years are required for two and three examinations respectively. Quigley, Addicks & Green (1982) compared the number of human optic nerve axons with the SAP data from the same eye and observed that up to 50% of ganglion cells needed to be lost before SAP would show a defect. Similar findings were obtained by Harwerth *et al.* (1999) study with trained monkeys. However, Harwerth and colleagues plotted their data with logarithmic scale, thus putting more emphasis on more advanced stages of RGCs loss. Later work by Garway-Heath *et al.* (2002) comparing SAP with structural measurements with the Heidelberg retina tomograph reported that, when the data are plotted on a standard linear scale, the structure and function relationship is linear, though the data still vary greatly.

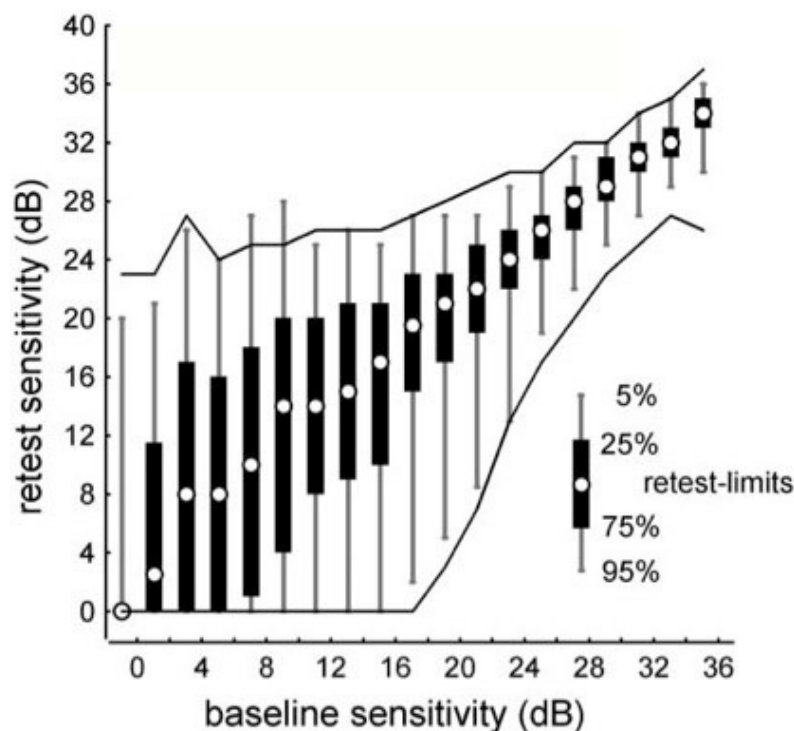


Figure 1.1 Test-retest limits of SAP measured with SITA standard. Thin vertical lines indicating 90% of the test-retest intervals between the 5th and 95th percentiles. Vertical bars indicate the interquartile ranges and solid lines represent 90% retest limits for Full Threshold strategy. Picture taken from Artes et al. (2002).

The inadequacies of SAP drove scientists to develop more accurate functional tests.

They argued that the white-on-white perimetry stimulated a wide range of RGC types, and thus had considerable redundancy that can mask early glaucomatous damage. The ideal test should isolate a specific population of RGCs that either is preferentially lost early in the disease, or has less redundancy.

In 1988, Quigley and colleagues suggested a preferential loss of large optic nerve fibers in glaucoma, which are mostly part of the magnocellular visual processing stream. As magnocellular cells are known to be sensitive to motion and high frequency flicker, it

was thought that tests that target this response property will detect glaucoma earlier (Dandona, Hendrickson & Quigley 1991; Quigley, Dunkelberger & Green 1988). Frequency doubling perimetry (FDP) and its successor, FDP – 2 which has a different thresholding algorithm and more refined test pattern, compared with the previous version, were developed for the purpose of isolating magnocellular cell activity, more specifically a subset of magnocellular cells first reported in cat named M_y cells, by employing flickering grating stimuli of fixed spatial frequency (Artes *et al.* 2005; Johnson & Samuels 1997). Frequency doubling is an illusion, in which alternating light and dark bars will appear to be twice the actual number of bars when low spatial frequency sinusoidal gratings are flickered at high temporal frequency ($>10\text{Hz}$) and the illusion is reportedly mediated by the M_y cell (Maddess and Henry 1992; Kelly 1966). However, although FDP is created based on the illusion, the task involved in this psychophysical test is detection of the gratings and not the illusion. Cross-sectional studies have reported constant test-retest variability over the dynamic range of the instrument and lower variability with increasing defect severity in both FDP and FDP2, suggesting they may be better tests for earlier detection and monitoring progression of glaucoma than SAP. The effects of eccentricity on variability are also less than those reported in SAP. These superior performances of FDP have been attributed to the larger stimulus size used by FDP, which might be less affected by small eye movements compared to SAP (Artes *et al.* 2005; Chauhan & Johnson 1999; Leeprechanon *et al.* 2007; Spry *et al.* 2001; Wall *et al.* 2009). FDP1 has been shown to be able to detect glaucoma earlier by as much as 4 years in 59% of 105 glaucoma suspects (Medeiros *et al.* 2004). However the result from Medeiros and colleagues should be viewed with caution, as the objective was to assess the strength of FDP in predicting future development of SAP visual field defect in glaucoma suspects, thus the majority of

participants had normal baseline SAP visual fields. This could have omitted populations of people that might have abnormal SAP, but normal FDP.

Direct comparison between the threshold estimate of FDP1&2 and SAP are difficult due to the different scale of measurement. In both versions of FDP, a 1-dB change in threshold equals a 0.05 log unit change in stimulus contrast, whilst with SAP, a 1-dB change equates to a contrast change of 0.1 log unit. They also differ in measurement ranges, with SAP showing a greater floor effect compared to FDP2 (Artes *et al.* 2005) and thus limiting the usefulness of results of previous studies comparing the techniques based solely on the mean and pattern standard deviations. Artes & Chauhan (2009) compared SAP and FDP2 using estimation of the ratio between signal and noise; here asymmetries in the differences in sensitivity between superior and inferior mirror pairs of sectors in the visual field, were taken as signal and the variability of sensitivity differences from test to test, as noise. This allows identification of localized VF loss that is independent of decibel scale, and thus gives better comparison between techniques. The authors found a higher signal to noise ratio in FDP2, supporting the hypothesis that FDP2 has superior ability compared to SAP in detection of glaucoma progression over time. However Redmond *et al.* (2013a) in a longitudinal study of 5 year on 100 patients using permutation point-wise linear regression, an analysis method that gives a single P value that is independent of the scale of original measurement, however, found no evidence that FDP2 is more sensitive than SAP in identification of visual field progression at fixed specificity.

Recent histological and psychophysical evidence has cast doubt on the preferential loss of magnocellular cells hypothesis (Ansari *et al.* 2002b; Morgan 2002; Sample,

Bosworth & Weinreb 1997; Weber *et al.* 1998). It is now presumed that RGCs are affected non-selectively in glaucoma (further explanation available in section 1.5). But this does not mean that tests which selectively target the magnocellular pathway have no more utility than SAP, as tests that only isolate one particular aspect of visual processing will also prevent the sparing in other visual systems from compensating for the damage caused by glaucoma and thus could detect glaucoma earlier (Ansari *et al.* 2002b). However it is unclear whether FDP actually preferentially stimulates the M_y cells, as studies looking at the presence of this subgroup of highly non-linear cells in primates with retrograde labeling and counter-phased modulated sinusoidal gratings recording have not been able to confirm their presence (Levitt *et al.* 2001; White *et al.* 2002). White *et al.* (2002) instead suggest that the illusion originated at the level of cortex and not the retina. Furthermore there is a large overlap between the respective response characteristics of the magnocellular and parvocellular pathways. The parvocellular pathway peak temporal frequency, cut off temporal frequency and peak spatial frequency only differ by 15% from those of magnocellular pathway (Merigan & Maunsell 1993). Swanson *et al.* (2011), looking at the response of magnocellular and parvocellular cells to SAP and FDP, reported that a Goldmann size III stimulus in SAP is better than sinusoidal gratings in FDP at preferentially stimulating magnocellular cells. They observed that the abrupt ON and OFF of the Goldmann stimulus provides it with high temporal frequency components, whilst the lack of a chromatic component causes a weak P cell response.

Short wavelength automated perimetry (SWAP) was developed following the finding of short wavelength colour vision defects in patients with early glaucoma (King-Smith, Lubow & Benes 1984). SWAP employed a blue Goldmann size V stimulus to

preferentially stimulate the blue cones. Yellow background of 100cd/m² is used to simultaneously adapt the green and red cones, and also to saturate the rod activity. Longitudinal studies on SWAP have shown it to be able to detect progression of glaucoma 6 months to 5 years earlier than SAP and also that the rate of VF progression is more rapid for SWAP in early glaucoma patients (Johnson *et al.* 1993; Sample, Boynton & Weinreb 1993; Bayer & Erb 2002). SWAP sensitivity to earlier damage is attributed to its ability to detect selective damage to the short wavelength sensitive pathway in early glaucoma (Heron *et al.* 1987; Sample *et al.* 1988). As it is now recognized that all pathways in the retina are affected equally in glaucoma, a more convincing alternative hypothesis states that its potential to monitor the small population of small bistratified ganglion cells (1-7%), which are responsible for mediating the short wavelength sensitive pathway, may be one reason behind the earlier detection by SWAP of glaucomatous damage (Dacey 1994; Johnson 1994; Morgan *et al.* 2000). However not all studies agree on the apparently superior performance of SWAP in early diagnosis of glaucoma. Conflicting studies have reported that SAP field loss can occur prior to or at the same time as SWAP, and some found that SWAP visual field loss is not followed by SAP even after 5 years follow up (Havvas *et al.* 2013; van der Schoot *et al.* 2010). Possible explanations for this discrepancy of findings are: different studies utilize different criteria of abnormality; sampling bias in which only participants with normal SAP are included, but not those with abnormal SAP and normal SWAP fields; failing to take into account the extended learning effect - up to 5 examinations (Wild *et al.* 2006); and different criteria of abnormality between studies. The major problem with SWAP is its use of blue stimulus that is heavily absorbed by the yellowing crystalline lens (Sample & Weinreb 1992), and thus cumbersome to be used in clinical routine, as the prevalence of glaucoma increases with age. SWAP has

also been reported to have higher variability compared to SAP (Blumenthal *et al.* 2003), possibly owing to the longer testing time. Recently, a faster thresholding algorithm called Swedish Interactive Threshold Algorithm (SITA) has been implemented on SWAP to reduce testing time, and Bengtsson & Heijl (2006) reported that SITA SWAP has comparable diagnostic sensitivity with SAP.

1.3.3. Measurement of Intraocular Pressure (IOP)

Goldman applanation tonometry was first introduced in the 1950s and has since enjoyed the reputation as the gold standard test for IOP measurement. It converts the force necessary to flatten the cornea into a measurement of pressure. Goldman applanation tonometry was designed/ calibrated for an estimated corneal thickness of 500 μm and thus the instrument tends to overestimate IOP in corneas with above the 'normal' thickness, and to underestimate IOP in corneas with thickness below normal. This can cause many patients to be misclassified as glaucoma suspect and thus the measurement of IOP in practice nowadays is accompanied by measurement of central corneal thickness, when deemed necessary (Doughty & Zaman 2000). Although glaucoma is now recognized as a multifactorial disease, and elevation of IOP over 21mmHg is not synonymous with glaucoma, measurement of IOP is still of paramount significance. Elevated IOP is the major risk factor for glaucoma and IOP lowering therapy remains the only treatment with proven benefit in slowing down progression of glaucoma (Chauhan *et al.* 2010; Leske *et al.* 2003).

1.4. Retinal ganglion cell dysfunction

Histological studies analyzing the RGC soma distribution in post-mortem humans and primates reported a selectively greater reduction in large RGCs in early stages of glaucoma (Glovinsky *et al.* 1991; Glovinsky *et al.* 1993; Quigley *et al.* 1987; Quigley, Dunkelberger & Green 1988). The RGC and axon sizes correspond roughly with the RGC type, midget and parasol cells (Perry *et al.* 1984). Midget cells represent 80% of the RGC population; they have medium sized soma with small to medium sized dendritic trees. The axons of the midget cells project to the parvocellular layers of the lateral geniculate nucleus (LGN). They respond best to chromatic stimulus with high spatial and low temporal frequency. Parasol cells on the other hand only represent 10% of the RGC population and have large somas and dendritic trees. They project to magnocellular layers of the LGN and respond best to achromatic stimuli of high temporal and low spatial frequency (Dacey & Petersen 1992; Dacey 1994; Rodieck *et al.* 1985; Leventhal *et al.* 1981).

The selective loss of large RGCs was interpolated as evidence of preferential damage of parasol cells in glaucoma. This hypothesis was supported by significant loss of cells in magnocellular laminae, but not in parvocellular laminae of the LGN in five post-mortem patients with glaucoma and thus drove the creation of psychophysical tests that target the properties of the parasol cells (Ansari *et al.* 2002a; Chaturvedi *et al.* 1993). Although psychophysical tests targeting parasol cell dysfunction demonstrated deficits in motion perception in patients with early glaucoma and ocular hypertension, defects were also reported with tests that target midget cell function (Casson, Johnson & Saphiro 1993; Johnson 1994; Sample *et al.* 1994). Noting the inconsistency between histological and psychophysical evidence, Morgan (1994) questioned the selective

parasol cell loss hypothesis. He reasoned that the inconsistency could be explained if there was cell shrinkage and theorized that if all RGC cells were to undergo the same percentage of shrinkage during the early stage of glaucoma, this effect would be greater for larger cells, and thus may generate cell size distributions that appear as if larger RGCs had been selectively affected. However, even though the hypothesis was consistent with the histological data from Quigley *et al.* (1987) and Quigley, Dunkelberger & Green (1988), the RGC shrinkage hypothesis was dismissed. The selective RGC damage hypothesis indicates that there is an absolute relationship between cell type and cell size, and that RGCs do not undergo shrinkage or any change prior to the onset of apoptosis. It means that RGCs go from the state of good structural health to death with no degenerative or “sickness” period in between. This is inconsistent with other degenerative conditions, such as Alzheimer’s (Hollingworth *et al.* 2011), Parkinson’s (Zaja-Milatovic *et al.* 2005) and Huntington’s (DiProspero *et al.* 2004) diseases, in which neuronal and dendritic shrinkage are two of the hallmarks in degenerative change preceding cell death. In 1998, a study looking at the degenerative effect of chronic elevation of IOP in primates found that the earliest structural changes observable in glaucoma were a reduction in RGC dendritic field size, followed by a decrease in axon diameter. The reduction of cell body size occurred at the same time as axonal thinning, or shortly after (Weber *et al.* 2000). Morgan *et al.* (2006) and Shou *et al.* (2003) in experiments with rodent and cat glaucoma models, respectively, supported the Weber *et al.* (2000) finding.

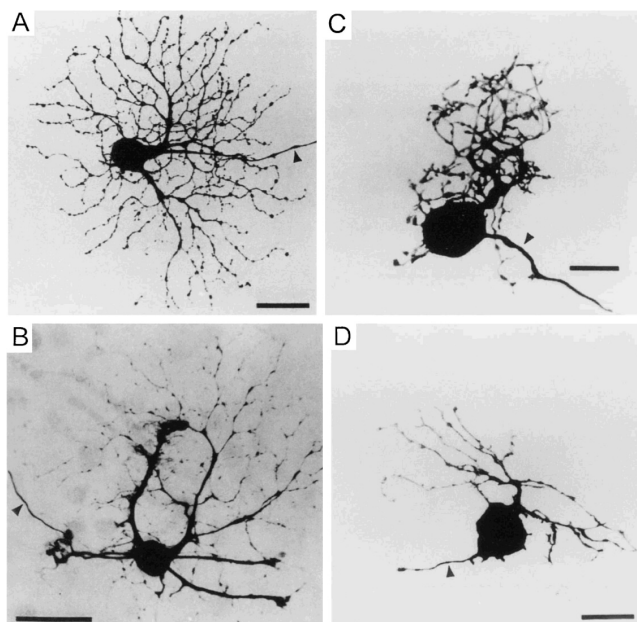


Figure 1.2. Confocal images of RGCs from primate retina. (A) Normal parasol cell. (B) Normal midget cell. (C) Parasol cell and (D) Midget cell in primate retina with severe ocular hypertension. Picture taken from Weber et al. (1998).

The pruning of dendrites as the first sign of structural change could be due to RGCs trying to conserve their energy initially, by shaving off the distal dendrites. The energy shortage in glaucomatous RGCs could be caused by aforementioned deprivation of neurotrophic factor (Weber *et al.* 2000) or could be the direct effect of mitochondrial insult due to elevated IOP (Lee *et al.* 2011). Retinal ganglion cell activity is dependent on the shape and functional integrity of its dendritic tree. It is the dendrites of RGCs that generate the characteristic center surround receptive field organization by summing input from bipolar cells; the soma then sends an action potential via its axon to the higher visual areas (Yang & Masland 1994). The shrinkage of the dendrites is expected to compromise signal integration from the outer retina and consequently reduces the accuracy of the RGC response to a stimulus (Morgan 2012). In living humans, it is impossible to perform a histological study to investigate the presence of a dysfunction period and it cannot be assumed that the RGC dysfunction period is also present in

humans due to the interspecies differences. Thus, the best way to investigate this is to look for changes in RGC signal integration activity. Pattern electroretinogram (PERG) employs a stimulus of contrast-reversal gratings or checkerboard to investigate the physiologic integrity of RGC objectively. The amplitude in PERG is labeled P50 and N95, which refer to a prominent positive peak at 50ms and a slow broad trough with a minimum at 95ms, respectively. P50 is reduced in glaucoma and other diseases of the optic nerve, coupled with its elimination by tetrodotoxin, which blocks the action potential of RGCs, suggesting that P50 is a signal generated by RGC. It is less clear where N95 originates from, as it is not affected by tetrodotoxin, but is reduced in monkeys and humans with glaucoma. Thus, it is speculated that N95 is generated by ganglion cell bodies or other structures distal to it. PERG amplitude and phase measure different aspects of RGC function (Holder 1987; Viswanathan *et al.* 2000). The reduction of PERG amplitude could be caused by a loss of RGCs, RGC dysfunction, or even a combination of the two. PERG phase reductions mostly suggest that the RGCs are still alive, but they respond in slower fashion, as it has been showed that PERG phase becomes delayed in aging (Porciatti & Ventura 2004; Porciatti & Ventura 2009).

Porciatti and Ventura (2005) were the first to employ PERG to investigate the presence of RGC dysfunction in humans. They compared the PERG amplitude and phase in 49 eyes of participants with ocular hypertension, chronic OAG, normal tension glaucoma and primary ACG that were under oculohypotensive treatment, with 44 eyes that were under observation/no treatment. They reported a PERG amplitude and/or phase increase beyond the test-retest variability in 40% of the treated group, compared to the non-treated group. The difference was for ocular hypertension, normal tension glaucoma and

chronic OAG. Even though one eye of primary ACG was included, there is no mention of its PERG amplitude/phase in the paper.

The increase in PERG amplitude and/or phase of the treated group suggests the presence of a population of RGC with IOP-dependent dysfunction, which was able to generate a stronger electrical signal after oculohypotensive treatment (Porciatti & Ventura 2005). The recovery of PERG amplitude following treatment has also been reported in a group treated with oculohypotensive treatment by North *et al.* (2010) and in an eye that underwent trabeculectomy, in Sehi *et al.* (2010).

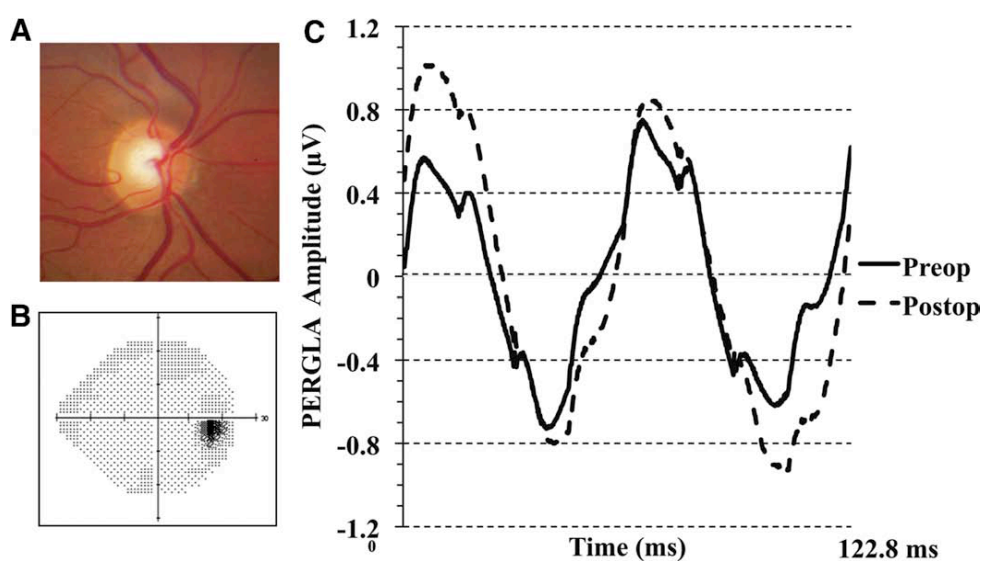


Figure 1.3. Right eye of a patient that was not responding to ocular hypertensive treatment that went on to undergo trabeculectomy in Sehi et al. (2010) study. This patient's mean IOP reduced from 26 to 11mmHg. (A) Normal optic disc in fundus photograph. (B) Normal SAP result. (C) The average amplitude of PERG that increases from 0.6 to 0.9 after surgery.

A very interesting finding by Porciatti and Ventura (2005) was that a greater PERG improvement was reported in participants with normal or early altered VF, implying the presence of a larger population of viable/sick RGCs in eyes with preserved VF. The research group then embarked on a longitudinal study (with a minimum of 6 years), investigating the progressive changes of retinal ganglion cell function before and after treatment in participants with normal SAP and glaucomatous disc (glaucoma suspect). Out of 59 eyes involved in the study, 28 eyes received treatment at some point during the follow up and 31 eyes remained untreated. As can be seen from Figure 1.4, PERG amplitudes decreased progressively with time in both treated and untreated groups. The negative amplitude trend was slowed or even inhibited after treatment in the treated group, but the negative trend of PERG amplitude carried on in the untreated group (Ventura *et al.* 2012). It is important to note, however that there is considerable variance in the data which will likely contribute to variability around the slope estimate. With such a small effect size between groups, it is difficult to have complete confidence in the effect of treatment. Another interesting point is that PERG amplitude in the treated group did not show a positive trend, suggesting that current glaucoma treatment might not be sufficiently effective to recover RGC function, but only to slow down progression.

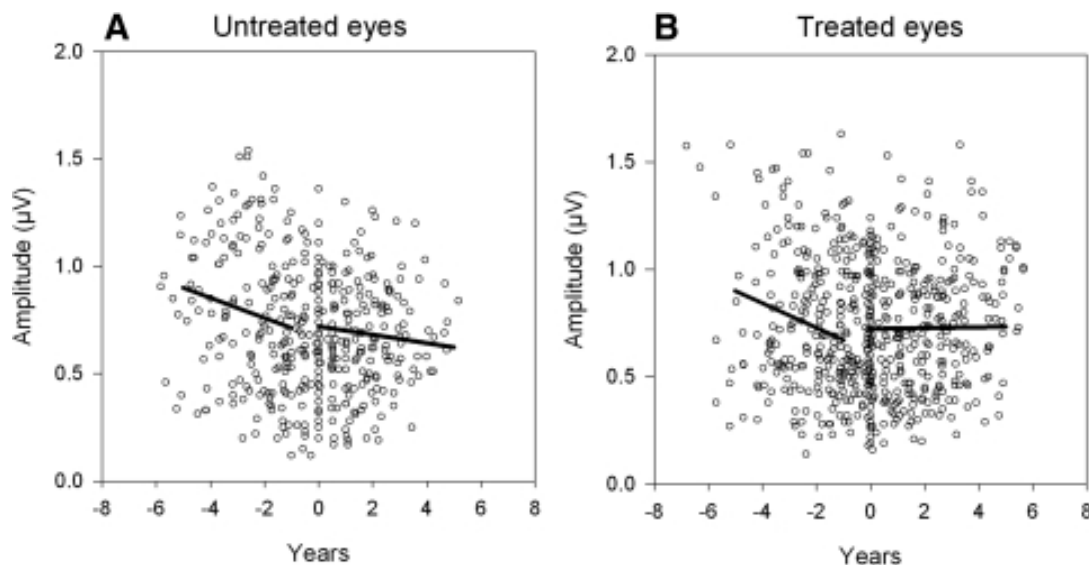


Figure 1.4. PERG amplitudes recorded throughout the entire follow up period in (A) untreated group and (B) treated group. Thick lines are the linear mixed models that fixed the data. Break point is assigned a zero value to normalize the time scale and represent the time of the first recording after initiation of treatment in (B) and randomly assigned in (A). Picture taken from Ventura *et al.* (2012)

Sehi *et al* (2011) conducted a placebo-controlled, double masked clinical trial with latanoprost 0.005% on 68 eyes of participants with OAG, ocular hypertension and those suspected of having glaucoma due to the elevated IOP. They reported no difference in PERG amplitude and phase after 4 weeks in either the participants receiving latanoprost therapy or placebo, supporting findings of Nesher *et al.* (1990) 6 years study, in which there were no meaningful differences in mean PERG amplitude between eyes treated with timolol 0.5% and those with placebo. Sehi *et al.* (2011) proposed a number of factors that might account for the discrepancy in findings between their two studies (Sehi *et al.* 2010), and those of Porciatti and colleagues even though they used the same PERG measurement protocol. One suggestion was that the magnitude of IOP reduction of 21% in the study was not significant enough to cause improvement in PERG

amplitude. Taking into account the improvement of IOP in all of the studies (Table 1.1), this is however questionable. Although there was a reduction in IOP (47%) following trabeculectomy in the study by Sehi *et al.* (2010) study, the other studies only reported mild to modest reduction in IOP. All the studies have been unable to find a relationship between the extent of IOP reduction and the recovery of PERG amplitude, and thus it is unlikely that IOP is the sole factor causing the discrepancy.

*Table 1.1. Summary of mean IOP in untreated and treated eyes in different studies investigating RGC dysfunction with PERG. *Although baseline IOP and IOP after treatment were measured as part of the protocol, they did not include any exact quantification of IOP, other than giving information that there were two different categories of baseline IOP on the study (<21mmHg, average 15±3 and >21mmHg, average 29±12). ** The untreated and treated IOP came from two different groups of participants (treated and untreated ocular hypertension groups). This is an observational study, with no influence on the decision of treatment.*

IOP (mmHg)	Porciatti and Ventura(2005)*	North <i>et al.</i> (2010)**	Sehi <i>et al.</i> (2010)	Sehi <i>et al.</i> (2011)	Ventura <i>et al.</i> (2012)
Untreated	NA	24.81	19.7±8.6	18.8±4.7	16.84±3.96
Treated	NA	19.17	10.4±4.6	14.9±3.8	14.8±3.24
Percentage	NA	23%	47%	21%	12%

Other more possible explanations between the discrepancy of PERG findings include; it is known that the diminishing of PERG amplitude in early glaucoma gives rise to the limited dynamic range of amplitude measurement for moderate or advanced glaucoma. It is possible that the participants recruited by Sehi *et al.* (2011) study were more

advanced than the others, and thus any changes that might had taken place went unnoticed. It is well documented that PERG measurement has moderate variability between participants and is affected by visual acuity (VA) and media opacities (Porciatti & Ventura 2004; Ventura *et al.* 2006; Yang & Swanson 2007). Although care was taken by Sehi and colleagues to exclude eyes with moderate cataract and poor vision, it is possible that the patients recruited for their study had inferior media clarity and/or VA compared to other studies. Lastly, as PERG amplitude is the sum activity of the RGCs and the neurons in inner retina, it is possible that there are changes in inner retina that masked the changes in PERG amplitude (Porciatti & Ventura 2004). It is also possible that they calculated the sample size incorrectly and thus were not able to observe effect.

PERG measurement has provided an invaluable support for the RGC dysfunction hypothesis. However, PERG measurement has many shortcomings over and above that mentioned in the previous paragraph. It is operator-dependent, has increased test-retest variability when the measurement is different from the mean; the amplitude does not reduce to noise level even when the participant has no light perception, there are wide ranges of normal PERG; and depending on the type of electrode used, the procedure might require topical anesthetic. Most importantly the PERG signal is very small with a high noise level and thus is difficult to differentiate from noise at times (Porciatti & Ventura 2004; Porciatti & Ventura 2009; Ventura *et al.* 2013; Walsh *et al.* 2005; Yang & Swanson 2007).

Supporting the hypothesis of RGC dysfunction in human is not the sole goal of the studies investigating RGC dysfunction in human. Another objective of this research is to establish a functional measure that is sensitive enough to detect the subtle changes

that take place when the viable RGCs are under stress, with low variability that could be easily implemented in clinical practice. Although PERG has potential as a tool to target the neuroprotective effects or other oculohypotensive agents under clinical trials, it is too cumbersome and non-patient friendly for clinical application. In addition, PERG only measures the consequences of damage at the level of the retina; there is no information on what might be happening higher in the visual pathway. When we are seeing, we are not only using photoreceptors and other retinal cells. We are seeing with the whole visual system, from photoreceptors to the cortical cells. Even when there is extensive retinal damage, it does not automatically mean that the patient is blind, because the brain might be compensating for the changes. Recent evidence from animal models of glaucoma has suggested effects on higher visual areas (Davis *et al.* 2016). PERG is useful if one wishes to understand the retinal structure and retinal function in the disease, but if detection of visual loss is required then we need to test the visual system as a whole. The technique that is able to measure the sum of activity of the whole visual system currently is perimetry. But it is highly variable and since it uses just a single sized spot of light, it is not likely to provide comprehensive information. Instead, we might borrow ideas from studies of early glaucoma in animals, that there is shrinkage of RGC dendrites that should in turn affect the way the visual system gathers light information over space. Redmond *et al.* (2010a) studied on changes of area of complete spatial summation (Ricco's area) in humans and found an anomaly of spatial summation in early glaucoma. However, before further explanation of the current study, and aim of this PhD, are provided, an extensive summary of what constitutes Ricco's area and its potential origin in the visual system will be provided.

1.5. Spatial summation and Ricco's area

1.5.1. Introduction

For a visual stimulus to be detected by the visual system, the strength of the stimulus signal must be greater than the intrinsic noise. In order to improve detection, the visual system increases its sensitivity by integrating or pooling signals over space (spatial summation) and time (temporal summation). Spatial summation improves detectability but unfortunately, it lowers the eye's resolution by impeding the discrimination of separations between targets and thus visual acuity (Barlow 1958; Richards 1967; Wilson 1970). In 1877, Ricco introduced the law of complete spatial summation (Ricco 1877). According to this law, the threshold needed for detection of a signal is inversely proportional to the area of the stimulus.

$$A \times I = k \qquad \qquad \qquad \text{(Equation 1)}$$

Where A represents stimulus area, I represents intensity and k is a constant.

The largest area for which this law holds true is called Ricco's area, or the area of complete spatial summation. It is also known, in some literature, as the critical area. Intensity thresholds for stimuli smaller than Ricco's area are governed by Ricco's law, while those for stimuli larger than Ricco's area are governed by incomplete spatial summation. There are various laws of incomplete spatial summation, such as Piper's law, where threshold is inversely proportional to the square root of area (Piper 1903); Other laws, including Piéron's law, Goldmann's approximation, and Weber's law, however only operate under very specific experimental conditions (Brindley, 1970).

Glezer (1965) reported an eventual absence of spatial summation when stimulus size increased to very large levels.

It is well established that Ricco's area varies under different experimental and adaptive conditions. It enlarges with increasing retinal eccentricity (Vassilev *et al.* 2003; Volbrecht *et al.* 2000; Wilson 1970), decreasing background luminance (Barlow 1958; Glezer 1965), and decreased duration of the stimulus (Glezer 1965). Even under the same experimental conditions, Ricco's area exhibits considerable inter-subject variability (Volbrecht *et al.* 2000; Scheffrin *et al.* 1998).

The physiological basis of Ricco's area is still a subject of debate. In an effort to understand this, Ricco's area has been investigated under, and compared between, different visual pathways (e.g. the achromatic and S-cone pathways), which involves measuring Ricco's area under conditions that preferentially stimulate or isolate the pathway of interest and comparing it to that found in the achromatic pathway, mindful of known differences in physiology and cellular morphology between the two pathways. The relationship between Ricco's area and structural features in the retina has also been investigated.

The traditional explanation for the basis of Ricco's area is that it represents the size of the RGC receptive field centre (Brown *et al.* 1989; Barlow 1958; Glezer 1965). Glezer (1965) reported a shrinkage of achromatic Ricco's area with increasing background luminance, and attributed this change to increased centre-surround antagonism in the receptive field of RGCs. Given the association between the RGC receptive field size and dendritic tree size (Wässle & Boycott 1991), it was reasonably assumed that Ricco's area would also be associated with RGC dendritic tree size and/or density. Based on this

notion, Volbrecht *et al.* (2000) assessed the relationship between Ricco's area and retinal field eccentricity, by using stimuli isolating the S-cone and L-cone pathway respectively from 0 – 20° retinal eccentricity. They reported a good correlation between Ricco's area size and the parasol dendritic field size with eccentricity. However, the pattern of change of Ricco's area with eccentricity did not correspond with the pattern of dendritic field change of the small bistratified RGCs (Volbrecht *et al.* 2000). Vassilev *et al.* (2000) reported a similar result. These results suggest that the size of Ricco's area is not solely governed by the RGC dendritic or receptive field size. This conclusion is further supported by Redmond *et al.* (2013b), who reported a shrinkage of Ricco's area with increased blue background luminance under experimental conditions preferentially stimulating the S-cone pathway; a finding similar to that of Glezer (1965) in the achromatic pathway. However, the receptive fields of small bistratified RGCs do not have antagonistic spatial (center-surround) organization (Dacey & Lee 1994). Thus, the finding of changes in Ricco's area with blue background luminance in the S-cone pathway are not what one would expect, if the hypothesis of Glezer (1965) for the physiological basis of Ricco's area holds true. Redmond *et al.* (2013) proposed an alternative hypothesis. Spatial antagonism is still required for the formation of Ricco's area and the changes observed with background luminance. However, this spatial antagonism should involve receptive field components that are reactive to the same chromaticity; in the S-cone pathway, this spatial antagonism should be of the configuration S+/S-, but receptive fields meeting this criterion are not found at the level of the retina. In fact, they are first encountered in double-opponent cells in the visual cortex (Conway 2001; Conway & Livingstone 2006; Hubel & Wiesel 1968; Shapley & Hawken 2011; Wiesel & Hubel 1966).

Volbrecht *et al.* (2000) suggested that there could be an equal number of RGCs underlying Ricco's area at each visual field location, because it was observed that even though Ricco's area increased with eccentricity, it retained a constant intensity threshold for that area. This hypothesis had been proposed earlier by Fischer (1973) and Ransom-Hogg & Spillmann (1980). To investigate this hypothesis, Scheffrin *et al.* (1998) compared Ricco's area in old and young individuals, to evaluate the effect of age related loss of RGCs. Indeed, they reported a slight increase in the size of Ricco's area with age under scotopic conditions. They suggested a possible alternate hypothesis that the RGC loss with age resulted in an increase in convergence of the photoreceptors onto the residual RGCs, that in turn causes an increase in the size of Ricco's area. This photoreceptor density hypothesis was not supported by the study of Volbrecht *et al.* (2000), in which Ricco's area was more strongly correlated with RGC density than with photoreceptor density. Furthermore, Zele *et al.* (2006) measured Ricco's area in participants with early age-related macular degeneration, a disease that is known to primarily affect the outer retina, and reported no changes in Ricco's area despite elevated thresholds.

Studies of the effect of age on Ricco's area, guided by the notion that spatial summation should change with age-related neural changes, were unable to identify an association (Brown *et al.* 1989; Redmond *et al.* 2010b). Redmond and colleagues suggested that it is possible that an enlargement of Ricco's area with age is masked by age-related optical changes, whereby an increase in wide angle scatter with age may give rise to an enlargement of the point spread function associated with the stimuli used to measure Ricco's area. If the point spread functions of the differently-sized stimuli are enlarged, this means that the stimulus area on the retina is larger than what the investigator had

intended. With this in mind, the critical area of complete spatial summation would *appear* to be smaller, simply because the stimuli are larger on the retina. Redmond *et al.* (2011, ARVO Abstract), using filters to simulate the wide-angle scatter associated with the optics of a given older age, demonstrated shrinkage of the measured Ricco's area. They calculated the expected RGC dropout for the simulated age, and then calculated the expected enlargement in Ricco's area given this level of RGC dropout. They found that the shrinkage of Ricco's area due to wide-angle scatter and the predicted enlargement of Ricco's area due to age-related RGC dropout were equal and opposite, suggesting that an age-related increase in intraocular stray light masks the effects of increased spatial pooling with age.

A less popular hypothesis for the physiological basis of Ricco's area is one by Davila & Geisler (1991). They performed a predictive calculation of the size of Ricco's area in the fovea in an 'ideal observer', including only pre-neural factors (pupil and lens effect) and photoreceptors in their calculation, and then compared this to their measurements of Ricco's area in four participants. They concluded that Ricco's area is the effect of photoreceptor summation and the optics of the eye (Davila & Geisler 1991). This conclusion has since been challenged by Dalimier & Dainty (2010) who used adaptive optics to correct for the effect of optical aberrations on Ricco's area. They reported that even though the optics of the eye account for most of the formation of Ricco's area in the fovea, and that optical factors influence the size of Ricco's area, in more peripheral regions there was still a break point on the spatial summation curve, indicating that Ricco's area is first and foremost a neural phenomenon.

Combining the evidence from multiple studies, it is likely that the physiological basis for Ricco's area does not lie in one specific region of the visual pathway. Although studies have provided evidence for and against various locations in the visual pathway as the basis for the phenomenon, it should be borne in mind that visual processing of light is a continuous process from cornea to cortex and that spatial summation can occur at multiple levels. Therefore, the size of Ricco's area is likely the product of spatial summation in the visual pathway. Specific spatial mechanisms in the visual cortex can be preferentially stimulated with specific experimental conditions. Under the conditions of SAP, it is likely that the spatial mechanism preferentially stimulated determines the size of Ricco's area (Pan & Swanson 2006; Redmond *et al.* 2010a).

1.5.2. Statistical fitting of spatial summation functions

A wide range of methods for determining the amount of spatial summation, or the size of Ricco's area has been reported in the literature, limiting direct comparisons between studies. Variations include different visual field locations measured (Glezer 1965), different stimulus sizes (Wilson 1970), different background luminance level (Barlow 1958), different stimulus chromaticity (Volbrecht *et al.* 2000), different psychophysical task (detection versus resolution) and different statistical methods to fit the data (Latham *et al.* 1994). Using temporal summation data, Mulholland *et al.* (2015) demonstrated the importance of using a statistical procedure that not only minimises residuals to the fitted curve, but also one that caters for the laws governing the thresholds.

Barlow (1958) and Wilson (1970) fitted their spatial summation data by manually approximating the point at which deviation is observed from a reference line with slope

of -1 (the manual estimation technique). Another method is called constrained least square analysis, which fits two lines to the spatial summation data, constraining the slope of the first line to -1, with respect to Ricco's law, and that of the second line to -0.5, with respect to Piper's law (used by Richards 1967) or slope of 0 (used by Brown *et al.* 1989; Davila & Geisler 1991). The point at which the two lines meet is taken as an estimate of Ricco's area. Scheffrin *et al.* (1998) fitted linear regression lines to their data, constraining the slope of the first line to -1, and allowing the slope and intercept of the second line to vary (two-phase regression analysis); the intersection/ break point gives an estimate of Ricco's area size.

The manual estimation technique can be variable, as the transition between complete to incomplete summation is gradual. In addition, the technique suffers from very strong operator bias. Mulholland *et al.* (2015) compared different fitting techniques for estimating the critical duration of temporal summation, (the relationship between intensity and stimulus duration is the same as that between intensity and area), which are the same techniques as those used for the estimation of area of complete spatial summation. They reported that the manual technique could give a larger estimation of Ricco's area, when compared to the other two techniques. In the same paper, Mulholland and colleagues showed that constraining the slope of the second line to 0 in the same data set resulted in a larger breakpoint value than was the ground truth. The problem with constraining the second line to -0.5 is that variable degrees of partial summation have been observed in the literature (Volbrecht *et al.* 2000; Scheffrin *et al.* 1998). As previously mentioned, these laws are only observable under very specific experimental conditions (Brindley 1970). Constraining the slope of the second line to 0 (an assumption that there is no summation) did not account for the presence of

incomplete summation. Although a varying degree of incomplete summation has been observed across published literature, it is evident in most cases. Iterative two-phase regression analysis addresses both the strong operator bias of manual technique and the wide range of slope in the second line. Importantly, it allows a close fit to the data, while also accounting for both Ricco's law and the variable nature of incomplete summation between locations, individuals, and conditions. However, it is still a semi-subjective method, in that it requires subjective estimation and input of an initial breakpoint value, intercept of the first line, and slope of the second line.

Comparing different fitting techniques available in the literature, the most suitable fitting technique should be the one respecting Ricco's law and not discounting the presence of varying levels of partial summation. Of all of the techniques described, iterative two-phase regression analysis best meets these criteria.

The following equation is used in the analysis outlined in the current thesis:

$$\text{Threshold} = (\text{intercept1} - \text{area}) * (\text{area} < \text{breakpoint}) + (\text{intercept1} - \text{breakpoint} + \text{slope2} * (\text{area} - \text{breakpoint})) * (\text{area} > \text{breakpoint}). \quad (\text{Equation 2})$$

c = estimated intercept of the first line

mb = estimated slope of the second line

A = stimulus area

AR = estimated breakpoint

1.5.3. Ricco's area in glaucoma

Fellman *et al.* (1989) observed that the difference in thresholds to Goldmann III and V stimuli was greater in participants with glaucoma than that in healthy controls. They also observed that enlarging the stimulus area caused a greater increase in measured contrast sensitivity than did increasing the stimulus intensity. They found that the opposite was true in healthy controls. They hypothesized that the greater increase in measured sensitivity to larger stimuli in glaucoma was due to either the stimulus covering more regions of normal retina, or to pathological spatial summation. Redmond *et al.* (2010b) measured achromatic and chromatic (S-cone pathway) Ricco's area in the visual field of 24 participants with early POAG and NTG (average TD at test locations: -1.3dB) and 26 age matched healthy participants. They reported an overall larger Ricco's area in patients with glaucoma, relative to that in healthy controls, under both chromatic and achromatic conditions. They demonstrated that when changes in Ricco's area are accounted for, thresholds for a range of perimetric stimulus sizes overlap between patients in controls, and that disproportionate differences in thresholds between large and small stimuli in glaucoma are no longer observable. They hypothesized that Ricco's area might be determined by the receptive field size of a cortical spatial mechanism that receives input from a critical number of RGCs (31 cells, in line with the report by Swanson *et al.* (2004) that approximately 31 RGCs underlie Ricco's area across the visual field).

To explain, as RGCs are lost in glaucoma, the mechanism that receives input from 31 RGCs now receives input from a smaller number of cells (Figure 1.5 cell B). However, a mechanism that previously received input from a greater number of RGCs (and hence has a larger receptive field), but has now lost input from some RGCs, might now meet

the criteria of 31 underlying RGCs (Figure 1.5 cell C). The extent of the receptive field associated with that mechanism would now determine the size of Ricco's area. This hypothesis would allow for the maintenance of a constant sensitivity at Ricco's area that has previously been reported in published literature.

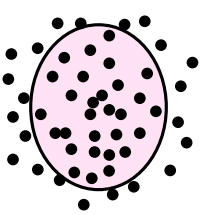
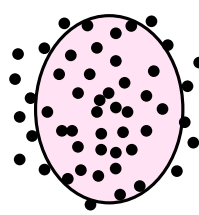
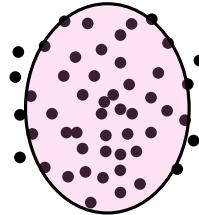
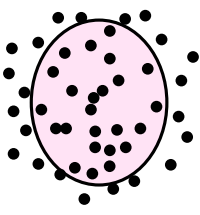
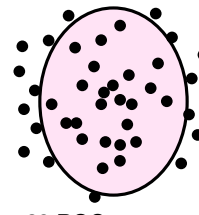
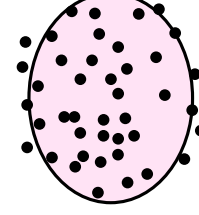
	Cell A	Cell B	Cell C
Healthy	 <p>Input: 24 RGCs Sensitivity: <31dB Complete spatial summation</p>	 <p>Input: 31 RGCs Sensitivity: 31dB Complete spatial summation</p>	 <p>Input: 40 RGCs Sensitivity: >31dB Probability spatial summation</p>
Glaucoma	 <p>Input: 19 RGCs Sensitivity: << 31dB Complete spatial summation</p>	 <p>Input: 28 RGCs Sensitivity: <31dB Complete spatial summation</p>	 <p>Input: 31 RGCs Sensitivity: 31dB Complete spatial summation</p>

Figure 1.5. Cortical cells A, B and C receiving input from different amount of RGCs on the same retinal locations.

An alternative hypothesis is that remaining healthy cells, likely in the visual cortex, extend their receptive fields in response to RGC death. Plasticity in the visual cortex has previously been observed in the monkey (Gilbert & Wiesel 1992). In that study, the investigators performed laser ablation of outer retinal cells, and observed an enlargement of receptive fields of cortical cells next to the region that would otherwise have received input from the damaged retinal region. Also, an enlargement of receptive

fields in the superior colliculus was observed following chronic elevation of IOP in rats (King *et al.* 2006).

It might reasonably be assumed that both RGC death and dysfunction would have an effect on how information of light is pooled by the visual system. Both would involve an absence, or reduction, respectively, of signal inputs into higher visual areas. A pre-morbid shrinkage of dendrites, or death of RGCs in early glaucoma could cause an anomaly of spatial pooling in the visual system, in an attempt to maintain a constant signal-to-noise ratio. If recoverable RGC dysfunction causes Ricco's area to enlarge, a shrinkage of Ricco's area might be observable after successful administration of treatment. Therefore, a comparison of the size of Ricco's area before and after the commencement of rigorous glaucoma treatment would provide a valuable opportunity to investigate pre-morbidity in RGCs in human glaucoma, and the visual effects associated with it.

1.6. Aims and objectives of the PhD

The main objective of this PhD is to investigate the presence of a period of RGC dysfunction in patients with glaucoma, by comparing the size of Ricco's area before and after trabeculectomy surgery. Two control cohorts, one of stable glaucoma patients and another of healthy individuals will also undertake identical experiments. A secondary objective is to better understand the physiological basis for Ricco's area, which is enlarged in glaucoma patients relative to that in age-similar healthy individuals, and to which reduced perimetric sensitivity to a Goldmann III stimulus can be mapped. This investigation will be undertaken in a cohort of individuals with amblyopia, a condition in which retinal receptive fields have previously been found to be normal, but in which deficits in visual function have a cortical origin. A third objective is to provide proof of concept that measurements of a change in Ricco's area have superior utility to measurements of a change in sensitivity to a Goldmann III stimulus in the identification of glaucomatous visual field damage.

Prior to addressing the aims and objectives, it was necessary to undertake a series of preliminary methodological studies, in order to determine the optimum experimental parameters for use in the main experiments. These are described in Chapter 2.

Chapter 2: Preliminary Studies and Optimisation of Experimental Methods

2.1. Introduction

This chapter goes into in-depth details on the factors influencing accurate experimental methodologies for the estimation of Ricco's area. As mentioned in Chapter 1, the measurement of Ricco's area involves measuring thresholds for a range of precisely circular stimulus sizes. Smaller stimulus sizes will need very high luminance level for the thresholds to be measured. Considering the large amount of stimulus presentations involved, thresholding algorithms with an acceptable test time and adequate precision should be chosen. Number of test locations should also be balanced with reasonable test times.

However, before going into the stimulus parameters, the first thing to be considered is experimental apparatus.

2.1.1. Experimental apparatus

In order to construct a spatial summation curve and extract Ricco's area estimate, circular stimuli need to be presented on the retina. The stimulus needs to be highly precise and the apparatus used needs to be able to present a very high luminance level in order to be able to measure thresholds for the smaller stimulus sizes. Currently available instruments are cathode ray tubes, liquid crystal displays and bowl projection systems.

Display monitors have been widely used in studies of visual field because they offer advantages such as accurate user control of the stimulus colour and luminance values on

a pixel-by-pixel basis. Display monitors also come at lower cost compared to bowl projection systems. However, the luminance of the display monitor can be inconsistent between the central and peripheral display locations and, depending on the monitor used, this can be up to 27% or more, affecting large stimulus size presentation (Bach *et al.* 1997; Ghodrati *et al.* 2015; Metha *et al.* 1993). The stimulus presented has also been reported to suffer from non-uniformity of pixel area across the range of luminance and thus there could be a difference between the intended stimulus area and the one actually presented, which was observed on study conducted by Pelli (1997). The projection angle of a pixel to the retina changes across the monitor affecting incident luminance. Display monitors also have limited dynamic range in display, which approximately ranges from 250 to 365 cd/m^2 depending on monitors, with OLED monitors having even lower luminance display (Ghodrati *et al.* 2015).

Up until recently, experiments were usually programmed with software and displayed on the monitor. Bowl and projection systems were not programmable due to the restriction from the manufacturer. New software has since been developed to allow vision scientists to use the open-source programming language, R to control commercially available perimeters: the Open perimetry interface (OPI). Currently the OPI can be accessed on three instruments: The Octopus 900, KOWA AP7000 and the Heidelberg Edge Perimeter (Turpin *et al.* 2012). Commercial perimeters tend to have a large usable dynamic range (e.g. up to 3185 cd/m^2 on the Octopus 900 perimeter) and this factor is of particular advantage for this project as it involves threshold measurement of stimulus sizes as small as Goldmann size I where more light energy is needed for the stimulus detection. The Octopus 900 and KOWA AP7000 have a hemispheric projection bowl of radius 33 cm ensuring a consistent projection angle of

stimulus to retina. The light reflected back from the bowl is polydirectional (i.e. not concentrated in a narrow angle as is the case with LCDs). Therefore, background luminance is more uniform across the surface of the bowl than it is with LCDs. The other advantages are uniform luminance over the area of a stimulus without the stimuli having a dot pitch, which is common in display monitors (i.e. spacing between two adjacent pixels in which no light energy is emitted). The surface of bowl projection systems means that the stimulus projected will be more circular than a stimulus projected on a flat screen (i.e. presentation of a circular stimulus on the periphery of a flat screen will be projected as a vertical oval to the retina because of perspective). An additional advantage of using a commercial perimeter machine, and indeed the OPI, is that if particular hypotheses are accepted following experiments on this platform, then the path to translation becomes much clearer and other groups could also replicate this work freely, if the stimuli was programmed on a monitor in matlab. Even though the problem with circular stimuli and screen background uniformity in the display monitor can be corrected, the problem with limited dynamic range remains a fundamental disadvantage. Given the requirements for the experiments outlined in this thesis, the decision was made to conduct experiments on the Octopus 900 perimeter (Haag Streit Ltd., Koeniz, Switzerland). The study by Redmond *et al.* (2010a) in which achromatic Ricco's area was measured showed that Ricco's area in glaucoma participants was between Goldmann III and IV, approximately, whilst for healthy participants it was between Goldmann II and III. Therefore, the use of Goldmann I – V stimulus sizes in our study enables measurements of Ricco's area size for both groups.

2.1.2. Choosing a thresholding algorithm

There are numerous thresholding strategies available for the psychophysical measurement of visual threshold. They have various methods to reach threshold, different testing speed, different repeatability, and adaptive or non-adaptive strategies. Non-adaptive strategy has the trials distribution that is specified in advance and can be called the method of constant stimuli. This method employs pre-determined stimuli with different intensities and presents them in a randomised order (Spearman 1908; Treutwein 1995). Due to the large number of stimulus presentations needed, this technique can be time consuming and inefficient if the pre-determined stimulus testing intervals do not include the true threshold. The fewer the trials needed to reach a particular standard deviation of the estimate, the more efficient that strategy is. Adaptive strategy involves the distribution of trials that are dependent upon the outcome of the previous trials and is considered to be more efficient, as it does not present a stimulus that is remote from thresholds that provide little information. One of the adaptive methods is the staircase method, whereby the stimulus intensity is changed by a pre-determined amount, depending upon the subject's previous response to the stimulus. If the subject perceived the stimulus, the intensity is decreased and vice versa. The change from seeing to non-seeing and from non-seeing to seeing is called a reversal. The staircase method stops after a certain number of reversals. There are different types of adaptive staircase methods available. One of the adaptive staircase methods is the X up and Y down procedure or more commonly known as a transformed staircase (Levitt 1971). The staircase could begin supra-thresholdly and each time the observer make Y number of correct responses consecutively, the contrast will be reduced. And when the observer cannot detect the stimulus by X amount of responses, then the contrast will be increased. The inflection point is named the reversal point. The procedure stops after a

certain number of reversals. The threshold can be taken as an average of whatever number of reversals is selected. Depending upon the starting threshold level, the steps of staircase and the reversals points, the staircase method can be more or less efficient than MOCS (Cornsweet 1962).

Another adaptive method is PEST or Parameter Estimation by Sequential Testing, which started by presenting a block trial at a fixed intensity. The next section of block trial is then presented at higher and lower intensities depending on the sequential likelihood test. It terminates when the amount of correct responses differ significantly from that expected from the threshold-criterion probability. (Taylor 1967).

Common adaptive methods with higher efficiency are the maximum likelihood methods of QUEST (Watson & Pelli 1983) and a modified version of QUEST, called ZEST (Zippy Estimation by Sequential Testing) (King-Smith *et al.* 1994). Both methods have been shown to exhibit narrower distribution of errors compared to the staircase method and PEST (King-Smith *et al.* 1994). Both strategies employ prior knowledge about the expected distribution of thresholds (the initial probability density function [pdf]) and the response that is made by the patient (seen or not seen) to alter the intensity on subsequent trials. The maximum likelihood technique reduces testing time and test-retest when compared to adaptive methods such as staircase method and PEST, especially when the initial threshold estimates used by the procedures are dissimilar to the true threshold of the location (King-Smith *et al.* 1994; Turpin *et al.* 2003). Although computer simulations have shown QUEST to exhibit less precision compared to ZEST (King-Smith *et al.* 1994), many of these same modifications that have been applied to ZEST have also been applied to QUEST, resulting in QUEST+ (Watson 2017).

QUEST+ was not available at the time of commencement of the experiment and therefore it was decided that ZEST would be the best option and only ZEST will be explained in great details.

The initial pdf used in ZEST contains information for each possible threshold (0-50dB): the probability of the subject's threshold at a particular location. Figure 2.1 illustrates how ZEST utilizes the pdf. The top panel of Figure 2.1a shows that the initial pdf assumes that 14dB is the most likely threshold for the subject ($P= 0.13$) and that it is very unlikely that the threshold will be 2, 3, 4, 19 or 20dB ($P= 0.001$). The first stimulus that is presented will have a contrast equal to the mean of the initial pdf, which is 12dB in this case denoted by the vertical dashed line in Figure 2.1. If the subject responds no, then the initial pdf is modified by multiplying it with a likelihood function, which is the frequency of seeing curve, to give greater probability to the lower values (decibels) (Figure 2.1a bottom panel). In other words, after each response, the [posterior] pdf is modified by multiplying each value in the pdf by the likelihood of observing that particular response, given that particular parameter value. The next stimulus presented will have intensity equal to the mean of the new pdf, which is 9dB. If the subject had responded yes to the initial 12dB, the pdf would have been modified to give greater probability to the higher values (decibels) (Figure 2.1b). The process continues until it is stopped by either one of two termination criteria: after a specified number of trials or when the estimated threshold has the confidence interval that is smaller than a criterion level, which is <1.5 dB of the pdf standard deviation (dynamic termination criterion). The subject threshold is the mean of the final pdf (Turpin *et al.* 2003; Turpin *et al.* 2007)

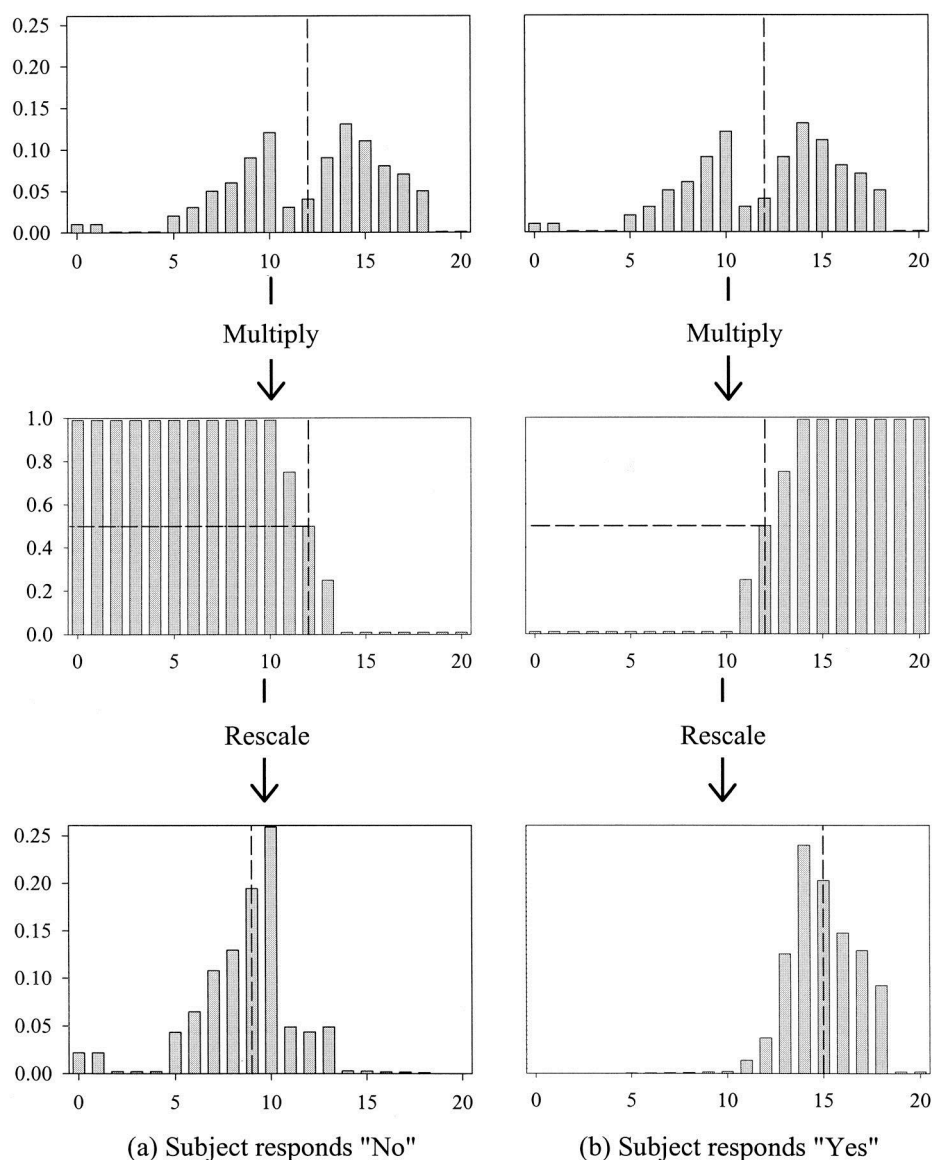


Figure 2.1. The first step of ZEST thresholding procedure. Top panel: initial pdf; middle: likelihood functions with the 50% seeing point aligned with the mean of initial pdf; bottom panel: the posterior/new pdf. Dashed vertical lines: mean of pdf. Picture taken from Turpin et al. (2002).

Anderson (2003) performed a computer simulation comparing the two different termination criteria, fixed number of trials and dynamic termination. Dynamic termination ends the thresholding procedure when the confidence interval for the estimated threshold is smaller than a criterion level. Anderson recommended the use of fixed number of trials criterion due to its reduced testing time and comparable

distribution of errors with dynamic criterion. However, he was using a starting pdf that only consisted of normal threshold data and therefore his observation might not be applicable for ZEST method in this study, as the pdf used will consist of threshold data from both healthy and glaucoma participants (bimodal pdf), derived by Turpin *et al.* (2002). Dynamic criterion tends to last longer in cases when the threshold estimate does not match the initial pdf value (Turpin *et al.* 2002), which could explain the observation of Anderson (2003). As the participants in this PhD study consist of both healthy and glaucoma individuals, the danger of using a fixed number of trials on all participants is that in some cases the thresholding procedure would stop before it reaches a patients' 'true' threshold level. Therefore, it was decided that the ZEST algorithm used in this study would use the bimodal pdf derived by Turpin and colleagues, which was derived for Goldmann size III. How appropriate the bimodal pdf is for other Goldmann sizes remains to be seen. The dynamic termination criteria met when the standard deviation of the pdf is <1.5 dB.

2.2. Optimisation of thresholding algorithm and test time

The ZEST codes used in this project were adapted from code written by Andrew Turpin and Luke Chong (University of Melbourne, accessed on 19th January 2014). The original code can be found at <http://people.eng.unimelb.edu.au/aturpin/opi/interface.html>. The modifications to the code are listed below:

- Measuring threshold for Goldmann size I-V as opposed to just GIII
- Stimulus presentation time was increased to 200ms
- Dynamic range of the thresholding method was increased from 30dB to 40dB, as the average dB value observed during the pilot study of this project for Goldmann V of healthy participants is 33dB
- Amendment to the test location patterns, as it was observed that the code miscalculated the presentation location and the test location is shifted 3° superior and 3° temporal away from the intended location.

Two-phase regression analysis in this study involved fitting two lines onto a set of threshold data. This iterative analysis is based on using two simple linear regressions ($y=mx+b$), where, within the estimated breakpoint, the data are best described by the first part of Equation 1, which incorporates a constraint on the slope ($m = -1$). For data beyond the estimated breakpoint, the data are best described by the second part of Equation 1. The two equations are fitted to the data in order to minimize residual sum of square. The equation for the two-phase regression analysis in the study can be found in Chapter 1. In our study, the slope of the first line will be constrained to -1 to respect Ricco's law whilst the intercept of the first line, and slope of the second line is allowed to vary. The break point between first and second lines denotes Ricco's area estimation.

The more variable the thresholds measured in the study, the harder it is to fit two-phase regression analysis. The fitting procedure is semi-objective with an initial breakpoint needed to be estimated subjectively and put into the formula to obtain a final breakpoint estimate. When the threshold data is variable, the initial breakpoint estimate could be off and the two-phase regression analysis can fail to run. Also, to ensure the accuracy of the Ricco's area estimate obtained, coefficient of determination (R^2) output from the linear regression on the data that is less than 0.9 will be excluded from further analysis. The lower the R^2 is, the worse the linear regression is able to fit the data and thus could give inaccurate Ricco's area estimates.

A pilot study investigating a good compromise of test precision and test duration was conducted on 3 participants. This exploratory study was conducted with two thresholding methods, ZEST (experiment 1) and the adaptive staircase method (experiment 2) to measure threshold of GI-V on different number of test locations to assess the parameters that produce more spatial summation curves with $R^2 > 0.9$.

2.2.1. Method for experiment 1

2.2.1.1. Subjects

Three participants (age: 23, 27 and 31 years) were recruited from students and staff of Cardiff University. One of the participants (P003) withdrew from the study after one session due to the length of time needed to complete the experiment. Two participants completed the study. All participants underwent ocular health investigation with slit lamp biomicroscopy and Topcon 3D OCT 1000. All participants had best corrected visual acuity of at least -0.2 LogMAR and IOP < 21mmHg with a Topcon CT-80 non-contact tonometer. All participants underwent visual field investigation with SAP (Humphrey visual field analyser [HFA] II, 24-2 SITA-Standard, Carl Zeiss Meditec, Dublin, CA) and all had full fields. Only the right eye of each participant was tested. All participants were recruited in accordance with declaration of Helsinki.

2.2.1.2. Apparatus and Stimuli

Stimuli were Goldmann sizes I-V (0.11° , 0.22° , 0.43° , 0.87° and 1.7°), presented on an Octopus 900 perimeter (Haag Streit, Koeniz, Switzerland) with background luminance of 10 cd/m^2 for 200ms, driven by the Open perimetry interface (Turpin *et al.* 2012).

2.2.1.3. Procedure

The study commenced using ZEST algorithm to measure thresholds for 5 Goldmann sizes with Yes/No criterion on the standard 24-2 pattern, (50 locations within 24° and two extra locations in nasal field, at 30° eccentricity) of the visual field. Based on the R^2 from the fitting of two-phase regression analysis at the 50 locations and the number of Ricco's area estimates that can be processed successfully with two-phase regression analysis, the number of test locations was reduced. When the R^2 and number of

successfully run two-phase regression analysis were low, the numbers of test locations were reduced to 44 and two-phase linear regression analysis was performed on the data again. This process was repeated with test locations cut down to 30 and 16 (Figures demonstrating the test patterns can be found in section 1.1.2). Threshold measurement procedure was conducted twice for 16 test locations, first with only one set of Goldmann I-V sensitivity measurements and then repeated with two sets of Goldmann I-V sensitivity measurements to assess improvement in R^2 . The time needed to finish the tests was recorded. ZEST gets the information of the starting value of a test location from the other locations adjacent to it. Therefore, when the test locations were excluded, the residual locations needed to be connected to neighbouring points. No initial starting values from each intensity was inputted manually as ZEST got its starting value from pdf that was collected by Turpin *et al.* (2002). All procedures were carried out with natural pupil sizes and full refractive correction (with full aperture trial lenses) in place for the relevant working distance. Fixation was monitored visually and patient position adjusted when the eye pupil drifted on the fixation camera on the instrument.

Data processing and statistical analysis.

Sensitivity values (dB) were converted into increment threshold (ΔI) and plotted against area. Two-phase regression analysis was performed in the freely available open-source statistical environment, R (version 3.1.0) to obtain Ricco's area estimates at each eccentricity. The slope of the first line was constrained to a value of -1, following Ricco's law, whilst the intercept of first line, slope of the second line and break point were allowed to vary. The breakpoint estimated was taken to be the Ricco's area estimate.

2.2.2. Results for experiment 1

Table 2.1 shows average test durations for GI-V for 52 test locations.

Table 2.1. Average test times for 4 different locations on 2 participants with ZEST

Goldmann Sizes	Number of test points			
	52	30	16	16 (2x)
I	11 mins 48 secs	7 mins 43 secs	5 mins 12 secs	10 mins 2 secs
II	10 mins 27 secs	7 mins 2 secs	4 mins 55 secs	10 mins 14 secs
III	7 mins 2 secs	3 mins 18 secs	2 mins 3 secs	3 mins 57 secs
IV	7 mins 50 secs	4 mins 10 secs	2 mins 46 secs	5 mins 17 secs
V	8 mins 30 secs	5 mins 6 secs	3 mins 3 secs	6 mins 9 secs
Total test durations	45 mins 37 secs	27 mins 19 secs	17 mins 59 secs	35 mins 39 secs

With the ZEST algorithm, the test time is longer for Goldmann sizes that are not Goldmann III. ZEST was initially run on 52 locations. The time listed on Table 2.1 is the test time without breaks. Participants needed at least 5 minutes rest after the threshold measurement of each Goldmann size, which added another 25 minutes to the test times in addition to the test time mentioned in the Table 2.1. This is in addition to regular breaks given to the participants. A total of 520 thresholds were measured, representing 104 test locations across two participants, and thus 104 data sets with which to plot 104 spatial summation functions. When data were arranged in order to plot spatial summation curves at each location, it was found that curves could not be fitted in 47 locations, which means only 54.81% of data could be processed to produce Ricco's area estimates (Figure 2.2). The mean R^2 of spatial summation curves that could be successfully fitted was 0.89, which does not reach the criteria of successful fitting of 0.9. The number of test locations was reduced further to 30 (Figure 2.3) and then to 16

(Figure 2.4) and the analysis was repeated each time. The proportion of locations for which spatial summation curves could be fitted successfully was 66.67% (40 out of 60) for the 30-location test grid (with mean R^2 of 0.91, Figure 2.3) and 75% (24 out of 32) for the 16-location test grid (mean R^2 of 0.94, Figure 2.4). Goldmann I-V thresholds were then measured twice with the 16-location test grid to assess any improvement in mean R^2 when thresholds for individual Goldmann sizes at individual locations were averaged. The success rate of curve fitting procedure increased from 75% to 87.5% (42 out of 48) with mean R^2 of 0.97.

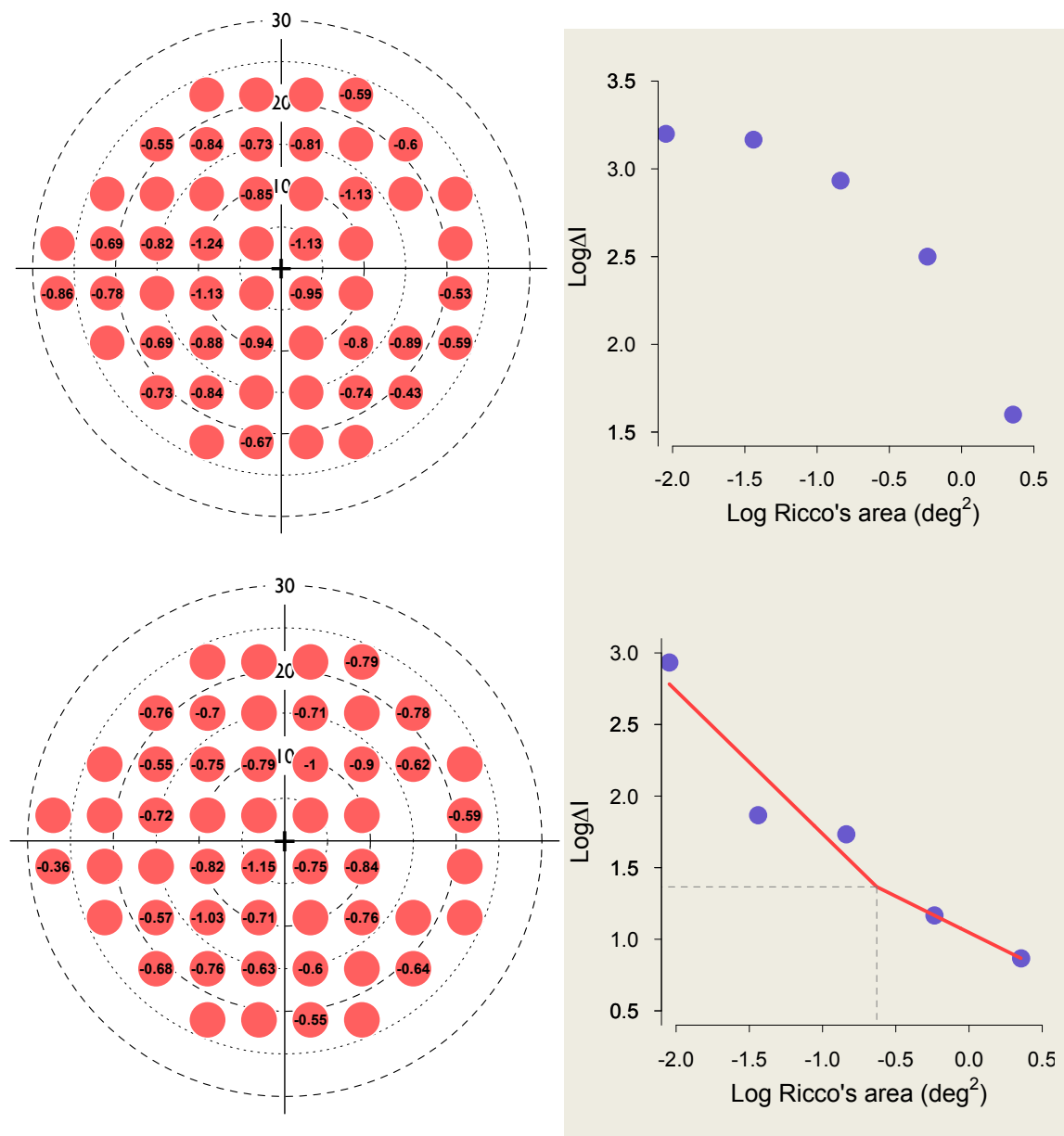


Figure 2.2. Top and bottom left images show 54 test locations visual field pattern with Ricco's area estimates for subjects P001 (top left) and P002 (bottom left). Top right image shows an example of one of the worst spatial summation curves and bottom right image shows an example of one of the best spatial summation curves with the 54-location test grid from both participants. The locations with numbers were those where the curve successfully fitted, whilst those without numbers were not successfully fitted.

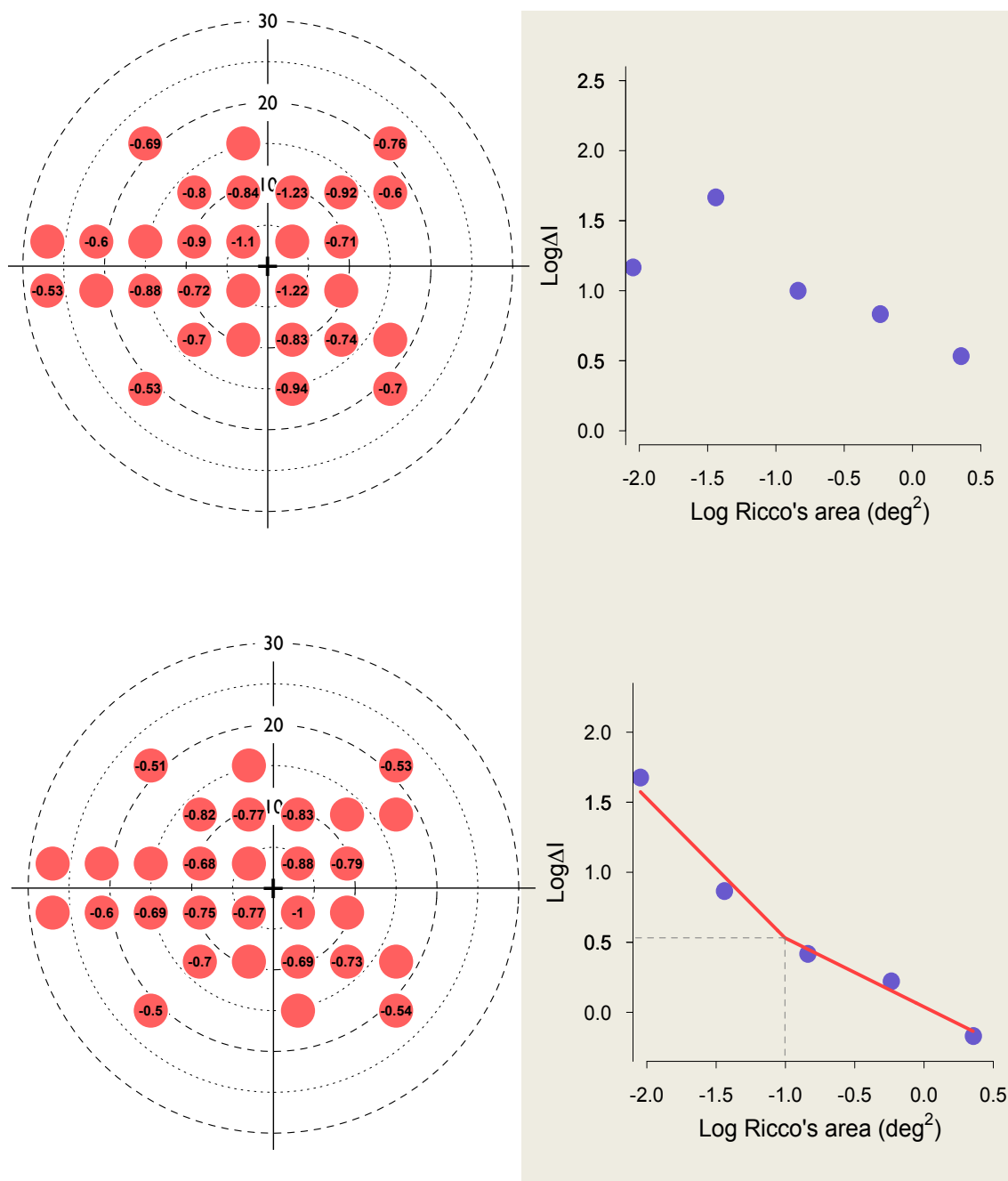


Figure 2.3. Top and bottom left images show the 30-locations visual field test pattern with Ricco's area estimates for subject P001 (top left) and P002 (bottom left). Top right image shows an example of one of the worst spatial summation curves and bottom right image shows an example of one of the best spatial summation curves with the 30-location test grid from both participants. The locations with numbers were those with curve successfully fitted, whilst those without numbers were not successfully fitted.

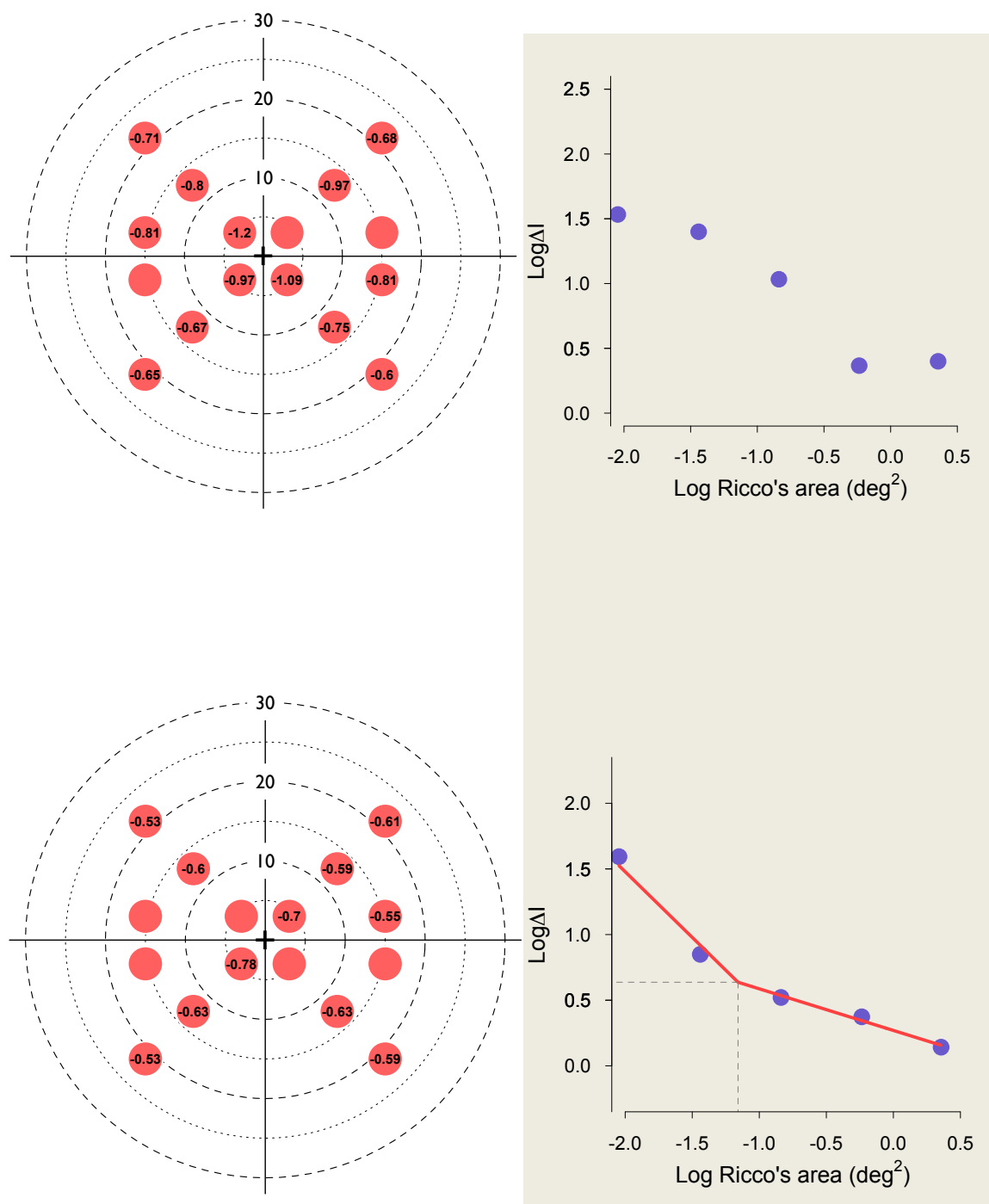


Figure 2.4. Top and bottom left images show 16 test locations visual field pattern with Ricco's area estimates for subject P001 (top left) and P002 (bottom left). Top right image shows an example of one of the worst spatial summation curve and bottom right image shows an example of one of the best spatial summation curves for the 16-locations test grid with two repeats from both participants.

2.2.3. Discussion for experiment 1

The goodness-of-fit of spatial summation functions, as denoted by mean R^2 , improved as the number of test locations was reduced. It increased to a satisfactory level of 0.97 and good successful fit on spatial summation curve of 87.5%, with two repeat threshold measurements at 16 test locations.

The increase of test time for Goldmann sizes other than Goldmann III agrees with the report of Turpin *et al.* (2002), that the testing time increases when the participant's threshold does not match the initial threshold estimate of the pdf, as more presentations are required (correct estimate = 2-3 presentations; incorrect = 4-6 presentations). The pdf used in this study is based only on a threshold of Goldmann III stimuli of 856 individuals and it was outside the scope of this project to create new pdf for the other Goldmann sizes. This defeated the purpose of using the ZEST algorithm, as one of the primary advantages of this procedure is reduced test time.

Another drawback became apparent when the number of test locations was reduced in that, a problem with randomisation of thresholding procedure arose. The majority of tests at 16 test locations involved spots of light appearing systematically at one test location at a time, changing in intensity until the threshold was reached, before it moved to the next location, i.e. disruption of the randomisation procedure. Phu *et al.* (2016) observed that when participants can anticipate where the stimulus is going to appear next, contrast sensitivity measurement increases for Goldmann I and III, but not V. This has the potential to affect the size of Ricco's area obtained.

Due to the randomisation problem, a staircase method was adapted from Andrew Turpin and Luke Chongs' codes (University of Melbourne) and tested in experiment 2 to assess the goodness-of-fit of spatial summation function, the number of successfully fitted curves, time taken to perform the test and any potential problems with the randomisation procedure.

mean R^2 of spatial summation function as an indicator of success, the following steps were taken:

- 1) Repeated threshold measurements for Goldmann I-V. Threshold measurements were repeated twice and then three times for the same 8 test locations. These were then averaged by location and stimulus size. Time needed to finish the tests was recorded.
- 2) Staircase step sizes were altered. The effect of a 4-1dB and 4-0.5dB strategy was assessed. A 4-1dB strategy means that before the first reversal, the step size was 4dB. For subsequent reversals, the step size was 1dB.

The first stimulus intensity was based on a range of threshold values for Goldmann I-V obtained in experiment 1. In order for the staircase method to run efficiently, the first stimulus intensity needed to be close to the threshold.

2.2.5. Results for experiment 2

Test durations increased as Goldmann sizes were reduced for the staircase thresholding algorithm, unlike for the ZEST algorithm, where the testing time increased for all Goldmann sizes except for Goldmann III (Table 2.2). Total test duration for the staircase method was reasonably short. The percentage of Ricco's area estimates obtained with the staircase method with twice repeated measure was 93.75% (15 out of 16) and mean R^2 was 0.98. Percentage stayed the same for the staircase method with triple repeated threshold measurement, however mean R^2 improved to 0.99.

Table 2.2. Test durations for staircase thresholding procedure

Goldmann Sizes	Number of test points	
	8 (2x)	8 (3x)
I	7 mins 30 secs	9 mins 36 secs
II	6 mins 44 secs	10 mins 9 secs
III	5 mins 20 secs	8 mins 15 secs
IV	5 mins 6 secs	7 mins 7 secs
V	5 mins 2 secs	7 mins 11 secs
Total test durations	29 mins 42 secs	42 mins 18 secs

Staircase method was then run with two different step sizes 4-1dB step and 4-0.5dB.

There was no difference between the mean R^2 of 4-1dB step and 4-0.5dB step sizes of 0.99. However test duration increased by half an hour with 4-0.5dB.

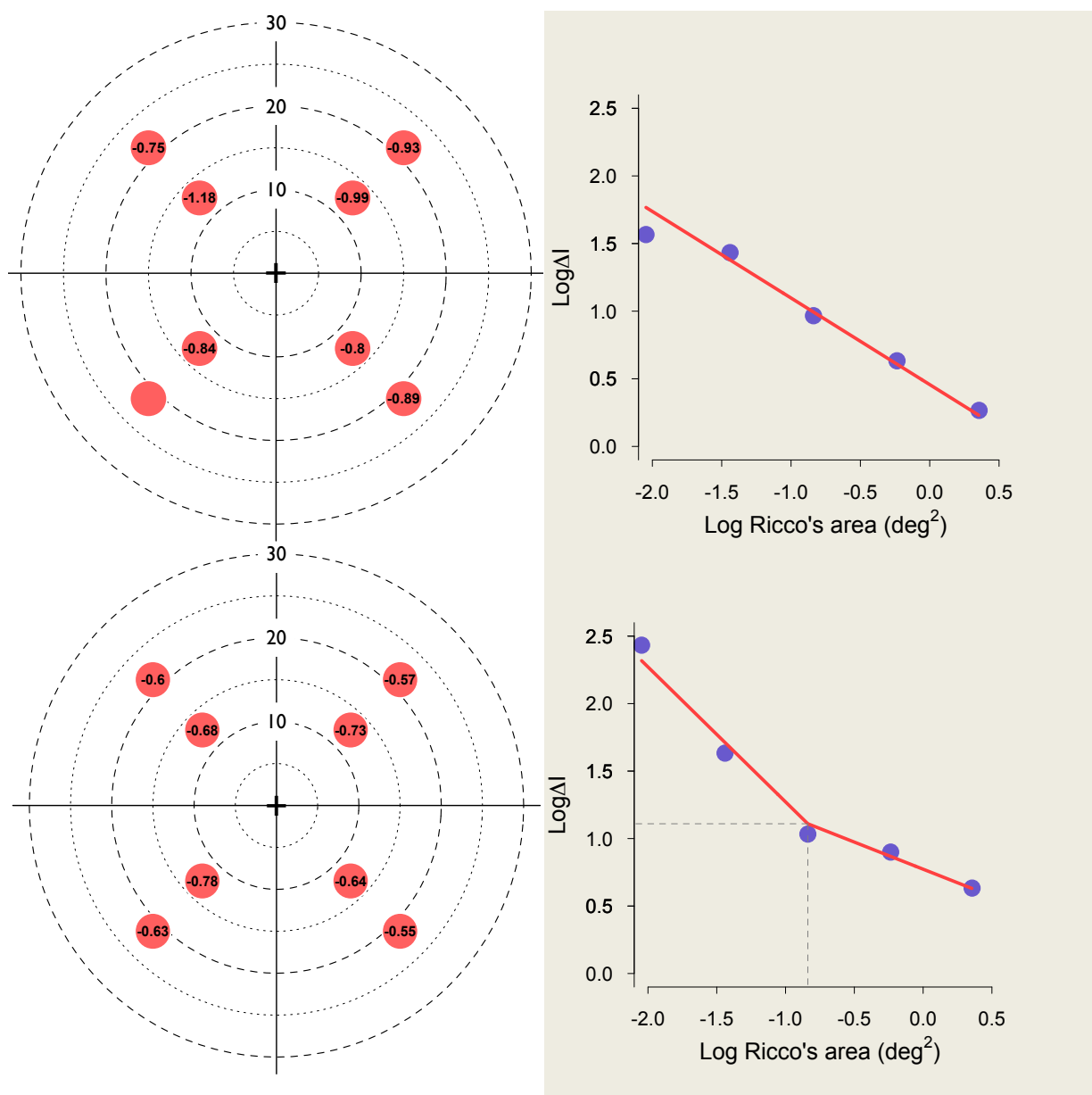


Figure 2.6. Top and bottom left images show 8 test locations visual field pattern with Ricco's area number for subject P001 (top left) and P002 (bottom left). Top right image shows an example of one of the worst spatial summation curves and bottom right image shows an example of one of the best spatial summation curves with the 54-location test grid from both participants.

2.2.6. Discussion for experiment 2

The staircase method exhibited no randomisation problem, had reasonable test time and allowed the determination of spatial summation data that could be fitted successfully. It is therefore a better thresholding algorithm compared to ZEST for this experiment. Mean R^2 improved by 12% with three repeats measured, indicating that increasing repeat threshold measurements improved the fit of spatial summation function substantially. Time needed to perform the triple repeated test measurement was also acceptable with 8 visual field test locations.

The 4 - 0.5dB strategy exhibited a similar mean R^2 with the 4 - 1dB strategy but with a substantially longer test time. Both participants reported that the test was very taxing and required additional rest times. One important consideration is that participants in this study were young researchers with relatively good concentration levels, so if the test was too difficult for these participants then we can assume that participants with glaucoma, who are more senior, would find the test even more challenging. Therefore a 4-1dB step staircase was considered a better option.

In conclusion, the optimum protocol for the main experiments was chosen as follows: 8 test locations in which three repeated threshold measurements are conducted with a staircase procedure, a 4 -1dB strategy, 8 reversal termination criterion and final threshold taken as the average of last 4 reversals. This protocol enabled a reasonable balance between test duration, number of satisfactory fitted spatial summation curves and the goodness-of-fit of these curves (as denoted by mean R^2 of more than 0.9).

2.3. Learning effect and variability

2.3.1. Introduction

SAP has been reported to exhibit a learning effect, whereby inexperienced participants present with artificial VF defects that disappear in subsequent tests as participants acquire more experience in performing the test (Kulze *et al.* 1990; Wild *et al.* 1989). The learning effect is characterized by an increase in absolute mean sensitivity with subsequent examinations, that is especially significant between the first and second examinations in SAP (Kulze *et al.* 1990; Wild *et al.* 1989). It has also been shown in FDP (Fujimoto *et al.* 2002; Iester *et al.* 2000) and SWAP (Wild *et al.* 2006; Rossetti *et al.* 2006). It is unclear whether Ricco's area measurement suffers from a learning effect. This needs to be investigated in order to establish which testing session measurement should be used as the baseline data, as any learning effect could minimise the possibility of detecting small changes in Ricco's area. It is expected that there will only be a learning effect for the thresholds for different sizes/ contrast detection (vertical arrows in Figure 2.7), but not for Ricco's area size (horizontal arrow), as intuitively we do not expect a participant to be able to learn to move the inflection point on spatial summation curves. To shift the inflection point, the mean sensitivity will have to be systematically greater (or smaller) with increasing stimulus size. Unlike the perception of being near threshold on a contrast detection task, participants have no way of perceiving the size of Ricco's area in relation to the stimuli being presented. Also, as outlined in the previous experimental chapter, the different stimulus sizes will be presented randomly, and thus making it difficult for participants to learn to shift the inflection point.

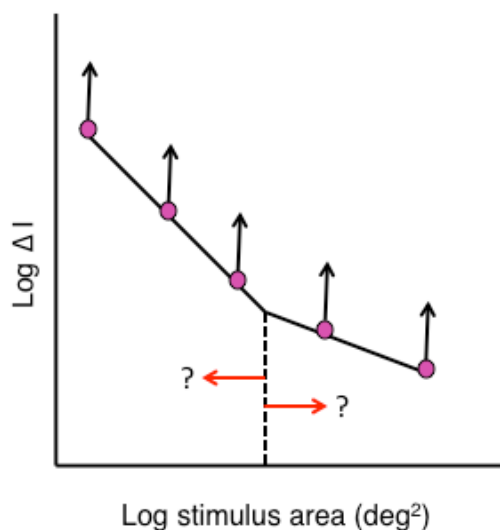


Figure 2.7. Illustration of possible improvement in Goldmann size thresholds (black vertical arrows) and Ricco's area size estimates (red horizontal arrows).

Nevertheless, it is prudent to conduct the study to eliminate such an effect. To the author's knowledge, no literature assessing a learning effect of different stimulus sizes is currently available. If a learning effect is indeed present, it is expected to appear in the form of systematic enlargement or reduction of size of Ricco's area between visits.

It is clear from the literature that Ricco's area size varies between individuals, but it is unclear what is the intra-individual variability in Ricco's area size (Redmond *et al.* 2010a; Volbrecht *et al.* 2000). Measurement of the variability of Ricco's area can better help inform true changes from physiological fluctuations between two visits (see Chapter 4).

The aims of this study are twofold: firstly, to explore the presence of a learning effect on Ricco's area measurements and, secondly to investigate the variability of Ricco's

area estimates between visits in observers with previous experience of visual field testing, compared to inexperienced observers.

2.3.2. Methods

2.3.2.1. Subjects

Four healthy participants (two aged 21 and two aged 22 years old) that were naïve to psychophysical testing, and 3 participants (aged 23, 28 and 51 years old) with prior experienced of performing psychophysical testing, were recruited from students and staff of Cardiff University. All participants underwent ocular health investigation with slit lamp biomicroscopy and Topcon 3D OCT 1000. All participants had best corrected visual acuity of at least -0.2 LogMAR and IOP<21mmHg with Topcon CT-80 non-contact tonometer. All participants underwent visual field investigation with Humphrey SITA-Standard, which was measured after completion of Goldmann I-V threshold measurements to confirm visual field normality. Only right eyes of all participants were tested.

2.3.2.2. Apparatus and Stimuli

Experiments were performed on an Octopus 900 perimeter (Haag Streit, Koeniz, Switzerland) controlled with OPI, presenting Goldmann sizes I-V (0.11°, 0.22°, 0.43°, 0.87° and 1.7° diameter) on a white background (10 cd/m²) for 200ms. Eight visual field locations were measured at eccentricities of 12.7° and 21.2° (Figure 2.8) based on previous experiments, where the success rate of spatial summation curve fitting was observed to be higher at these eccentricities.

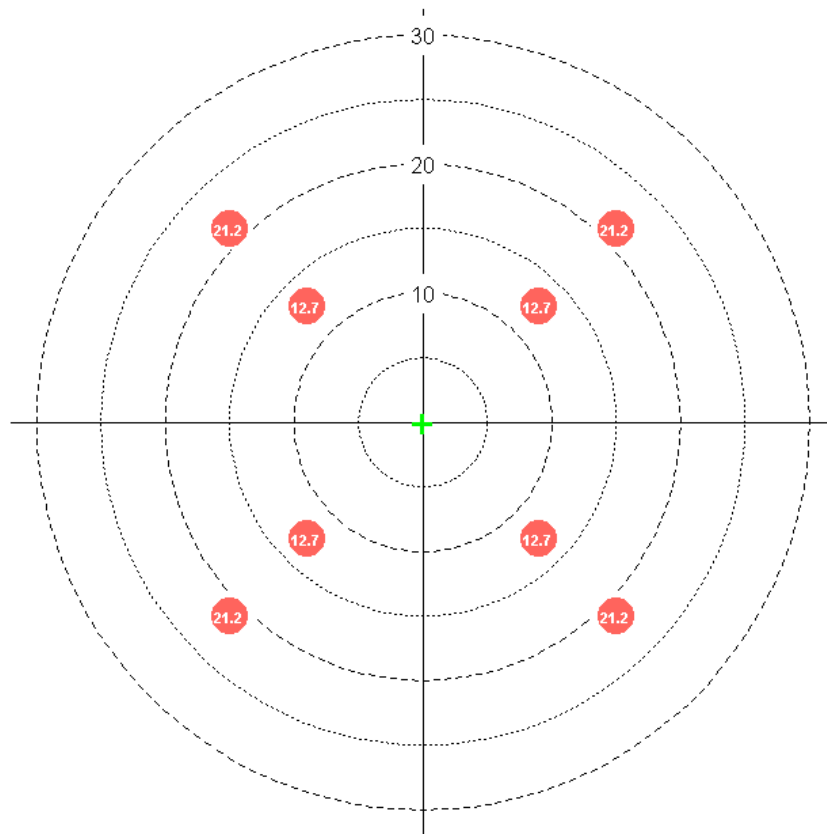


Figure 2.8. 8 visual field test locations

2.3.2.3. Procedure

Sensitivity (in dB) was measured for each of the Goldmann sizes (I-V) at each visual field location in an interleaved manner. In each test, a different Goldmann size was used, chosen at random. A 4:1 staircase procedure was used, which was adapted from that produced by Andrew Turpin and Luke Chong (University of Melbourne, <http://people.eng.unimelb.edu.au/aturpin/opi/interface.html>, accessed on 15th March 2014). Step size was 4 dB before the first reversal and 1dB thereafter. A yes/no response criterion was used. At each location, the procedure stopped after 8 reversals and the final threshold returned was an average of the last 4 reversals. The entire procedure was repeated twice more. So at each test location, 3 values for sensitivity

were obtained for each Goldmann size. Therefore a total of 15 sets of sensitivity measurements were obtained per location, and 120 measurements per participant for each appointment visit. Sensitivity measurements of Goldmann I-V were conducted for 4 appointment visits over the period 3 weeks for experienced participants and 5 appointment visits for naïve participants. All procedures were carried out with natural pupil sizes and central refractive error corrected fully with full aperture trial lenses. Fixation was monitored visually and patient position adjusted when fixation began to drift from central. Breaks were given approximately every 10 minutes (roughly two threshold measurements) and whenever a patient asked for a break.

2.3.2.4. Data analysis

Sensitivity values (dB) for Goldmann I-V were converted into increment threshold (ΔI) and plotted against area. Two-phase regression analysis was performed in the freely available open-source statistical environment, R (version 3.1.0) to obtain Ricco's area estimates at each location. The slope of the first line was constrained to a value of -1, following Ricco's law, whilst the intercept of first line, slope of the second line and break point were allowed to vary. The breakpoint estimated was taken to be the Ricco's area estimate. For each appointment visit, eight Ricco's area estimates were obtained from each participant. Ricco's area estimates were compared between visits to explore any learning effect and variability between visits. Kolmogorov-Smirnov test was conducted and showed the data to be non-normally distributed and therefore a two-way Friedman test was used to investigate significant differences between sessions. Research was conducted in accordance with the tenets of the Declaration of Helsinki.

2.3.3. Results

When the Ricco's area data from all locations were pooled together, averaged for each participant and plotted by each visit, all 3 experienced participants exhibited different patterns of Ricco's area changes between visits (Figure 2.9). P006 Ricco's area seemed to exhibit a pattern of enlargement from visit 1 to 3 that was not observed for the other participants. P004 Ricco's area got smaller from visit 1 to 2, but then enlarged. P005 Ricco's area appeared to stay relatively stable from visit 1 to 2 and then got smaller, before it stayed somewhat stable again. The same was observed with naïve participants, where different participants exhibited different patterns of Ricco's area changes between visits, with P009 showing the largest change in Ricco's area estimates between visits.

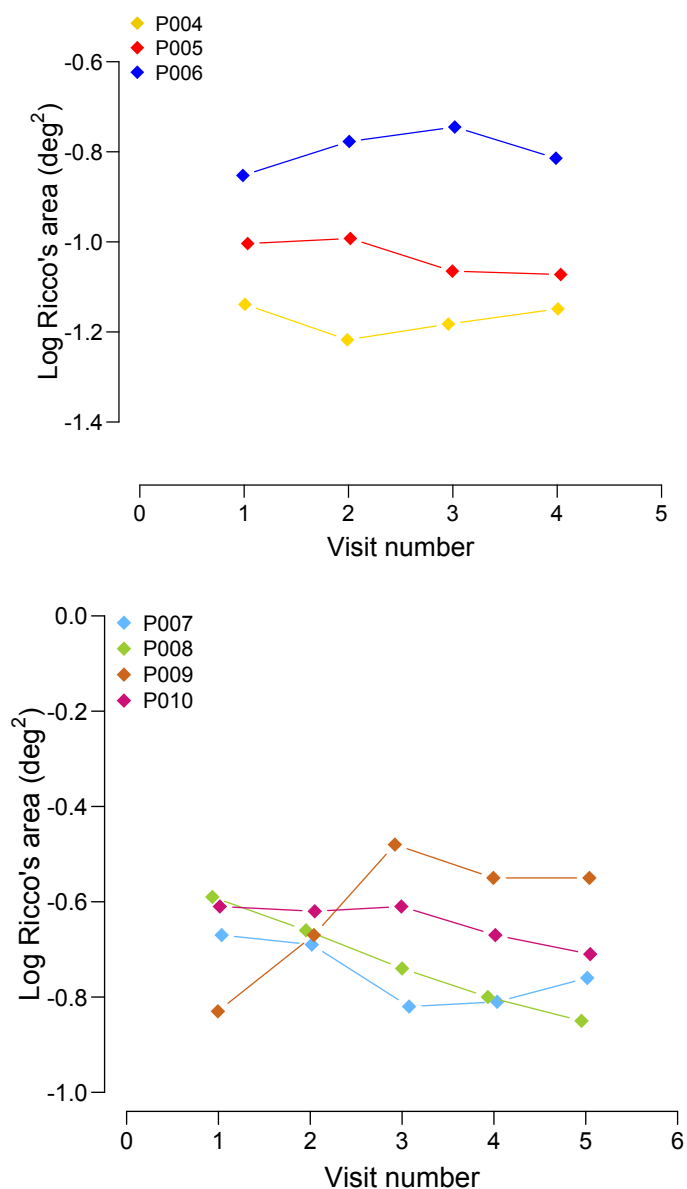


Figure 2.9. Ricco's area estimates of all 3 experienced (top) and naïve (bottom) averaged across all locations.

The Friedman test showed no statistically significant difference in Ricco's area estimates between visits in experienced ($p=0.96$) and naïve ($p=0.48$) participants. Mean and standard deviation between visits for P004, P005, and P006 are -1.18 ± 0.03 , -1.03 ± 0.05 , and -0.78 ± 0.08 respectively. Slightly larger standard deviation is observed with naïve participants, mean and standard deviation for P007, P008, P009, and P010 are -0.75 ± 0.07 , -0.73 ± 0.10 , -0.62 ± 0.14 and -0.64 ± 0.04 respectively.

2.3. *Threshold values of Goldmann I, III and V for 4 visits in experienced participants.*

Standard deviation depicting range of threshold values found in 8 test locations.

Goldmann size	Visit 1 (dB)	Visit 2 (dB)	Visit 3 (dB)	Visit 4 (dB)
I	18.91 ± 1.95	18.39 ± 2.45	18.88 ± 1.72	18.88 ± 1.71
III	30.41 ± 0.75	30.48 ± 0.86	30.68 ± 0.67	30.19 ± 0.82
V	34.41 ± 0.38	34.59 ± 0.56	34.58 ± 0.31	34.23 ± 0.5

There was no improvement in sensitivity values with visits in experienced participants for any Goldmann I, III and V (Table 2.3). Mean and standard deviations of sensitivity (dB) between visits for Goldmann I, III and V are 18.77 ± 0.25 , 30.44 ± 0.20 and 34.45 ± 0.17 respectively.

Table 2.4. Threshold values of Goldmann I, III and V for 5 visits in naïve participants.

Standard deviation depicting range of threshold values found in 8 test locations.

Goldmann size	Visit 1 (dB)	Visit 2 (dB)	Visit 3 (dB)	Visit 4 (dB)	Visit 5 (dB)
I	15.44 ± 1.46	16.02 ± 1.37	15.80 ± 1.22	15.82 ± 1.34	16.00 ± 1.52
III	28.30 ± 1.21	28.82 ± 0.91	28.58 ± 1.02	28.63 ± 1.04	28.67 ± 0.89
V	33.56 ± 0.42	33.78 ± 0.62	34.04 ± 0.48	33.77 ± 0.42	33.91 ± 0.42

There was a slight improvement of sensitivity values from first to second visit in naïve participants, more so for smaller Goldmann sizes. Mean and standard deviations of sensitivity values (dB) between visits for Goldmann I, III and V are 15.81 ± 0.23 , 28.6 ± 0.19 and 33.81 ± 0.18 respectively.

2.3.4. Discussion

The learning effect is reportedly present with SAP, FDP and SWAP in the form of an increase in absolute mean sensitivity that is most notable between the first and second examinations (Fujimoto *et al.* 2002; Iester *et al.* 2000; Kulze *et al.* 1990; Rossetti *et al.* 2006; Wild *et al.* 1989; Wild *et al.* 2006). However, such an effect does not appear to be present in Ricco's area measurements. The lack of systematic changes of Ricco's area estimates and the random pattern of changes of Ricco's area estimates between visits in both experienced and naïve participants suggest an absence of a learning effect in Ricco's area measurement.

A slight improvement in sensitivity values of Goldmann III in the range of 0.20 - 0.58dB was observed in naïve participants, which is smaller than reported in the published literature (Kulze *et al.* 1990; Wild *et al.* 1989). One possible explanation is that repeated threshold measurements of different Goldmann sizes in one session allowed participants to learn the visual field task better than in SAP. In this study, as thresholds of Goldmann I-V were repeatedly measured, if Goldmann size II was taken as an example, by the time the observer takes the second Goldmann II threshold measurement, he/she would have undertaken the threshold measurement for all the other Goldmann sizes and will be on at least the 6th test at this point. The observer would have learned how brief the stimulus duration was, the test locations, and how far into the periphery, etc. Because even though the Goldmann sizes were different, the task was the same, consisting of detecting achromatic contrast.

There was no obvious learning effect for different stimulus sizes in experienced participants. Neither the experienced nor the naïve participant data exhibited an increase

in variability with decreasing stimulus sizes, disagreeing with Wall *et al.* (2009) study, where they observed reduced variability with Goldmann V when compared to Goldmann I and III.

The good repeatability of Ricco's area measurement in the current study is encouraging, with the largest standard deviation being 0.14. The participants recruited in this study were students and research associates with a high level of concentration and motivation. When the test is conducted on participants from elderly populations (as glaucoma prevalence increases with age), although it is expected that the concentration will affect threshold measurements, the variability of Ricco's area is expected to remain unchanged.

In conclusion, a learning effect was not observed in the participants that had performed SAP and those with no visual field task experience. Therefore, in the main PhD study there is no need to exclude Ricco's area measurement from the first session. The good repeatability exhibited by the current study, together with the trials of different parameters in previous sections suggested that the psychophysical protocol for the main experiment is optimised.

2.4. Corneal wavefront aberrations.

2.4.1. Introduction

One of the main aims of the PhD was to test the hypothesis that Ricco's area shrinks following more rigorous IOP-lowering treatment. The treatment form chosen in the study was trabeculectomy surgery. Trabeculectomy surgery is a procedure that allows the lowering of IOP by creating a corneoscleral fistula that causes subconjunctival bleb formation (Cairns 1968). A more detailed explanation of the surgery can be found in Chapter 4. This procedure had been documented to cause changes in corneal curvature (Egrilmez *et al.* 2004; Hong *et al.* 1998) and it was felt that this could affect the projected size, on the retina, of stimuli used in the measurement of Ricco's area. Thus, it was felt to be important to investigate between-visit changes in corneal aberrations and their effect on between-visit measurements of Ricco's area. More details about that experiment can be found in Chapter 4. Here, the principles of corneal aberrations will be described, and a preliminary study of the repeatability of measurements will be reported.

Wavefront aberrations illustrate the distortion of wavefronts as they go through a non-optimal optical system. Wavefront aberrations can be described mathematically by a polynomial series, with Zernike polynomial expansion chosen to become the standard for describing ocular wave aberrations (Thibos *et al.* 2002). The Zernike polynomial is a set of basic functions, with each having a coefficient. Coefficients depict how much contribution that aberration has to the overall wavefront aberration. The Zernike terms are construed by radial order n and frequency m over a unit circle with orthogonal polar co-ordinates ρ and θ .

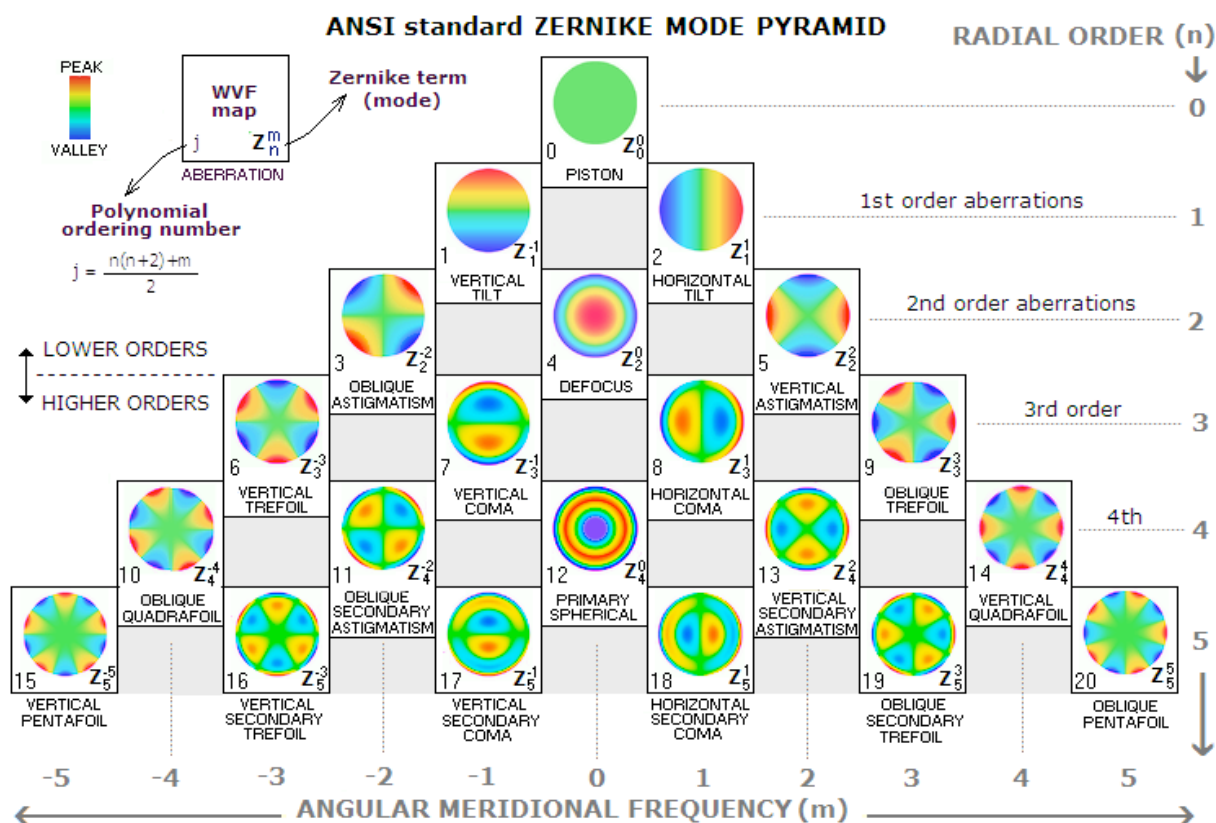


Figure 2.10. Pyramids of Zernike term up to 5th order. Image reproduced from http://www.telescope-optics.net/monochromatic_eye_aberrations.htm.

The Zernike pyramid organizes aberrations into a hierarchy with an increasing radial order (Figure 2.10). Lower order aberrations are zero (piston), first (tilt), and second order (astigmatism and defocus), and can be corrected with spectacle lenses. Higher order aberrations consist of third order aberrations and above; these imperfections cannot be corrected with spectacle lenses.

The cornea, as the contributor of approximately two-thirds of the power of the relaxed eye, has great influence on ocular aberration. Trabeculectomy causes a change in corneal curvature, and has previously been observed to cause a change in corneal higher order aberrations, which return to pre-operation values 3 months after surgery (Fukuoka

et al. 2011). Corneal aberrations are estimated based on corneal elevation data, where the Zernike polynomial is fitted as close as possible to the measured height data. Given the possibility of misinterpreting normal variability in wavefront aberration measurements as true surgery-related changes, it was considered important to gain an understanding of normal measurement variability in otherwise healthy individuals.

Here, an exploratory study is described in which corneal wavefront aberrations are measured over multiple visits in a cohort of healthy participants, to gain an understanding of normal between-visit variability. The Optical Society of America (OSA) recommendations were followed throughout the study (Thibos *et al.* 2002).

2.4.2. Methods

In this experiment, corneal aberrations were measured in 4 healthy participants, on 5 visits, over a period of 3 weeks.

2.4.2.1. Participants

Four healthy participants (two aged 21 and two aged 22 years old) were recruited from students of Cardiff University. All participants underwent an ocular health investigation with slit lamp biomicroscopy and optical coherence tomography (OCT) with a Topcon 3D OCT 1000 (Topcon Corp., Tokyo, Japan). All participants had a best corrected visual acuity of at least -0.2 LogMAR and IOP < 21mmHg, as measured with a Topcon CT-80 non-contact tonometer (Topcon Corp., Tokyo, Japan). All participants had a normal visual field, as determined with Standard Automated Perimetry (SAP; 24-2 SITA-Standard, Humphrey Field Analyser, Carl Zeiss Meditec, Dublin, CA, USA). The right eye of each patient was tested.

2.4.2.2. Apparatus and Stimuli

An Oculus Pentacam (Oculus, Wetzlar, Germany) was used to obtain measurements of corneal wavefront aberrations. The instrument uses a 475nm UV-free LED and two cameras, and a method based on the Scheimpflug principle to capture the size and orientation of the pupil and capture images from the cornea. An attempt to calibrate the instrument with a steel ball of known radius was unsuccessful because, in order to take the measurement, the Pentacam relies on the backward light scattering properties of the front and back surface of the transparent cornea. The instrument was instead calibrated with a 3D-printed model eye.

2.4.2.3. Procedure

Three repeated measurements of corneal aberrations were acquired each visit. Each acquisition lasted approximately two seconds. On occasions when data were missing from the Pentacam report, (e.g. due to ptotic eyelids or long eyelashes), an attempt was made to hold the eyelid. Care was taken to ensure that the eyelids were held against the brow, avoiding any manual compression of the globe, or moving the eyelid to an abnormal position. Room lights were switched off during the measurement to ensure a reflection-free image. The automatic release mode was used, in order to reduce operator dependency for all tests, wherein the Pentacam automatically captured the scan when it decided that correct alignment with the corneal apex had been achieved.

2.4.2.4. Data analysis

Due to raw data export restrictions with the Pentacam, Zernike numbers had to be hand-typed from a screenshot of the report from each acquisition. Forty-five Zernike coefficients were obtained from each acquisition from the front surface of the cornea, and 45 from the back surface of the cornea. As three acquisitions were made per visit, the total number of Zernike coefficients obtained per participant, per visit, was 270. Therefore, 1,350 Zernike coefficients were recorded in total, across the 5 visits for each participant. As a quality control, Zernike coefficients were hand-typed three times, in order to check for transcription errors. To do this, every third Zernike number was transcribed again on two separate occasions. Coefficients, transcribed on the 2nd occasion were subtracted from their corresponding data, transcribed on the first occasion, to ensure that a value of zero was obtained (i.e. no transcription error). This was repeated for the 1st and 3rd data sets, and the 2nd and 3rd data sets. For each participant, on average 24 minutes were needed to type out the Zernike numbers per visit. As recommended by Atchison (2004), Zernike polynomials up to the 6th order

were included in the analysis so that the error of the fit that comes with a coefficient does not become as significant as the coefficient itself.

Data from all participants, at all five visits, were pooled by polynomial. The median coefficient was calculated for each front surface polynomial in each participant. These were plotted by polynomial number. Then, the median coefficient for all participants was calculated for each polynomial. The coefficient range (i.e. difference between the maximum and minimum measurement for each polynomial) was calculated per participant and plotted by polynomial. The mean coefficient range was then calculated for each polynomial and plotted together on the same graph. All analysis was then repeated for the back surface data.

2.4.3. Results

Front surface data

In the front surface data, the polynomial with the highest mean aberration coefficient is polynomial 0 (median = 0.13, Figure 2.11), followed by polynomial 4 (median = 0.08). The polynomial with the lowest median between-visit difference in coefficients was polynomial 20 (median = -9.45×10^{-5} , Figure 2.12). The polynomial with the highest mean coefficient range (i.e. mean(maximum – minimum) across all four participants) was polynomial 2 (0.0013; Figure 2.13), and that with the lowest variance was polynomial 23 (8.05×10^{-5}).

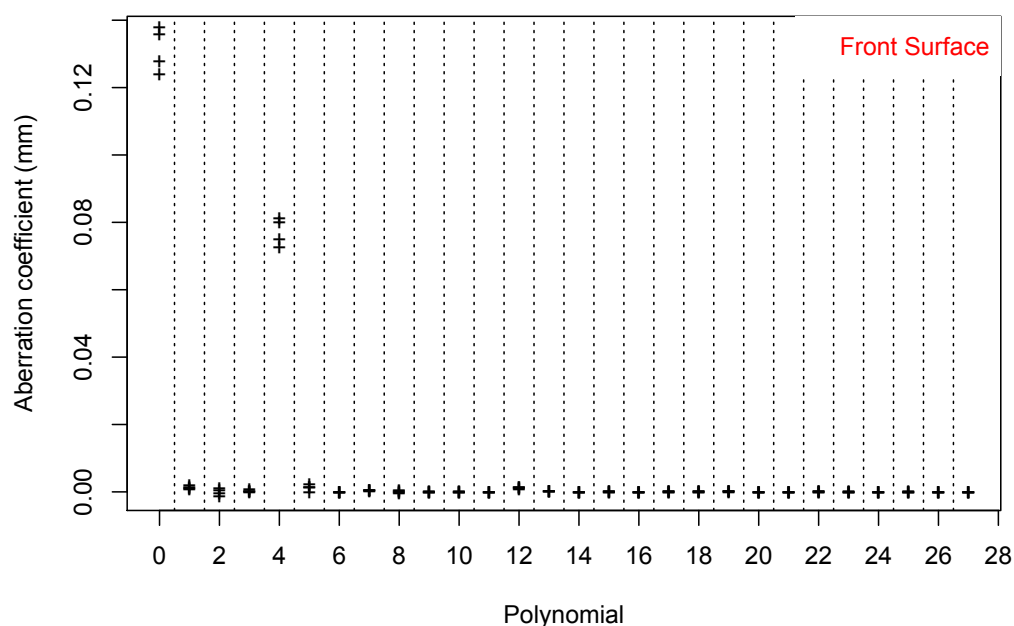


Figure 2.11. Aberration coefficients for polynomials 0 – 28 for all four participants (front surface).

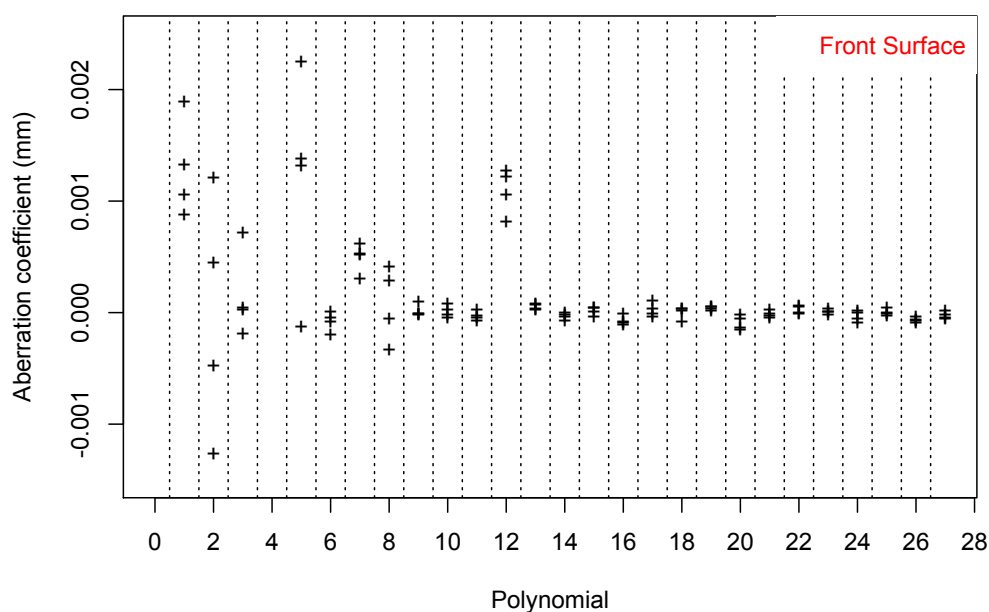


Figure 2.12. Aberration coefficients for polynomials 0 -28 for all participants. Data are the same as those in Figure 2.11 above, except that polynomials 0 and 4 are removed for ease of visualisation of the remaining data.

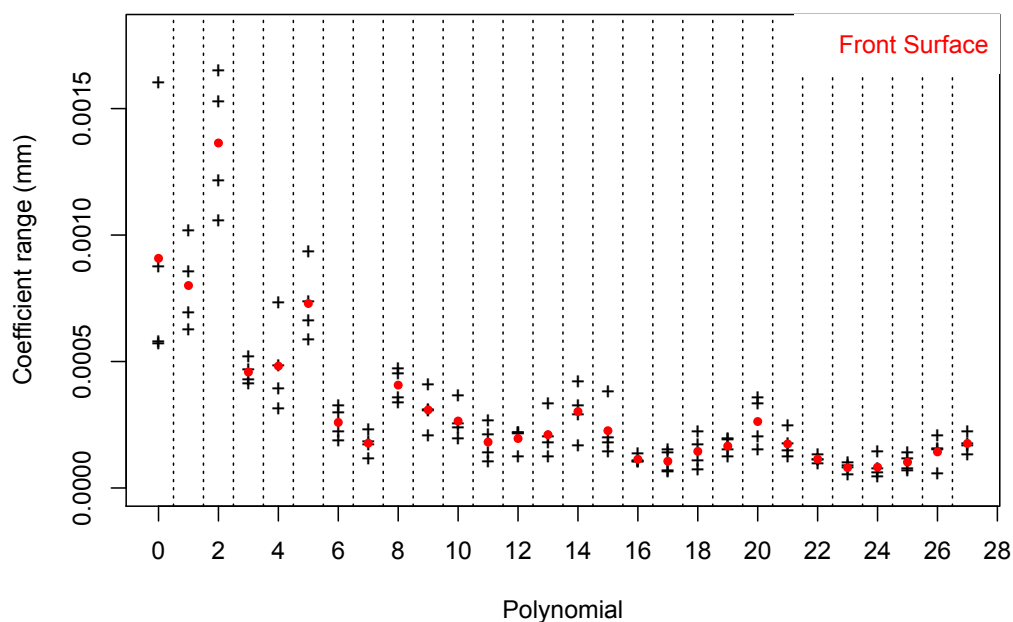


Figure 2.13. Coefficient range (maximum – minimum) for each front surface polynomial pooled across all participants (+ symbols). Mean coefficient range for each polynomial is denoted by the red symbols.

Back surface data

In the back surface data, the polynomial with the highest mean aberration coefficient is polynomial 0 (median = 0.17, Figure 2.14), followed by polynomial 1 (median = -0.003). The polynomial with the lowest median between-visit difference in coefficients was polynomial 1 (median = -0.003, Figure 2.15). The polynomial with the highest mean coefficient range (i.e. mean(maximum – minimum) across all four participants) was polynomial 0 (0.0003; Figure 2.16), and that with the lowest variance was polynomial 24 (0.00028).

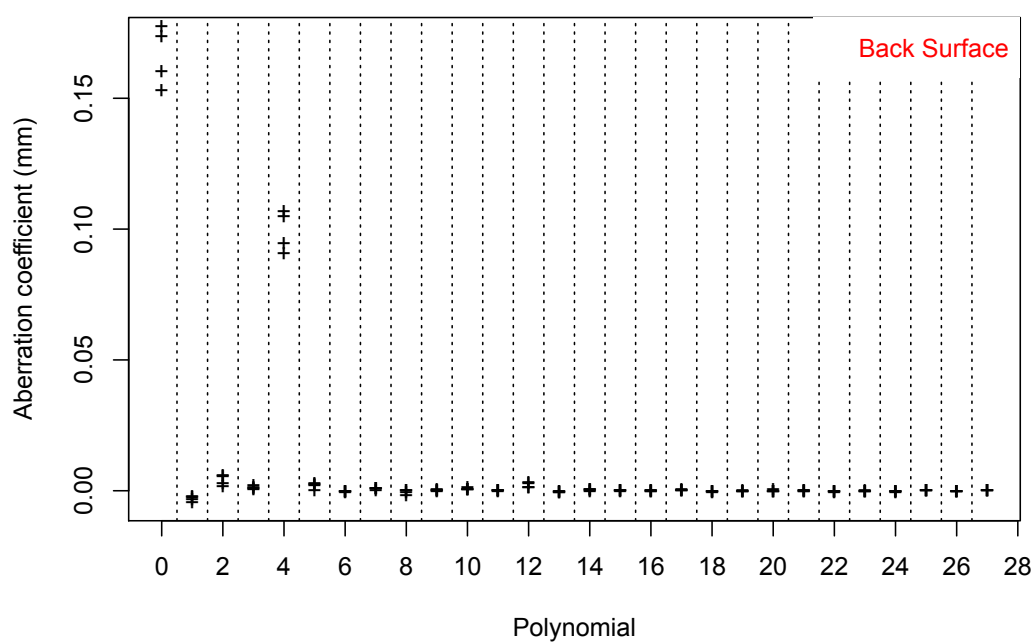


Figure 2.14. Aberration coefficients for polynomials 0 – 28 for all four participants (back surface).

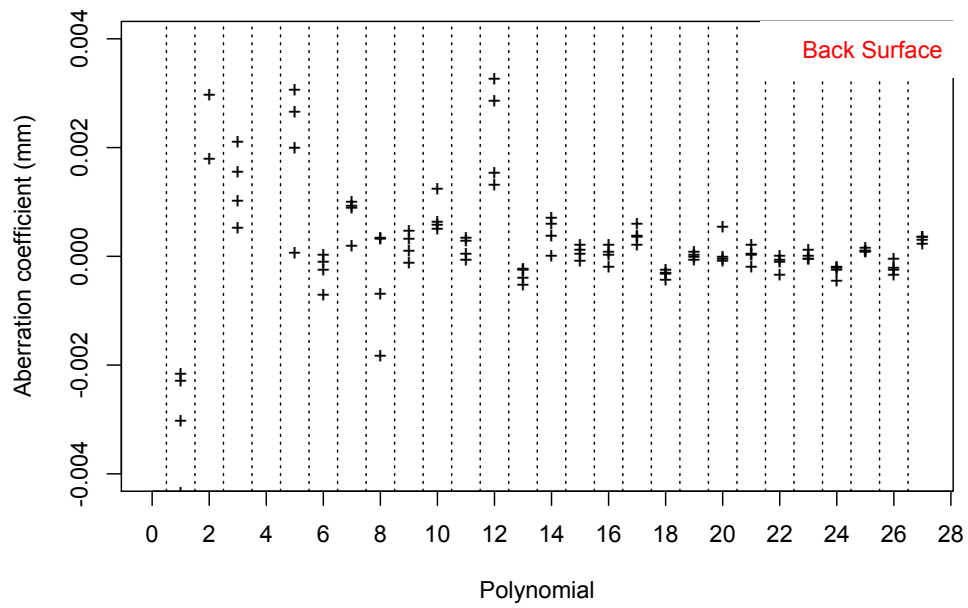


Figure 2.15. Aberration coefficients for polynomials 0 -28 for all participants (back surface). Data are the same as those in Figure 2.14 above, except that polynomials 0, 1, and 4 are removed for ease of visualisation of the remaining data.

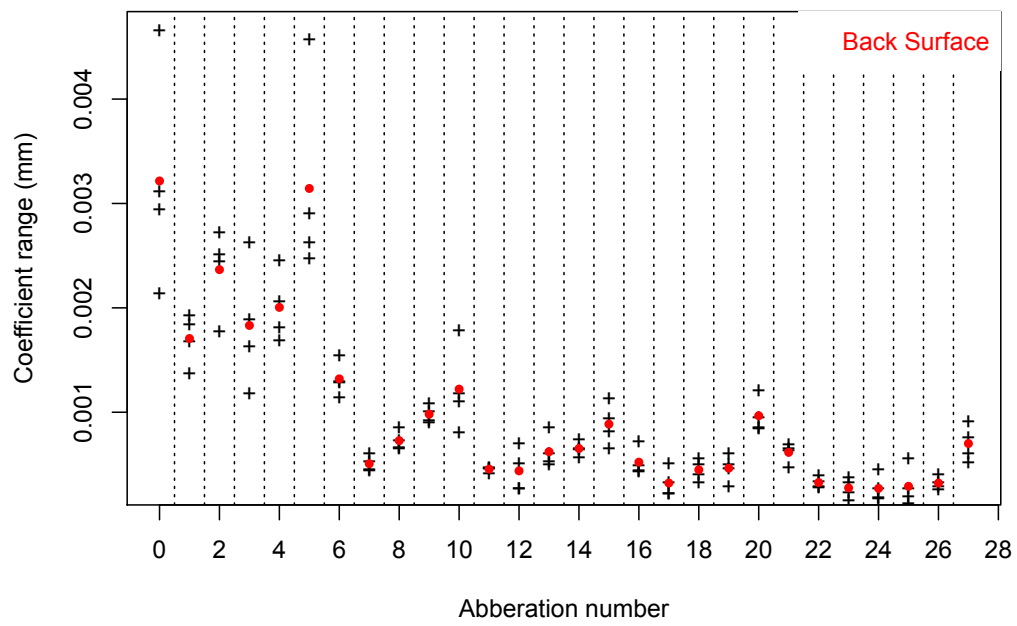


Figure 2.16. Coefficient range (maximum – minimum) for each back surface polynomial pooled across all participants (+ symbols). Mean coefficient range for each polynomial is denoted by the red symbols.

2.4.3. Discussion

This exploratory study enabled an understanding of normal between-visit and between-participant differences. It can be seen that the largest variation is found in lower order aberrations, with this variation becoming considerably less with increasing order.

It is difficult to comment, at this stage, on whether or not the variation observed is clinically meaningful, but these data serve to provide a context for any between-visit differences in polynomial coefficients observed in patients undergoing trabeculectomy in the study described in Chapter 4.

2.5. Effect of localised defocus on measurements of Ricco's area

Trabeculectomy surgery has been observed to cause a shallowing of the anterior chamber up to 5 years post-surgery (Husain *et al.* 2013; Man *et al.* 2015), shortening of axial length up to 5 years following surgery (Husain *et al.* 2013; Pakravan *et al.* 2015) and changes in corneal curvature in the form of flattening of anterior curvature, resulting in increase in with-the-rule astigmatism in some cohorts by up to 2.00D at 12 months post-surgery (Hong *et al.* 1998; Kook *et al.* 2001). The resultant dioptric blur could mask subtle changes in Ricco's area after trabeculectomy surgery and thus need to be investigated.

Low spatial frequency stimuli have been observed to be more robust to the effect of defocus, compared to high spatial frequency stimuli (Campbell & Green 1965). It is well documented that refractive error increased with visual field eccentricity, with the astigmatic component going up to 2.00D at 30° eccentricity (Calver *et al.* 2007; Millodot 1981; Rempt *et al.* 1971; Taberero & Schaeffel 2009). Anderson *et al.* (2001) reported that a higher detection threshold with small stimulus sizes at more peripheral locations and thus their finding is in agreement with the robust effect of bigger stimulus sizes. This suggests that with increased dioptric blur, small stimulus sizes lead to point spread function enlargement with increasing defocus, whilst at larger stimulus sizes the point spread function remained unaffected. Considering that the assessment of Ricco's area involved measurement of Goldmann I-V threshold, if the smaller stimulus size threshold is affected whilst the larger stimulus size is not, it is expected that the Ricco's

area estimate will be affected as well. Therefore qualification and quantification of the effect of dioptric blur on Ricco's area is needed.

The aim of this study is to investigate the effect of optical defocus on the measurement of Ricco's area at three different retinal eccentricities.

2.5.2. Methods

2.5.2.1. Subjects

Five healthy participants (mean age: 23, range 21 – 25 years) were recruited from students of Cardiff University. All participants underwent an ocular health investigation with slit lamp biomicroscopy and indirect ophthalmoscopy to ensure no retinal pathology or abnormalities were present. All participants had a best corrected visual acuity of -0.2 logMAR, IOP <21 mmHg (Topcon CT-80 non-contact tonometer) and demonstrated full visual fields with a Humphrey field analyser with SITA-Standard. Only right eyes of all participants were tested. All participants were recruited in accordance to Declaration of Helsinki.

2.5.2.2. Apparatus and stimulus

Goldmann I-V stimuli were presented on a white background (10 cd/m²) for 200 ms. Five different stimulus areas were used, GI-V (0.11° , 0.22° , 0.43° , 0.87° and 1.7°). The Octopus 900 perimeter (Haag Streit, Koeniz, Switzerland) controlled with OPI was used to present the stimuli at all measured visual field locations. Stimuli was presented on 6 visual field locations at eccentricities of 12.7° , 21.2° , and 29.7° (Figure 2.17). Three test stimuli were located at 12.7° , 21.2° , and 29.7° inferotemporally, with three control locations at the same eccentricities superonasally to aid central fixation. The inferotemporal test location was chosen to avoid possible influence of shadow cast by nose bridge and eyelid. A Keeler retinoscope was used to assess refractive error at central locations and three inferotemporal test locations (more details in section 2.5.2.3).

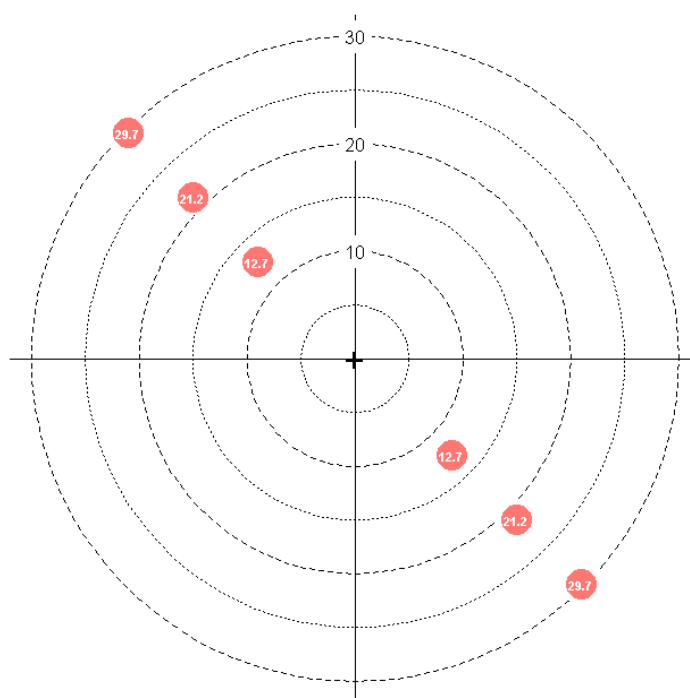


Figure 2.17. 6 test locations in visual field of right eye

2.5.2.3. Procedure

1. Ricco's area measurement

Sensitivity (in dB) was measured for each of the Goldmann sizes (I-V) at each visual field location in an interleaved manner. In each test, a different Goldmann size was used, chosen at random. A 4:1 staircase procedure was used, which was adapted from that produced by Andrew Turpin and Luke Chong (University of Melbourne, <http://people.eng.unimelb.edu.au/aturpin/opi/interface.html>, accessed on 15th March 2014). Step size was 4 dB before the first reversal and 1dB thereafter. A yes/no response criterion was used. At each location, the procedure was terminated after 8 reversals and the final threshold returned was an average of the last 4 reversals. The entire procedure was repeated twice more. So at each test location, 3 values for sensitivity were obtained for each Goldmann size. Therefore, a total of 15 sets of sensitivity measurements were obtained per location, and 45 measurements per participant. Thresholds for five Goldmann sizes were measured three times each, first

with central refractive correction in place and a +3.00D lens to control accommodation, then with addition of induced optical blur in the form of full aperture trial lenses of +1.00D and +2.00. Only plus lenses are used in this study, as the effect of refractive blur is the same for plus and minus lenses. Participants included in the study were young with healthy accommodation; adding a minus lens will prevent accurate assessment of an influence of refractive blur on Ricco's area estimates by triggering their accommodation. All procedures were carried out with natural pupil sizes. Fixation was monitored visually and participants' head position adjusted whenever needed.

Sensitivity values (dB) for Goldmann I-V were converted into increment threshold (ΔI) and plotted against area. Two-phase regression analysis was performed in the freely available open-source statistical environment, R (version 3.1.0) to obtain Ricco's area estimates at each location. The slope of the first line was constrained to a value of -1, following Ricco's law, whilst the intercept of the first line, slope of the second line and break point were allowed to vary. The breakpoint estimated was taken to be the Ricco's area estimate. Three Ricco's area estimates were obtained from each participant, one for each eccentricity inferotemporally. Superonasal location data was not analysed as only the spot of light used to maintain fixation was used here. The average test time including breaks for each participant was 4 hours 30 minutes.

2. *Peripheral refractive error*

For peripheral refractive error measurements, a central black fixation target and six peripheral targets corresponding to test locations (12.7°, 21.2°, and 29.7° at superonasal and inferotemporal visual field locations) were attached to a white wall. The required locations of the targets were calculated for a working distance of 3 metres:

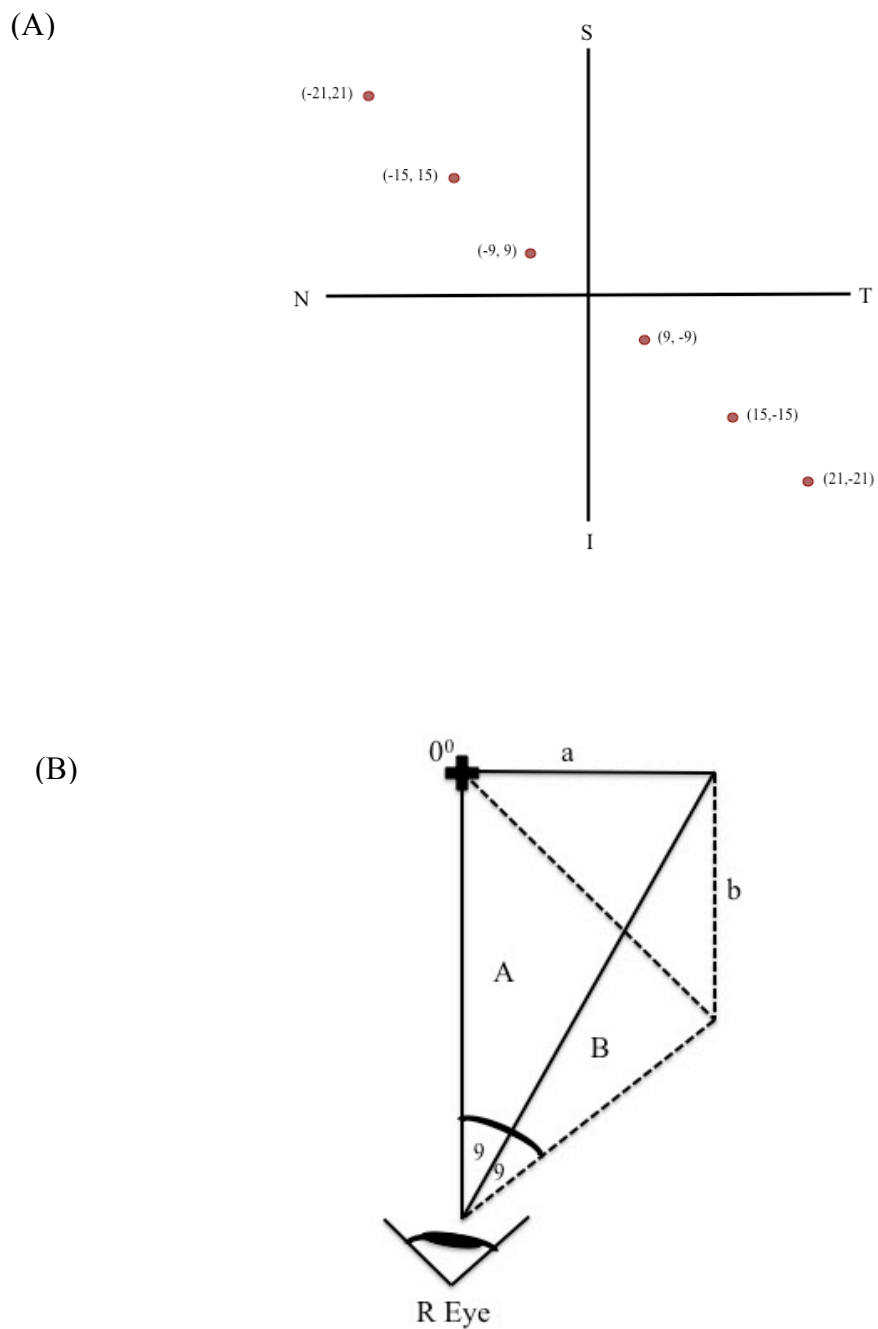


Figure 2.18. (A) X and Y coordinates of Octopus 900 testing locations; (B) schematic representations for target distance calculation.

Based on Figure 2.18 (B) the viewing angle for test location (9, -9) coordinate (Figure 2.18(A)) or 12.7° inferotemporally is 9° . In order to establish the peripheral target

distance, a and b in Figure 2.18(B) calculation with trigonometry was required. So for a working distance of 3m:

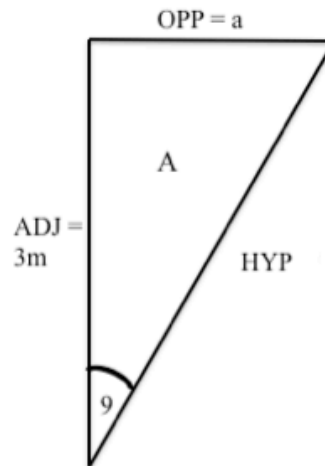


Figure 2.19. Right angle triangles for calculations of peripheral target distance.

$$\tan 9 = a/3; a=0.4752\text{m (47.5cm)}$$

The same method of calculation was applied to inferotemporal peripheral targets at 21.2° and 29.7° , with resultant target set up that was shown in Figure 2.19.

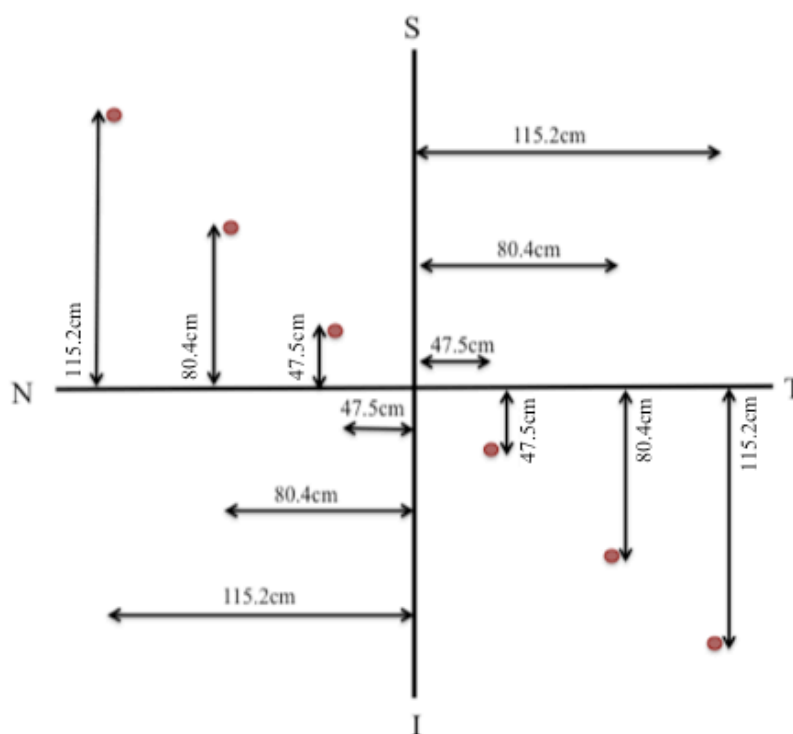


Figure 2.20. Target set up for peripheral refractive error measurement.

Participants were seated 3m away and instructed to look at a central fixation target for measurement of central refractive error. Retinoscopy was used with sphero-cylindrical lenses to estimate the amount of refractive error. All measurements were performed with the participants' head held straight in primary position (0°) and the investigator seated straight in line with the participant's visual axis. To get the peripheral refractive error at 12.7° inferotemporal visual field location, participants were instructed to look to the target located at 12.7° superonasal visual field location whilst the practitioner continued to be positioned on the former central axis.

Total defocus

Peripheral refractive error measurements were used to estimate the amount of total peripheral defocus. Estimates of peripheral ocular blur were obtained by subtracting the

central refractive error value from the peripheral refractive error value at each location. When a central refractive correction was worn the amount of ocular blur at the primary position was always zero. The amount of optical blur at the peripheral location was taken to be the difference between the peripheral refractive error, at that location, and the central refractive error. For example, if a participant had a central refractive error of -2.00 and peripheral refractive error of -2.50 , after the correction of central refractive error, the amount of ocular blur left at 12.7° eccentricity would be 0.50 D. The total amount of defocus induced was a combination of ocular blur at the test location and the induced optical blur (blur resulting from introduction of positive spherical lenses, Figure 2.21).

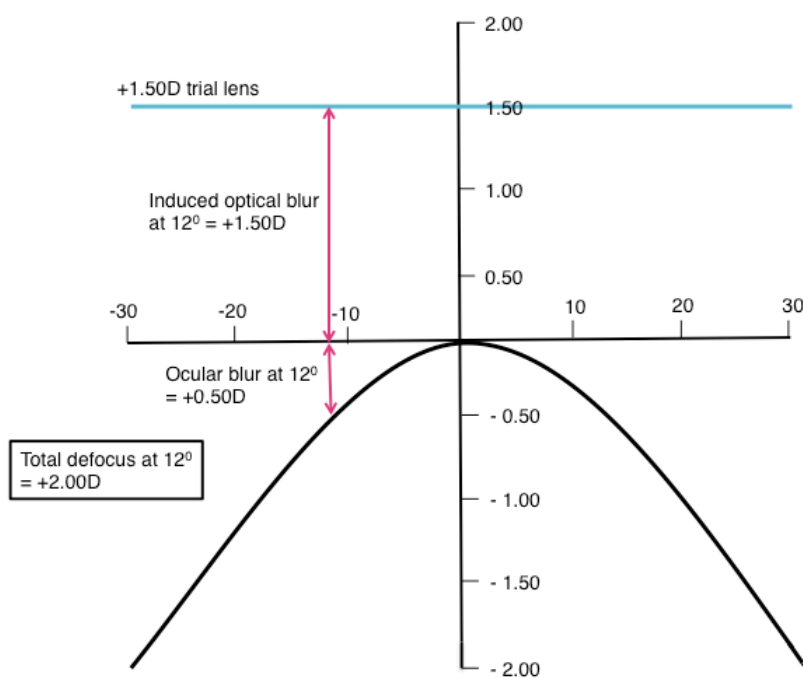


Figure 2.21. Illustration of estimation of total defocus (the sum of optical and ocular blur) at 12° eccentricity (adapted from Charman & Radhakrishnan (2010)).

Data of Ricco's area estimates was observed to be normal based on Kolmogorov-Smirnov test. Ricco's area estimates with added blur were separated into 3 groups with increasing amount of dioptric blur (0-1.00D, 1.10-2.00D and 2.10-3.00D). Data from each dioptric blur group was plotted against visual field eccentricity and repeated measures ANOVA performed to check whether there were significant differences of Ricco's area changes at different level of blur with increasing visual field eccentricity.

Another investigation involved looking at changes of dioptric blur at each measured eccentricity and performing repeated measured ANOVA comparing Ricco's area estimates at each measured eccentricity with increasing dioptric blur. A Holm-Bonferroni correction was used when the same hypothesis was tested multiple times, and only when $p \leq 0.05$ was achieved, to reduce the likelihood of a type I error.

2.5.3. Results

Forty-five spatial summation curves were generated in total. There was a general increase in astigmatism in 4 out of 5 participants. All but one participant exhibited peripheral myopic shift with increasing eccentricity (Table 2.5).

Table 2.5. Peripheral refractive errors in all participants

Eccentricity	P007		P008		P009		P010		P011	
	Sph	Cyl	Sph	Cyl	Sph	Cyl	Sph	Cyl	Sph	Cyl
0	+2.00	-1.50	-0.25	0.00	+0.75	0.00	+1.00	-0.50	+0.50	-0.25
12.7	+1.25	-0.75	-0.50	0.00	+0.75	0.00	+2.00	-0.25	+0.25	-0.25
21.2	+1.00	-0.25	-0.75	0.00	+0.50	-0.25	+2.50	-0.50	0.00	-0.50
29.7	+0.25	-0.25	-1.00	0.00	+0.50	-1.00	+3.00	-1.50	-0.50	0.00

Mean refractive errors of all participants, at different eccentricities is represented in Table 2.6.

Table 2.6. Values of the mean refractive errors at all test locations in all participants

Eccentricity	Peripheral refractive errors (D)
0	0.70/-0.05 x 90
12	0.75/-0.25 x 90
21	0.65/-0.30 x 90
29	0.45/-0.55 x 180

The averages of ocular blur after central correction at 12.7°, 21.2°, and 29.7° inferotemporally were 0.53D, 0.81D, 1.14D respectively. The maximum of total defocus at 12.7°, 21.2°, and 29.7° inferotemporally were 2.53D, 2.81D and 3.14D respectively.

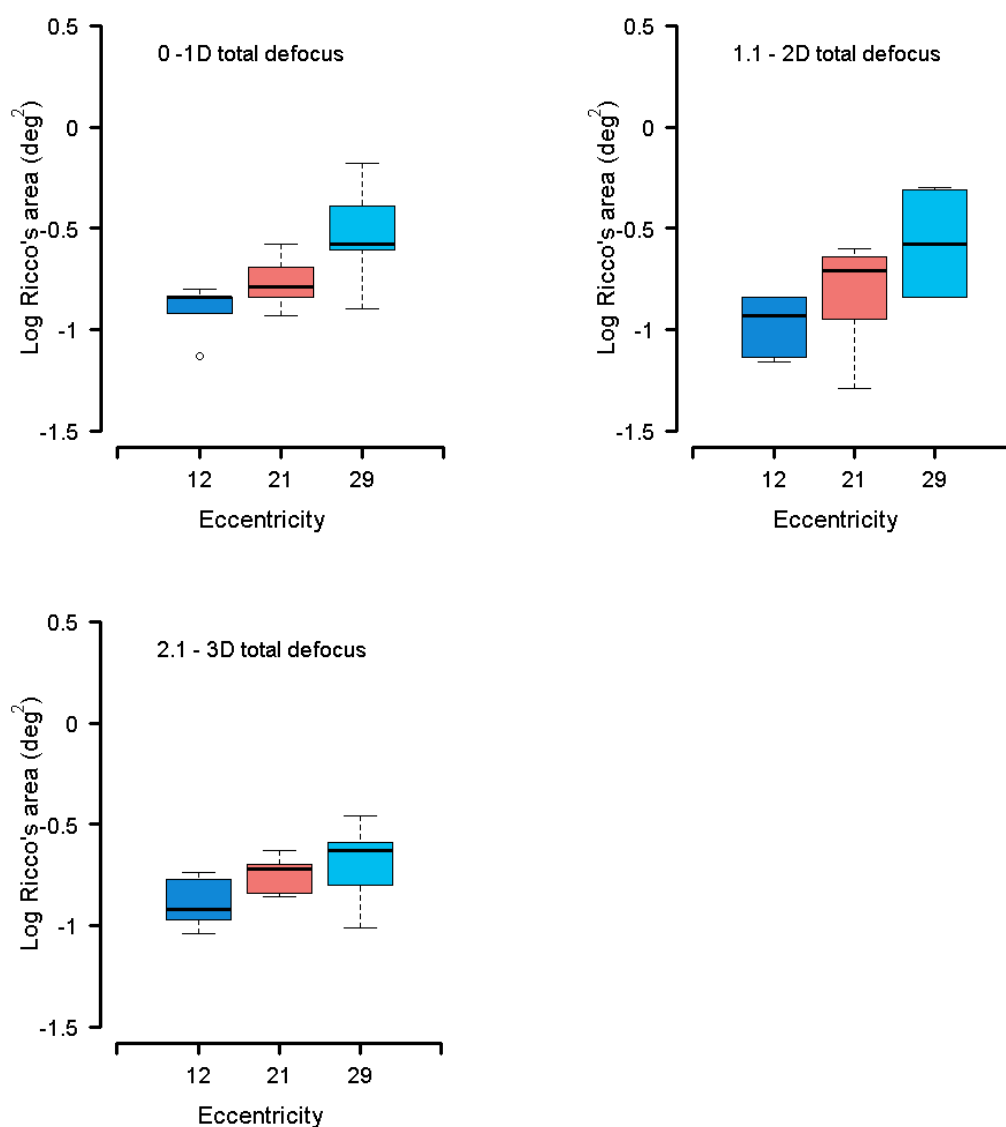


Figure 2.22. Ricco's area estimates obtained at three eccentricities under 3 different levels of optical blurs

There was a general trend towards enlargement of Ricco's area with eccentricity at all 3 levels of total defocus (Figure 2.22), however the magnitude of Ricco's area size change with eccentricity seemed to reduce with increasing amount of total defocus. The trend to enlargement with eccentricity did not reach statistical significance at any level of blur (repeated measures ANOVA, all $p > 0.12$).

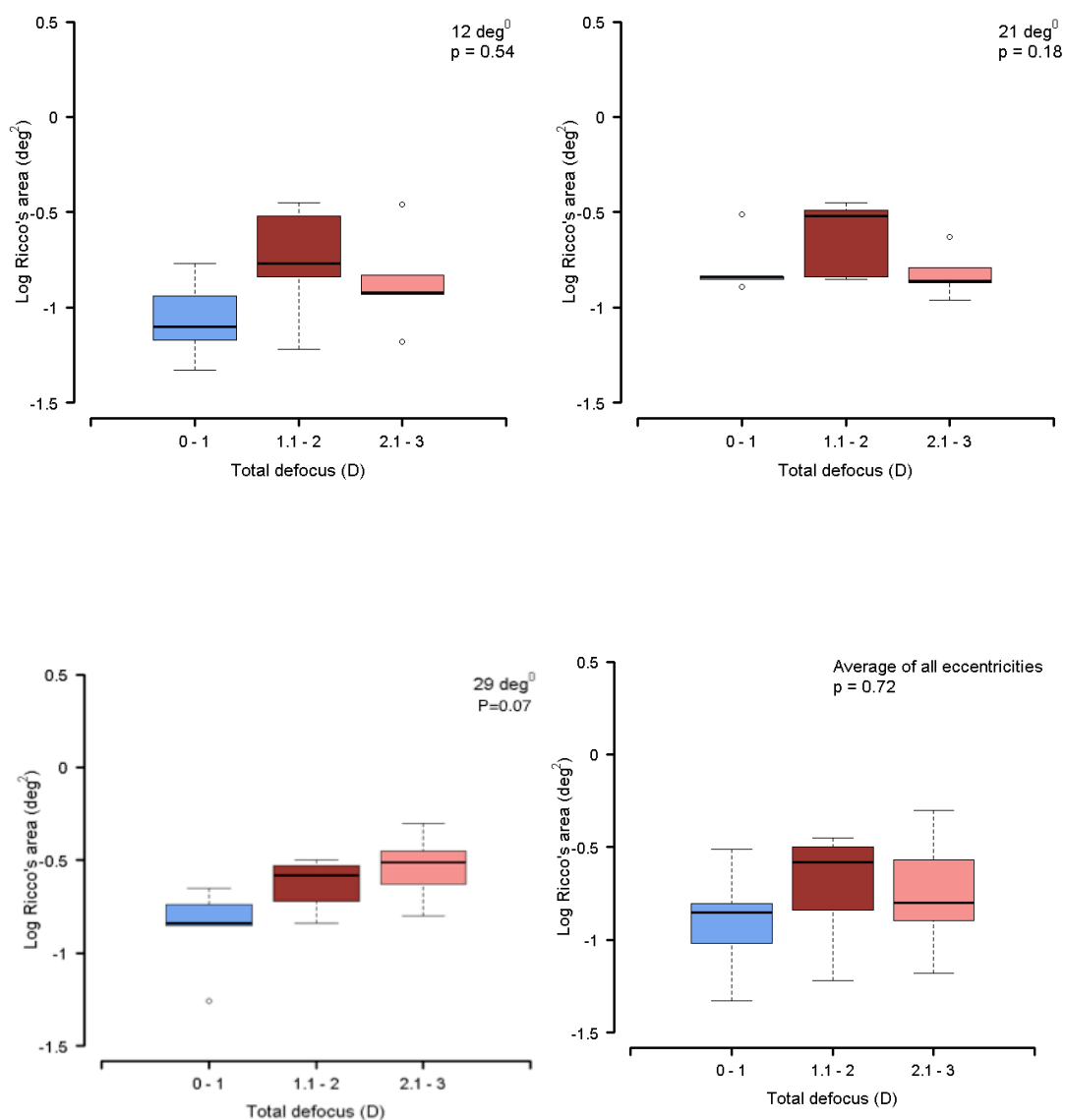


Figure 2.23. Ricco's area estimates at individual test eccentricities (12.7° , 21.2° and 29.7°) and averaged.

There was no clear pattern of change in Ricco's area size, nor was there a statistically significant change of Ricco's area size with increasing amount of optical blur at 12.7° ($p=0.54$), 21.2° ($p=0.18$), or 29.7° ($p=0.07$). When the data from all eccentricities were averaged, there was still no statistically significant change in Ricco's area size with increasing defocus ($p=0.72$).

There is a large difference between sensitivity measured in between total defocus of 0 and 3D of total defocus for Goldmann I of 4.43dB. The differences of sensitivities measured between total defocus of 0 to 3D lessen to 3.28dB for Goldmann III and 1.11dB for GV respectively.

2.5.4. Discussion

The peripheral myopic shift observed in four out of five emmetropic and myopic participants in this study is in agreement with the finding of Calver *et al.* (2007) and Gustafsson *et al.* (2001). Other studies observed hyperopic shift in myopes and myopic shift in hyperopes (Millodot 1981; Mutti *et al.* 2000).

In agreement with previous studies investigating peripheral refractive error changes with eccentricity, there is an increase in the astigmatic components of the refractive error. The increase in astigmatism with eccentricity is smaller than that found in other studies. Here we demonstrate an average increase of 0.50D compared to an average of 2.00D in Gustafsson *et al.* (2001), Millodot (1981), Rempt *et al.* (1971), and Seidemann *et al.* (2002). This could be attributed to the different measurement techniques, as other studies had used different methods, such as a double pass method and auto-refractor, as they were concerned that peripheral refractive error measurement with retinoscopy could be too variable and subjective. Retinoscopy was chosen as the measurement method for the study because the only available autorefractor was unable to measure peripheral refractive error and the person undertaking the retinoscopy was skilled in the technique. On the other hand, it is also clear from the literature that there is large inter-subject variability in patterns of peripheral refractive error changes (Millodot 1981; Rempt *et al.* 1971; Seidemann *et al.* 2002). This is a more likely reason for the discrepancy of current study astigmatism in the literature.

Although there is a general trend for enlargement, the increase in Ricco's area size with eccentricity under normal conditions in this study did not reach statistical significance. Comparing the extent of Ricco's area enlargement in the current study with the findings

of Khuu & Kalloniatis (2015), where they showed that the average enlargement of Ricco's area from 10° to 20° in 28 participants was 0.35 log unit in the temporal meridian, there were lesser changes of Ricco's area size with eccentricity in current study; here the change from 12.7-21.2° was 0.17 log unit. Ricco's area had also been shown to exhibit large inter-subject variability (Redmond *et al.* 2010a; Volbrecht *et al.* 2000) and therefore could have different level of change of Ricco's area with eccentricities even between normal subjects causing different of changes of Ricco's area estimates with eccentricity between results from Khuu & Kalloniatis (2015) with our study.

The lack of significant changes of Ricco's area size with increasing defocus up to 3.14D, was unexpected because of two factors. Firstly, the enlargement of point spread function (PSF) with defocus. Figure 2.24 shows the point-spread function of a projected stimulus without a blurring lens, on the left and with additional blur, on the right. When a blurring lens is added, the image of the stimulus on the retina will be larger than the image of a stimulus without a blurring lens. Ricco's area would be expected to be 'filled' sooner and as a consequence, Ricco's area should *appear* to reduce in size. This hypothesis was also proposed by Redmond *et al.* (2010b) who observed no change in Ricco's area with age. They hypothesized that changes in the crystalline lens with age causes an increase in PSF, which causes Ricco's area to be filled sooner. No effect on Ricco's area was observed in Redmond *et al.* (2010b) study and they further hypothesized that the increase in PSF was cancelled out by loss of RGC with age.

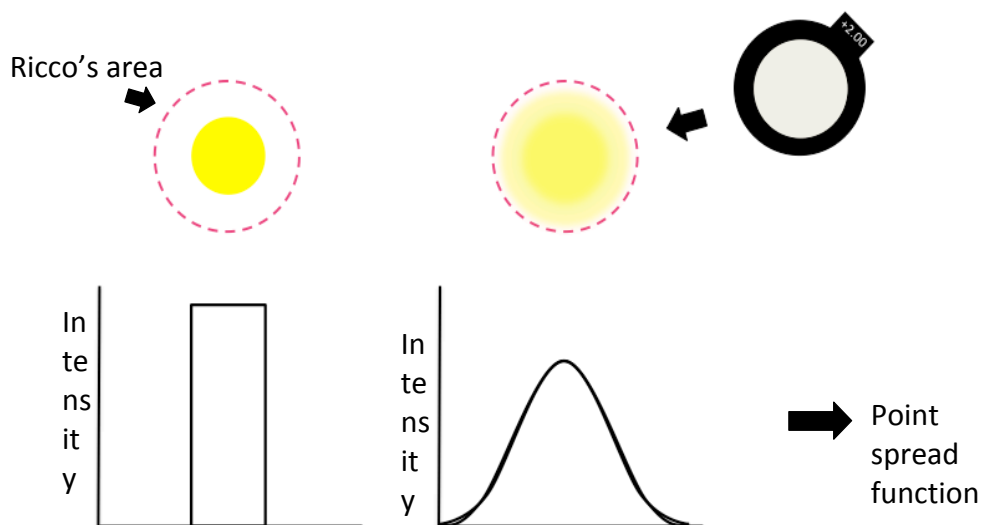


Figure 2.24. Top left image shows a projected stimulus without any optical filtering falling onto one Ricco's area, and its point-spread function is shown bottom left. Top right image is of a projected stimulus with added blurring lens, causing widening of its point spread function (bottom right).

This study observed no reduction in Ricco's area either. The lack of changes could be due to the conventional fitting method used to obtain Ricco's area estimates in both studies. Perhaps the greater effect to thresholds of small Goldmann sizes causes steepening of the left limb of the spatial summation functions. Two-phase regression analysis, that is used to obtain Ricco's area estimates in this study, constrained the slope of the first line to -1 would have the effect of dragging the inflection point from the true point to a larger value along the x axis, and thus causing an apparent enlargement in Ricco's area size, negating the smaller Ricco's area caused by an increase in defocus (Figure 2.25).

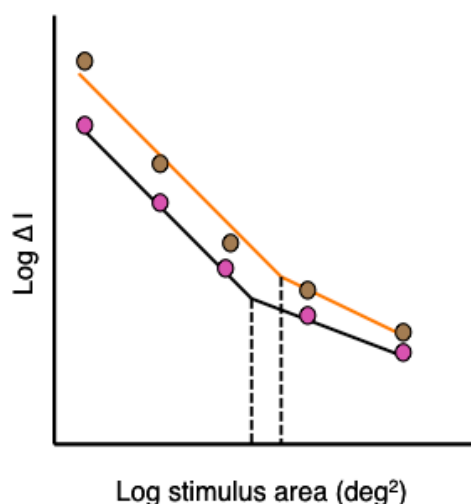


Figure 2.25. Two spatial summation curves. Pink dots are the thresholds for Goldmann I-V without any blurring lens, whilst brown dots are thresholds after addition of blurring lens.

According to the hypothesis above, the effect of optical blur on threshold data for a Goldmann I should be greater than that for a Goldmann III, which in turn should be greater than that for the Goldmann V. This is supported by the data here where the difference in sensitivity for Goldmann I, III and V is 4.43dB, 3.28dB and 1.11dB respectively when 3D of optical blur is added.

It should be noted that this study by no means supports the idea of no changes in Ricco's area with defocus, as it is clear from published literature that optical factors influence the measurement of Ricco's area (Dalimier & Dainty 2010; Davila & Geisler 1991). Nevertheless, the absence of obvious changes in Ricco's area observed in this study is in support of the notion that the effect of small refractive changes (at least up to 3.14D) on Ricco's area, and induced astigmatism with trabeculectomy, will likely not be a major cofounder in the determination changes in Ricco's area, owing to neural change following trabeculectomy surgery. Considering that changes of refractive error

up to 6 months after trabeculectomy surgery was reported to be a maximum of 3.00D, the measurement obtained for Chapter 4 is unlikely to be influenced by optical blur.

Chapter 3: On the Physiological Basis for Ricco's Area: A Study of Amblyopia

3.1. Introduction

For a visual stimulus to be detected, the strength of the stimulus signal must overcome intrinsic noise that is inherent in the visual pathway. Pooling of signals over space (spatial summation), increases detectability, but at the expense of reduced visual resolution. Ricco's law of spatial summation (Ricco 1877) states that for a range (Piper 1903) of small stimulus areas, stimulus area and intensity are inversely proportional at threshold ($A \times I = k$), i.e. spatial summation is complete. However, Ricco's law applies only within a critical area, known as Ricco's area. Beyond Ricco's area, spatial summation is incomplete and, depending on the precise conditions under which it is measured, threshold is governed by laws of incomplete summation, such as Piper's law (Piper 1903), or Pieron's law (Kleitman & H 1929)

The physiological basis for Ricco's area is not entirely understood. The traditional explanation has been that it is the psychophysical correlate of the area of the RGCs receptive field centre (Glezer 1965; Lie 1980). Initially, this may seem reasonable, given that it has been found to vary with retinal eccentricity (Vassilev *et al.* 2003; Wilson 1970) and background adaptation level (Glezer 1965; Lelkens & Zuidema 1983) in healthy observers. However, despite the close association between Ricco's area and RGC size (Vassilev *et al.* 2005) as well as eccentricity-related changes in RGC density (Volbrecht *et al.* 2000), it was demonstrated by Pan & Swanson that spatial summation

of circular incremental stimuli, as used in clinical visual field testing, cannot be accounted for by probability summation across retinal ganglion cells, but rather spatial pooling by multiple cortical mechanisms (Pan & Swanson 2006). Further support for the physiological basis of Ricco's area lying at a cortical level comes from Redmond *et al.*, who found changes in Ricco's area in the S-cone pathway, as a function of the blue background adaptation level (Redmond *et al.* 2013b). The traditional explanation of changes in Ricco's area with background luminance, that it is a manifestation of increased spatial antagonism in RGC receptive fields (Glezer 1965), cannot account for these changes, as centre-surround spatial antagonism is not found in receptive fields of the small bistratified cells that mediate the S-cone signal response. Rather, the blue/yellow ON and OFF receptive field regions are spatially coextensive (Dacey & Lee 1994). Receptive fields of the arrangement S+/S- are required to observe such changes, and these are not found at the level of the retina. Ricco's area was also found to be larger in patients with glaucoma, a disease characterized by the death of RGCs, with respect to age-similar healthy controls. Following reports that RGCs may shrink in early glaucoma (Morgan 2002; Morgan *et al.* 2006), it is difficult to reconcile these changes in structure and function using the traditional explanation of Ricco's area as a retinal phenomenon. However, if cortical pooling contributes a sizeable component to Ricco's area, it may partly explain this difficulty.

Given the observation of an enlarged Ricco's area in glaucoma, that can account for disproportionate deficits in contrast sensitivity to perimetric stimuli of different area, it is of great importance to better understand the underlying mechanisms responsible for Ricco's area and anomalies thereof, not just for an improved understanding of a fundamental attribute of visual processing, but also for a more scientifically sound design of diagnostic functional tests of the visual field that can be used clinically. To

achieve a better understanding of the role of spatial summation in glaucoma and more broadly in reconciling visual function with retinal structure, one must also investigate the possible role of non-retinal sites, and therefore must look to a neurological condition affecting vision that is not characterised by anomalies at the retinal level. One such condition is amblyopia, a developmental disorder in which there is a reduction of vision in one eye, or more infrequently, both eyes, even with optimum optical correction and in the absence of detectable ocular abnormality.

Approximately 3.6% of the UK population has amblyopia (Williams *et al.* 2008). Histological studies of experimentally induced amblyopia have suggested that the primary site of neural deficit in amblyopia is V1 (Hendrickson *et al.* 1987; Kiorpes *et al.* 1998). RGCs have been observed to be anatomically and functionally normal in experimental models of amblyopia (Kratz *et al.* 1979; Sherman & Stone 1973; Spear & Hou 1990). LGN cells have been observed to change in size, their spatial resolution has been found to be unaffected (Derrington & Hawken 1981; Jones, Kalil & Spear 1984; Movshon *et al.* 1987; von Noorden 1970), suggesting the possibility of subtle binocular interactions. Amblyopia is therefore a suitable eye condition to investigate post-retinal involvement in the formation of Ricco's area. Previous studies of spatial summation in amblyopia reported an accelerated rise in sensitivity with greater of stimulus width in amblyopic eyes, reaching maximum sensitivity at much greater stimulus widths than in non-amblyopic eyes (Hagemans & van der Wildt 1979; Katz, Levi & Bedell. 1984); a finding that is suggestive of an enlargement of Ricco's area in amblyopia.

The aim of this study was to form a better understanding of the physiological basis of Ricco's area, by investigating differences in spatial summation of perimetric stimuli between amblyopic observers and normally-sighted controls with binocular vision.

Amblyopia is an eye condition that has been widely documented to be of cortical origin with no retinal and LGN involvement. Investigating spatial summation in amblyopia and comparing it to normally-sighted controls with binocular vision can help ascertain the cortical involvement in formation of Ricco's area.

3.2. Methods

Spatial summation functions were measured in both eyes of adults with strabismic or anisometric amblyopia, as well as normally-sighted controls with binocular single vision. Ricco's area was estimated at each test location and analysed as a function of visual field eccentricity.

3.2.1. Participants

Fourteen adults (median [IQR] age: 20.5 [19.25, 22.00] years) with amblyopia and 15 normally-sighted participants with normal binocular vision (median [IQR] age: 24 [22, 25] years) were recruited from staff and students of Cardiff University, as well as a participant database at the Cardiff University Eye Clinic. All participants underwent an ophthalmic and orthoptic assessment, including a visual acuity test (Bailey-Lovie chart, logMAR notation), optical coherence tomography (Topcon 3D OCT 1000, Topcon Corp, Tokyo, Japan), and slit-lamp biomicroscopy with anterior eye assessment, to screen for any other ocular or visual abnormalities that may affect visual performance. Binocular status was confirmed using tests for simultaneous perception (Bagolini lenses), suppression (Worth's 4 dot test), stereopsis (TNO, Oculus, Wetzlar, Germany), eccentric fixation (ophthalmoscope grid), and the prism cover test. Binocular vision was confirmed if the participant demonstrated simultaneous perception, no suppression, and measurable stereopsis. Participants were included in the amblyopic group if they had an inter-ocular difference in visual acuity of ≥ 0.2 logMAR (\geq two lines on the Bailey-Lovie chart). Anisometric amblyopia was classified on the basis of an inter-ocular difference in refractive error of ≥ 1.00 DS, or a history of anisometropia in the absence of strabismus or strabismus surgery. Strabismic amblyopia was classified on the basis of

a manifest strabismus, history of childhood strabismus, or previous strabismus surgery. Patients' current distance refractive error was recorded or, if his/her refractive correction had been >2 years old, a refraction was undertaken as part of the research visit. Refractive correction, appropriate for the test distance of 33cm, was worn during experiments. Appropriate refractive correction was also used for the relevant orthoptic assessments. Both eyes were included in the study.

3.2.2. Apparatus and stimuli

Experiments were conducted on an Octopus 900 perimeter (Haag Streit Ltd, Koeniz, Switzerland), driven by the Open Perimetry Interface. Stimuli were achromatic circular increments of different area (Goldmann I – V; 0.01, 0.04, 0.15, 0.58, and 2.27 deg²), modulating in contrast on an achromatic background of 10cd/m². Presentation duration was 200ms, with a square temporal profile. Stimuli were presented to 12 visual field locations (4 locations at each of 12.7°, 21.2°, and 29.7° eccentricity, Figure 3.1).

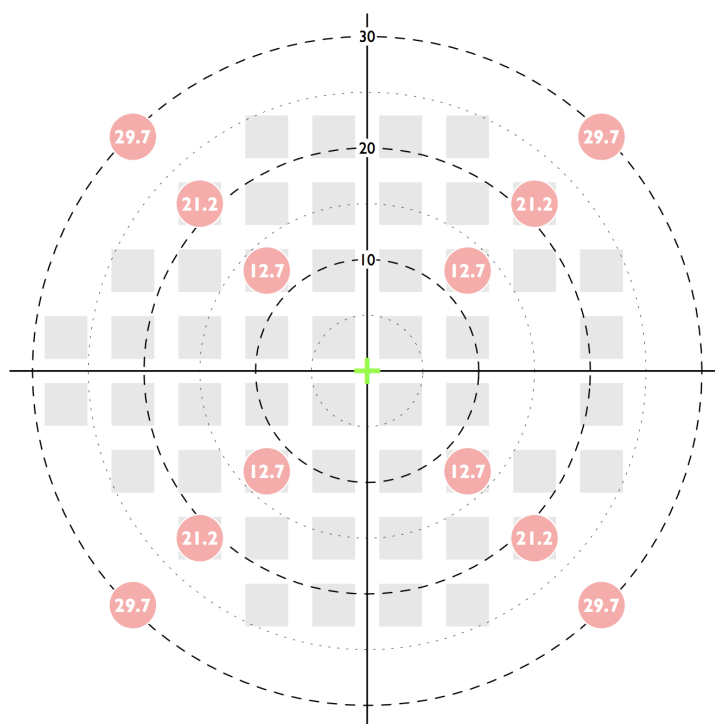


Figure 3.1. Visual field locations tested in the current study. A conventional 24-2 visual field pattern (right visual field), used in clinical visual field tests, is displayed for clinical reference

3.2.3. Procedure

Thresholds were measured at each visual field location with one of the five Goldmann stimuli at twelve visual field locations in an interleaved fashion. This was then repeated with the other four Goldmann stimuli, in a randomised order. Thresholds were measured a second time for each of the five Goldmann sizes, in a randomised order, and averaged with the first set of measurements by stimulus size and location. Experiments were carried out on both eyes separately, with the order in which eyes were tested randomised between subjects. In all experiments, a 1:1 staircase and yes/no response

criterion were used to determine threshold. Fixation was monitored visually, on the Octopus 900 fixation monitor.

3.2.4. Statistical analysis

Thresholds were averaged by eccentricity in each eye, giving one spatial summation function for each of the three visual field eccentricities. In order to estimate Ricco's area at each eccentricity, an iterative two-phase regression analysis was performed on the eccentricity-averaged data. The fitting procedure is described in depth in our previous work; briefly, a two-phase regression function was fitted to the threshold data for the five stimulus areas, constraining the slope of the first line to -1 (respecting Ricco's law), and allowing the intercept of the first line, the slope of the second line, and the breakpoint value to vary. The breakpoint, estimated by the model, was taken to represent Ricco's area. Each eye had three Ricco's area estimates, one for each eccentricity.

In the amblyopic participants, Ricco's area estimates were compared between amblyopic and non-amblyopic eyes at each eccentricity. Similarly, Ricco's area estimates were compared between the right and left eyes of normal participants. Inter-ocular differences were tested for at each eccentricity with a paired t-test. A Holm-Bonferroni correction was applied to p-values obtained for each of the three eccentricities.

To investigate the effect of a) type of amblyopia, b) binocularity, and c) inter-ocular difference in central visual acuity on the difference in Ricco's area between amblyopic and fellow non-amblyopic eyes, linear mixed effects model analysis was performed, with the inter-ocular difference in Ricco's area as the dependent variable, and type of

amblyopia, binocularity, and inter-ocular difference in VA as fixed effects. Subject and eccentricity were included as random effects, with random intercepts added to the by-subject and by-eccentricity effects. For this analysis, data from each eccentricity and from each subject were pooled into a single dataset. The magnitude of each of the effects was determined from the analysis. A likelihood ratio test of the model (including all effects), and the same model with the effect in question removed, was performed in order to determine the statistical significance of that effect.

Statistical analysis was performed with the open source statistical environment R and the lme4 package where applicable.

The datasets generated and analysed during the current study are available from the corresponding author on reasonable request.

Ethical approval was granted by the Wales Research Ethics Committee 1. Informed consent was obtained before participants were included. The research was conducted in accordance with the tenets of the Declaration of Helsinki.

3.3. Results

Table 3.1. Clinical characteristics of amblyopic participants in the current study

Subjects	Refractive error	Acuity (LogMAR)	Stereoacuity	History
RB (18) Strab	R +4.50/ -1.50 x 50 R +4.50/ -1.50 x 15	-0.1 -0.3	Absent	RE 2pd Esotropia; 3pd Hypertropia Patched and glasses @3, No surgery
TN (23) Strab	R -4.25/ -0.75 x 100 L -3.75/ -0.50 x 82	-0.08 0.32	Absent	LE 8pd Esotropia Patched and glasses @ 5, No surgery
IH (19) Strab	R +1.00/ -0.50 x 100 L +1.50/ -0.50 x 65	-0.1 0.12	200 seconds	LE Esotropia noticed at age 5 Patched and glasses @ 5, Surgery @ 5
AG (21) Strab	R +7.25 L +6.75/ -0.25 x 170	0.36 -0.16	Absent	RE 6pd Esotropia Patched and glasses @2
RT (27) Strab	R +1.25/ -1.50 x 155 L +1.25/ -0.75 x 55	-0.1 0.2	Absent	LE 6pd Esotropia Patched and glasses @ 2
AR (22) Strab	R +1.25/ -0.50 x 90 L +1.00/ -0.25 x 130	0.16 -0.22	400 Seconds	Microtropia Not patched, No surgery
BE (22) Strab	R +0.75/ -0.50 x 180 L +1.00/ -0.75 x 173	0.3 -0.12	400 Seconds	LE 16pd Hypotropia Not patched, No surgery
EE (35) Aniso	R +6.00/ -1.50 x 180 L +0.50	0.86 -0.26	Absent	Patched and glasses @7 No surgery
SJ (21) Aniso	R +5.00/ -0.50 x 30 L +0.75/ -0.25 x 120	0.2 -0.2	Absent	Patched and glasses @4
KF (20) Aniso	R +2.25/ -2.75 x 3 L -5.00/ -3.75 x 171	-0.14 0.36	400 Seconds	Patched and glasses @3 No Surgery
DE (20) Aniso	R+2.50/ -0.25 x 180 L Plano	0.62 -0.1	Absent	Patched and glasses @6 No surgery
KO (18) Aniso	R +3.50/ -1.50 x 180 L +1.25/ -0.25 x 180	0.1 -0.1	240 seconds	Patched and glasses @6 No surgery
JS (20) Aniso	R +1.50/ -4.50 x 28 L -0.75/ -1.25 x 142	-0.1 0.16	200 seconds	Optical penalization @4 No surgery
FK (19) Aniso	R +0.50/ -0.25 x 90 L +2.75/ -0.25 x 10	-0.2 0	400 seconds	Not patched, glasses @8 No surgery

Table 3.2. Clinical characteristics of control participants in the current study.

Subjects	Refractive error	Acuity (LogMAR)	Stereoacuity	History
SR (29) Control	R plano L plano	-0.1 -0.1	40 seconds	No binocular vision anomalies
SJ (25) Control	R -5.50 L -4.50	-0.2 -0.2	40 seconds	No binocular vision anomalies
LT (24) Control	R -2.50/ -1.00 x 175 L -3.00/-0.75 x 180	-0.2 -0.2	40 seconds	No binocular vision anomalies
TR (32) Control	R -1.50/ -2.50 x 82 L -2.50/ -2.00 x 81	-0.1 -0.1	40 seconds	No binocular vision anomalies
VS (21) Control	R -5.00/ -0.50 x 120 L -5.00/ -0.25 x 45	-0.2 -0.2	40 seconds	No binocular vision anomalies
SL (25) Control	R plano L plano	-0.2 -0.2	40 seconds	No binocular vision anomalies
KB (25) Control	R Plano L Plano	-0.1 -0.1	40 seconds	No binocular vision anomalies
AN (48) Control	R plano L plano	-0.2 -0.2	40 seconds	No binocular vision anomalies
KB (24) Control	R +0.50 L +0.50	-0.2 -0.2	40 seconds	No binocular vision anomalies
SM (22) Control	R +0.50/ -0.25 x 160 L +0.50/ -0.25 x 180	-0.22 -0.22	60 seconds	No binocular vision anomalies
KB (23) Control	R -0.75/ -0.25 x 180 L -0.50/ -0.25 x 180	-0.16 -0.22	40 seconds	No binocular vision anomalies
JR (25) Control	R -0.25 L Plano	-0.3 -0.3	40 seconds	No binocular vision anomalies
HJ (22) Control	R -0.25/ -0.75 x 80 L -0.25/ -0.50 x 55	-0.2 -0.2	40 seconds	No binocular vision anomalies
KE (19) Control	R +0.25/ -0.25 x 180 L +0.25/ -0.25 x 180	-0.24 -0.28	40 seconds	No binocular vision anomalies
ZD (21) Control	R +0.25 L Plano	-0.24 -0.22	40 seconds	No binocular vision anomalies

Clinical characteristics of amblyopic and control participants are outlined in Tables 3.1 and 3.2 respectively. Seven of the amblyopic participants had strabismic amblyopia (of which three had binocular vision), while the remaining seven had anisometropic amblyopia (of which four had binocular vision). Visual acuity was, on average, 0.42 logMAR (approx. 4 lines), lower in the amblyopic eye than in the fellow non-amblyopic eye (paired t-test, $p < 0.001$). Acuity in the non-amblyopic eye was, on average, 0.04 (2 letters) better than the average visual acuity for the right and left eyes in the control cohort, but this was not statistically significant (Student's t-test, $p = 0.12$).

A total of 174 spatial summation functions (3 eccentricities in 58 eyes) were determined across both groups and included in the analysis. Figure 3.2 shows average Ricco's area as a function of visual field eccentricity for amblyopic eyes, non-amblyopic eyes of the same participants, as well as left and right eyes of control participants. Ricco's area is shown to be larger at more peripheral test locations, as reported in previous literature (Vassilev *et al.* 2003; Volbrecht *et al.* 2000; Wilson 1970).

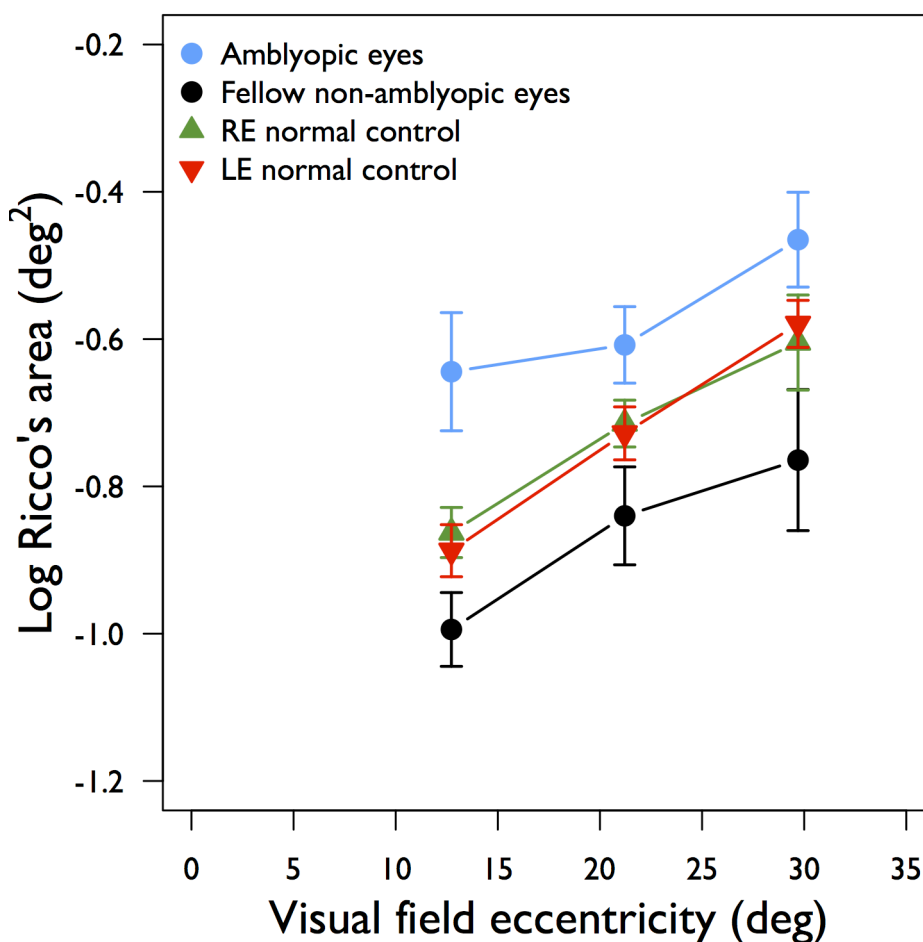


Figure 3.2. Ricco's area as a function of visual field eccentricity in amblyopic and fellow non-amblyopic eyes (blue, black discs respectively), as well as the left and right eye of a normal control cohort (red, green triangles respectively). Error bars: SEM

At all eccentricities, mean Ricco's area was larger in amblyopic eyes, compared with that in fellow non-amblyopic eyes (all $p < 0.01$). Inter-ocular differences in Ricco's area in the normal control group were negligible (Figure 3.2), and thus values for the right and left eyes were averaged at each eccentricity for further analysis. Compared to the average normal at each eccentricity, mean Ricco's area was larger in amblyopic eyes, and smaller in fellow non-amblyopic eyes (Figure 3.2 and Table 3.3).

*Table 3.3. Difference in mean Ricco's area between amblyopic participants and normal controls (normal Ricco's area averaged by eye). *Statistically significant at 0.05 level*

(Student's t-test, Holm-Bonferroni-corrected p-values)

<i>Eccentricity (deg)</i>	<i>Amblyopic eyes (deg²)</i>	<i>p-value (Student's t-test)</i>	<i>Fellow non-amblyopic eyes (deg²)</i>	<i>p-value (Student's t-test)</i>
<i>12.7</i>	<i>0.35</i>	<i>0.047*</i>	<i>-0.12</i>	<i>0.166</i>
<i>21.2</i>	<i>0.11</i>	<i>0.125</i>	<i>-0.13</i>	<i>0.255</i>
<i>29.7</i>	<i>0.13</i>	<i>0.125</i>	<i>-0.18</i>	<i>0.255</i>

The difference in mean Ricco's area between amblyopic eyes and those of normal controls was statistically significant at 12.7° eccentricity ($p = 0.047$, following a Holm-Bonferroni correction). In subsequent analyses involving linear mixed effects models, inspection of the residuals confirmed normality and no heteroscedasticity.

Binocular vs non-binocular vision in amblyopes

Data were separated according to binocular and non-binocular vision status.

Distributions of Ricco's area values for the amblyopic and non-amblyopic eyes of each group can be seen in Figure 3.3.

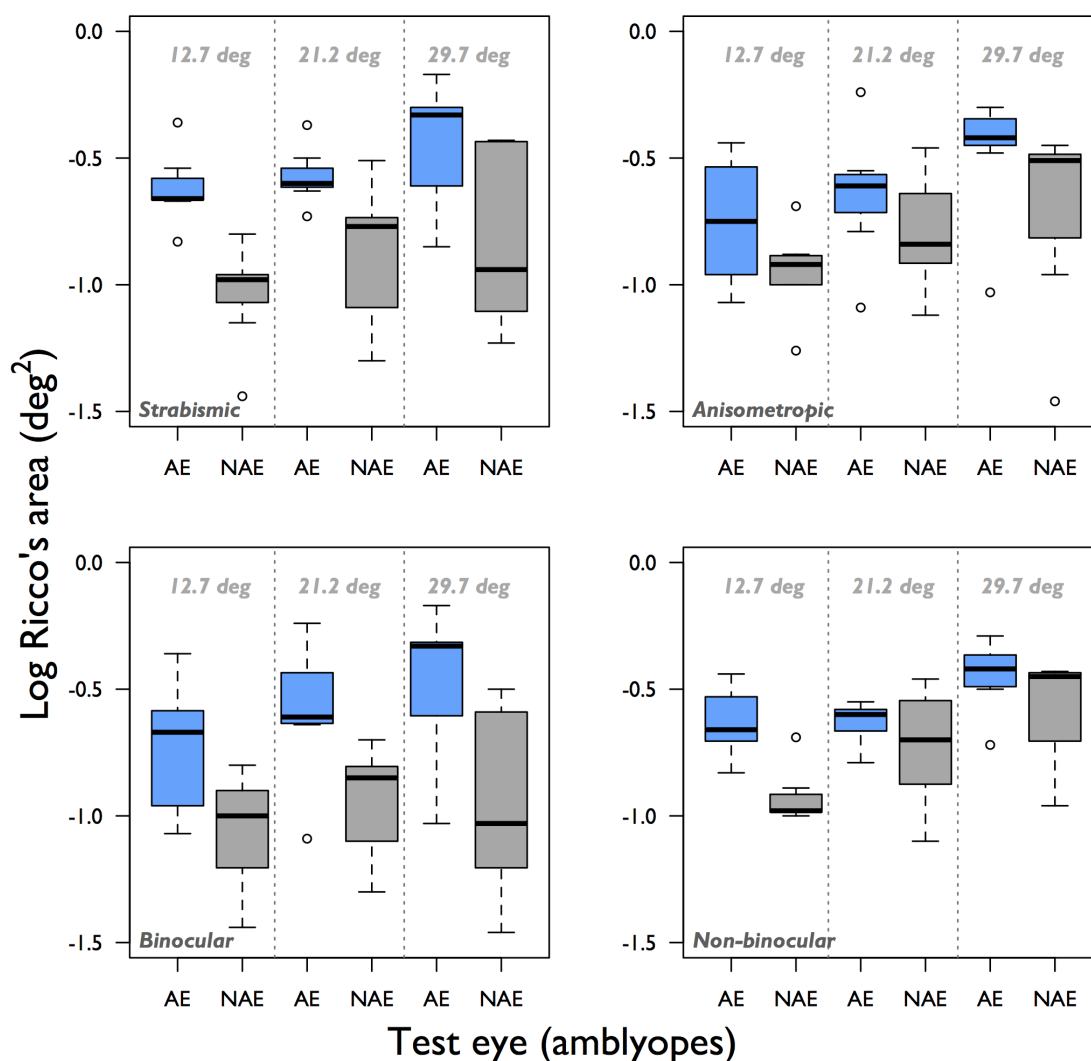


Figure 3.3. Ricco's area in amblyopic (blue boxes) and non-amblyopic (grey boxes) eyes at each eccentricity when amblyopes are separated into strabismic (top left) and anisometropic (top right) groups, as well as binocular (bottom left) and non-binocular (bottom right) groups Error bars: SEM

Linear mixed effects model analysis reported that the inter-ocular difference in Ricco's area was $0.33 \log \text{deg}^2$ ($\pm 0.1 \text{ SE}$) larger overall in the binocular group than in the non-binocular group ($p = 0.005$). Separate linear mixed effects analyses, with Ricco's area in the amblyopic and non-amblyopic eyes as dependent variables (with the same fixed and random effects), revealed that most of this effect can be attributed to a smaller Ricco's

area overall in the non-amblyopic eyes of binocular amblyopes, compared with that in non-binocular amblyopes (by $-0.327 \log \text{deg}^2$, $\pm 0.1 \text{ SE}$, $p = 0.004$). This difference can be seen in Figure 3.4 (left panel; solid lines: binocular group, dotted lines: non-binocular group).

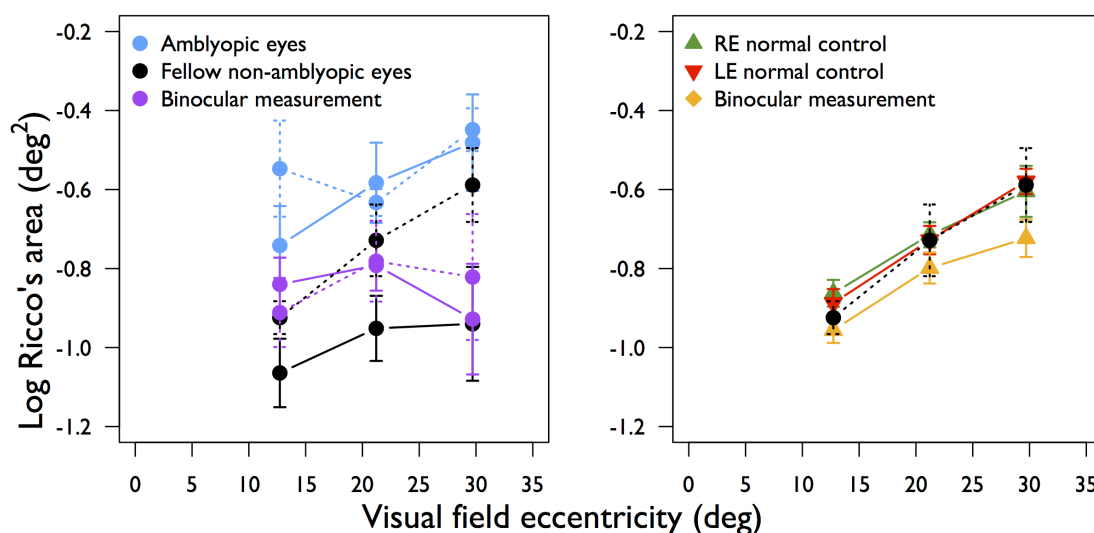


Figure 3.4. Mean Ricco's area as a function of eccentricity in amblyopic participants, separated by binocular and non-binocular status (solid and dotted lines respectively, left panel). Mean Ricco's area as a function of eccentricity in normal controls are shown in the right panel. For ease of comparison, Ricco's area data from the fellow non-amblyopic eyes of non-binocular amblyopes are superimposed on data from normal controls (right panel, black symbols). Error bars: SEM

In fact, mean Ricco's area in the non-amblyopic eye of non-binocular amblyopes is comparable to that in normal controls at each eccentricity. The overall difference in Ricco's area in the amblyopic eye between binocular and non-binocular groups was negligible ($-0.003 \log \text{deg}^2$, $\pm 0.1 \text{ SE}$, $p = 0.96$).

Strabismic vs anisometropic amblyopia

None of the strabismic participants in the study had anisometropia (Table 3.1).

The distributions of Ricco's area values for the amblyopic and non-amblyopic eyes of strabismic and anisometropic amblyopes are shown in Figure 3. Linear mixed effects model analysis showed that type of amblyopia was significantly associated with the inter-ocular difference in Ricco's area ($p = 0.01$) with this difference being $0.28 \log \text{deg}^2$ larger ($\pm 0.1 \text{ SE}$) overall in strabismic amblyopes. A smaller Ricco's area in the non-amblyopic eyes of strabismic amblyopes relative to that in anisometropic amblyopes (by $-0.20 \log \text{deg}^2$, $\pm 0.1 \text{ SE}$, $p = 0.06$) contributed most to this effect. A slightly larger Ricco's area in amblyopic eyes of strabismic amblyopes relative to that in anisometropic amblyopes contributed to the effect by a negligible amount ($+0.08 \log \text{deg}^2$, $\pm 0.1 \text{ SE}$, $p = 0.40$).

Severity of amblyopia

The inter-ocular difference in central visual acuity to standard optotypes was taken as a clinical measure of severity of amblyopia. The linear mixed effects model showed that inter-ocular difference in VA was significantly associated with the inter-ocular difference in Ricco's area ($p = 0.04$).

Monocular vs binocular measurements of Ricco's area

A subset of amblyopic participants ($n = 12$) and all controls ($n = 15$) underwent binocular measurements of Ricco's area with an identical test protocol to that described in the Methods. In controls, Ricco's area estimates measured binocularly are smaller, on average, than those measured monocularly at all eccentricities, with the largest difference in mean Ricco's area observed at 29.7° (Figure 3.5).

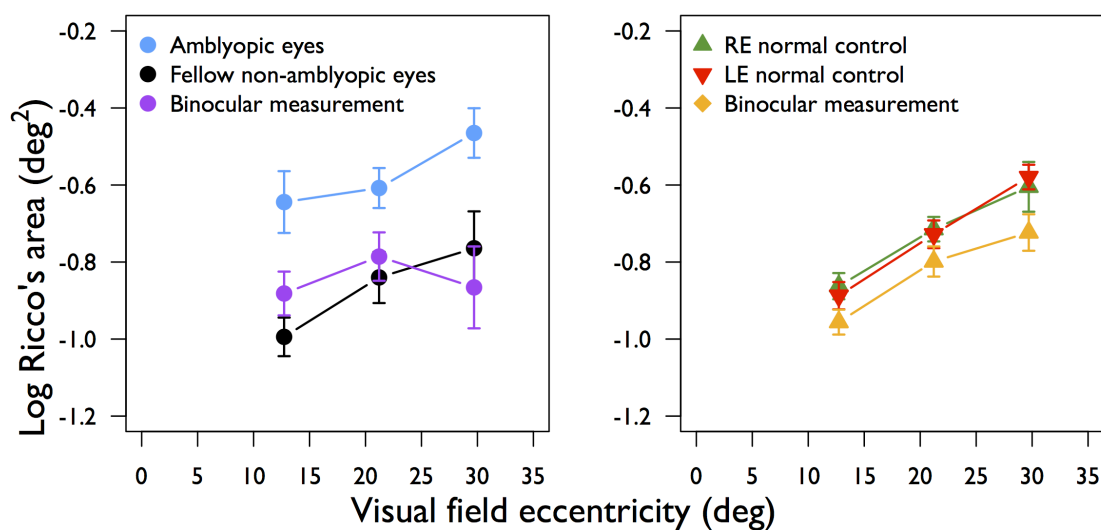


Figure 3.5. Mean Ricco's area, measured binocularly, in amblyopic participants (purple discs) and normal controls (gold triangles) in left and right panels respectively.

Mean Ricco's area estimates in amblyopes and normal controls are also shown, for reference. Error bars: SEM

In amblyopes, binocularly measured Ricco's area was, on average, smaller than that measured monocularly in amblyopic eyes but larger than those measured monocularly in fellow non-amblyopic eyes, at 12.7° and 21.2° (Figure 3.5). At 29.7° eccentricity, binocularly-measured Ricco's area was, on average, smaller than that in both amblyopic and non-amblyopic eyes. Mean Ricco's area, measured binocularly was, on average, larger at 12.7° and smaller at 29.7° eccentricity in amblyopic eyes than in control eyes, with a negligible difference at 21.2° eccentricity. When data were separated by binocular vision status, mean binocularly measured Ricco's area was comparable between groups at 21.2° eccentricity. On average, binocularly measured Ricco's area was slightly smaller in the non-binocular than in binocular amblyopes at 12.7°, while the opposite was found at 29.7° (Figure 3.4, purple symbols).

3.4. Discussion

This study is the first to formally report on measurements of Ricco's area in amblyopic participants. The finding of a larger mean Ricco's area, and thus greater spatial summation, in amblyopic eyes supports previous findings of disproportionately higher thresholds for small stimuli than for larger stimuli in amblyopic cohorts (Hagemans & van der Wildt 1979; Flynn 1967). Intriguingly, not only is mean Ricco's area larger in amblyopic eyes compared with that in eyes of control participants, but unexpectedly, it is smaller in fellow non-amblyopic eyes (particularly in non-binocular amblyopes) compared with that in controls.

These findings offer some clues as to the loci along the visual pathway that contribute to the basis for Ricco's area. RGCs and the LGN were previously reported to be normal in amblyopia (Derrington & Hawken 1981; Jones *et al.* 1984; Movshon *et al.* 1987; Sherman & Stone 1973; von Noorden 1970), even in stimulus deprivation amblyopia, the most severe form. Also, the general consensus is that retinal nerve fibre layer thickness is unaffected in the condition (Chen *et al.* 2013; Ersan *et al.* 2012; Walker *et al.* 2011; Xu *et al.* 2013). Therefore, the findings of the current study support predictions that Ricco's area is not solely a retinal phenomenon, and that it likely represents summation by multiple mechanisms along the visual pathway (Pan & Swanson 2006), i.e. a 'net' receptive field, or 'perceptive field' (Anderson 2006; Vassilev *et al.* 2005) for a given location in visual space. Indeed, differences in spatial summation in pathological conditions affecting the visual pathway from the retina to visual cortex (Redmond *et al.* 2010a; Wilson 1967), as well as under changing S-cone adaptation conditions (Redmond *et al.* 2013b), also support this.

The findings of the current study are suggestive of either a shift in signal processing to the most responsive spatial frequency channels (as has been hypothesized to occur in glaucoma (Redmond *et al.* 2010a)), or a difference between the pathways from each eye to the brain, in terms of convergence of signals from a group of lower level neurons on to a group of higher level neurons. While both are plausible explanations, it is worth considering the finding of a smaller Ricco's area in fellow non-amblyopic eyes. It is difficult to understand how the visual system may gain from a shift to a channel tuned to lower spatial frequencies in the amblyopic eye and a shift to a channel tuned to higher spatial frequencies in the fellow non-amblyopic eye. Such an adaptation would be suggestive of the amblyopic eye being optimized for contrast sensitivity, with the fellow eye optimized for visual resolution. Here we put forward an alternative hypothesis. If receptive fields of retinal cells and the LGN are unaffected in amblyopia, and the number of RGCs is similar between amblyopic eyes and fellow non-amblyopic eyes (as denoted by a lack of any notable difference in retinal nerve fibre layer thickness in published literature), the first site at which disrupted circuitry, and thus an anomaly of spatial summation, might occur is layer 4 of V1, where an asymmetry of ocular dominance (OD) columns has been noted in primates (Hubel *et al.* 1977) and humans with early-onset amblyopia (Goodyear *et al.* 2002), as well as an asymmetry in population receptive field size (Clavagnier *et al.* 2015). In normal observers, ocular dominance columns relating to the right and left eyes in a given hypercolumn are equal in width, and contain comparable numbers of cells sampling the visual field. Therefore, 1 minute of visual angle is represented by the same cortical space when viewing with the right or left eye. Likewise, the number of geniculocortical axons relaying right eye signals from the LGN to layer 4 is equal to the number of geniculocortical axons relaying left eye signals. In amblyopia, the region of the hypercolumn sampling the

visual field of the non-amblyopic eye is larger (wider OD columns), and that devoted to sampling the visual field of the amblyopic eye is smaller (narrower OD columns). Therefore, 1 minute of visual angle, viewed through the fellow non-amblyopic eye is represented by a larger area of cortex than the same visual angle viewed with the amblyopic eye, despite no perceptual difference in object size. Importantly, the proportions of geniculocortical axons relaying eye-specific signals from the LGN remain unaffected. Increased axonal arbor complexity in the geniculocortical cells mediating the signal response of the non-amblyopic eye would mean that those axons are available to synapse with a greater number of cells in the hypercolumn, while reduced axonal arbor complexity in geniculocortical cells mediating the signal response from the amblyopic eye would mean that fewer cells in V1 will synapse with them (Antonini & Stryker 1993). Assuming that the density of cells in OD columns is unaffected in amblyopia, greater spatial summation might therefore be observed as signals from the amblyopic eye converge on to a smaller region of the cortex (smaller number of cells), and vice versa. A third, alternative explanation for an enlarged Ricco's area in amblyopic eyes may be increased topographical disarray in receptive fields of V1 to at least V3, as reported in a recent fMRI study of amblyopia (Clavagnier *et al.* 2015). However, the finding of a smaller-than-normal Ricco's area in the non-amblyopic eye raises challenges for this hypothesis.

The finding of a smaller Ricco's area in fellow non-amblyopic eyes was unexpected, and so peripheral resolution acuity was not measured prospectively. Given the inverse association between spatial summation and resolution acuity, however, this finding suggests that resolution acuity should be higher in the non-amblyopic eye than in normal controls, albeit at the expense of spatial pooling. Conventionally, the non-amblyopic eye has been referred to as 'the normal eye' by clinicians, due to its largely

unaffected performance in visual acuity tasks on a high contrast letter chart. However, published evidence of the visual performance of fellow non-amblyopic eyes is, as yet, inconclusive (Chatzistefanou *et al.* 2005; Freeman & Bradley 1980; McKee *et al.* 2003; Thompson *et al.* 2011; Leguire *et al.* 1990). McKee *et al.* (2003) reported superior contrast sensitivity in the non-amblyopic eyes in participants with visual acuity of 6/30 or better, but this superiority is only observed in participants without residual binocular function. Numerous studies comparing the visual function of the fellow non-amblyopic eye have, however, reported impairment in other attributes of visual function, such as contrast sensitivity (Chatzistefanou *et al.* 2005; Reed *et al.* 1996), Vernier acuity (Cox *et al.* 1996; Levi & Klein 1985), global motion processing (Simmers *et al.* 2003), dark adaptation (Bedell & Kandel 1976), and rarebit sensitivity (Agervi *et al.* 2010), as well as an increase in neural noise (McKee *et al.* 2003). Standard optotype visual acuity, measured in the fovea in the current study, was not significantly different between fellow non-amblyopic eyes and those of normal controls. However, although these measurements were not performed at the same test locations as measurements of Ricco's area, the findings in the current study indicate that non-amblyopic eyes would otherwise be inappropriately considered 'normal' in the clinical setting, despite a possible anomaly of Ricco's area. A formal investigation of peripheral grating resolution acuity at the same test locations in those eyes is warranted.

In this study, the finding of a larger-than-normal Ricco's area in amblyopia, and smaller-than-normal area in the fellow eye, was in a cohort containing an equal proportion of anisometric and strabismic amblyopes. Binocular and non-binocular participants were also represented in equal proportions, with strabismic and anisometric amblyopes represented in both groups. Statistical analysis indicated that binocularity had the largest effect on inter-ocular differences in Ricco's area in

amblyopic participants. While the difference in mean Ricco's area between the two groups for amblyopic eyes was negligible, most of the effect of binocularity could be explained by a smaller Ricco's area in the non-amblyopic eyes of binocular amblyopes, compared to those of non-binocular amblyopes and normal controls. On inspection of Figure 3.4, it can be seen that when Ricco's area estimates were divided into binocular and non-binocular groups, mean values in the non-amblyopic eyes of the non-binocular group closely resemble those of normal controls, and that it is, in fact, those estimates in the non-amblyopic eyes of the binocular group that are smaller than normal. This finding could be explained by a simple cortical model similar to that proposed by McKee *et al.* (2003) (their Appendix A). Suppose that in a given region of the visual cortex of a binocular amblyope, 60% of neurons are binocularly-driven (i.e. they receive input from both eyes), and the remaining 40% of neurons are monocularly-driven (20% from each eye). If one supposes that in non-binocular amblyopes, the same region of the visual cortex contains only monocularly-driven neurons; 50% receiving in input from one eye, and the other 50% receiving input from the fellow eye. Full-field monocular stimulation in binocular amblyopes would result in stimulation of up to 80% of cortical cells in that region, whereas in non-binocular amblyopes, the same degree of monocular stimulation would elicit a response of up to 50% of cortical cells in that region. If a stimulus of a fixed area is projected on to the retina of one eye, the number of responding RGCs should be equal in both groups. However, if the number of cortical cells responding to the stimulus is smaller in the non-binocular group, this may manifest as a larger Ricco's area, because of greater convergence of signals from the same number of geniculocortical axons on to a smaller cortical region. Conversely, in the binocular group, the same level of convergence would not be required, which may manifest as a smaller Ricco's area. Swanson *et al.* (2004) determined that Ricco's area

is sampled by a critical number of RGCs ($n = 31$) across the visual field of a normal observer under perimetric conditions equivalent to those employed in the current study (Swanson *et al.* 2004). If one assumes that Ricco's area is also sampled by a critical number of cortical cells across the visual field, a monocularly-presented stimulus of a fixed area would be sampled by approximately 16% more cortical cells in a given cortical region in binocular amblyopes than in non-binocular amblyopes. In this case, the critical number of cortical cells, and thus the criterion for the extent of Ricco's area, would be met with a smaller stimulus, resulting in a smaller Ricco's area in those eyes.

The findings of the current study also have important implications for our understanding of visual field sensitivity deficits in glaucoma. Attempts to understand the nature of sensitivity loss in glaucoma have typically involved investigations of the relationship between RGC number (or a surrogate) and visual field sensitivity to achromatic circular luminance increments on a uniform achromatic background. Guided by the fact that glaucoma is characterised by death of RGCs, many investigations do not consider changes that may occur at extra-retinal levels, but instead make decisions on the utility of one functional test over another based on the strength of association between the test output and measurements of retinal structure. Given that an enlarged Ricco's area is also observed in glaucoma (Redmond *et al.* 2010a), the findings of the current study provide further support for the case that changes in cortical mechanisms should be taken into account when attempting to understand the nature of visual loss in glaucoma, as measured with conventional circular incremental stimuli.

In conclusion, an enlarged Ricco's area has been found in amblyopic eyes, and a smaller-than-normal area has been found in fellow non-amblyopic eyes. This finding is suggestive of Ricco's area being the psychophysical consequence of multiple pooling

mechanisms in the visual cortex, rather than in retinal receptive fields alone. Greater attention should therefore be given to alterations in cortical processing in glaucoma, given that a loss of sensitivity to conventional stimuli can be mapped to an enlarged Ricco's area. The findings in the current study also highlight differences in fundamental attributes of visual function between binocular and non-binocular amblyopes as well as strabismic and anisometropic amblyopes that warrant further investigation.

Chapter 4: Changes in Ricco's area in Glaucoma, in Response to IOP-lowering Treatment

4.1. Introduction

Subtle structural changes in RGC before the onset of apoptosis have been well documented in experimental model of glaucoma, with the earliest sign being the pruning of RGC dendrites, followed by shrinkage of the RGC soma (Morgan 2002; Shou *et al.* 2003; Weber *et al.* 2000). This has raised the suggestion that perhaps RGCs undergo a period of dysfunction before death in animal models of glaucoma (Morgan 2002; Shou *et al.* 2003; Weber *et al.* 1998) and that the same process could occur in human glaucoma (Porciatti & Ventura 2012). However this cannot be ascertained currently in human glaucoma, as an *in-vivo* study of the relationship between the structure and function of isolated RGCs is not yet possible in the living human. Although early structural changes were observed in experimental glaucoma, it is not an absolute indication that RGC function is compromised or absent; it is unclear whether RGC function would be lost before the pruning of dendrites occurred or it reduces proportionally with structural change. RGC dysfunction in humans was first suggested following PERG measurements by Ventura & Porciatti (2005). They observed an increase in PERG amplitude and phase in participants with OAG and NTG undergoing IOP-lowering treatment, compared with those who were not treated. This result has since been supported by other PERG studies where PERG amplitude and/or phase have been observed to stabilise or increase following treatment in glaucoma participants (North *et al.* 2010; Sehi *et al.* 2010). For a more extensive review please refer to Chapter 1.

4.2. Measuring RGC dysfunction

True dysfunction could only be determined in one of two ways: a) evidence of functional loss prior to, or proportional with the loss of structural integrity of the damaged cells, or b) evidence of functional improvement in response to treatment. The former method is difficult, because precise measurements of RGC structural integrity *in vivo* are not yet possible. Surrogate measures, such as RGC layer thickness with OCT, would be much less imprecise. Furthermore, a precise comparison of structure and function, as is needed to provide such subtle evidence, is hampered by the fact that these measures have incomparable scales and normative databases. The latter method is arguably less difficult.

The ability to measure reduced visual function in glaucoma with PERG is well documented, however PERG is not a technique that is widely used or available in clinical practice. Currently, there is no other clinical test that has been definitively shown to measure RGC dysfunction. In fact, the presence of dysfunction is difficult to conclude *in vivo*. Although it is possible to measure a reduction in contrast sensitivity with conventional perimetry, it is not clear how much of this reduction in sensitivity is due to cell death and how much is due to dysfunction; this would require precise knowledge of the integrity of individual ganglion cells in isolation. Furthermore, clinical measures of visual field sensitivity are a result of not only retinal processing, but also cortical pooling by multiple spatial mechanisms (Pan & Swanson 2006). Therefore, even if a ganglion cell does become dysfunctional prior to death, knowledge of the extent of dysfunction of that cell is not enough to adequately assess the effect on perimetric sensitivity at that location. It is perhaps more important, clinically, to attempt

to identify dysfunction by measuring alterations in spatial pooling that may occur in response to RGC damage.

4.3. Changes in spatial summation as a measure of RGC dysfunction?

A study investigating changes in spatial summation over time in glaucoma may provide some clues as to whether or not dysfunction occurs, while at the same time offering some insight into the impact of such damage on the resulting functional deficit in visual field sensitivity. Redmond *et al.* (2010a) reported a statistically significantly larger Ricco's area in participants with early glaucoma (MD better than -8dB), when compared to that in healthy controls, in visual field locations that had, on average, minimal visual field damage, with conventional perimetry (average TD -1.3dB; 24-2 SITA-Standard, HFA II, Carl Zeiss Meditec, Dublin, CA). They suggested that changes in Ricco's area may be due to cortical remodelling, or a result of a greater capacity for complete spatial summation in otherwise larger cortical receptive fields due to ganglion cell damage. Due to the cross-sectional nature of the study, it could be argued that the difference in Ricco's area found by Redmond *et al.* (2010a) was due to RGC death only. It is impossible to deduce from their data how Ricco's area changed over time. One method of ascertaining this is by measuring Ricco's area before and after the commencement of intra-ocular pressure-lowering treatment (or more rigorous treatment, if treatment has already been initiated) and observe whether Ricco's area a) continues to enlarge, b) remains at a constant size, or c) becomes smaller, after treatment. The possible options are illustrated in the schematic in Figure 4.1.

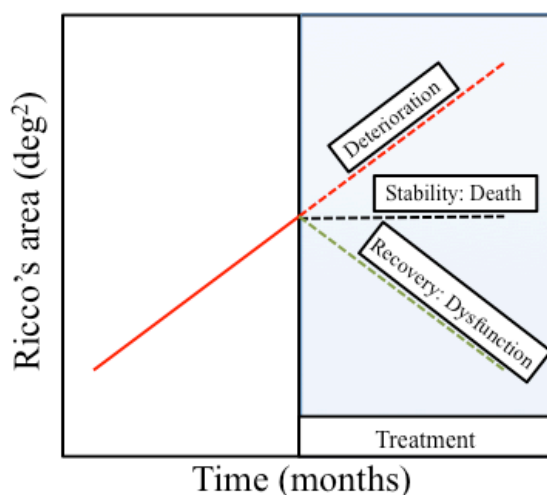


Figure 4.1. Possible changes in Ricco's area in response to treatment (or more rigorous treatment). A further increase would indicate further deterioration, a reduction would indicate recovery and thus that any previous enlargement of Ricco's area was due to RGC dysfunction, and no change would indicate stability and that any previous enlargement of Ricco's area may have been due to RGC death.

Pruning of RGC dendrites might be expected to cause impairment in the ability of the cell to gather light signals over space. With cell death, there would be a complete inability to gather light signals over space. Ricco's area might be expected to enlarge accordingly in order to maintain the signal/noise ratio, as is observed with visual field eccentricity in the healthy eye (Wilson 1970). If the enlargement of Ricco's area represents RGC dysfunction, one might expect to observe a shrinkage of Ricco's area after administration of treatment, as the cell recovers. If the enlargement represents RGC death, one might expect to observe no change in Ricco's area after treatment. If Ricco's area enlarges further after treatment, it might be concluded that either death and/or dysfunction continue to occur and that treatment had little or no effect. If Ricco's area shrinks to normal (or near normal) levels following treatment, this might be an

indication that dysfunction does initially occur, but that recovery occurs in response to treatment.

An investigation into changes in Ricco's area after intraocular pressure-lowering treatment is problematic in that compliance to a treatment regime involving topical medicine by patients cannot be easily ascertained. Research has shown that nearly half of glaucoma patients who know they are being monitored electronically do not use their medication as prescribed, 75% of the time (Okeke *et al.* 2009). The only way to ensure maximal compliance is to carry out the investigation on patients in which there is no reliance upon adherence to the prescribed use of medication. Patients undergoing trabeculectomy surgery to lower intraocular pressure are therefore an ideal cohort in which to carry out such an investigation, as they are not required to take regular medical treatment at home. Thus, concerns about compliance are greatly reduced.

Trabeculectomy surgery was first introduced by Cairns (1968) and has since undergone numerous modifications. It is a procedure that allows the lowering of IOP by creating a corneoscleral fistula that causes subconjunctival bleb formation. The use of antimetabolites such as mitomycin C increases post-operative success and thus is commonly added to the procedure (Chen 1983). Generally patients who undergo trabeculectomy surgery tend to be those for whom topical IOP-lowering treatment has not been successful, and those in which compliance is a concern.

Given that measurements of Ricco's area involve projection of spot stimuli on the retina, it is important, when determining the neural component to any changes in Ricco's area in response to treatment, that any surgically-induced changes to pre-neural

structures that might alter the stimulus configuration between pre- and post-surgery experiments are accounted for, or at least considered. Trabeculectomy surgery has been observed to cause a shallowing of the anterior chamber up to 5 years post-surgery (Husain *et al.* 2013; Man *et al.* 2015), shortening of axial length up to 5 years following surgery (Husain *et al.* 2013; Pakravan *et al.* 2015) and changes in corneal curvature in the form of flattening of anterior curvature, resulting in increase in with-the-rule astigmatism in some cohorts by up to 2.00D at 12 months post-surgery (Hong *et al.* 1998; Kook *et al.* 2001). As previously discussed in Chapter 2, there do not appear to be any notable systematic changes in Ricco's area, even with a substantial increase in optical blur. Therefore it is expected that any small refractive changes that might occur in participants undergoing trabeculectomy will not contribute a great deal to any observed change in Ricco's area following surgery. However, refractive blur is not the only optical factor that can cause degradation in retinal image quality. In this chapter, changes in wavefront aberrations and how these will affect the measurement of Ricco's area will also be taken into account.

4.4. Measurement of corneal wavefront aberrations

Wavefront aberrations illustrate the distortion of wavefronts as they go through a non-optimal optical system. Wavefront aberrations can be described mathematically by a polynomial series, with Zernike polynomial expansion chosen to become the standard for describing ocular wave aberrations (Thibos *et al.* 2002). The Zernike polynomial is a set of basic functions, each having a coefficient. Coefficients depict how much contribution that aberration has to the overall wavefront aberration. The Zernike terms

are construed by radial order n and frequency m over a unit circle with orthogonal polar co-ordinates ρ and θ .

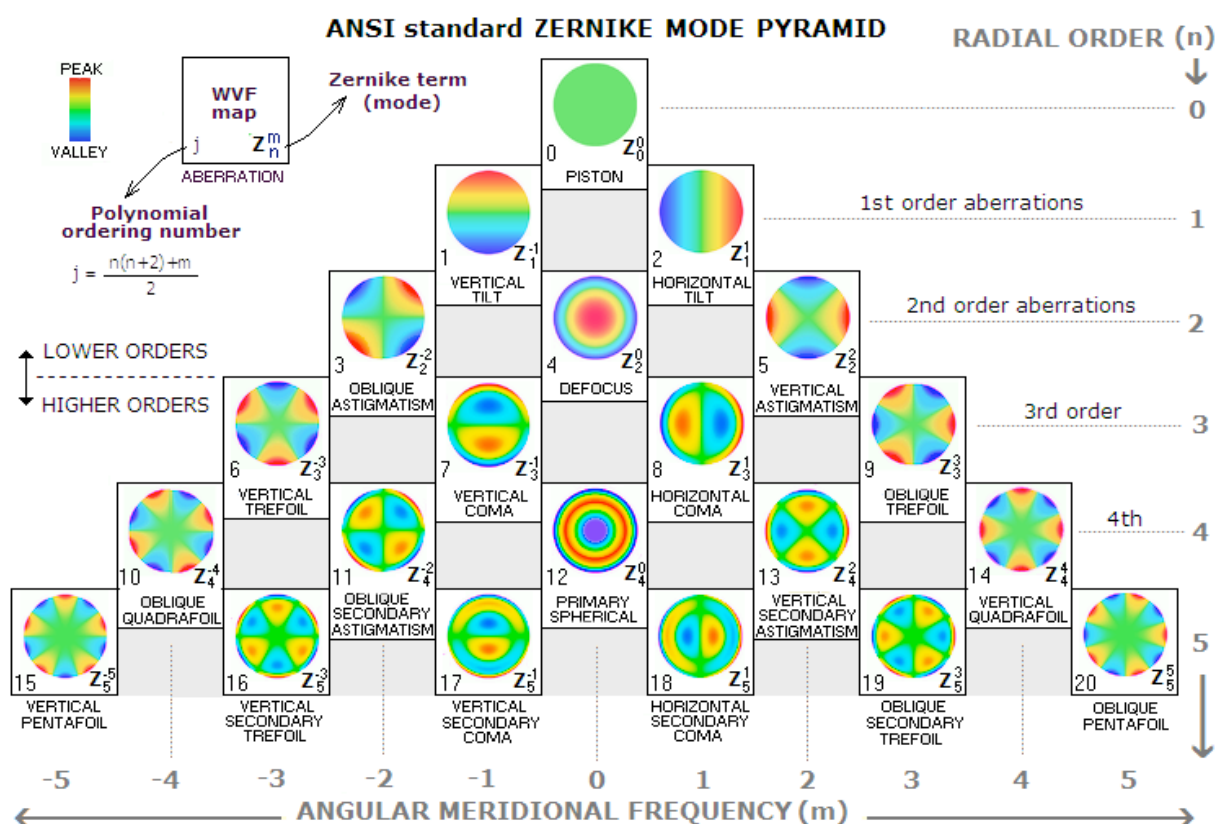


Figure 4.2. Pyramids of Zernike term up to 5th order. Image reproduced from

http://www.telescope-optics.net/monochromatic_eye_aberrations.htm.

The Zernike polynomial organizes aberrations into a hierarchy with an increasing radial order (Figure 4.2). Lower order aberrations are zero (piston), first (tilt) and second order (astigmatism and defocus) and can be corrected with spectacle lenses. Higher order aberrations consist of third order aberrations and above; these imperfections cannot be corrected with spectacle lenses.

The cornea, as the contributor of two-thirds of the power of the relaxed eye, has great influence on ocular aberration. Trabeculectomy causes a change in corneal curvature, and has previously been observed to cause a change in corneal higher order aberrations

post-surgery, returning to pre-operation values 3 months after surgery (Fukuoka *et al.* 2011). Corneal aberrations are estimated based on corneal elevation data, where the Zernike polynomial is fitted as close as possible to the measured height data.

In any study of spatial summation following a procedure involving anterior eye insult, it is imperative that changes in corneal aberrations be investigated before and after the procedure has taken place. This will help determine the likelihood that any change (or absence of change) in Ricco's area post-surgery is due to surgically-induced changes in aberrations.

The aim of this study is to compare measurements of Ricco's area before and after trabeculectomy surgery, in order to test the hypothesis that an enlarged Ricco's area in glaucoma returns to normal (or near normal) levels following IOP-lowering surgery. Secondary aims are to investigate whether or not Ricco's area is enlarged in patients requiring trabeculectomy surgery, relative to that in stable glaucoma participants for whom surgery is not required, and to investigate any changes in Ricco's area that may have occurred during this timescale in stable glaucoma participants, relative to that in normals, in the absence of any change in sensitivity to a conventional perimetric stimulus. As verification of the quality of the data, an additional aim is to confirm the finding of Redmond *et al.* (2010a), of an enlarged Ricco's area in glaucoma participants relative to that in healthy controls. Patients in the trabeculectomy group were recruited on the basis of having already been listed for trabeculectomy surgery. All clinical decisions regarding treatment were made prior to, and independently of, patients' involvement in the study and were not based on any findings from the current thesis). All participants will undergo the same experimental procedures twice, using the same

experimental protocol, spaced at least six months apart. Patients undergoing surgery will undergo experiments within the 2 weeks prior to their surgery and again, approximately 6 months after the surgery. The outcome of this study will enable a firmer hypothesis to be made regarding the presence, or otherwise of neural dysfunction in humans, as well as enable a determination to be made about whether or not Ricco's area can enlarge with glaucoma severity, given that the results of Redmond *et al.* (2010a) were cross-sectional.

4.5. Methods

Spatial summation curves were measured and Ricco's area compared between multiple visual field locations in one eye of patients with stable glaucoma, patients with glaucoma requiring trabeculectomy surgery as part of their normal clinical care, and healthy control participants on two separate visits, spaced approximately 6 months apart (Experiment 1). In the case of patients requiring trabeculectomy, experiments were conducted within a matter of days before their surgery, and again, approximately 6 months after their surgery. Spatial summation curves were determined from contrast thresholds measured with Goldmann size 1-V stimuli. Given that corneal changes might be expected as a result of trabeculectomy surgery, it was considered that these changes might have an effect on the area of the stimulus being projected on the retina, and thus the measurement of threshold. Therefore, corneal aberrations were also measured on the same visits in each participant group. In all cases, differences in aberrations between visits were determined and the effect of this difference on any changes in Ricco's area was investigated (Experiment 2).

4.5.1. Experiment 1

4.5.1.1. Participants

Patients with Primary OAG or NTG (herein referred to as the 'stable glaucoma participants (S)' and 'trabeculectomy participants (T)') were recruited from glaucoma clinics at the University Hospital of Wales, Cardiff. Age-similar healthy controls (herein referred to as 'healthy participants (H)' or normal controls) were recruited from staff and students of Cardiff University and a research volunteer database at the Cardiff University Eye Clinic. Any decisions regarding treatment or otherwise were made by

the patients' care team, and were made on the basis of clinical findings during the patients' visits to the hospital clinic. No decisions on treatment were made on the basis of the findings of the current study, nor were they influenced by patients' inclusion in the study. Participants were advised to continue following the advice of the glaucoma clinic regarding any topical medication or planned procedures, and not to alter their regime because of their inclusion in the study.

Inclusion criteria for all participants were a) spherical refractive error $\leq \pm 6.00$ DS, b) astigmatism < 1.50 DC, and c) best corrected visual acuity better than or equal to 0.3 logMAR. Specific inclusion criteria for glaucoma patients were a) diagnosis of POAG or NTG by the hospital eye service and b) a visual field defect consistent with glaucomatous optic nerve appearance. Specific inclusion criteria for *stable* glaucoma were: a) a diagnosis of stable glaucoma by the glaucoma consultant on the basis of stable IOP < 21 mmHg, b) no identifiable visual field progression, c) stable optic disc appearance, and d) no previous trabeculectomy in the eye to be tested. The specific inclusion criterion for the trabeculectomy group was a decision by the consultant ophthalmologist to list the patient for trabeculectomy surgery, based on a clinical determination of progression, or high risk of progression, that could not be controlled with medication. Specific inclusion criteria for healthy participants were a) full visual field b) healthy optic discs, and c) IOP < 21 mmHg. Exclusion criteria were a) media opacities greater than those expected for the participant's age (e.g. in older participants, no more than mild cataract, graded with LOCS III; grade of ≤ 2), b) ocular or systemic conditions or medication that might be expected to affect visual performance, except for glaucoma, where appropriate (e.g. diabetes, thyroid disease), c) corneal opacities, d) ocular surgery which might affect visual performance (apart from trabeculectomy,

where appropriate), e) inability to steadily fixate during the test (e.g. individuals who have nystagmus or macular degeneration), f) a family history of glaucoma (first degree relative; healthy participants only), and g) brimonidine treatment (e.g. Alphagan) for high IOP (glaucoma participants only).

All participants underwent an ocular health investigation with slit lamp biomicroscopy, binocular indirect ophthalmoscopy, perimetry (24-2 SITA-Standard; Humphrey Field Analyzer II; HFA II, Carl Zeiss Meditec, Dublin, CA), and optical coherence tomography (OCT; Topcon 3D OCT-1000, Tokyo, Japan) to confirm that each group met the relevant inclusion criteria. Corneal aberrations were measured with an Oculus Pentacam (Oculus, Wetzlar, Germany). Only one eye, the eye that best met the inclusion criteria, was tested in all participants. In stable and healthy participants, the test eye was chosen at random when both eyes met the inclusion criteria.

4.5.1.2. Apparatus and Stimuli

In all experiments, stimuli were achromatic circular spots of light, presented on a grey background (luminance: 10 cd/m^2) for 200 ms. Sensitivity was measured at 8 different visual field locations across two different eccentricities (12.7° and 21.2° ; Figure 4.3) with five different stimulus areas (Goldmann sizes I-V; 0.11° , 0.22° , 0.43° , 0.87° and 1.7° diameter). Stimuli were presented on an Octopus 900 perimeter (Haag Streit, Koeniz, Switzerland), controlled with the Open Perimetry Interface (Turpin *et al.* 2012).

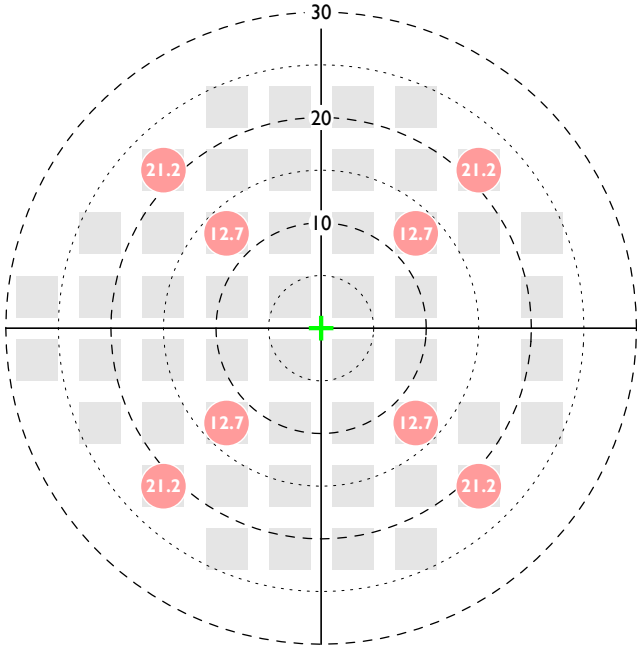


Figure 4.3. Visual field test locations (red), superimposed on a 24-2 HFA II visual field test grid, for reference. Visual field eccentricities are given inside each symbol.

4.5.1.3. Procedure

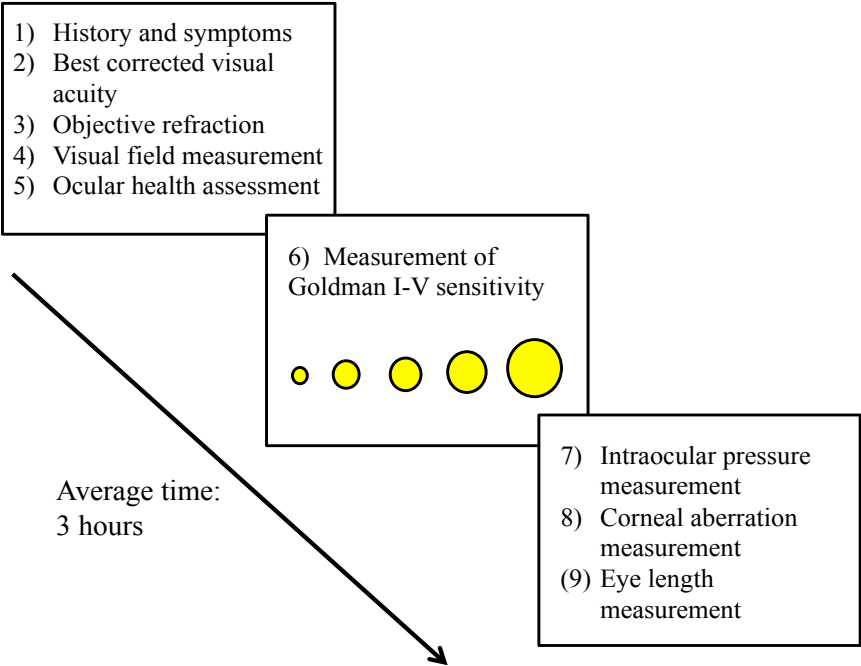


Figure 4.4. Schematic timeline of tests for both visits.

A summary of the preliminary tests and experiments, and the order in which they were performed, is shown in the schematic in Figure 4.4. For the Ricco's area measurement, sensitivity (in dB) was measured with each of the Goldmann sizes (I-V) at each visual field location in an interleaved manner. In each test, a different Goldmann size was used, chosen at random. A 4:1 staircase procedure was used, which was adapted from that produced by Andrew Turpin and Luke Chong (University of Melbourne, <http://people.eng.unimelb.edu.au/aturpin/opi/interface.html>, accessed on 15th March 2014). Step size was 4 dB before the first reversal and 1dB thereafter. A yes/no response criterion was used. At each location, the procedure stopped after 8 reversals. The final sensitivity returned was an average of the last 4 reversals. The entire procedure was repeated twice more. So, at each test location, 3 values for sensitivity were obtained for each Goldmann size. Therefore a total of 15 sets of sensitivity measurements were obtained per location, and 120 measurements per participant. All procedures were carried out with natural pupil sizes and central refractive error, corrected fully with full aperture trial lenses. A near addition was given for the appropriate working distance (33 cm). Fixation was monitored visually and eye position was adjusted when the pupil moved from the optimum position in the eye monitor. Breaks were given approximately after every 10 minutes and whenever requested by the patient.

4.5.1.4. Data analysis

Severity of glaucoma is classified based on Hodapp-Parrish-Anderson criteria. Sensitivity values (dB) for Goldmann I-V were averaged by stimulus size for each location (by unlogging, averaging, and then re-logging), converted to increment threshold (ΔI), and plotted against area. Two-phase regression analysis was performed

in the freely available open-source statistical environment, R (version 3.1.0) to obtain Ricco's area estimates at each location. The slope of the first line was constrained to a value of -1, following Ricco's law, whilst the intercept of first line, slope of the second line and break point were allowed to vary. The breakpoint estimated was taken to be an estimate of Ricco's area. Pooling all Ricco's area data together in participants with glaucoma can lead to masking of any subtle changes, as different glaucomatous visual fields (and locations within each field) have a different level of severity, and it is possible that some will have progressive loss while others will not. To address this potential problem, data from each participant group were divided into 3 equally sized strata based on total deviation (TD) values ascertained from conventional perimetry (24-2 SITA-Standard, HFAII). Stratum 1 contained data with more positive / less negative TD values (less visual field loss) and level 3 contained data with most negative TD values (most severe visual field loss). A paired t-test was performed on data from each group to test for overall changes in Ricco's area between visit 1 and 2. A Holm-Bonferroni correction was performed on all p values to reduce possibility of a type 1 error (increased likelihood of statistical significance due to multiple tests of the same hypothesis). Given that it was favourable to investigate whether Ricco's area changes between visits in the trabeculectomy group, relative to the other groups, it was necessary to account for the multiple factors that might otherwise influence the size of Ricco's area in this study. Linear mixed model analysis was therefore used to assess the relationship between participant type and the difference in Ricco's area between visits. The difference in Ricco's area between visits (ΔRA) was the dependent variable. Participant type (without an interaction term) was entered as a fixed effect, while intercepts for subjects and test locations, as well as by-subject random slopes were entered as random effects. There were no obvious deviations from normality, nor

heteroscedasticity. A likelihood ratio test of the model (including all effects) and the same model with the effect of interest removed was conducted in order to establish the statistical significance of that effect. Individual Ricco's area values were then plotted for both visits to assess changes of Ricco's area across all locations. Binomial test conducted on trabeculectomy group data to assess possibility of the result happening by chance. Ricco's area was also plotted as a function of age and linear regression performed to assess age-related enlargement with Ricco's area size. Slopes of the second lines were plotted against total deviation from SITA-Standard 24-2 and independent samples t-test run to assess relationship between two variables. Difference in RA between visits was plotted against difference in IOP between visits to assess their relationship. Sensitivity to a single stimulus area (each of Goldmann I-V stimuli) was compared between visits to test for possible changes between visits in each of the participant groups.

RGC density

RGC density was calculated from measures of sensitivity to a Goldmann III stimulus from the preliminary perimetry test using the 'hockey-stick' method of Swanson *et al.* (2004), at each experimental test location, in all participants, on both visits, to give some context, (in terms of the number of functional RGCS lost, or gained), to the findings of functional change between visits for the trabeculectomy, stable glaucoma, and healthy groups. The 'hockey-stick' structure/function model of Swanson *et al.* (2004) predicts that beyond 15° eccentricity, where Ricco's area in normal eyes is, on average, larger than the Goldmann III stimulus, log RGC number ($<1.5 \log \text{RGCs}$) is linearly related to perimetric sensitivity (dB) and well described with a line that has a slope of +1. Within 15° visual field eccentricity, Ricco's area is smaller than the

Goldmann III stimulus, and the relationship between sensitivity and log RGC number is well described with a line that has a slope of +0.25 (2.5dB per 1 log unit difference in RGC number). When Ricco's area is equal to the size of the Goldmann III stimulus, the sensitivity is predicted to be 31.25dB. The following calculations can be used to estimate RGC density.

When sensitivity to a Goldmann III stimulus is less than 31.25dB:

$$\text{Log} \left(\frac{RGC}{GIII} \right) = \frac{(\text{Sensitivity (dB)} - 16)}{10}$$

(Equation 3)

When sensitivity to a Goldmann III stimulus is greater than 31.25dB:

$$\text{Log} \left(\frac{RGC}{GIII} \right) = \frac{(\text{Sensitivity (dB)} - 27.44) \times 4}{10}$$

(Equation 4)

RGC/mm² is then calculated by converting the log RGC/GIII to linear units and dividing by 0.0119, the area (in mm²) of a Goldmann III on the retina, calculated using the conversion of Drasdo & Fowler (1974).

4.5.2. Experiment 2

Given the effect of optical factors on the size of Ricco's area (Davila & Geisler 1991; Dalimier & Dainty 2010), it was considered prudent to determine the effect of changes in optical quality, owing to trabeculectomy surgery, on any changes in Ricco's area between visits. If a change in Ricco's area is found between visits in the trabeculectomy group, it is important to ascertain whether this change is due to surgically-induced alterations of the cornea, or true neural changes. In this experiment, corneal aberrations were measured on both visits in the trabeculectomy group, as well as the stable glaucoma and healthy groups (control groups).

Corneal wavefront aberrations were measured before surgery in trabeculectomy participants and at least 6 months after surgery. Corneal wavefront aberrations were observed to vary greatly even among healthy individuals (Wang *et al.* 2003). An additional advantage in the current longitudinal study is that aberrations (and Ricco's area values) can be compared before and after trabeculectomy in the same participants, thus each participant acts as his/her own control. The Optical Society of America recommendations were followed throughout the study (Thibos *et al.* 2002).

4.5.2.1. Participants

Participants were the same as those who took part in Experiment 1. Full participant details can be found in Chapter 4.

4.5.2.2. Apparatus and Stimuli

An Oculus Pentacam (Oculus, Wetzlar, Germany) was used to obtain measurements of corneal wavefront aberrations. The instrument uses a 475nm UV-free LED and two

cameras and a method based on based on Scheimpflug principle to capture size and orientation of the pupil and capture images from the cornea. An attempt to calibrate the instrument with a steel ball of known radius was unsuccessful because, in order to take the measurement, the Pentacam relies on the backward light scattering properties of the front and back surface of the transparent cornea. The instrument was instead calibrated with a 3D-printed model eye.

4.5.2.3. Procedure

Three repeated measurements of corneal aberrations were taken each visit. Each acquisition lasted approximately two seconds. When the Pentacam gave reports with missing data, (e.g. due to droopy eyelids or long lashes), attempt were made to hold the eyelid up. Care was taken to ensure that the eyelids were held against the brow, avoiding any manual compression of the globe. Room lights were switched off during the measurement to ensure a reflection-free image. The automatic release mode was used, in order to reduce operator dependency for all tests, wherein the Pentacam automatically captured the scan when it decided that correct alignment with the corneal apex had been achieved.

4.5.2.4. Data analysis

Due to raw data export restrictions with the Pentacam, the Zernike coefficients had to be hand-typed from a screenshot of the report from each acquisition. Forty-five Zernike coefficients were obtained from each acquisition from the front surface of the cornea, and 45 from the back surface of the cornea. As three acquisitions were made per visit, for each visit the total number of Zernike coefficients obtained per participant were 270. The total numbers of Zernike coefficients collected was 15,360 at the first visit and

12,000 at second visit, owing to participant dropout. In order to minimize chances of subjective error, for every third Zernike coefficient typed out, that coefficient was typed out three times on separate occasions. To conclude the quality control check, the numbers were subtracted from each other to see whether a value of zero was obtained. An error of zero indicated no transcription error. For each participant, on average 24 minutes were needed to type out the Zernike coefficients per visit.

To correct for mirror asymmetry between right and left eyes, following suggestion of OSA (Thibos *et al.* 2002), signs of Zernike coefficients from left eyes with Zernike polynomials with negative, even meridional and positive, odd meridional indices were changed for example: C_2^{-2} , C_3^1 . As suggested by Atchison (2004), Zernike polynomials up to the 6th order are included in the analysis so that the error of the fit that comes with a coefficient does not become as significant as the coefficient itself.

The difference in Zernike coefficients between visits for the front and back surfaces for each participant group was plotted. The median for both cornea surfaces was calculated for all groups. They are compared qualitatively with the healthy subjects' Zernike coefficients results obtained from Chapter 3. Linear mixed model analysis was used to assess the relationship between between-visit differences in aberrations (ΔA) and ΔRA in the superior hemifield. Only ΔRA from the superior visual field were included in this analysis, as a) it is most likely that if any disruption to the corneal surface occurs in trabeculectomy, it is most likely that this will be in the superior cornea, and b) inclusion of the inferior locations could contaminate the identification of any small effects of surgical changes on the measurement of Ricco's area. ΔRA , pooled across all superior visual field locations, participants, and participant groups, was the dependent variable.

ΔA , corneal surface, and participant group were entered as fixed effects. Intercepts for polynomial number, test location, and subjects were entered as random effects. There were no obvious deviations from normality, nor heteroscedasticity. A likelihood ratio test of the model (including all effects) and the same model with the effect in question removed, was conducted in order to establish the statistical significance of the removed effect on the dependent variable.

4.6. Results

4.6.1. Experiment 1

The average testing time for each participant was 3-hours/visit.

Participants

Trabeculectomy participants

Twelve trabeculectomy participants with open-angle or normal tension glaucoma met the inclusion criteria out of 36 participants listed for trabeculectomy surgery within the period of study recruitment from June 2015 to August 2016. All participants underwent trabeculectomy with adjunctive Mitomycin C. Three out of 12 participants were lost to follow-up after the first visit, and their data were removed from subsequent analysis.

The trabeculectomy group had a range of VF loss from early to advanced.

Stable glaucoma participants

Twenty-six glaucoma participants with OAG or NTG were classified as stable by the consultant ophthalmologist in the hospital eye service, on the basis of no identifiable visual field progression, stable optic disc appearance, and stable IOP < 21mmHg. All participants continued to use any topical treatment prescribed to them by the hospital eye service throughout the period of the study. None of the participants had any change in their prescribed eye drops between the first and second visit. Following the first visit, six out of 26 participants in this group were lost to follow up, and their data were removed from subsequent analysis.

Healthy participants

Twenty-six participants with no family history of glaucoma or any other eye disease were recruited. All participants had IOP < 21mmHg, normal optic disc appearance C/D ratio < 0.5 in the test eye, with < 0.2 inter-ocular difference). All had full, normal visual fields. Six participants out of 26 were lost to follow-up and their data were removed from subsequent analysis.

*Table 4.1. Data from preliminary tests in each participant group. *Data from those participants lost to follow-up after the first visit have been excluded.*

	Trabeculectomy	Stable glaucoma	Healthy
n (first visit)	12	26	26
n (second visit)	9	20	20
Median [IQR] age	67 [58 to 77.50]	69 [62.50 to 76.50]	67 [63.25 to 71.75]
Median [IQR] refractive error (DS)	-3.25 [+1.50 to -4.75]	-2 [+3.75 to -4.50]	-0.75 [+2.75 to -2.25]
Median [IQR] VA (logMAR)	0.02 [-0.14 to +0.1]	0.04 [-0.12 to +0.16]	0.06 [-0.08 to +0.2]
Median [IQR] MD (dB) 1 st visit*	-5.3 [-8.7 to -3.5]	-1.9 [+1.1 to -8.1]	+0.5 [-0.6 to +1.4]
Median [IQR] MD (dB) 2 st visit	-5.1 [-11.6 to -1.4]	-1.2 [+3.8 to -8.2]	+0.9 [+0.1 to +1.6]

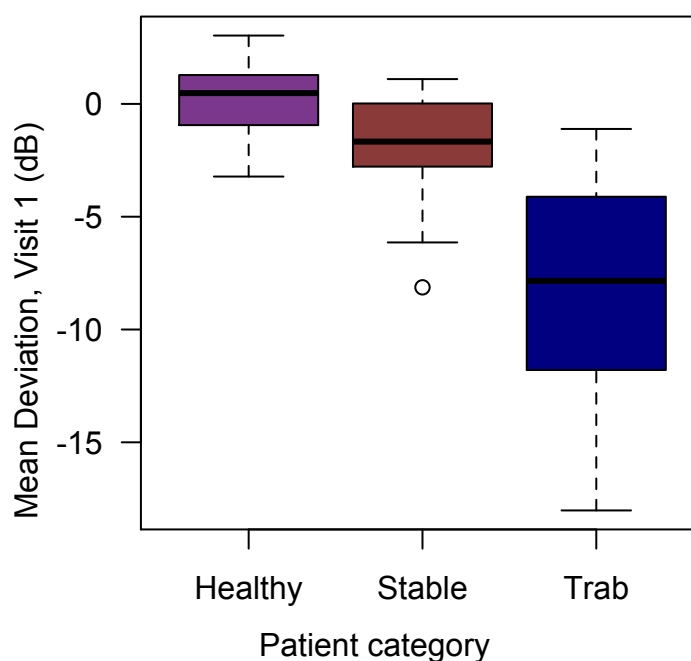


Figure 4.5. Graphical representation of MD from first visit of all participant groups.

Overall, changes in refractive error between visits were less than 0.50 D for all participant groups, and this was not statistically significant ($p=0.76$). Median logMAR visual acuity between visits was unchanged between visits in the stable glaucoma and healthy groups. The overall difference between visits was not statistically significant ($p=0.69$). Eleven participants in the trabeculectomy group had the same logMAR visual acuity between visits, but one participant had a small reduction of 0.04 logMAR on the second visit. Median (IQR) IOP up to 2 weeks pre-operation and at approximately 6 months post-operation for trabeculectomy groups were 25 (17-30) mmHg and 14 (9-18.75) mmHg respectively. Median (IQR) IOP for the stable glaucoma group's first and second visits were 14mmHg (10-19) and 12mmHg (10-16.5), respectively. Median (IQR) IOP for the healthy glaucoma group's first and second visits were 13mmHg (9-15) and 14.5mmHg (10-16), respectively.

Table 4.2. Time difference, in days, between first and second visits of participants in the healthy group. LTF = Lost To Follow-up.

Participant ID	Date of Visit 1	Date of Visit 2	Time between visits (days)
N001	12/05/16	20/11/16	192
N002	21/10/15	28/04/16	190
N003	26/08/15	24/02/16	182
N004	20/09/15	18/03/16	180
N005	03/09/15	02/03/16	181
N006	20/08/15	01/03/16	194
N007	30/08/15	29/02/16	183
N008	19/08/15	22/02/16	187
N009	09/09/15	21/03/16	194
N010	04/09/15	03/03/16	181
N011	07/10/15	15/04/16	191
N012	11/09/15	10/03/16	181
N013	18/03/16	20/09/16	186
N014	07/04/16	10/10/16	186
N015	24/04/16	01/11/16	191
N016	08/08/15	10/02/16	186
N017	17/03/16	21/09/16	188
N018	25/11/15	26/05/16	183
N019	26/11/15	24/05/16	180
N020	11/03/16	LTF	NA
N021	31/03/16	LTF	NA
N022	09/05/16	LTF	NA
N023	06/05/16	LTF	NA
N024	11/05/16	LTF	NA
N025	06/10/15	LTF	NA
N026	27/04/16	25/10/16	181

Tables 4.2, 4.3 and 4.4 show the time (in days) between visits in healthy, stable and trabeculectomy groups respectively. These data are graphically represented in Figure 4.6. At least 174 days (5.8 months) had passed between the first and second visit for all participant groups. The maximum time difference between first and second visits was 198 days (6.6 months). At least 172 days (5.7 months) had passed between the date of surgery and the second visit for the trabeculectomy group.

Table 4.3. Time difference in days between first and second visits of participants in stable glaucoma group. LTF = Lost To Follow-up.

Participant ID	Date of Visit 1	Date of Visit 2	Time between visits (days)
S001	02/09/15	11/03/16	191
S002	15/10/15	25/04/16	193
S003	30/09/15	08/04/16	190
S004	08/10/15	06/04/16	181
S005	15/10/15	LTF	NA
S006	14/10/15	25/04/16	194
S007	21/10/15	18/04/16	180
S008	10/11/15	09/05/16	181
S009	22/10/15	LTF	NA
S010	11/11/15	16/05/16	187
S011	19/10/15	21/04/16	185
S012	11/11/15	18/05/16	189
S013	23/11/15	27/05/16	186
S014	04/02/16	16/08/16	194
S015	05/11/15	17/05/16	194
S016	14/01/16	LTF	NA
S017	17/02/16	LTF	NA
S018	02/02/16	11/08/16	191
S019	05/01/16	16/07/16	193
S020	15/02/16	19/08/16	186
S021	17/02/16	23/08/16	188
S022	24/02/16	01/09/16	190
S023	29/03/16	LTF	NA
S024	10/04/16	20/10/16	193
S025	20/06/16	LTF	NA
S026	14/04/16	19/10/16	188

Table 4.4. Time difference, in days, between the first and second visits of participants in the trabeculectomy group. The time difference between the date of the operation and the second visit is also shown. LTF = Lost To Follow-up

Participant ID	Date of Visit 1	Date of Visit 2	Date of Surgery	Time between visits (days)	Time between surgery and Visit 2 (days)
T001	06/10/15	08/04/16	10/10/15	185	182
T002	25/11/15	25/05/16	27/11/15	182	181
T003	22/03/16	20/09/16	29/03/16	182	182
T004	05/11/15	10/05/16	09/11/15	187	183
T005	12/10/15	27/04/16	16/10/15	198	190
T006	21/10/15	28/04/16	25/10/15	190	186
T007	15/09/15	20/03/16	20/09/15	187	182
T008	30/03/16	20/09/16	01/04/16	174	172
T009	18/02/16	30/08/16	27/02/16	194	185
T010	31/03/16	LTF	04/04/16	NA	NA
T011	15/09/15	LTF	19/09/15	NA	NA
T012	30/03/16	LTF	02/04/16	NA	NA

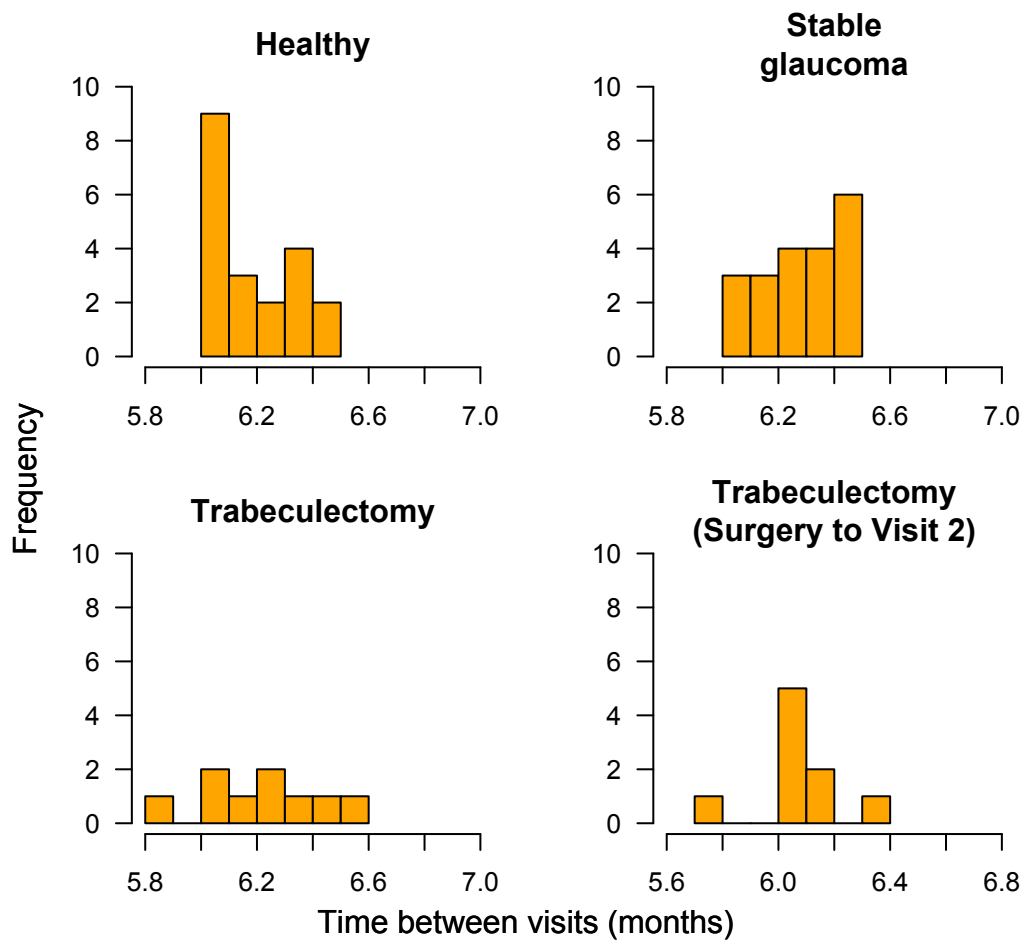


Figure 4.6. Time differences between visits for all participant groups in months. Also time between surgery and visit 2 for trabeculectomy group.

Spatial summation

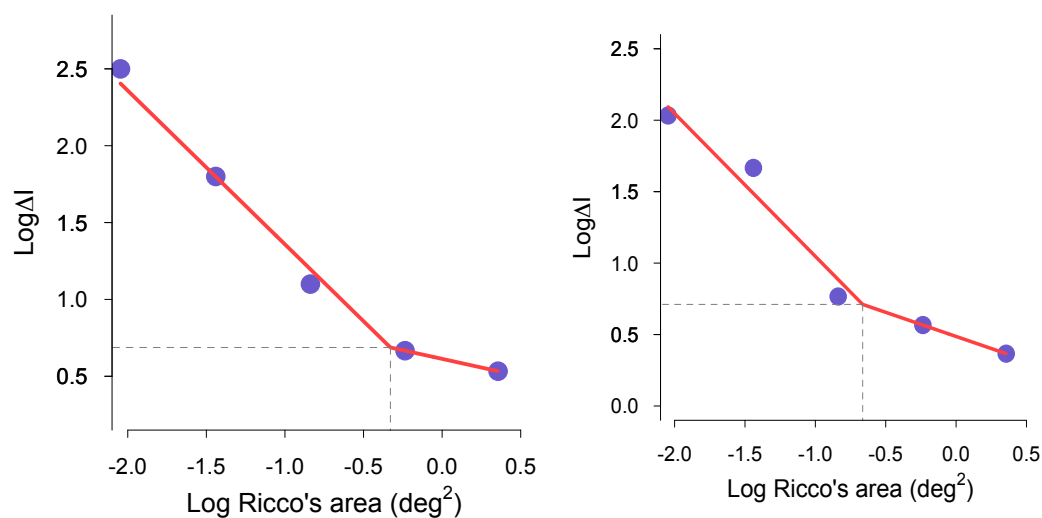


Figure 4.7. Examples of spatial summation curves determined in this study. Left: an example of typical data obtained in the study (two-phase regression line fit $R^2 > 0.9$). Right: an example of variable data from the study that still met the inclusion criterion of $R^2 > 0.9$.

Data were excluded from further analysis if a) a two-phase regression line could not be fitted to the data, or b) r^2 was < 0.9 from the regression.

On this basis, 8 out of 160 spatial summation functions from the first visit, and 15 out of 160 functions from the second visit were excluded from further analysis in the healthy control group. Fifteen out of 160, and 10 out of 160 spatial summation functions were excluded from first and second visit data, respectively, in the stable glaucoma group. Five out of 72, and 3 out of 72 spatial summation functions were excluded from first and second visit, respectively, in the trabeculectomy group.

It can be seen in Table 4.5 and Figure 4.8 that median Ricco's area was larger in the stable group than in the healthy participant group. In addition, median Ricco's area was larger in the trabeculectomy group than that in the healthy participant group at visit 2, but not at visit 1. In all groups, median log Ricco's area enlarged from visit 1 to visit 2.

Table 4.5. Median [IQR] log Ricco's area in each participant group for both visits.

Data were pooled from all locations in all participants with in each group.

	Median [IQR] Ricco's area (deg ²)		P values
	Visit 1	Visit 2	
Healthy	-0.79 [-0.97, -0.61]	-0.73 [-0.93, -0.58]	0.36
Stable glaucoma	-0.67 [-0.84, -0.47]	-0.63 [-0.84, -0.43]	0.34
Trabeculectomy	-0.84 [-1.02, -0.53]	-0.57 [-0.78, -0.41]	0.21

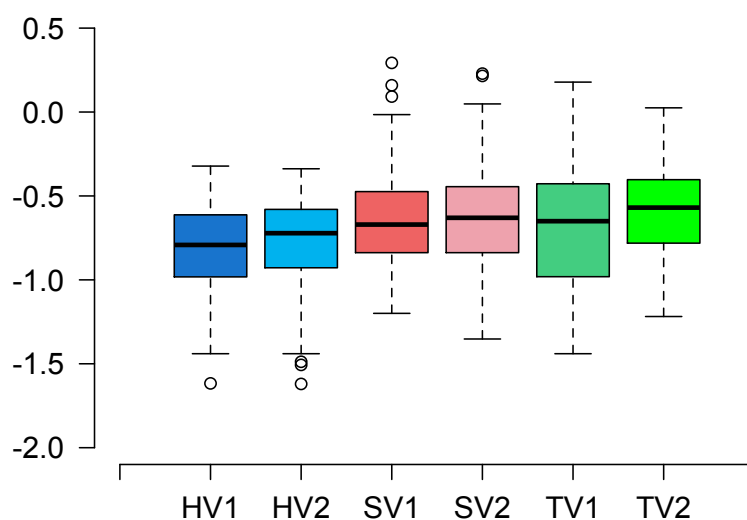


Figure 4.8. Comparison of Ricco's area data pooled for all locations between visits in each participant group (H= healthy group, HV1= visit 1, HV2= visit 2; S= stable glaucoma group, SV1= visit 1, SV2= visit 2; T= trabeculectomy group, TV1=visit 1, TV2= visit 2.)

Table 4.6. Median [IQR] Ricco's area for each participant group, divided into 3 different strata according to TD. The higher the stratum the more negative the TD values are. Note: strata are not continuous across all groups, but are based on TD values in each of the groups, separately.

	Median [IQR] Ricco's area (deg ²)					
	Stratum 1		Stratum 2		Stratum 3	
	Visit 1	Visit 2	Visit 1	Visit 2	Visit 1	Visit 2
Healthy	-0.84 [-0.99 to -0.63]	0.72 [-0.94 to -0.57]	-0.76 [-0.92 to -0.61]	-0.75 [-0.94 to -0.56]	-0.77 [-0.98 to -0.62]	-0.71 [-0.91 to -0.60]
Stable glaucoma	-0.65 [-0.84 to -0.48]	-0.66 [-0.94 to -0.54]	-0.67 [-0.91 to -0.47]	-0.66 [-0.84 to -0.41]	-0.66 [-0.84 to -0.46]	-0.56 [-0.84 to -0.33]
Trabeculectomy	-0.60 [-0.85 to -0.52]	-0.68 [-0.84 to -0.49]	-0.84 [-0.97 to -0.50]	-0.56 [-0.68 to -0.40]	-0.85 [-1.08 to -0.51]	-0.55 [-0.80 to -0.39]

On initial observation of the pooled data, divided by stratum (Figure 4.9), there does not appear to be any meaningful difference in median Ricco's area between visits for the healthy and stable glaucoma groups in any stratum. However, there does appear to be a slightly smaller median Ricco's area at the second visit for the trabeculectomy group in stratum 1, but a larger median Ricco's area on the second visit in strata 2 and 3.

To gain an overall impression of changes in Ricco's area between visits, Ricco's area values, pooled from all locations per participant group, were plotted for each visit (Figure 4.10). A paired t-test was carried out on these data (with a Holm-Bonferroni correction). This showed a statistically significant difference between visits in stratum 3 for the trabeculectomy group ($p=0.04$), but not in any of the other strata in any other participant group.

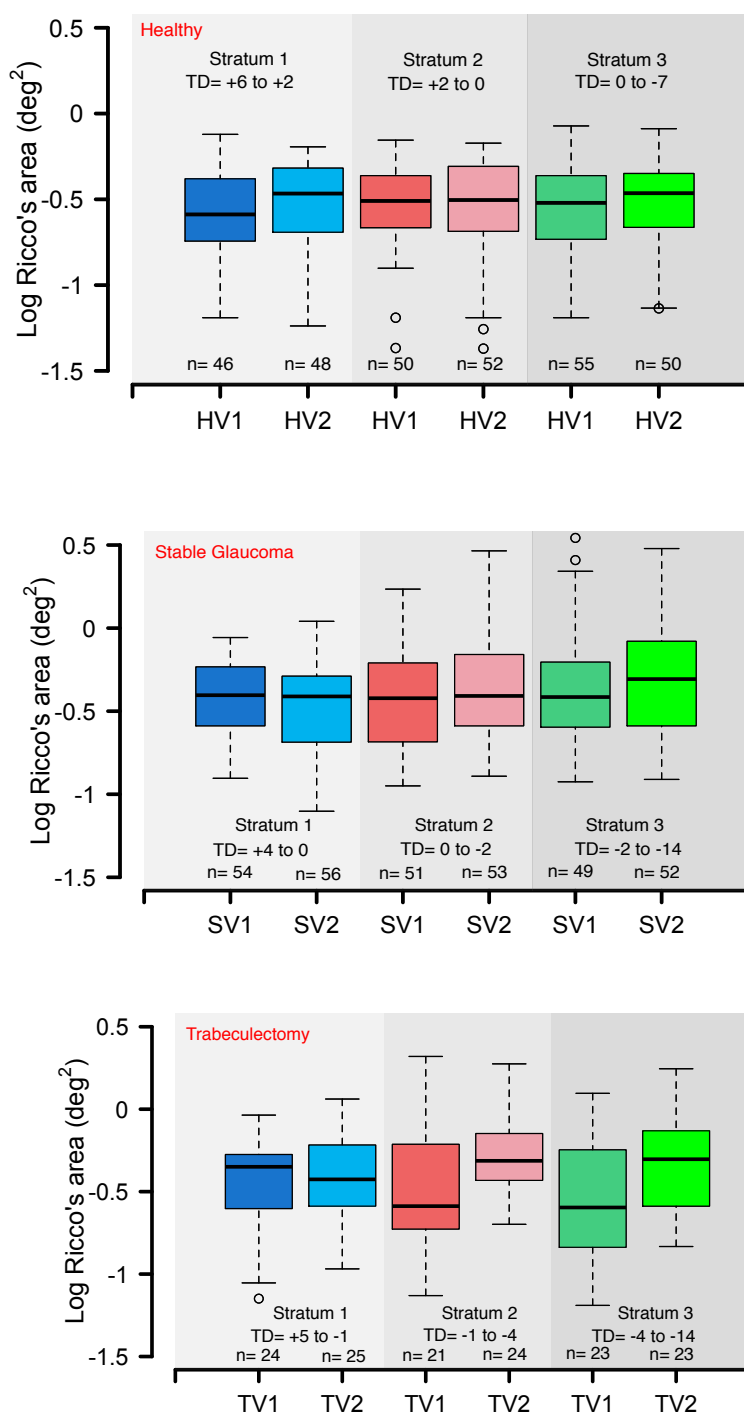


Figure 4.9. Comparison of Ricco's area data pooled for all locations between visits across different strata in each participant group (Top: healthy group. HV1= visit 1, HV2= visit 2; middle: stable glaucoma group SV1= visit 1, SV2= visit 2; bottom: trabeculectomy group. TV1=visit 1, TV2= visit 2.)

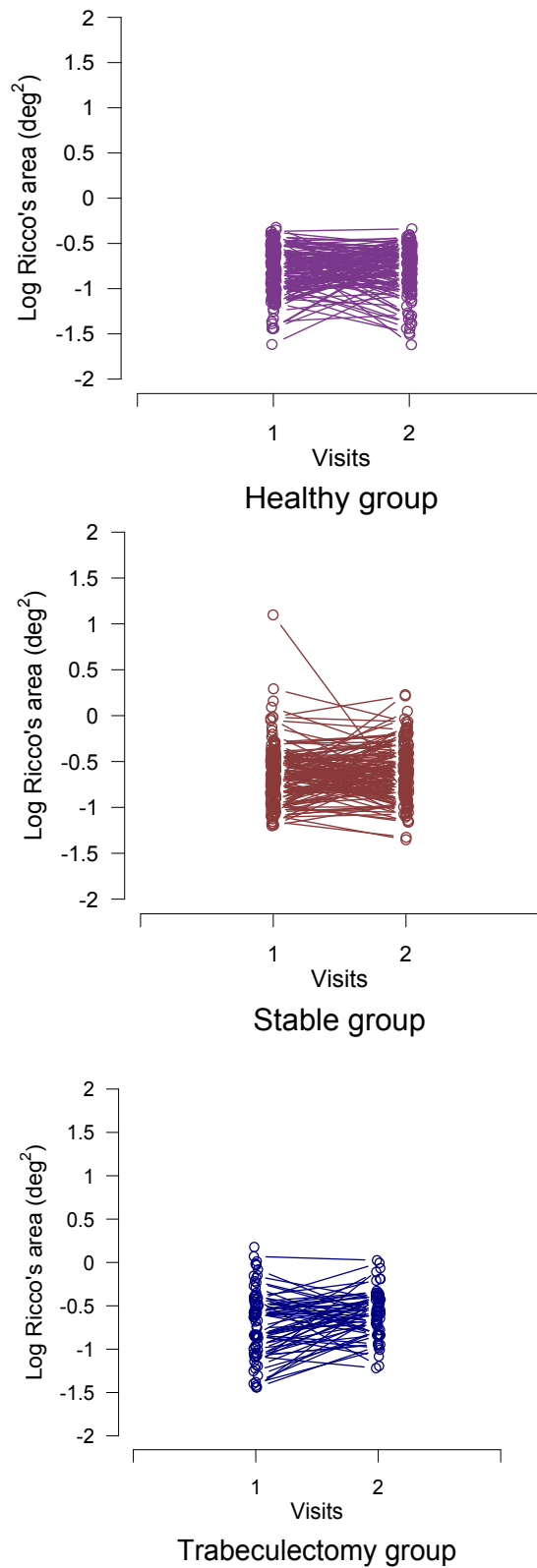


Figure 4.10. Ricco's area at each location on visits 1 and 2 in healthy (top left), stable (top right) and trabeculectomy groups (bottom).

When data are separated and shown paired by location in this way (rather than pooling all locations), it can be seen that while in some locations, Ricco's area is larger in the second visit than in the first, the opposite can be seen in other locations. There are also locations in which no notable change in Ricco's area can be seen. The spread of the data is approximately equal for the first and second visit in the healthy group, and also in the stable glaucoma group, with the exception of one location that shows a large reduction between visits. The spread of data is larger in the stable group compared to healthy. The spread of the data in the trabeculectomy group is larger in the first visit compared to that of data at the second visit. Even though not all locations showed an enlargement of Ricco's area, there was a greater number of positive than negative slopes (i.e. more instances in which Ricco's area was larger on the second visit) in this group. Overall, positive slopes were also steeper than negative slopes. The finding from the binomial test suggests that the greater occurrence of positive slopes was not due to chance ($p=0.005$).

Linear mixed model analysis revealed that the effect of participant type on the between-visit difference in Ricco's area was not statistically significant. However, when we view the effect sizes, it can be observed that the between-visit difference in Ricco's area for the stable glaucoma group was just 0.01 (SE = ± 0.05) $\log \text{deg}^2$ greater than that found in the healthy control group. In contrast, the between-visit difference in Ricco's area in the trabeculectomy group was 0.15 (SE = ± 0.07) $\log \text{deg}^2$ greater than that found in the healthy control group (and 0.14 $\log \text{deg}^2$ greater than that found in the stable glaucoma group). The median enlargement of Ricco's area in healthy controls was 0.06 $\log \text{deg}^2$, therefore, the model reports between-visit differences in Ricco's area of 0.07 $\log \text{deg}^2$ in the stable glaucoma group, and 0.21 $\log \text{deg}^2$ in the trabeculectomy group. Inspections

of the residuals confirmed normality and no heteroscedasticity. When the analysis was repeated with data for the healthy group removed from the dataset, the effect of participant type on between-visit Ricco's area was borderline statistically significant ($p=0.05$).

Table 4.7. Median [IQR] sensitivity (dB) in all participant groups at both visits

Participant group	Visit	Median [IQR] sensitivity (dB)				
		GI	GII	GIII	GIV	GV
Healthy	1	17.67 [16.83 to 19.34]	23.71 [23.22 to 25.90]	28.98 [28.12 to 29.76]	31.77 [31.51 to 32.04]	33.66 [32.84 to 34.58]
	2	17.73 [16.12 to 18.63]	23.78 [22.69 to 25.95]	29.14 [28.67 to 29.79]	31.96 [30.86 to 32.44]	33.62 [32.87 to 34.65]
Stable	1	15.62 [14.66 to 15.98]	22.63 [21.85 to 23.66]	28.24 [26.99 to 28.93]	29.87 [28.67 to 31.63]	31.75 [31.18 to 32.86]
	2	15.97 [13.93 to 16.95]	21.95 [20.18 to 24.50]	27.84 [26.78 to 28.77]	30.42 [29.11 to 31.39]	32.16 [31.68 to 33.31]
Trabeculectomy	1	17.62 [17.02 to 17.94]	24.62 [21.68 to 24.95]	28.23 [27.99 to 28.66]	30.74 [26.60 to 30.57]	32.99 [32.69 to 34.27]
	2	14.66 [13.24 to 16.62]	21.97 [20.21 to 23.67]	27.92 [24.97 to 28.62]	30.26 [30.15 to 31.26]	32.68 [29.87 to 32.78]

Sensitivity values were pooled across all locations in all participants, in each participant group. Sensitivity was greater to larger stimuli in all participant groups, in line with spatial summation (Table 4.7). Median sensitivity to a Goldmann I stimulus was lower in both visits for stable glaucoma group, compared to that in the healthy group. The

difference in median sensitivity to a Goldmann II stimulus (and larger stimuli) was less between these participant groups. Median sensitivity to a Goldmann I stimulus in the trabeculectomy group was more similar to that in the healthy group at the first visit. However, median sensitivity to the Goldmann I stimulus in the trabeculectomy group was reduced in visit 2 and closer to that in the stable group. For each Goldmann stimulus, a one-tailed paired t-test was performed on pooled data to investigate changes in sensitivity between visits. Between-visit changes in sensitivity to all stimuli were not statistically significant (all $p > 0.12$), except for the reduction in sensitivity between visits for a Goldmann I ($p = 0.03$).

Figure 4.11 shows that there is no relationship between changes in IOP between visits with changes of RA between visits, it appears that changes in Ricco's area is not dependent on the reduction of IOP. This absent of relationship persisted through all stratum/ no different pattern detected with worsening of TD values. There is wide variation of Ricco's area sizes at different level of IOP changes.

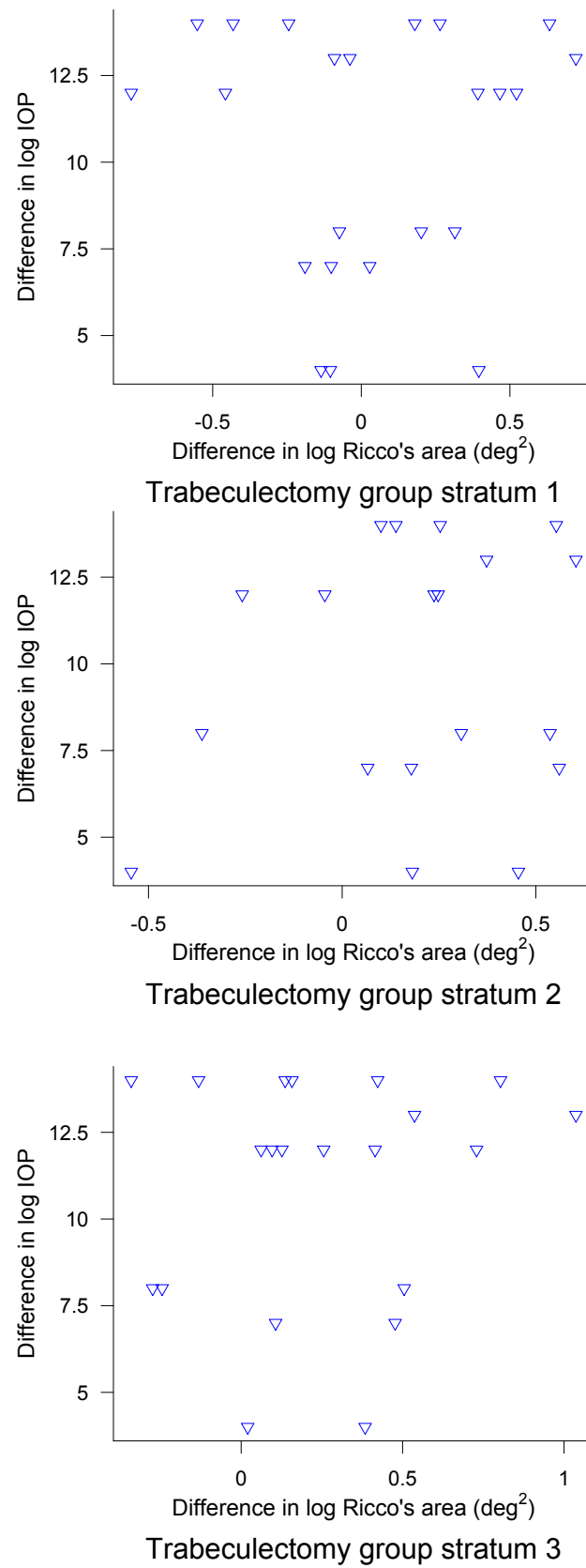


Figure 4.11. Difference in IOP between visits as a function of difference in Ricco's area on trabeculectomy group.

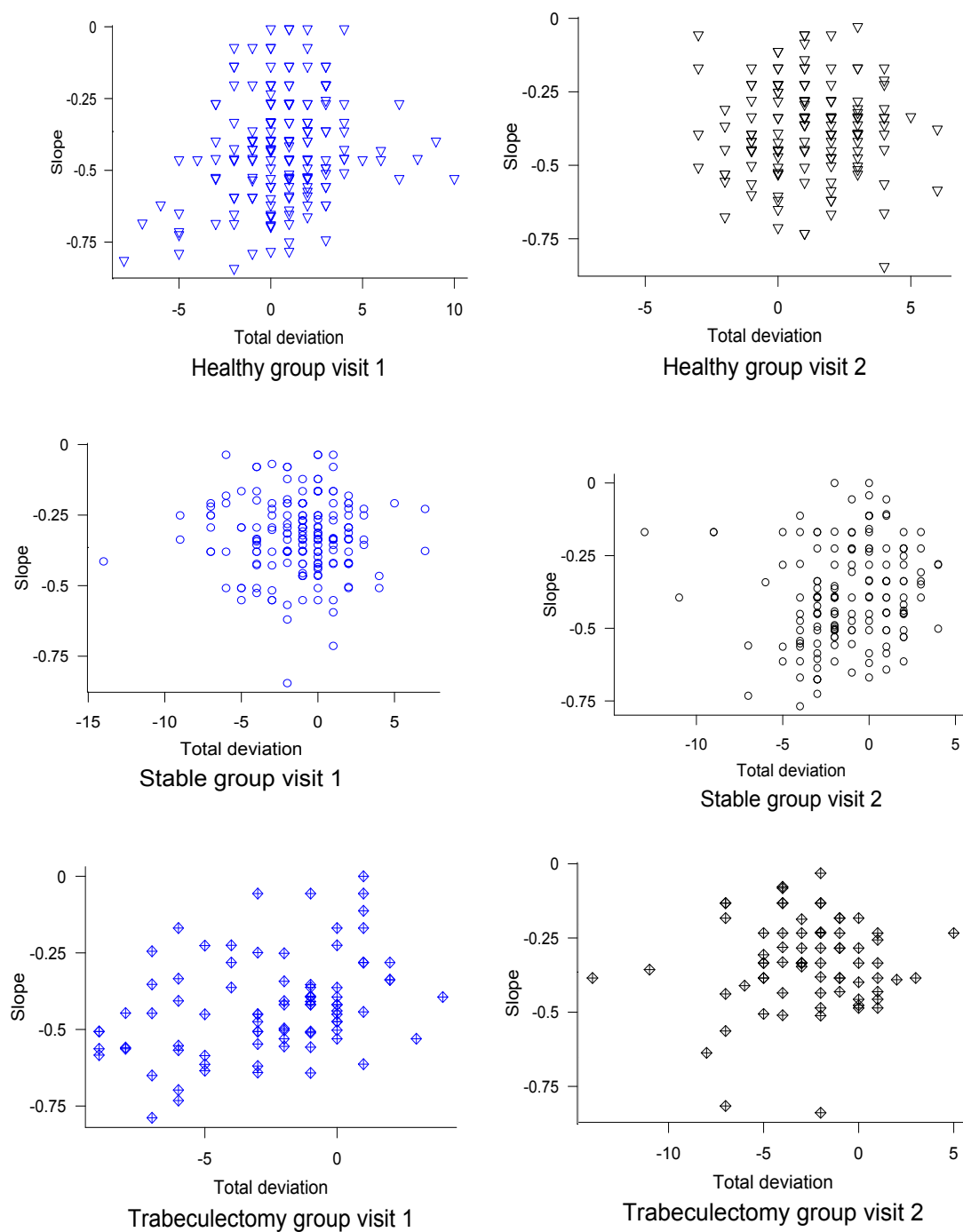


Figure 4.12. Slope of second line as a function of total deviation in all participant groups on both visits.

Figure 4.12 shows that there is a wide variation of slope of the second line of the two-phase regression in all participant groups. For reference, a slope of 0 in the second line of the spatial summation function means that the line is flat and there is no summation

with increasing stimulus area. A slope close to -1 indicates that the relationship between intensity and area at threshold is close to that described by Ricco's law. The two phase-regression analysis determines the breakpoint as the point at which Ricco's law no longer holds. Therefore, in this analysis, the slope of all second lines will be between -1 and 0. Second line slopes were averaged per participant, giving 20 values for the healthy group, 20 for the stable glaucoma group, and 9 for the trabeculectomy group, for each visit. An independent samples t-test showed that there was no statistically significant difference in second line slope between glaucoma patients (combined stable glaucoma and trabeculectomy group data) and healthy controls ($p(\text{visit1}) = 0.47$, $p(\text{visit2}) = 0.62$). When comparing the second slope between the stable glaucoma group and healthy controls, there was still no statistically significant difference ($p(\text{visit 1}) = 0.98$, $p(\text{visit 2}) = 0.69$). Finally, there was no statistically significant difference in the slope of the second line between the stable glaucoma group and the trabeculectomy group ($p(\text{visit 1}) = 0.18$, $p(\text{visit 2}) = 0.93$).

To add context to the changes between visits reported here, the average change in linear RGC number from the first to the second visit was +1.19 in the healthy group, +0.45 in the stable glaucoma group, and -7.8 in the trabeculectomy group.

There is no statistically significant relationship between log Ricco's area and age in the healthy participant group for both visits ($p(\text{visit1}) = 0.39$, $p(\text{visit2}) = 0.1$, $\text{slope}(\text{visit1}) = -0.68$, $\text{slope}(\text{visit 2}) = -0.53$) (Figure 4.13).

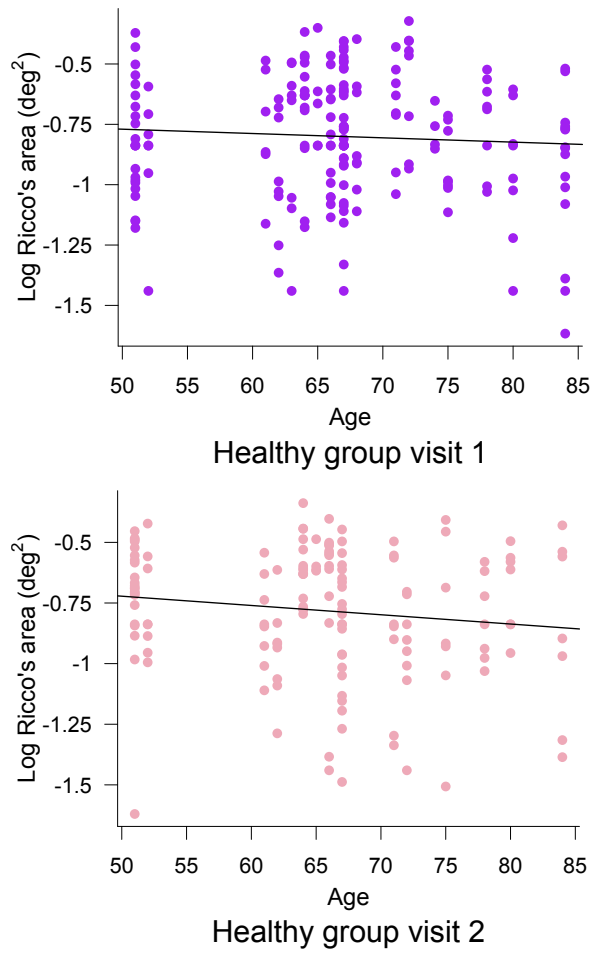


Figure 4.13. Ricco's area size obtained per location from healthy participants' against age for different visits.

4.6.2. Experiment 2

Figures 4.14, 4.15 and 4.16 show the between-visit difference in front (ΔA_f) and back (ΔA_b) corneal surface Zernike coefficients for the 28 Zernike polynomials within the first 6th radial orders in all participant groups.

ΔA_f is smaller than ΔA_b in the healthy group. However ΔA_f appears to be highest for Zernike polynomial 9, but this is not observed for ΔA_b . Likewise, low ΔA_b is observed for the lowest order polynomials, which is not apparent to the same extent with ΔA_f .

Although there is some variance in ΔA_f and ΔA_b across all 28 polynomials in the stable glaucoma group, qualitatively there are no obvious deviations from 0 (Figure 4.15). In the trabeculectomy group, however, the variance in ΔA_f and ΔA_b across polynomials appears qualitatively larger than that in the stable glaucoma and healthy groups, and with greater magnitude, particularly for the lower order polynomials (Figure 4.16). However, there is little consistency between groups in the polynomials for which ΔA_f and ΔA_b are greatest.

When compared with the Zernike coefficient data obtained from healthy subjects in Chapter 2, the polynomial with the greatest ΔA_f and ΔA_b do not match. In the exploratory study explained in Chapter 2, the greatest ΔA_f is Zernike polynomial 2. In the current study, although the healthy group also has the greatest A_b in Zernike polynomial 0, the extent of difference is larger and the stable glaucoma group has the greatest ΔA_f and ΔA_b in different Zernike polynomials.

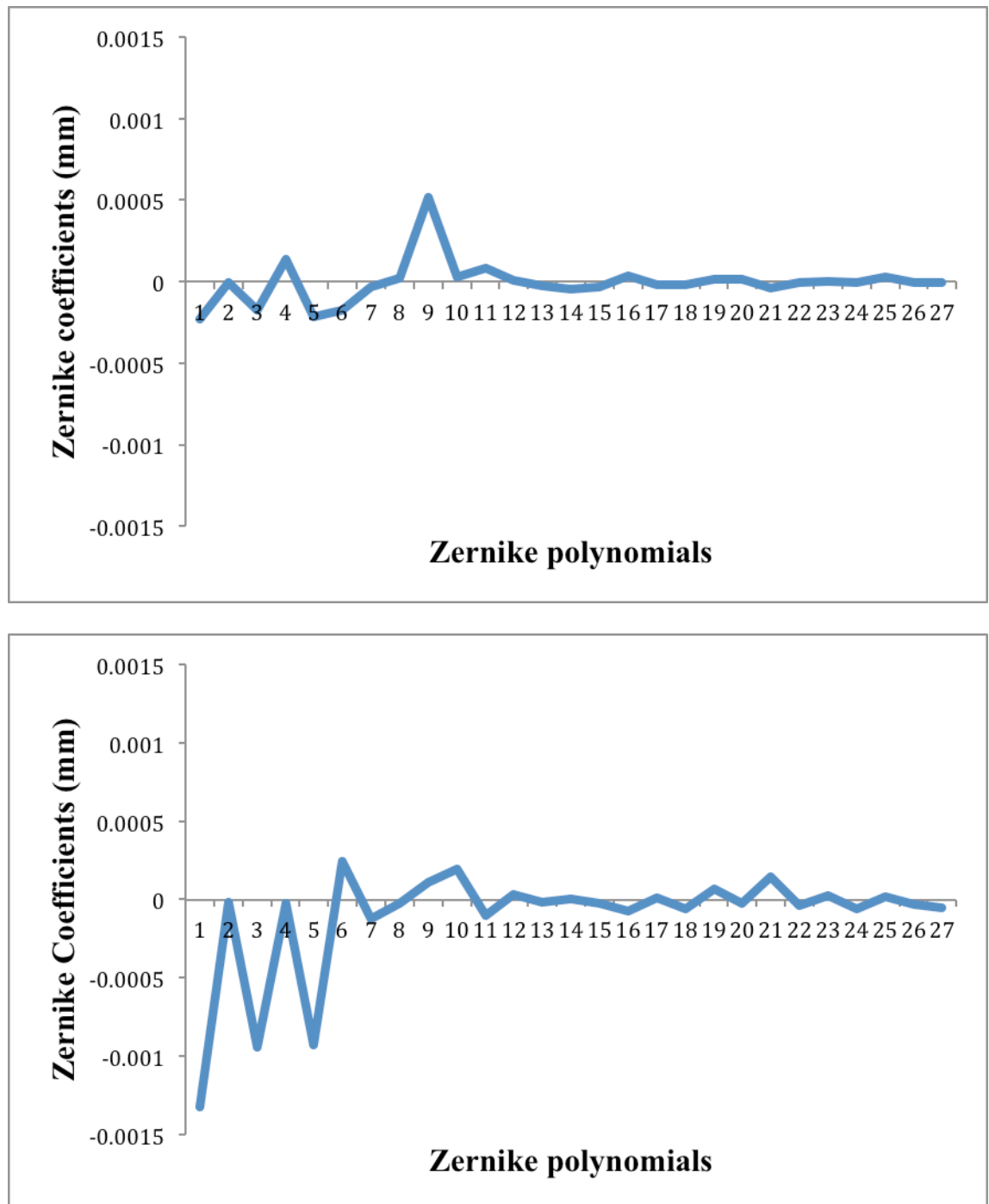


Figure 4.14. Difference in Zernike coefficients for 28 Zernike polynomials contained in the first 6 radial orders for the front (top) and back (bottom) surface of the cornea in the healthy group.

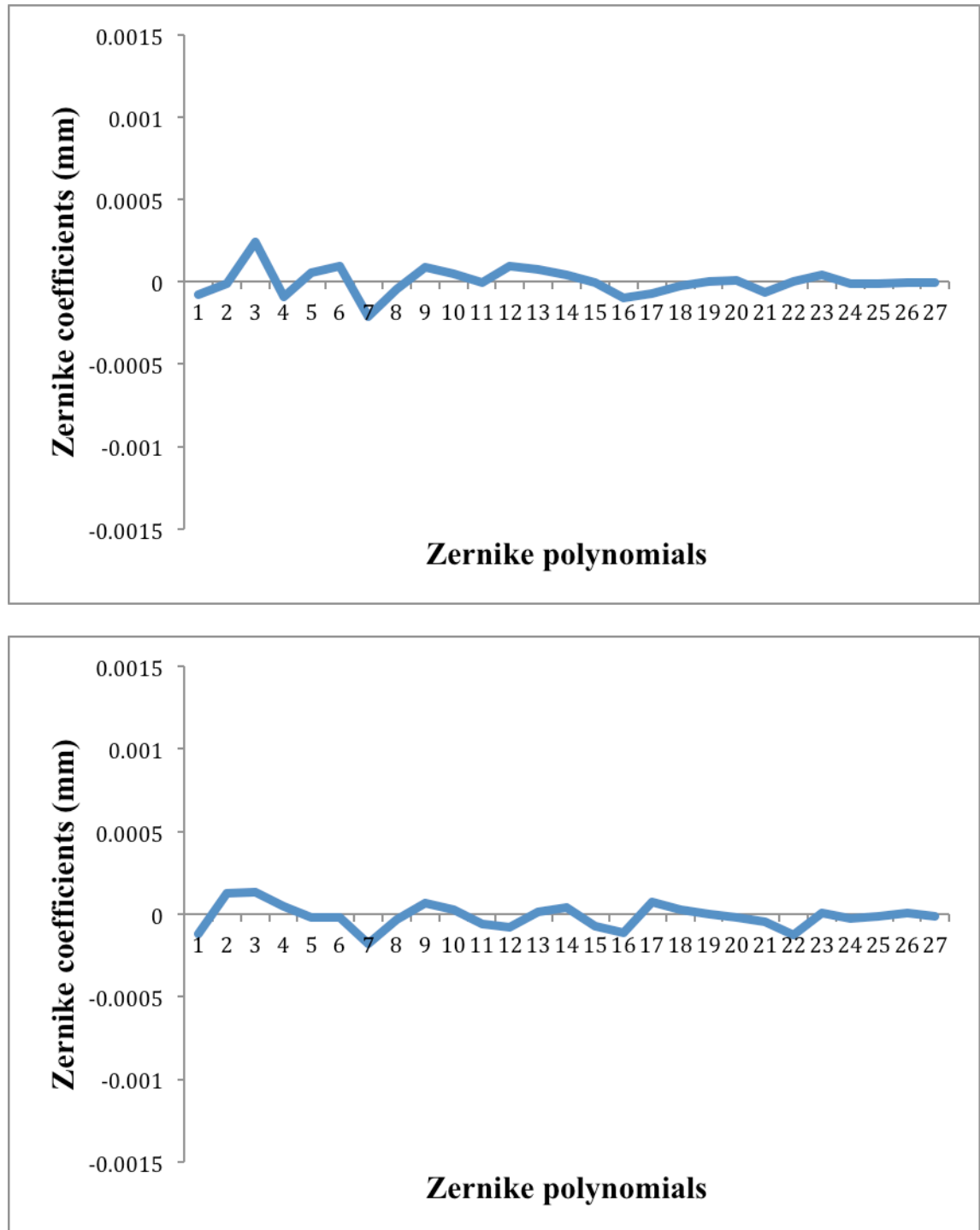


Figure 4.15. Difference in Zernike coefficients for 28 Zernike polynomials contained in the first 6 radial orders for the front (top) and back (bottom) surface of the cornea in the stable glaucoma group.

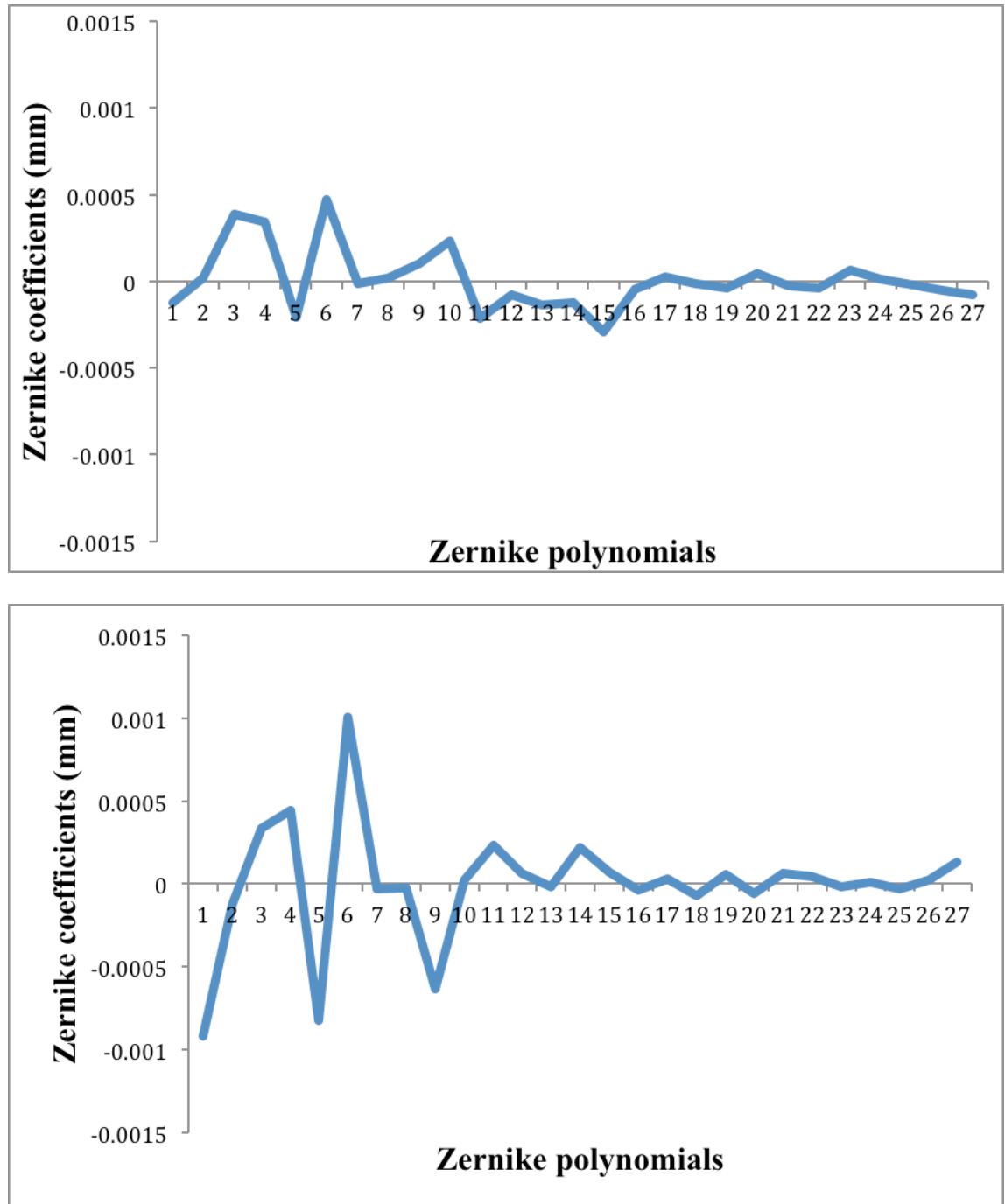


Figure 4.16. Difference in Zernike coefficients for 28 Zernike polynomials contained in the first 6 radial orders for the front (top) and back (bottom) surface of the cornea in the trabeculectomy group.

Table 4.8. Zernike coefficients (mm) for polynomials of the first 6 radial orders from the front surface of the cornea of all participant groups in both visits.

Types		0	1	2	3
Median healthy 1st visit		0.135128667	0.000125333	0.000705	-0.00000233
Median stable 1st visit		0.136450167	0.000509167	-0.0006	3.69835E-05
Median trabeculectomy 1st visit		0.135	0.000281	-0.001446667	-0.000377333
Median healthy 2nd visit		0.134320333	0.000180333	0.000955	0.000322333
Median stable 2nd visit		0.136277833	0.000516334	-0.000256834	0.000005
Median trabeculectomy 2nd visit		0.133415333	0.000456333	-0.000507	0.000364
4	5	6	7	8	9
0.080192	0.000586333	0.0000363	0.000101333	0.0000907	0.0000277
0.080805334	0.000542	0.0000275	0.000105	-0.000278833	0.0000065
0.079533333	0.000815333	-0.0000443	0.000204	-0.000162667	0.0000747
0.079496	0.000506333	-0.000021	0.0000967	0.0000537	0.0000727
0.080722167	0.000363	-0.00008	9.33165E-05	-0.00013515	0.00007415
0.078664667	0.001265	-0.000113	0.000271	0.000263	0.000199333
10	11	12	13	14	15
0.000042	0.0000227	0.001460333	-0.0000367	-0.000123	-0.000029
0.0000045	0.000019185	0.00143	-0.00000165	-0.000048	-0.000009485
0.000238667	0.0000297	0.001491667	-0.00000133	-0.000158	-0.000075
0.0000743	0.0000253	0.001412667	-0.0000837	-0.000057	0.0000157
0.00003185	-0.00003215	0.001470167	0.000010165	-0.000028835	-0.00007515
0.000160667	0.00000367	0.001393	-0.000201	-0.000317	-0.0000727
16	17	18	19	20	21
-0.0000273	0.000074	-0.000126	-0.0000337	-0.00000133	-0.000062
-0.0000355	-0.000002	-0.000032	-0.00003185	-0.00007635	-0.0000545
-0.000119667	0.000034	0.0000653	0.000103667	0.0000527	-0.0000977
0.000000333	0.0000333	-0.000109667	0.00000767	-0.0000927	-0.0000437
-0.000068	0.000004	0.00001915	-0.00002835	-0.000078	-0.000036
-0.000101	0.000015	-0.00000167	0.000204	-0.0000607	-0.000208333
22	23	24	25	26	27
0.0000653	0.000011	-0.0000873	-0.0000183	0.000006	0.000008
0.0000412	0.000025	-0.00003665	-0.000003	-0.000019685	0.000011185
0.0000293	0.000000333	-0.0000427	-0.0000143	0.000007	0.000068
0.000077	0.00000667	-0.0000593	-0.0000163	-0.000007	-0.0000187
0.0000605	0.000024	-0.0000538	-0.0000105	-0.000004835	0.00000167
0.000122	0.0000117	-0.000105	-0.0000453	-0.000069	-0.000065

Table 4.9. Zernike coefficients for polynomials of the first 6 radial orders from the back surface of the cornea of all participant groups in both visits.

Types		0	1	2	3
Median healthy 1st visit		0.163817	-0.000383	0.001034	0.001744333
Median stable 1st visit		0.1588005	0.000167667	0.000564333	0.001119833
Median trabeculectomy 1st visit		0.163272167	0.0003745	0.0000425	0.000715334
Median healthy 2nd visit		0.163556333	-0.000283333	0.001228667	0.001456
Median stable 2nd visit		0.158681	0.000202667	0.000652833	0.0013725
Median trabeculectomy 2nd visit		0.160702667	0.00053	0.001107	0.0012
4	5	6	7	8	9
0.096768667	0.001353333	-0.000112	0.000695333	-0.000499333	0.000319333
0.093582	0.000964667	-0.000118167	0.000371	-1.16665E-05	0.000504
0.0958585	0.001216167	-0.000113684	0.000536184	-0.000534	0.000223334
0.096425	0.000668	-0.000235333	0.000573333	-0.000297333	0.000399
0.093474667	0.001551667	-0.000283667	0.000297	0.000272834	0.000306667
0.094996	0.001544	-0.000152667	0.000575	-0.0003	0.000188
10	11	12	13	14	15
0.000666667	0.0000717	0.001593333	-0.000247333	0.000423667	0.000113333
0.000684167	0.000134834	0.001365333	-0.000314167	0.000544	0.0001325
0.000370667	0.0001685	0.001394334	-0.000262834	0.0004395	0.00007315
0.000593	0.0000583	0.001598333	-0.000178667	0.000499333	0.0000467
0.000408	0.00007065	0.001489334	-0.0003075	0.000633	-0.0000688
0.000569667	-0.00003	0.001196667	-0.000117333	0.000308333	0.000071
16	17	18	19	20	21
0.0000883	0.000063	-0.000127333	-0.0000627	0.000037	0.000149333
0.00004465	0.000036	0.0000305	0.00004865	-0.0000705	0.00005785
0.000134833	-0.000019985	-4.99835E-05	0.00006765	-0.0000812	-0.00005715
0.0000713	0.000031	-0.0000623	-0.0000127	0.000237333	0.00000567
0.000107684	0.000024015	0.000054	0.00007885	5E-07	-0.000018685
0.0000583	-0.000178667	0.0000157	-0.00000267	-0.0000537	0.000042
22	23	24	25	26	27
-0.000202667	-0.000042	0.0000207	0.0000317	-0.000209667	0.00027
-0.000182834	-0.000003685	-0.00004065	0.0000225	-0.000226334	0.0000585
-0.000144484	-0.0000542	-0.000001665	0.0000595	-0.000357	0.0001885
-0.000148333	-0.0000353	0.0000157	0.000048	-0.000248333	0.000241
-0.000163167	-0.0000555	-0.0000267	0.000001665	-0.000327167	9.43335E-05
-0.000225333	-0.0000663	0.0000313	0.000057	-0.00014	0.000257

The linear mixed model analysis showed that the effect of ΔA on ΔRA is not statistically significant ($p = 0.98$). Incorporating ΔA , polynomial number, and corneal surface into the model (but only on superior visual field data), reveals that ΔRA in the stable glaucoma group is 0.053 [SE: ± 0.07] smaller than that in the healthy group, and that ΔR in the trabeculectomy group is 0.16 [SE: ± 0.09] larger in the trabeculectomy group than in the healthy group. However, the effect of participant type still did not

reach statistical significance ($p = 0.09$). Inspection of the residuals in both models confirmed normality and no heteroskedasticity.

4.7. Discussion

The aim of this study was to investigate changes in Ricco's area in glaucoma patients, before and after IOP-lowering treatment, in order to test the hypothesis that an enlarged Ricco's area in glaucoma returns to normal (or near normal) levels following IOP-lowering treatment. Secondary aims were to investigate whether or not Ricco's area is enlarged in patients requiring trabeculectomy surgery, relative to that in stable glaucoma participants for whom surgery is not required; and also, to investigate any changes in Ricco's area that may have occurred during this timescale in stable glaucoma participants, relative to that in normals, in the absence of significant change in sensitivity to a conventional perimetric stimulus. Patients requiring trabeculectomy as part of their clinical care underwent measurements of spatial summation, from which Ricco's area was determined, within a matter of days prior to surgery, and again, approximately 6 months later. The same experiments were performed at the same intervals in two control groups, one of which consisted of stable glaucoma patients and the other, healthy individuals without glaucoma.

In agreement with the findings of Redmond *et al.* (2010a), This study has also found that Ricco's area is, overall, larger in trabeculectomy and stable glaucoma groups compared to that in healthy participants in our study. The enlargement of Ricco's area between the first and second visit in the trabeculectomy group reached statistical significance only for the most severe TD group (stratum 3, moderate-to-advanced visual field damage). When analysing the effect of participant group on between-visit differences in Ricco's area, linear mixed effects model analysis reported a greater difference between visits for the trabeculectomy group than for the stable glaucoma and

healthy control groups, though the effect of participant type, overall, was not statistically significant ($p = 0.09$). When the data from the healthy group were eliminated from the data set, the model reported that the effect of participant type on between-visit differences in Ricco's area was borderline significant ($p = 0.05$). This suggests that there are indeed genuine differences between first and second visits for trabeculectomy participants, particularly given the short timescale over which measurements were repeated (approximately 6 months), and the fact that the median between-visit differences in normals was much smaller ($0.06 \log \text{deg}^2$). It is worth noting, that in the study of Redmond *et al.* (2010a), the average difference in Ricco's area between glaucoma patients and controls was $0.65 \log \text{deg}^2$, so the change in Ricco's area observed over approximately 6 months in this study is approximately 33% of what was found between groups by Redmond *et al.* (2010a).

The magnitude of IOP reduction is related to the risk of glaucoma progression, with each mmHg reduction of IOP causing a lowering of the risk of glaucoma progression by 10% (Leske et al. 2003). Therefore, the pattern of Ricco's area changes could be different with topical treatment of IOP, as the lowering of IOP would not be as drastic when compared to that encountered following the trabeculectomy procedure. Hence, the risk of progression may be greater with topical treatment. This perhaps could result in larger Ricco's area post-treatment compared to what was found following the trabeculectomy procedure.

As previously discussed, trabeculectomy can affect the curvature of the corneal surface, and therefore the retinal image size of the stimulus which, in turn, can have an effect on the measured Ricco's area. Therefore, an investigation of the effect of between-visit differences in corneal aberrations on between-visit differences in Ricco's area was also

warranted. A comparison of Zernike coefficients between visits showed high within-subject variability even in healthy participants. This is further supported by the fact that there is no consistency in the polynomial coefficient that changes most between visits in stable glaucoma patients and healthy controls. As there is no expected change in corneal curvature in both stable glaucoma and healthy participants, they would be expected to have similar changes (if any) in the Zernike coefficients between visits. In fact, in some of the Zernike polynomials, the between-visit difference in coefficients is actually larger in the healthy group than that in the trabeculectomy group. When the linear mixed effects model analysis was repeated, this time only including psychophysical data from the superior hemifield and including the effects of between-visit differences in aberrations (back and front surface), it is evident that the effect of participant type on between-visit differences in Ricco's area was largely unchanged. This suggests that any observed changes in Ricco's area between visits in the current study are unlikely to be related to surgically-induced corneal changes, and more likely owing to true neurological changes.

Sensitivity to Goldmann I-V is similar between visits in healthy and stable glaucoma groups. However, this is not the case for the trabeculectomy group. There are differences in sensitivity, between visits, to all Goldmann sizes in this group, however the difference becomes less obvious with increasing stimulus area. This supports the notion of a rightward shift of the spatial summation curve between visits, along the area axis (Figure 4.1 from into aim). This difference between visits does not reach statistical significance however, nor does the overall between-visit difference in Goldmann III sensitivity (average: 0.31dB). Sensitivity to Goldmann I and Goldmann II stimuli are reduced in the stable glaucoma group, compared to that in healthy controls. Again, this

difference is less obvious with increasing stimulus size, supporting the notion of an enlarged Ricco's area in glaucoma, relative to that in healthy controls. The reason for such an obviously lower sensitivity to smaller Goldmann sizes could be due to the fact that the stimulus falls within Ricco's area in that region of the visual field. According to the hockey-stick model of Swanson *et al.* (2004), the relationship between log RGC number and visual field sensitivity (in dB) is 1:1 when the stimulus is smaller than Ricco's area. Therefore, for a given RGC dropout, a reduction in sensitivity to smaller stimuli will be more obvious.

The data showed a wide range of second line slope values (ranging from 0 to close to -1) in all participant groups that are not influenced by changes in total deviation values measured with SITA-Standard 24-2 test. Although probability summation is frequently described by Piper's law (Piper, 1903), among others, this finding suggests caution should be exercised in making assumptions regarding the slope of the second line in future experiments aimed at mapping to the spatial summation function with perimetric stimuli or modelling of perimetric sensitivity based on measures of Ricco's area. As Brindley (1970) points out, Piper's law is only demonstrable under precise experimental conditions. The findings here are also in agreement with the previous study of (Redmond *et al.* 2010b), that there is no statistically significant association between Ricco's area and age. However, there are large variations in the size of Ricco's area size at different ages.

There are several possible explanations for the enlargement of Ricco's area between the first and second visit that is observed in the second and third stratum of the trabeculectomy group. What is unknown is how Ricco's area might have changed had the trabeculectomy procedure not been undertaken, and the patient had continued with

their previous treatment regime. It is possible that even though Ricco's area enlarged between visits in the trabeculectomy group, it might have enlarged by a greater degree, had the patients not have received this surgery. This is illustrated in Figure 4.17. It might be assumed that, had the trabeculectomy procedure not been carried out just after visit 1 (V1 in the Figure), Ricco's area would have reached a value of A, instead of B. However this cannot be ascertained, as we do not have a measurement from a period of time before the surgery. We only have one measurement taken up to 2 weeks before the surgery, so it is not possible to know the rate at which Ricco's area enlarged before the first visit, and what trajectory the trend would have taken had the trabeculectomy not been performed.

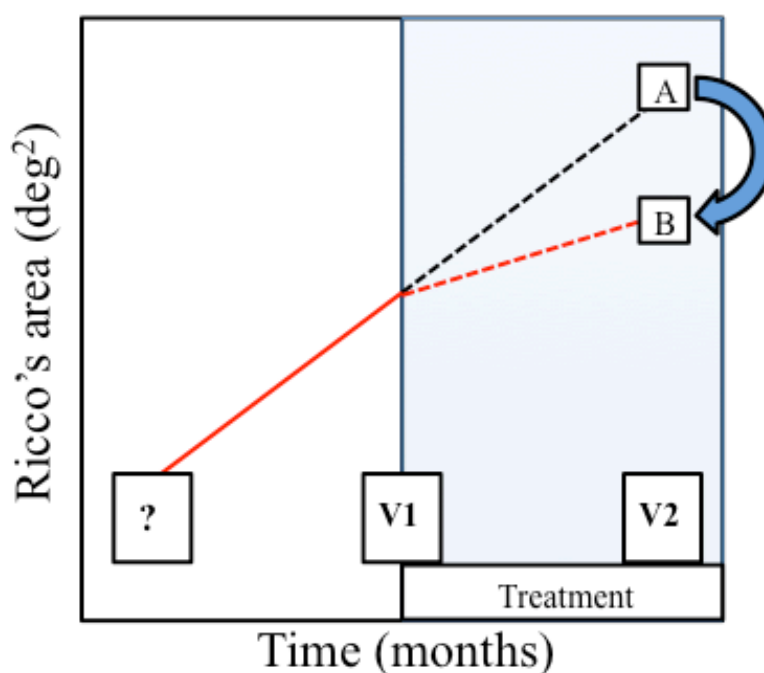


Figure 4.17. Graphical explanation of one of the hypothesis. B is where current Ricco's area size is after trabeculectomy surgery. A is the possible Ricco's area size if

trabeculectomy surgery had not been performed. However this cannot be ascertain as measurement was not taken some time before surgery. V1= visit 1, V2= visit 2.

Even though trabeculectomy surgery eliminates issues of compliance with topical medication, it may be that the surgery is not as effective as one might hope, given that changes in Ricco's area are measurable approximately 5.5 – 6 months following surgery. An alternative hypothesis is that the trabeculectomy did, in fact, slow down, or halt (in the case of the lower stratum), what might have been a greater change in Ricco's area had the eye not undergone the trabeculectomy procedure. Again, it is difficult to confirm or refute these ideas, given that the pre-surgery rate of change of Ricco's area is unknown. Such a study would require > 5 years of follow-up to establish baseline levels. Lowering IOP has previously been observed to improve visual function in some cases however this treatment method is mostly chosen because IOP is the only modifiable risk factor in glaucoma. In the absence of an alternative treatment that does not rely on patient compliance, and a longitudinal study observing the effects of intervention with trabeculectomy on a range of visual functions, one cannot make firm recommendations on the optimum treatment regime.

It is possible that the slight reduction in overall Ricco's area in stratum 1 is the result of recovery from what was originally RGC dysfunction and that the enlargement of Ricco's area observed 6 months after surgery in strata 2 and 3 of the trabeculectomy group is due to a delayed neural compensation mechanism to RGC dropout i.e. that the trabeculectomy did, in fact, prevent further retinal damage, but that the visual cortex continued to recover thereafter. In support of the former point, it was hypothesised that dysfunction would occur in very early glaucoma, and the locations represented in

stratum 1 meet this criterion. In support of the latter notion, the findings in amblyopia (Chapter 3), together with evidence in previously published literature suggest that Ricco's area represents spatial pooling at multiple hierarchies in the visual pathway, including cortical loci (Pan & Swanson 2006; Redmond *et al.* 2010a) (see Chapter 3 for a full review). Pan & Swanson (2006) demonstrate that spatial summation of perimetric stimuli cannot be accounted for by probability summation across RGCs, but rather multiple cortical pooling mechanisms. Therefore it is possible that changes in Ricco's area observed in glaucoma participants, as measured with perimetric stimuli, have a cortical basis. Studies have shown that even when Ricco's area enlarges with retinal eccentricity, the threshold at Ricco's area is constant overall (Fischer 1973; Ransom-Hogg & Spillmann 1980; Volbrecht *et al.* 2000; Wilson 1970).

Swanson *et al.* (2004) reported that Ricco's area covers, on average, 31 RGCs across the normal visual field. Based on this report, Redmond *et al.* (2010a) put forward a hypothesis to explain the larger Ricco's area in glaucoma patients, relative to that in healthy controls. The hypothesis states that in the visual cortex, there are receptive fields of different area that receive input from different numbers of RGCs, and it is those receptive fields that receive input from 31 RGCs that determine the size of Ricco's area. Therefore, if (for example) 8 RGCs are lost, the cortical receptive field previously determining the size of Ricco's area would now receive input from only 23 RGCs and no longer meet the criterion for determining the size of Ricco's area.

However, if a cortical receptive field that previously received input from 39 RGCs now receives input from only 31 cells, then its size determines the size of Ricco's area. A similar hypothesis could be used to explain the findings of the current study (Figure 4.18). It has previously been shown that the visual cortex has remodelling capabilities

under certain conditions. As discussed in Chapter 3, geniculocortical axon arbor complexity can change within a very short timescale, in response to interocular differences in visual input (Antonini & Stryker 1993). Laboratory work in monkeys (Gilbert & Wiesel, 1992) and rats (Linden & Perry 1982) has shown that when a cortical insult is inflicted, those adjacent cells involved in visual processing can extend their dendritic arbors to cover damaged areas. Therefore, it is not implausible that cortical, and thus visual adaptation can occur in response to RGC dropout.

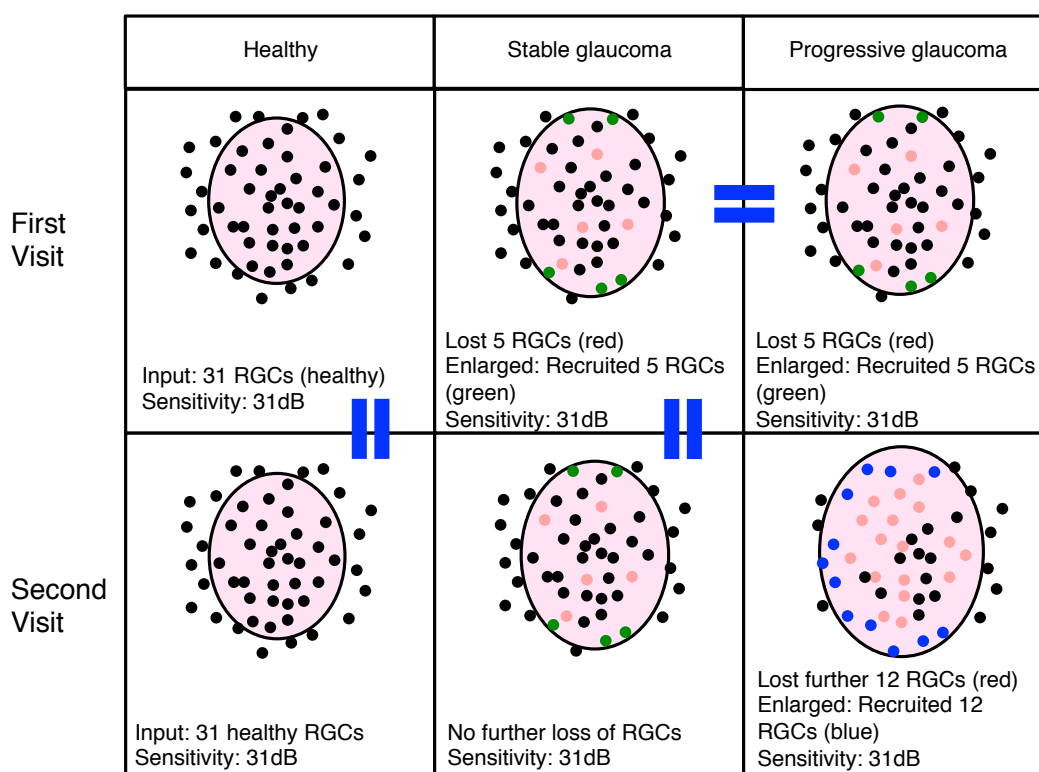


Figure 4.18. Hypothesis on possible cause of enlargement of Ricco's area in the trabeculectomy group second visit.

In conclusion although Ricco's area does not change by a sizeable amount in stable glaucoma patients and healthy controls over an approximately 6 month period, there are observable changes in a group of patients who have undergone a trabeculectomy

procedure for lowering IOP. When surgically-induced changes in corneal aberrations were accounted for, these observable changes in Ricco's area between visits remain, suggesting that they are, in fact, true neural changes, rather than optical in nature. Although, given the findings in amblyopia outlined in Chapter 3, as well as those reported in published literature, this is suggestive of a cortical adaptation mechanism, it cannot be ascertained, in the current study, how the rate of change in Ricco's area was affected by IOP-lowering treatment. Changes in Ricco's area between visits were modest and fell just short of statistically significant, but in the context of previously published literature on how Ricco's area differs in glaucoma patients and healthy controls, this effect size is noteworthy. Importantly, these changes were observed in the absence of statistically significant changes in sensitivity to a conventional Goldmann III stimulus. Further analysis of the comparative utility of Ricco's area measurements and sensitivity to a Goldmann III stimulus is described in Chapter 5, with a view to ascertaining whether novel perimetric methods, designed to map to the changing spatial summation function in glaucoma may have superior utility to conventional stimuli in identifying visual field damage and/or change over time.

Chapter 5: Signal/Noise Analysis for Comparison of Methods of Mapping to the Changing Spatial Summation Curve in Glaucoma

5.1. Introduction

RGCs have been observed to undergo subtle premorbid changes, including pruning of dendritic tree size and changes in axonal diameter, in experimental glaucoma (Morgan *et al.* 2006; Shou *et al.* 2003; Weber *et al.* 2000). This suggests that there may be a period of cell dysfunction before death in glaucoma. This raises the possibility that if the period of dysfunction can be identified and treated early then improvement in visual function may be possible. The goal of treatment for glaucoma is preservation of vision. Although several methods have been proposed to measure changes in glaucoma over time, including ocular imaging with technology such as OCT and scanning laser ophthalmoscopy, perimetry are the only way to quantify functional deficits or improvements. Perimetry is commonly used for the identification and monitoring of glaucoma in conjunction with imaging of the retinal nerve fiber layer and optic disc with techniques such as OCT and confocal scanning laser tomography. Structural measures can provide information about structural integrity of RGC, however just because RGCs are present, it does not mean that they are functionally healthy. Therefore, structural measurements cannot provide information on whether a RGC is sick, healthy, or recently dead. The conceptual model of Porciatti and Ventura (2012) illustrates this point. The model points out that, rather than a functionally sound cell undergoing spontaneous apoptosis, it likely undergoes a period of treatable dysfunction

before it dies and also there is time lag between loss of function and loss of structure. Figure 5.1 stage 1 illustrates an RGC in its normal state. With an increase in IOP, the cell undergoing stress becomes dysfunctional (stage 2). At this stage, it may be possible to recover the health of the cell if appropriate and adequate treatment were to be administered. If IOP were to increase further, the RGC would then undergo apoptosis (stage 3). From this stage onwards, no residual function would be left in the RGC. However the presence of the death RGC would still be measurable with imaging techniques, as its cell body would not have disappeared. According to the model, in order to prevent cell loss, treatment would have to be administered at stage 1 or 2.

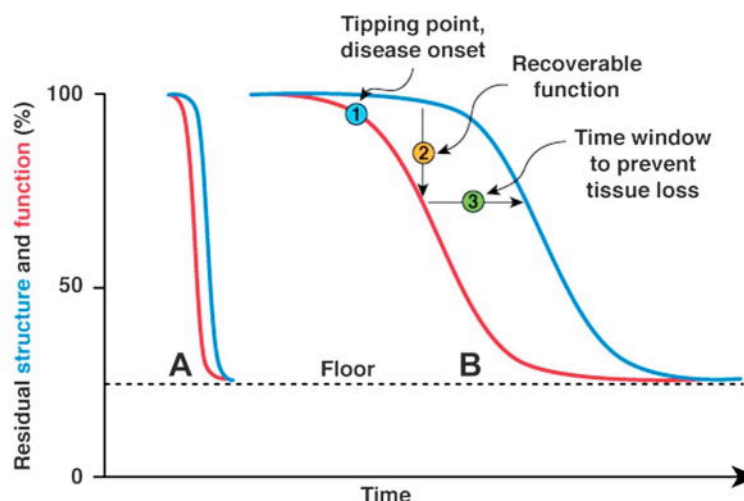


Figure 5.1. Conceptual model for RGC dysfunction and death by Porciatti and Ventura.

Picture taken from Porciatti and Ventura (2012)

Although several studies of optimum methods for glaucoma detection claim that structural loss occurs prior to functional loss (Kamal *et al.* 1999; Kamal *et al.* 2000; Kerrigan-Baumrind *et al.* 2000), it is difficult to understand how cells can retain function but lack structure or be absent altogether. Thus, it is more likely that high variability in current clinical functional techniques (Artes *et al.* 2002; Henson *et al.* 2000; Wall *et al.* 2009) mean that they lack the required sensitivity to identify pre-morbid changes in RGCs.

SAP remains the clinical standard for identifying and following functional visual loss over time in glaucoma. Despite its clinical standard status, as discussed extensively in Chapter 1, it has three cardinal limitations. Firstly, it has low sensitivity for subtle changes in early disease (Tafreshi *et al.* 2009). Although test-retest variability is lowest in early disease (Artes *et al.* 2002), it is unacceptably high if one wishes to identify differences from normality. Secondly, variability increases with depth of defect (Artes *et al.* 2002; Henson *et al.* 2000), meaning that it is more difficult to identify changes over time in glaucoma that is already established. Thirdly, it has a limited dynamic range and very high test-retest variability in advanced disease, in that remaining vision cannot be accurately quantified (if at all), and the limits of variability span almost the entire measurement range (Artes *et al.* 2002), thus making it difficult to distinguish true progression from variability of test results. Chauhan *et al.* (2008) performed a simulation of perimetric variability on different rates of change in sensitivity over time and found that, for example, if two visual field examinations are performed per year with SAP, it would take 8.5 years to identify mild progression (-0.25dB/year) in the presence of moderate variability (with statistical power of 80%). Considering that, in many clinics, only one visual field is typically undertaken every year (or sometimes even over a longer period), the time taken to identify subtle visual field damage will be much greater. Many attempts had been made to improve the ability to identify functional loss, such as the creation of new types of perimetry tests e.g. FDT and SWAP (Bayer & Erb 2002; Johnson *et al.* 1993; Sample *et al.* 1993). Caution should be exercised when interpreting research comparing SWAP and FDT to SAP, as some are limited by participant selection bias, in that they recruited participants with normal SAP but normal SWAP or FDT, or vice versa. The utility of these more recently developed tests has been inconclusive, predominantly owing to difficulty in directly comparing the

tests with the clinical standard (a more extensive discussion can be found in Chapter 1), because of the use of different stimuli, measurement scales, and measurement ranges to those used in SAP. Furthermore, the tests have different normative databases that have their own ranges, each determined with the previously mentioned different stimuli and measurement scales.

Other methods for improving the ability to identify glaucoma and changes in sensitivity over time are the development of statistical paradigms, aimed at disentangling the signs of true damage (signal) from variability (noise). Artes & Chauhan (2009) developed a statistical technique to estimate the signal/noise ratio (SNR) for hemifield differences in sensitivity, which they then compared between SAP and FDT in the same cohort of glaucoma patients. To calculate signal, they took the mean of 6 visual field sector mean deviations (sMD) inferior visual field from the mean of 6 sMDs in the superior field and constructed a null distribution of differences in sMD for all patients, for 36 different combinations of test order. The signal was the mean of the distribution and the noise was the standard deviation. In this way, they were able to compare the utility of SAP and FDT, two techniques independently of stimulus configuration and measurement scale, and without the need for normative databases. They found that, on average, SNR was greater for FDT than for SAP when identifying hemifield differences. Although this analysis was useful in determining the utility of the two tests in identifying such differences, it could not be assumed that FDT had superior utility for identifying progression. On the basis of the findings of Artes & Chauhan (2009), Redmond *et al.* (2013a) used permutation of pointwise linear regression (PoPLR) (O'Leary *et al.* 2012), a technique based on SNR analysis, to compare the utility of FDT and SAP in identifying overall change over time in patients enrolled in a longitudinal visual field

study. This technique was designed to report whether or not there was statistically significant overall visual field deterioration. This analysis also allows techniques to be compared independently of stimulus configuration, measurement scale, and normative databases. They found that, despite the greater cross-sectional SNR for FDT (Artes & Chauhan 2009), SAP identified more instances of change over time than FDT.

Accurate identification of change over time in glaucoma is important for the initiation of timely, and thus more successful, treatment, and a larger amount of attention has been given to this over the past few decades (for an extensive review please refer to Vianna & Chauhan, 2015). However the findings of this research have been poorly translated to clinical practice. One of the contributing factors is that some research was undertaken on laboratory equipment that limits its ability to be readily translated into the techniques available with clinical equipment. Patients are familiar with SAP, and many clinics have many years' worth of data on which to base clinical decisions. The introduction of a new test strategy with a very different appearance or task for the patient can potentially cause problems such as new learning effects that could last over several visits, affecting continuity and thus the ability to identify pathological change over time. These new strategies also might not allow for direct comparison with patients previous SAP clinical data. Although the current parameters of SAP were imported directly from kinetic perimetry without any scientific basis, and at a time when the pathophysiological basis for glaucoma was not well understood, the risks to continuity associated with a major change in the task for the patient are too great. What is needed, therefore, is an optimization of the parameters used in SAP to enable greater sensitivity to glaucoma in the first instance as well as to changes over time. As shown in Chapter 4, Ricco's area was enlarged in the second research visit, relative to that in the first visit, in

patients who had undergone trabeculectomy surgery, with no notable difference in Goldmann III sensitivity in the same test locations. Redmond *et al.* (2010a) also previously showed an enlarged Ricco's area in clinically normal visual field locations of glaucoma patients, glaucoma patients, relative to that in age similar healthy participants. They indicated that, on average, sensitivity loss to a Goldman III stimulus in glaucoma could be mapped to the horizontally-displaced spatial summation curve. Therefore, it is probable that clinical measures of Goldmann III sensitivity loss are simply measures of displacement of the spatial summation curve. Considering the schematic spatial summation curves in Figure 5.2, this measurement could be considered inefficient, in that the effect of a horizontal displacement of the curve is smallest where the slope is shallow (i.e. when the stimulus is larger than Ricco's area) and the stimulus is varying in contrast (along the y-axis). The largest 'signal' associated with a horizontally displaced spatial summation curve should be encountered when measuring the difference between the curves along the area axis (x-axis) within Ricco's area (vector A in Figure 1; vector B shows the 'signal' for a conventional Goldmann III varying in contrast). Changes in Ricco's area are a direct measure of this 'signal'. As there is a larger theoretical signal at vector A: (changes in Ricco's area) than at vector B (changes in Goldmann III sensitivity) it could be that progression is better determined by measuring the horizontal displacement of the spatial summation curve with a stimulus scaled to Ricco's area, varying in area, than with a Goldmann III stimulus varying in contrast. In other words, the disease signal might be boosted if one measures the horizontal difference between spatial summation curves, within Ricco's area than the vertical distance between curves outside Ricco's area (as is the case with a Goldmann III). Indeed, in a recent study comparing different stimulus paradigms optimised for measuring altered spatial summation in glaucoma, stimuli smaller than Ricco's area,

varying in area showed a significantly greater SNR than conventional Goldmann III stimuli (Rountree *et al.* 2018) for identification of glaucomatous damage. Area-modulated stimuli demonstrated more uniform response variability with increasing damage, and therefore hold promise for identification of deterioration over time also. Area-modulated stimuli were not employed in the current study, but it is possible to understand the likely utility of such measurements in the current study by calculating the longitudinal SNR for measurements of Ricco's area relative to measurements of Goldmann III sensitivity.

The purpose of this study was to investigate whether, in a short timescale, measurements of changes in Ricco's area over time (herein referred to as the Ricco's area method or RA method) offer a higher SNR than measurements of changes in GIII sensitivity (herein known as the Goldmann III method or GIII method). If the RA method reveals a higher SNR than the GIII method, the finding could be used in support of the employment of area-modulated stimuli (within Ricco's area) for identification of glaucomatous damage over time in the clinical setting.

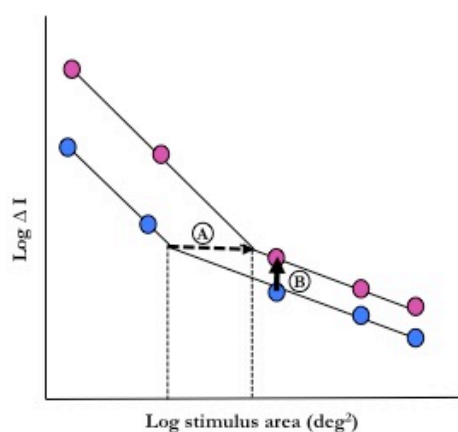


Figure 5.2. Schematic spatial summation curve for two points in time, assuming progression between the two visits (blue symbols: visit 1; pink symbols: visit 2). A larger signal to damage might be encountered when measuring the displacement of the spatial summation curve along the area axis within Ricco's area (A) than when

measuring vertical displacement in the curves (difference along the intensity axis) for a Goldmann III stimulus outside Ricco's area (B). The length of arrows A and B denotes the disease signal.

In this chapter comparison of SNR for the RA and GIII methods are compared with data collected over a 6 months interval was performed. One difficulty in comparing the utility of different instruments and tests in identifying change over time is that they are often on different measurement scales and have different units. This is also the case in the current study. Ricco's area measurements are in deg^2 while Goldmann III sensitivity measurements are in decibels (dB). The problem of having different measurement scales can be addressed by comparing signal-to-noise ratio (SNR) for between-visit differences in RA and Goldmann III sensitivity. The method of Artes & Chauhan (2009) is unsuitable for our aim as they were investigating cross-sectional hemifield data. In addition, their method of comparing mirror sectors may have masked diffuse loss of sensitivity in glaucoma. Similarly, PoPLR is inappropriate for use in the current study as this is a trend-based analysis, rather than an event-based analysis, as is required in the current study. Gardiner *et al.* (2013) compared the longitudinal SNR of SAP and OCT by applying linear regression of mean deviation (MD) of SAP and retinal nerve fiber layer thickness of OCT over time. They then used the rate of change over time (slope) as signal and standard deviation (SD) of the residuals as the noise measure. However the decibel scale is a logarithmic scale, while the retinal nerve fiber layer thickness scale is linear. Using linear trend lines on a decibel scale over time might not be the best methodology as it could give larger estimates of noise in MD residuals with increasing depth of defect (heteroscedasticity). Here, an alternative approach for event-based analysis of SNR is described.

5.2. Methods

Data for this study were the same as those described in Chapter 4. Participant characteristics, psychophysical methods (including apparatus and stimuli), and analysis used to determine Ricco's area and Goldmann III thresholds are described in detail in Chapter 4, but are briefly outlined below for clarity.

5.2.1. Participants

A comprehensive overview of participant characteristics can be found in Chapter 4. The difference in this chapter is that only data from participants that completed 2 visits are included. Nine glaucoma patients who were listed for trabeculectomy surgery ('trabeculectomy group'; median age [IQR]: 67 [58, 77.50] years) and 20 stable glaucoma participants ('stable glaucoma group'; median age [IQR]: 69 [62.50, 76.50] years) were recruited from the glaucoma clinic in the University Hospital of Wales. Twenty healthy participants ('healthy group'; median age [IQR]: 67 [63.25, 71.75] years) were recruited from the database of Cardiff University eye clinic. Severity of glaucoma is classified based on Hodapp-Parrish-Anderson criteria. The trabeculectomy group had a range of visual field loss from early to advanced with median MD [IQR] visit 1: -5.27 [-8.70 to -3.50] dB; median MD (IQR) visit 2: -5.06 [-11.56 to -1.36] dB. The stable glaucoma group had minimal to early visual field damage in both visits (median MD [IQR] visit 1: -1.88, [+1.10 to -8.13] dB; median MD [IQR] visit 2: -1.15 [+3.83 to -8.21] dB).

5.2.2. Apparatus and stimulus

Stimuli were achromatic circular stimuli, presented on a white background (10 cd/m^2) for 200 ms. Five different stimulus sizes were used, Goldmann sizes I-V (0.11° , 0.22° , 0.43° , 0.87° and 1.7° diameter). An Octopus 900 perimeter (Haag Streit, Koeniz, Switzerland), controlled with the Open Perimetry Interface, was used to present the stimuli at 8 visual field locations at eccentricities of 12.7° and 21.2° (Figure 4.3 in Chapter 4).

5.2.3. Thresholding procedure

Achromatic contrast detection thresholds were measured for each of the Goldmann sizes I-V in a randomized order. A 4:1 staircase procedure was used, which was adapted from that produced by Andrew Turpin and Luke Chong (University of Melbourne, <http://people.eng.unimelb.edu.au/aturpin/opi/interface.html>, accessed on 15th March 2014; adapted code can be found in Appendix 2). The initial step size was 4 dB until the first reversal was encountered, after which point it reduced to 1dB. A yes/no response criterion was used. At each location, the procedure stopped after 8 reversals and the final threshold returned was taken as an average of sensitivity at the final 4 reversals. The entire procedure was repeated twice more, such that for each participant, 3 sets of threshold measurements were obtained for each Goldmann size (a total of 15 sets of threshold measurements per participant). All procedures were carried out with natural pupil sizes and central refractive error corrected fully with full aperture trial lenses. Fixation was monitored visually and eye position was adjusted when the pupil moved from the optimum position in the eye monitor. Breaks were given approximately after every 10 minutes, with additional breaks granted when requested by the patient.

5.2.4. SNR procedure

Whereas many previous studies have compared clinical tests based on disease signal or variability separately, Rountree *et al.* (2018) point out the importance of considering both simultaneously, as a signal/noise ratio. In the current study, signal, noise, and SNR were calculated for a) the difference in Ricco's area between visits (RA method) at each location in each individual, and b) the difference in predicted Goldmann III threshold (GIII method) between visits at each location in each individual. The procedure for calculating SNR is described as follows, with reference to Figure 5.3.

Signal

Ricco's area values used to calculate the signal are the same as the Ricco's area data in Chapter 4. In summary, the three threshold values for each of the Goldmann I-V were averaged to give one threshold value for each of the Goldmann sizes. For example, in Figure 5.3, the threshold for a Goldmann I stimulus in visit 1 was calculated as $mean(A, B, C)$, threshold for a Goldmann III in visit 2 was calculated as $mean(V, W, X)$, etc.

Two-phase regression analysis was applied to averaged threshold data to obtain a spatial summation curve, and thus a Ricco's area estimate, per location per visit. The difference in Ricco's area (Δ_{RA}) and difference in predicted GIII thresholds from the fitted curves (Δ_{GIII}) between first and second visits was calculated, and taken as the signal for the RA and GIII methods respectively. This procedure was repeated for each of the 8 test locations in each participant. Data were then averaged to give 1 final signal value per method per participant.

Noise

Given that the threshold for Goldmann I-V was measured 3 times for each location per visit, 3 values were available for each of the Goldmann I-V stimuli per visit. This is

illustrated in the Tables in Figure 5.3. For example, at each location, threshold measurements for the Goldmann I stimulus on the first visit were named A, B, and C, and each of the three threshold measurements for the GIII stimulus on the second visit were named P, Q and R etc. Instead of averaging by stimulus area, as in the calculation of the signal, a program was created to randomly select one of the three values for each stimulus area per location for each visit. An example is shown in Figure 5.3, where the pink shaded areas in each of the tables indicate randomly chosen thresholds per stimulus area per location. With these data, two spatial summation functions were determined, one for each visit. Two-phase regression analysis was then applied to the randomly selected Goldmann I-V threshold values to obtain a Ricco's area estimate for each visit. The difference in Ricco's area estimates between visits ($\Delta_{RA} = \text{Ricco's area, visit 2} - \text{Ricco's area, visit 1}$) was calculated. The difference between the fitted two-phase regression lines for an area of $-0.84 \log \text{deg}^2$ (GIII) was also calculated (Δ_{GIII}). The entire procedure was repeated, with both Δ_{RA} and Δ_{GIII} calculated each time. As there are 3 available values for each of the Goldmann sizes, 243 ($3 \times 3 \times 3 \times 3 \times 3$) sets of threshold data were permuted and thus 243 Δ_{RA} and Δ_{GIII} values were estimated per location. Therefore for each participant at each visit, a total of 1944 Δ_{RA} and Δ_{GIII} estimates were obtained across 8 different test locations. Spatial summation curves were excluded if $R^2 < 0.9$. Null distributions of Δ_{RA} and Δ_{GIII} values were constructed. The SD of each of these distributions was taken to represent the noise for each method. The aforementioned process was repeated for all participants.

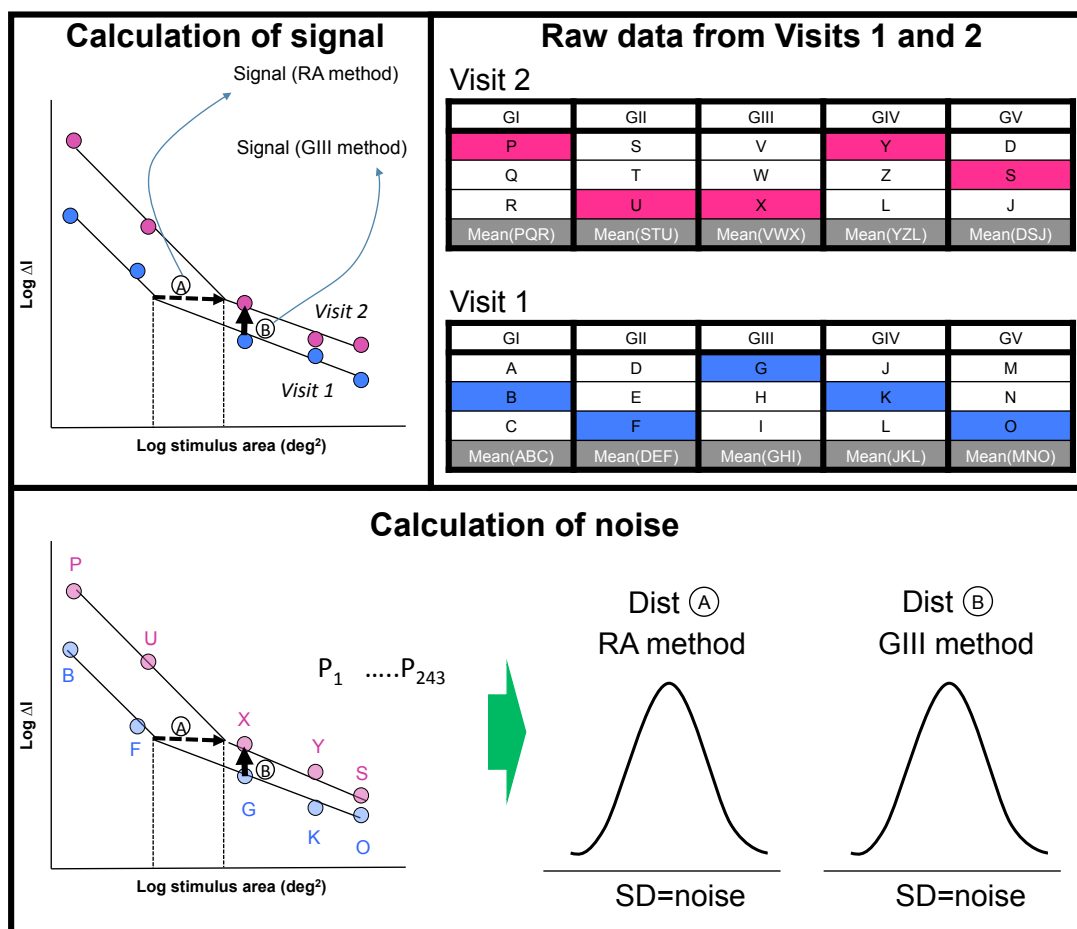


Figure 5.3. SNR protocol for Ricco's area calculation on each participant.

Signal/noise ratio

Signal values were calculated for individual participants per location and then averaged to give one signal value per participant. Therefore, 9 signal values were obtained for the trabeculectomy participants, 20 for stable participants and 20 for the healthy participants for each method. Noise values were also averaged per location and then per participant. Therefore, for each method, one value per participant was obtained. To calculate SNR signal was divided by noise for each method and for each participant. Signal was then averaged across all participants per participant groups, per method and the same was done for the noise.

5.2.5. Data analysis

The average signal and average noise values were then compared between RA and Goldman III data across the same participant group to explore differences between signal and noise separately between the two methods. A comparison was also made between different participant groups to investigate whether signal and/or noise differ substantially between participant groups for each method. Mean SNR was calculated for the RA and GIII methods for each of the participant groups, to investigate whether the RA method demonstrates a greater signal/noise ratio longitudinally than the GIII method. The standard deviation of SNR values was calculated to investigate whether there was greater variance in the SNR for one method over the other and between participant groups.

5.3. Results

Table 5.1. Mean and SD of signal, noise and SNR of the RA and GIII methods in all participant groups. T=trabeculectomy group; S=stable glaucoma group; H=healthy group.

Participant groups	Data types	RA method		GIII method	
		Mean	SD	Mean	SD
T	signal	0.32	0.23	0.25	0.32
	noise	0.34	0.18	0.93	0.47
	SNR	2.04	1.25	0.41	0.6
S	signal	0.2	0.12	0.02	0.58
	noise	0.33	0.15	0.73	0.36
	SNR	1.11	0.68	0.21	0.84
H	signal	0.16	0.2	1.11	0.73
	noise	0.23	0.08	1	0.52
	SNR	1.34	0.96	0.94	0.95

The signal is higher in stable glaucoma and trabeculectomy groups with the RA method when compared to the Goldmann III method (Table 5.1). The noise is smaller with the RA method for all participant groups. The SNR is larger across all participant groups for the RA method than for the Goldmann III method. It is worth noting that the SNR in the trabeculectomy group is substantially larger with the RA method than for the GIII method. The SD of SNR values in the trabeculectomy group is larger for the RA method than for the GIII method. The SD of SNR values in the stable glaucoma group is smaller for the RA method than for the GIII method, while in the healthy group the SD of SNR values is comparable between methods.

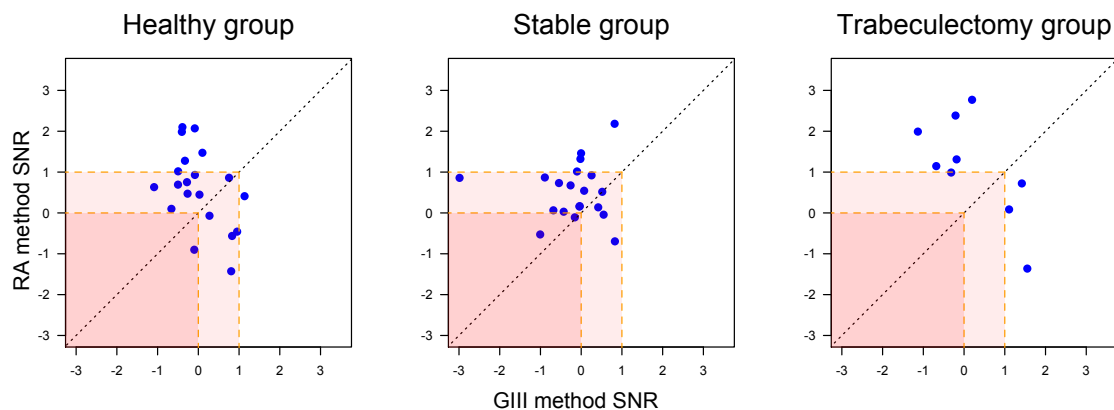


Figure 5.3, Scatterplots with lines of equality for all participant groups. The deeply shaded area emphasizes SNR values below zero and the lightly shaded area marks SNR values from 0-1.

Based on Figure 5.3, a greater number of data points fall above the line of equality, indicating that there are more participants for whom SNR with the RA method is greater than that with the GIII method. This observation is consistent in all participant groups, when data are partitioned into two strata: a) $0 < \text{SNR} < 1$, and b) $\text{SNR} > 1$. In addition, almost all of the SNR values are > 0 for both methods, indicating that, for the most part, Ricco's area enlarges and Goldmann III sensitivity is reduced in visit 2, compared with visit 1.

5.4. Discussion

The purpose of this study was to investigate whether, in a short timescale, measurements of changes in Ricco's area over time offer a higher SNR than for measurements of change in GIII sensitivity.

With SAP, tests need to be repeated multiple times per year before progression of visual field damage can be ascertained with a high degree of confidence (Chauhan *et al.* 2008).

A test with a high cross-sectional SNR is needed clinically for identification of glaucoma in the first instance. Similarly, a high longitudinal SNR is needed for a confident and timely identification of deterioration over time. If variability (noise) is high and masks true change (signal), then much time will have passed, and a great deal of damage will have occurred, before a confident identification of change is made. In the current study it can be observed that the SNR is higher for the RA method than that for the GIII method in all participant groups. This suggests that the RA method (or similar method for measuring the horizontal separation of spatial summation curves between visits) has greater utility for the identification of deterioration in the visual field over time than the conventional method of measuring changes in sensitivity to a Goldmann III stimulus. The estimated global rate of visual field deterioration per year is -0.22 dB (range: -4.9 to +1.9), -0.46 dB (range: -8.7 to 0.2) and -1.13dB (range: -11.3 to -0.1) for untreated NTG, Primary OAG, and pseudoexfoliative glaucoma respectively (Heijl *et al.* 2003), while for treated Primary OAG and pseudoexfoliative glaucoma, the rate of deterioration is -0.80 dB/year (range: -5.58 to +1.24) (Heijl *et al.* 2013).

Pseudoexfoliative glaucoma has a more advanced rate of deterioration compared to other glaucoma types. Considering that the glaucoma groups included in the current

study protocol were Primary OAG and NTG, and that measurements were only taken at 2 visits spaced 6 months apart, it is unsurprising that no meaningful differences were observed in our Goldmann III threshold measurements between visits for trabeculectomy and stable groups. This is evidenced in Table 4.5 in Chapter 4, that compared the values for sensitivity to a Goldmann III obtained between 2 visits. In the current chapter, SNR is substantially lower with the GIII method than with the RA method for both trabeculectomy groups. Although no meaningful inter-visit difference in Ricco's area estimates was observed in the stable group (Chapter 4), the RA method nonetheless demonstrated a greater SNR compared to the GIII method in this chapter. The SNR was observed to be positive with both methods in most participants in the healthy and stable glaucoma groups, indicating an enlargement of Ricco's area or reduction in sensitivity to a Goldmann III stimulus between visits. This could suggest that the analysis is sensitive to subtle changes over time, or it could just indicate normal fluctuations of measurement technique. The fact that the majority of SNR values were greater than 0, particularly for the glaucoma groups, indicates that this is a real effect that is being observed within a very short timescale, rather than simply measurement noise. The mean SNR is closer to 0 for the healthy control group (in which one would expect no meaningful change over time), which lends further support to this argument.

A six-month timescale was chosen for the study because Ricco's area was previously observed to change in clinically normal regions of the visual field in glaucoma and considering that, in a clinical setting, 2-3 visual field examinations are recommended per year (i.e. a 3-6 month interval), it is reasonable to investigate whether or not changes are observable over such a short timescale. Secondly it was considered essential to ensure that our participants with stable glaucoma were in fact stable, particularly for the

experiments outlined in Chapter 4. If the timescale of investigation were too long, then progression may have occurred in the stable participant group, and it would have been difficult to identify effects specific to the trabeculectomy group. It was therefore considered prudent to ensure that any effects observed within the trabeculectomy group could be solely attributed to particulars for that group (e.g. treatment). Thirdly, the main research objective was to look for very subtle changes in response to pressure-lowering treatment. Measurements of Ricco's area immediately after lowering of pressure (Chapter 4) could provide insight into how the visual system adapts after treatment.

In conclusion, the SNR was higher in all-participant groups for the RA method compared to the GIII method. This suggests that a clinical test, optimised to map changes in spatial summation in glaucoma (e.g. a stimulus smaller than, but scaled to Ricco's area, modulating in area) could have greater utility in identifying visual field deterioration (or improvement) over a short timescale than a test employing conventional Goldmann III stimuli. It should be noted that measurements of Ricco's area or spatial summation curves are not advocated here for use in clinical practice. Such a procedure would be much too time consuming. Rather, the findings provide some evidence that a change in sensitivity to a Goldman III stimulus is an inefficient measure of subtle visual field deterioration in glaucoma, and that a better method might be to undertake a test employing a stimulus that is optimised to follow the changing spatial summation curve (Rountree *et al.* 2018). Additionally, data were gathered with a clinically available instrument suggesting that it is possible to measure such subtle changes with existing clinical instrumentation, albeit with an optimised approach. Therefore, if the task of the patient is unchanged with the optimised approach, it might be expected that any required adaptation to the new test strategy by patients and perimetrists could easily be overcome.

Chapter 6 Conclusion and Future works

The main objective of this PhD was to investigate, with measurements of Ricco's area before and after the commencement of rigorous IOP-lowering treatment on subjects with glaucoma, whether or not visual consequences of RGC dysfunction (as separate to death) are observable. Based on the finding of Redmond *et al.* (2010a) that Ricco's area is larger in early glaucoma than in healthy controls, the hypothesis was that an observation of any shrinkage of Ricco's area after IOP-lowering treatment would be suggestive of recovery from pre-morbid dysfunction, whereas the absence of shrinkage, or indeed a continued enlargement of Ricco's area would be suggestive of RGC death or cortical adaptation to RGC death. As such, Ricco's area estimates were compared with those in participants with stable glaucoma as well as healthy individuals (both control groups).

In order to investigate this, a series of experiments was conducted in Chapter 2 to find the optimum test parameters for the measurement of spatial summation (specifically, Ricco's area) to be used in the main experiments, described in subsequent chapters. The most suitable experimental apparatus, number of stimuli, thresholding algorithm, and test locations were carefully considered through a review of published literature and by conducting preliminary experimental tests. It was decided that the Octopus 900 perimeter was the most appropriate apparatus for measuring spatial summation in glaucoma patients. Goldmann I – V stimuli were found to sufficiently sample the spatial summation curve across much of the visual field regions of interest, thus experiments entailed measurements of sensitivity (converted to threshold) to these stimuli. It was

decided that, on balance, a test paradigm incorporating a 4:1 staircase algorithm, terminating after 8 reversals (and threshold taken as an average of the last 4 reversals), to measure threshold at 8 visual field test locations enabled the measurement of good quality spatial summation curves (with $R^2 > 0.9$ and minimal failure of spatial summation curve fitting) within a reasonable time period. Given that the spatial extent of perimetric stimuli on the retina could be changed due to uncorrected (or ill-corrected) refractive error, the effect of dioptric blur on measurements of Ricco's area was quantified. Such effects were minimal, for up to 3.00D of induced blur, and were not statistically significant. It was considered that a change in corneal wavefront aberrations post-trabeculectomy surgery could potentially affect the retinal image size formed between visits, and thus give rise to an apparent change in the neural contribution to Ricco's area. Therefore, between-subject and between-visit variance in corneal wavefront measurements (specifically, Zernike polynomial coefficients up to the 6th radial order) were also investigated over 5 visits in a small number of healthy individuals in order to contextualise any surgically-induced changes found as part of the main experiments. Finally, an exploratory study of any potential learning effect on measurements of Ricco's area was conducted, in order to investigate how many times Ricco's area was required to be measured before and after surgery so that accurate surgery-related effects on sizes could be established. Although it is widely documented in published literature that initial measurements of visual field sensitivity with SAP are usually discarded due to a learning effect, such a learning effect was not anticipated for measurements of Ricco's area (it was considered almost impossible for subjects to learn or bias the position of the breakpoint on the spatial summation curve, because of the randomization of tests of sensitivity to different stimulus sizes). No learning effect was

observed, and therefore it was decided that initial measurements would not need to be discarded in the main experiments.

Redmond *et al.* (2010a) showed that when the difference in Ricco's area between glaucoma patients and healthy controls was taken into account, sensitivity to a range of perimetric stimulus areas overlapped between the two groups. This finding supported previous publications describing the importance of spatial summation in the determination and interpretation of perimetric sensitivity. Pan & Swanson (2006) demonstrated that probability summation across RGCs could not account for spatial summation of perimetric stimuli, but rather cortical pooling by multiple spatial mechanisms. An overview of findings from the literature suggests that losses of sensitivity to fixed-area perimetric stimuli may be an indirect measurement of a displaced spatial summation curve, arising from changes in spatial pooling at a cortical level.

In order to better understand the physiological basis for Ricco's area (the second objective of this PhD) and the mechanisms involved in determining sensitivity to a perimetric stimulus, an investigation of spatial summation in amblyopia was conducted. Amblyopia is a condition in which retinal receptive fields have previously been shown to be normal, and one in which functional deficits are largely attributed to regions of the visual cortex. Therefore, an investigation into changes in Ricco's area in amblyopia was undertaken, in order to provide an improved understanding the physiological basis for Ricco's area, and by extension, possible explanations for the change in Ricco's area in glaucoma. It was observed that Ricco's area is larger, compared to that in healthy controls, when measured through amblyopic eyes, and smaller than that in healthy controls when measured through non-amblyopic eyes. In healthy observers, it was

observed that Ricco's area is smaller, when measured binocularly, than when measured monocularly. In amblyopic participants, binocularly-measured Ricco's area is smaller than monocularly-measured Ricco's area through the amblyopic eye, and larger than that measured through the non-amblyopic eye. A likely basis for these findings is in layer 4 of V1, where dendritic arbors of geniculocortical cells from the non-amblyopic eye have previously been shown to be more complex, and those from the amblyopic eye have been shown to be less complex. These arbors have the potential for greater and less spatial pooling, respectively. This finding has important implications for glaucoma, as it adds to the growing literature suggesting that spatial summation of perimetric stimuli has a cortical origin.

Redmond *et al.* (2010a) hypothesized that the larger Ricco's area in glaucoma patients is due to a switch in the spatial frequency channel that determines Ricco's area, based on the report that approximately 31 RGCs underlie Ricco's area across the visual field (Swanson *et al.* 2004). In many perimetry studies in glaucoma, it is generally assumed that a loss of visual function is due to RGC death, but as previously mentioned, it is possible that early deficits may be a result of RGC dysfunction. If RGCs become dysfunctional before death, one might reasonably assume that the visual cortex receives fewer signals from these cells. Assuming the hypothesis of Redmond *et al.* (2010a) is correct, a switch in the spatial frequency channel determining Ricco's area should take place in response to dysfunction, given that signals to that channel ordinarily determining Ricco's area are reduced in number or weighting. A spatial frequency channel that previously pooled signals from a greater number of RGCs (> 31 RGCs), but because of RGC dysfunction, now pools signals from exactly 31 RGCs, would determine Ricco's area in these patients. However, should dysfunctional cells recover in response to rigorous IOP-lowering treatment, the spatial frequency channel determining

the larger Ricco's area should regain lost signals, in which case it would pool signals from > 31 RGCs once more. If all dysfunctional RGCs were to recover, the spatial frequency channel originally determining Ricco's area would re-recruit signals, enabling it to meet the critical number of inputting RGCs (31 RGCs) once again. This would manifest as a shrinkage of Ricco's area from a previously enlarged state. On the other hand, if RGCs had died, rather than become dysfunctional, they would not recover in response to IOP-lowering treatment, and Ricco's area would not be expected to shrink to normal (or near-normal) levels. In fact, depending on the timescale for cortical adaptation to RGC loss, Ricco's area might continue to enlarge for a period following damage, despite any cessation in further RGC death. It is difficult to ascertain whether the enlargement of Ricco's area in glaucoma is a response to cell sickness or cell death by undertaking a cross-sectional study. Therefore, a longitudinal study in which Ricco's area is compared before and after commencement of a more rigorous treatment such as trabeculectomy surgery, would provide an opportunity to test this hypothesis. In the study outlined in Chapter 4, Ricco's area was measured over 2 visits in participants listed for trabeculectomy surgery during the course of their clinical care. Experiments were undertaken once within 2 weeks before the surgery and once approximately 6 months after the surgery. Identical experiments were undertaken on two control groups: a cohort of participants determined to have stable glaucoma by the hospital eye service, and a cohort of healthy participants. When Ricco's area estimates were compared between visits over this short timescale, it was observed that Ricco's area of participants that had undergone trabeculectomy surgery showed a slight overall reduction from the first to the second visit in those locations with very early damage, but an enlargement from first to the second visits in those locations with early-moderate-advanced damage, although these differences were not statistically significant overall. In the control

cohorts, minimal or no overall change in Ricco's area was found between visits. Although the effect of participant type on between-visit changes in Ricco's area was not found to be statistically significant (though it was borderline significant), the effect size in trabeculectomy patients was greater than that of the stable glaucoma group by a meaningful amount. Furthermore, a reduction in Ricco's area in one disease stratum and an enlargement in the other two strata may account for the lack of statistical significance of an overall effect of participant type. The potential effect of between-visit differences in aberrations on measurements of Ricco's area, particularly in the trabeculectomy group, was investigated in a linear mixed effects model of effects on between-visit differences in Ricco's area that included participant type, subject, and test location. No statistically significant effect of between-visit difference in aberrations was found on the between-visit difference in Ricco's area. The size of the effect of participant type on between-visit differences in Ricco's area was largely unchanged when between-visit differences in aberrations were included in the model. This finding, along with the lack of an effect of dioptric blur on Ricco's area measurements in healthy individuals (Chapter 2), suggests that optical factors are not sizeable contributors to between-visit differences in Ricco's area in the study described in Chapter 4. Taking into account the findings of the study of Ricco's area in amblyopia (Chapter 3), it is entirely possible that the changes observed in the trabeculectomy group are the result of cortical changes in response to RGC dysfunction (stratum 1), and death (strata 2 and 3). Indeed, animal studies of induced damage in the visual cortex have shown changes in dendritic arbors of remaining healthy cells over a period of time after the initial insult (Gilbert & Wiesel, 1992). Changes in Ricco's area were observable even over a very short timescale, in the absence of statistically significant changes in Goldmann III sensitivity measured over the same time period.

Lastly, the third objective of this PhD was to investigate whether, in a short timescale, measurements of changes in Ricco's area over time offer a higher SNR than for measurements of change in GIII sensitivity. Given the findings in Chapter 4, a statistical comparison of the signal/noise ratio (SNR) for changes in Ricco's area and Goldmann III sensitivity measurements in glaucoma was conducted, to assess whether novel perimetric methods using a stimulus scaled to Ricco's area, that measure the horizontal displacement of the spatial summation function in glaucoma, are likely to be superior in identifying change over time in glaucoma. Measurements of inter-visit differences in Ricco's area were observed to offer a higher longitudinal signal/noise ratio when compared to measurements of differences in Goldmann III sensitivity. This thesis does not advocate the measurement of Ricco's area or spatial summation curves in glaucoma clinics, but the findings do provide support for the hypothesis that stimuli optimised to map changes in spatial summation in glaucoma (Rountree *et al.* 2018) may have a higher longitudinal SNR than conventional Goldmann III stimuli.

Study limitations

Although changes in Ricco's area were observed between visits in the trabeculectomy group, true dysfunction or death of RGCs (i.e. the ground truth) cannot easily be ascertained in specific locations in the human retina *in vivo*. As the term suggests, dysfunction can only be measured with a functional test. In this study, it is possible that there is indeed a recovery of RGCs from a dysfunctional state, and that trabeculectomy actually succeeded in halting progression by reducing what would otherwise have been a greater enlargement. However, a change in trajectory cannot be ascertained as measurements of Ricco's area were obtained on two visits only. One measurement was

taken up to 2 weeks before the surgery and the other was taken approximately six months after the surgery.

The finding of a smaller Ricco's area in the non-amblyopic eye of amblyopic participants in Chapter 3 is suggestive of greater visual acuity in the non-amblyopic eye. However, this finding was unexpected, and therefore spatial acuity at the test locations was not measured prospectively. Although beyond the scope of this thesis, ongoing separate work within our group is aimed at better understanding the functional capabilities of the non-amblyopic eye of amblyopic individuals.

Future study

In order to build a more comprehensive picture of the effect of trabeculectomy surgery (or other IOP-lowering treatment) on visual function (including the ability to ascertain whether or not recovery from dysfunction has indeed occurred), a longer longitudinal study should be conducted, following subjects with glaucoma for a period of time before the surgery, and then a period of time afterwards. The availability of several measurements of Ricco's area during a stable period would allow for a calculation of projected changes (or otherwise) in Ricco's area over time, so that any departure from the normal rate of change can be easily identified. This would also enable a more accurate determination to be made regarding the success, or otherwise, of IOP-lowering treatment that might not otherwise be determinable with a conventional Goldmann III stimulus. The availability of several measurements of Ricco's area post-treatment would provide a more accurate picture of the success (or otherwise) of the treatment, how the visual system adapts to the treatment, and whether or not there is a limit to the enlargement of Ricco's area. Such a large venture is beyond the scope of a PhD

however, as this would require several years of repeated experiments. However, the findings presented in this thesis provide some preliminary data to inform the design of more definitive experiments, in addition to providing initial data on the likelihood of measurable dysfunction and neuro-recovery.

Another interesting investigation to pursue is that of changes in cortical adaptation in glaucoma patients, with functional imaging techniques, to better understand how cortical function is altered in response to changes in RGC function and/or population.

A study of grating resolution acuity in amblyopic and non-amblyopic eyes will be beneficial to investigate whether or not a smaller Ricco's area in non-amblyopic eyes is accompanied by 'super-normal' acuity, and to gain a better understanding of the functional capabilities and limitations of eyes that have traditionally been considered 'normal'.

A higher SNR for the RA method compared to the GIII method suggests that stimuli optimised to map changes in Ricco's area in glaucoma (i.e. stimuli smaller than Ricco's area, varying in area) may have greater utility for the identification of visual field change over time than the Goldmann III stimulus. A formal comparison of the utility of area-modulated stimuli and conventional contrast-modulated Goldmann III stimuli for identifying change over time in glaucoma is warranted.

Appendices

Appendix 1: CURRICULUM VITAE

Full Name: Shindy Je

Current Position: PhD student
Cardiff University
Maindy Road
Cardiff, CF24 4HQ
United Kingdom

Email: JeS@cardiff.ac.uk

EDUCATION

Oct 2013 – present	PhD student School of Optometry and Vision sciences Cardiff University (anticipated completion year: 2017)
Sep 2010 – Jul 2013	BSc (1 st class Hons) Optometry and Vision Sciences Cardiff University
Jul 2007 – Dec 2009	International University College of Technology Twintech, Malaysia (course closure during study for Dip. Optometry)
Jun 2004 – Jun 2007	W.R. Supratman High School, Indonesia

RESEARCH EXPERIENCE

Oct 2016 – May 2017	Cardiff University, UK <ul style="list-style-type: none">• Co-supervisor of undergraduate 3rd year dissertation project (student: Luke Summers)
Oct 2015 – May 2016	Cardiff University, UK <ul style="list-style-type: none">• Co-supervisor of undergraduate 3rd year dissertation project (student: Julia Rose)• Co-supervisor of undergraduate 3rd year dissertation project (student: Anisha Chowlia)
June – Sept 2015	Cardiff University, UK <ul style="list-style-type: none">• Co-supervisor of undergraduate 2nd year summer research project (student: Julia Rose)
Oct 2012 – Jul 2013	Cardiff University, UK <ul style="list-style-type: none">• Dissertation on ‘Tissue Engineering of Corneal Epithelium’• Supervisor: Prof. Andrew J Quantock
Jul – Aug 2012	Kyoto Prefectural University of Medicine and Doshisha University, Japan <ul style="list-style-type: none">• Selected to represent Cardiff University as a summer research intern in the laboratory of Prof. Shigeru Kinoshita and Dr Noriko Koizumi

PUBLISHED CONFERENCE ABSTRACTS

Je S, Ennis FA, Morgan JE, Redmond T. Spatial summation of perimetric stimuli across the visual field in anisometric and strabismic amblyopia. *Invest Ophthalmol Vis Sci* 2015;56;2212 E-Abstract (ARVO Abstract)

TEACHING EXPERIENCE

Cardiff University

Oct 2015 - present Assessor on Master of Research (MRes) in Vision Sciences

Oct 2013 – present Supervisor and examiner on the BSc Optometry undergraduate course:

OP2201 Clinical Studies & Dispensing (2nd year)

OP2203 Investigative Techniques (2nd year)

OP1201 Basic clinical techniques (1st year)

OP1207 Physiology of Vision (1st year)

Scholar Science Tuition Centre, Medan, Indonesia

Jul 2011 – Sep 2013 Private tutor to O-level biology and physics, and A-level biology students

Appendix 2: Conference presentations and Awards

CONFERENCE PRESENTATIONS

- 2016 Oxford-Bristol-Cardiff-Southampton (OBCS) Alliance in Vision Research, Cardiff University, UK **(invited)**
- 2016 22nd International Visual Field Imaging Symposium, Udine, Italy **(paper)**
- 2016 British Congress of Optometry and Vision Science (BCOVS), Ulster University, UK **(paper)**
- 2016 “Advances in eye research towards the prevention of visual loss” - the pioneering UK-Kazakhstan Vision workshop, Almaty, Kazakhstan **(paper)**
- 2016 Postgraduate research seminar, School of Optometry and Vision Sciences, Cardiff University, UK **(paper)**
- 2016 MARV seminar, School of Optometry and Vision Sciences, Cardiff University, UK **(paper)**
- 2016 Sensational seminar, School of Psychology, Cardiff University, UK **(paper)**
- 2015 British Congress of Optometry and Vision Science (BCOVS), City University London, UK **(paper)**
- 2015 Bristol Vision Institute (BVI) Young Researchers Colloquium, Bristol University, UK **(paper)**
- 2015 MARV seminar, School of Optometry and Vision Sciences, Cardiff University, UK **(paper)**
- 2015 Association for Research in Vision and Ophthalmology (ARVO), Denver, CO, USA **(poster)**
- 2014 Speaking of Science, Cardiff University, UK **(paper)**
- 2014 MARV seminar, School of Optometry and Vision Sciences, Cardiff University, UK **(paper)**
- 2012 Ophthalmology Seminar at Kyoto Prefectural University of Medicine, Department of Ophthalmology, Kyoto, Japan **(paper)**

AWARDS AND FINANCIAL SUPPORT

- 2016 Travel grant, International Perimetric Society (IPS) for attendance, Udine, Italy -**\$1000**
- 2015 Highly commended oral presentation, British Congress of Optometry & Vision Science (BCOVS), City University London, UK
- 2014 'People's Choice Oral Presentation Award', Speaking of Science conference, UK
- 2013 Cardiff University Overseas Research Scholarship (CUORS) - **£42,500**
- 2012 Best performance in clinical practice award; BSc (Hons) Optometry course, Cardiff University **£100**
- 2011 Best performance in dispensing award; BSc (Hons) Optometry course, Cardiff University **£100**

Appendix 3: Publications

Je S, Ennis FA, Morgan JE, Redmond T. Spatial summation of perimetric stimuli across the visual field in anisometropic and strabismic amblyopia. (*in review*)

Je S, Ennis FA, Morgan JE, Redmond T. Spatial summation of perimetric stimuli across the visual field in anisometropic and strabismic amblyopia. *Invest Ophthalmol Vis Sci* 2015;56;2212 E-Abstract (ARVO Abstract)

Appendix 4: Ethical approval

Part of the research infrastructure for Wales funded by the National Institute for Social Care and Health Research, Welsh Government.
Yn rhan o seilwaith ymchwil Cymru a ariannir gan y Sefydliad Cenedlaethol ar gyfer Ymchwil Gofal Cymdeithasol ac Iechyd, Llywodraeth Cymru



Wales Research Ethics Committee 1
Sixth Floor, Churchill House
17 Churchill Way
Cardiff CF10 2TW

Telephone: 029 2037 6823

E-mail: jagit.sidhu@wales.nhs.uk

Website: www.hra.nhs.uk

20 May 2014

Dr Tony Redmond
Lecturer
Cardiff University
School of Optometry and Vision Sciences
Maindy Road
Cardiff
CF24 4HQ

Dear Dr Redmond

Study title: Measuring changes over time in the retina in eye disease
REC reference: 14/WA/0105
Protocol number: SPON 1272-2013
IRAS project ID: 141319

Thank you for your letter of 13 May 2014, responding to the Committee's request for further information on the above research [and submitting revised documentation](#).

The further information has been considered on behalf of the Committee by the [Chair, Dr K. Craig](#).

We plan to publish your research summary wording for the above study on the HRA website, together with your contact details. Publication will be no earlier than three months from the date of this opinion letter. Should you wish to provide a substitute contact point, require further information, or wish to make a request to postpone publication, please contact the REC Manager, Mrs Jagjit Sidhu, jagit.sidhu@wales.nhs.uk.

Confirmation of ethical opinion

On behalf of the Committee, I am pleased to confirm a favourable ethical opinion for the above research on the basis described in the application form, protocol and supporting documentation [as revised](#), subject to the conditions specified below.

Conditions of the favourable opinion

The favourable opinion is subject to the following conditions being met prior to the start of the study.



Cynhelir Cydweithrediad Gwyddor Iechyd Academaidd y Sefydliad Cenedlaethol ar gyfer Ymchwil Gofal Cymdeithasol ac Iechyd gan Fwrdd Addysgu Iechyd Powys

The National Institute for Social Care and Health Research Academic Health Science Collaboration is hosted by Powys Teaching Health Board



Management permission or approval must be obtained from each host organisation prior to the start of the study at the site concerned.

Management permission ("R&D approval") should be sought from all NHS organisations involved in the study in accordance with NHS research governance arrangements.

Guidance on applying for NHS permission for research is available in the Integrated Research Application System or at <http://www.rdforum.nhs.uk>.

Where a NHS organisation's role in the study is limited to identifying and referring potential participants to research sites ("participant identification centre"), guidance should be sought from the R&D office on the information it requires to give permission for this activity.

For non-NHS sites, site management permission should be obtained in accordance with the procedures of the relevant host organisation.

Sponsors are not required to notify the Committee of approvals from host organisations

Registration of Clinical Trials

All clinical trials (defined as the first four categories on the IRAS filter page) must be registered on a publically accessible database within 6 weeks of recruitment of the first participant (for medical device studies, within the timeline determined by the current registration and publication trees).

There is no requirement to separately notify the REC but you should do so at the earliest opportunity e.g when submitting an amendment. We will audit the registration details as part of the annual progress reporting process.

To ensure transparency in research, we strongly recommend that all research is registered but for non clinical trials this is not currently mandatory.

If a sponsor wishes to contest the need for registration they should contact Catherine Blewett (catherineblewett@nhs.net), the HRA does not, however, expect exceptions to be made. Guidance on where to register is provided within IRAS.

It is the responsibility of the sponsor to ensure that all the conditions are complied with before the start of the study or its initiation at a particular site (as applicable).

Ethical review of research sites

NHS sites

The favourable opinion applies to all NHS sites taking part in the study, subject to management permission being obtained from the NHS/HSC R&D office prior to the start of the study (see "Conditions of the favourable opinion" below).

Approved documents

The final list of documents reviewed and approved by the Committee is as follows:

<i>Document</i>	<i>Version</i>	<i>Date</i>
Copies of advertisement materials for research participants	1.0	25 February 2014
Covering letter on headed paper		04 March 2014

Evidence of Sponsor insurance or indemnity (non NHS Sponsors only)		18 September 2013
GP/consultant information sheets or letters	1.0	25 February 2014
Letter from sponsor		04 February 2014
Letters of invitation to participant	1.0	06 March 2014
Other [CV]	Shindy Je	25 February 2014
Other [CV]	Prof Morgan	06 March 2014
Other [Letter from funder]		14 August 2013
Other [Website Advertisement]	1.0	25 February 2014
Other [CV]	Lindsay Rountree	25 February 2014
Participant consent form [Healthy Participants]	1.0	25 February 2014
Participant consent form	1.0	25 February 2014
Participant information sheet (PIS)	2.0	16 April 2014
Participant information sheet (PIS) [Healthy Participants]	2.0	16 April 2014
REC Application Form	1.0	11 March 2014
Research protocol or project proposal	1.0	25 February 2014
Summary CV for Chief Investigator (CI)	Dr T Redmond	04 March 2014

Statement of compliance

The Committee is constituted in accordance with the Governance Arrangements for Research Ethics Committees and complies fully with the Standard Operating Procedures for Research Ethics Committees in the UK.

After ethical review

Reporting requirements

The attached document "*After ethical review – guidance for researchers*" gives detailed guidance on reporting requirements for studies with a favourable opinion, including:

- Notifying substantial amendments
- Adding new sites and investigators
- Notification of serious breaches of the protocol
- Progress and safety reports
- Notifying the end of the study

The HRA website also provides guidance on these topics, which is updated in the light of changes in reporting requirements or procedures.

Feedback

You are invited to give your view of the service that you have received from the National Research Ethics Service and the application procedure. If you wish to make your views known please use the feedback form available on the HRA website: <http://www.hra.nhs.uk/about-the-hra/governance/quality-assurance/>

We are pleased to welcome researchers and R & D staff at our NRES committee members' training days – see details at <http://www.hra.nhs.uk/hra-training/>

14/WA/0105

Please quote this number on all correspondence

With the Committee's best wishes for the success of this project.

Yours sincerely



p.p.
Dr K Craig
Chair

Email: jagit.sidhu@wales.nhs.uk

Enclosures: "After ethical review – guidance for researchers" [\[SL-AR2\]](#)

Copy to: R& D Office, Cardiff & Vale University Health Board
R&D Office, Cardiff University



GIG
Cymru
NHS
Wales
Bwrdd Iechyd Prifysgol
Caerdydd a'r Fro
Cardiff and Vale
University Health Board

Ysbyty Athrofaol Cymru
University Hospital of Wales

Heath Park,
Cardiff, CF14 4XW
Phone 029 2074 7747
Fax 029 2074 3638
Minicom 029 2074 3632

Parc Y Mynydd Bychan,
Caerdydd, CF14 4XW
Ffôn 029 2074 7747
Ffacs 029 20743838
Minicom 029 2074 3632

Tel: 029 20746986
Fax: 029 20745311
CAV_Research.Development@wales.nhs.uk

From: Professor C Fegan
R&D Director
R&D Office, 2nd Floor TB2
University Hospital of Wales
Cardiff
CF14 4XW

21 May 2014

Professor James Morgan
Consultant Ophthalmology
University Hospital of Wales
Heath Park
Cardiff
CF14 4XW

Dear Professor Morgan

Cardiff and Vale UHB Ref and Study Title : 14/CMC/5886 : Measuring Changes Over Time In The Retina In Eye Disease

IRAS Project ID: 141319

The above project was forwarded to Cardiff and Vale University Health Board R&D Office by the NISCHR Permissions Coordinating Unit. A Governance Review has now been completed on the project.

Documents approved for use in this study are:

Document	Version	Date of document
NHS R&D Form	3.5	Received 10/04/14
SSI form	3.5	Received 10/04/14
Protocol	1	25/02/2014
Participant Information Sheet	2	16/04/2014
Participant Information Sheet: Healthy Participants	2	16/04/2014
Invitation Letter	1	14/05/2014
GP Letter	1	25/02/2014
Website Advertisement	1	25/02/2014
Advertisement Material: Poster	1	25/02/2014
Participant Consent Form: Glaucoma	1	25/02/2014
Participant Consent Form: Healthy Volunteers	1	25/02/2014

I am pleased to inform you that the UHB has no objection to your proposal. You have informed us that Cardiff University is willing to act as Sponsor under the Research Governance Framework for Health and Social Care.

CC Mr Kadaba Rajkumar, Clinical Director
Dr Tony Redmond, School of Optometry and Vision Sciences
Miss Shindy Je, School of Optometry
Miss Lindsay Rountree, School of Optometry
Chris Shaw, Research Innovation Enterprise Services, Cardiff University

Please accept this letter as confirmation of permission for the project to begin within this UHB.

The UHB considers that this study is likely to be suitable for adoption onto the NISCHR Clinical Research Portfolio (CRP). This is important so that the UHB can receive funding to support this study. An application for adoption should be made by the Chief Investigator before commencing the study. If you wish to begin the study before it has been adopted, you must first obtain permission to do so from the Ophthalmology Clinical Director, Mr Rajkumar.

If your study is adopted onto the NISCHR CRP, it will be a condition of this NHS research permission, that you will be required to regularly upload recruitment data onto the portfolio database.

To apply for adoption onto the NISCHR CRP, please go to:

<http://www.wales.nhs.uk/sites3/page.cfm?orgid=580&pid=31979>. Once adopted, NISCHR CRP studies may be eligible for additional support through the NISCHR Clinical Research Centre. Further information can be found at:

<http://www.wales.nhs.uk/sites3/page.cfm?orgid=580&pid=28571>

If your study is adopted onto the portfolio, please inform NISCHR PCU and the R&D Office of your portfolio ID number.

To upload recruitment data, please follow this link:

http://www.crnc.nihr.ac.uk/about_us/processes/portfolio/p_recruitment Uploading recruitment data will enable NISCHR to monitor research activity within NHS organisations, leading to NHS R&D allocations which are activity driven.

May I take this opportunity to wish you success with the project and remind you that as Principal Investigator you are required to:

- Inform the R&D Office if this project has not opened within 12 months of the date of this letter. Failure to do so may invalidate R&D approval.
- Inform NISCHR PCU and the UHB R&D Office if any external or additional funding is awarded for this project in the future
- Submit any substantial amendments relating to the study to NISCHR PCU in order that they can be reviewed and approved prior to implementation
- Ensure NISCHR PCU is notified of the study's closure
- Ensure that the study is conducted in accordance with all relevant policies, procedures and legislation
- Provide information on the project to the UHB R&D Office as requested from time to time, to include participant recruitment figures

Yours sincerely,



Professor Christopher Fegan
R&D Director / Chair of the Cardiff and Vale Research Review Service (CaRRS)

References

- Agervi, P., Nilsson, M. & Martin, L., 2010. Foveal function in children treated for amblyopia. *Acta Ophthalmologica*, 88(2), pp.222–6.
- Alexandrescu, C. *et al.*, 2010. Confocal scanning laser ophthalmoscopy in glaucoma diagnosis and management. *Journal of Medicine and Life*, 3(3), pp.229–34.
- Anderson, A.J., 2003. Utility of a dynamic termination criterion in the ZEST adaptive threshold method. *Vision Research*, 43(2), pp.165–70.
- Anderson, R.S., 2006. The psychophysics of glaucoma: improving the structure/function relationship. *Progress in Retinal and Eye Research*, 25(1), pp.79–97.
- Anderson, R.S., McDowell, D.R. & Ennis, F.A., 2001. Effect of localized defocus on detection thresholds for different sized targets in the fovea and periphery. *Acta Ophthalmologica*, 79(1), pp.60–3.
- Ansari, E.A., Morgan, J.E. & Snowden, R.J., 2002a. Glaucoma: squaring the psychophysics and neurobiology. *British Journal of Ophthalmology*, 86(7), pp.823–6.
- Ansari, E.A., Morgan, J.E. & Snowden, R.J., 2002b. Psychophysical characterisation of early functional loss in glaucoma and ocular hypertension. *British Journal of Ophthalmology*, 86(10), pp.1131–5.
- Antonini, A. & Stryker, M.P., 1993. Rapid remodeling of axonal arbors in the visual cortex. *Science*, 260(5115), pp.1819–21.
- Armaly, M.F., 1967. Genetic determination of cup/disc ratio of the optic nerve. *Archives of Ophthalmology*, 78(1), pp.35–43.

- Artes, P.H. *et al.*, 2002. Properties of perimetric threshold estimates from Full Threshold, SITA Standard, and SITA Fast strategies. *Investigative Ophthalmology & Visual Science*, 43(8), pp.2654–9.
- Artes, P.H. *et al.*, 2005. Threshold and variability properties of matrix frequency-doubling technology and standard automated perimetry in glaucoma. *Investigative Ophthalmology & Visual Science*, 46(7), pp.2451–7.
- Artes, P.H. & Chauhan, B.C., 2009. Signal/noise analysis to compare tests for measuring visual field loss and its progression. *Investigative Ophthalmology & Visual Science*, 50(10), pp.4700–8.
- Atchison, D.A., 2004. Recent advances in representation of monochromatic aberrations of human eyes. *Clinical & Experimental Optometry*, 87(3), pp.138–48.
- Bach, M., Meigen, T. & Strasburger, H., 1997. Raster-scan cathode-ray tubes for vision research--limits of resolution in space, time and intensity, and some solutions. *Spatial Vision*, 10(4), pp.403–14.
- Barlow, H.B., 1958. Temporal and spatial summation in human vision at different background intensities. *The Journal of Physiology*, 141(2), pp.337–50.
- Bayer, A.U. & Erb, C., 2002. Short wavelength automated perimetry, frequency doubling technology perimetry, and pattern electroretinography for prediction of progressive glaucomatous standard visual field defects. *Ophthalmology*, 109(5), pp.1009–1017.
- Bedell, H.E. & Kandel, G.L., 1976. Experimentally induced variations in the dark adaptation functions of a severe strabismic amblyope. *Documenta Ophthalmologica*, 41(1), pp.129–56.
- Bengtsson, B. & Heijl, A., 2006. Diagnostic sensitivity of fast blue-yellow and standard

- automated perimetry in early glaucoma: a comparison between different test programs. *Ophthalmology*, 113(7), pp.1092–7.
- Bengtsson, B., Heijl, A. & Olsson, J., 1998. Evaluation of a new threshold visual field strategy, SITA, in normal subjects. Swedish Interactive Thresholding Algorithm. *Acta Ophthalmologica*, 76(2), pp.165–9.
- Blumenthal, E.Z. *et al.*, 2003. Evaluating several sources of variability for standard and SWAP visual fields in glaucoma patients, suspects, and normals. *Ophthalmology*, 110(10), pp.1895–902.
- Brown, B. *et al.*, 1989. Spatial summation in young and elderly observers. *Ophthalmic & Physiological Optics*, 9(3), pp.310–3.
- Buhrmann, R.R. *et al.*, 2000. Prevalence of glaucoma in a rural East African population. *Investigative Ophthalmology & Visual Science*, 41(1), pp.40–8.
- Bussel, I.I., Wollstein, G. & Schuman, J.S., 2014. OCT for glaucoma diagnosis, screening and detection of glaucoma progression. *British Journal of Ophthalmology*, 98(Suppl 2), p.ii15-ii19.
- Cairns, J.E., 1968. Trabeculectomy: Preliminary report of a new method. *American Journal of Ophthalmology*, 66(4), pp.673–9.
- Calver, R. *et al.*, 2007. Peripheral refraction for distance and near vision in emmetropes and myopes. *Ophthalmic & Physiological Optics*, 27(6), pp.584–93.
- Campbell, F.W. & Green, D.G., 1965. Optical and retinal factors affecting visual resolution. *Journal of Physiology*, 181(3), pp.576–93.
- Casson, E.J., Johnson, C.A. & Shapiro, L.R., 1993. Longitudinal comparison of temporal-modulation perimetry with white-on-white and blue-on-yellow perimetry in ocular hypertension and early glaucoma. *Journal of the Optical Society of*

America, 10(8), pp.1792–806.

Casson, R.J. *et al.*, 2012. Definition of glaucoma: clinical and experimental concepts.

Clinical & Experimental Ophthalmology, 40(4), pp.341–349.

Charman, W.N. & Radhakrishnan, H., 2010. Peripheral refraction and the development of refractive error: a review. *Ophthalmic & Physiological Optics*, 30(4), pp.321–38.

Chaturvedi, N., Hedley-Whyte, E.T. & Dreyer, E.B., 1993. Lateral geniculate nucleus in glaucoma. *American Journal of Ophthalmology*, 116(2), pp.182–8.

Chatzistefanou, K.I. *et al.*, 2005. Contrast sensitivity in amblyopia: the fellow eye of untreated and successfully treated amblyopes. *Journal of American Association for Pediatric Ophthalmology and Strabismus*, 9(5), pp.468–74.

Chauhan, B.C. *et al.*, 2008a. Canadian Glaucoma Study: 2. risk factors for the progression of open-angle glaucoma. *Archives of Ophthalmology*, 126(8), pp.1030–6.

Chauhan, B.C. *et al.*, 2008b. Practical recommendations for measuring rates of visual field change in glaucoma. *British Journal of Ophthalmology*, 92(4), pp.569–73.

Chauhan, B.C. *et al.*, 2010. Canadian Glaucoma Study: 3. Impact of risk factors and intraocular pressure reduction on the rates of visual field change. *Archives of Ophthalmology*, 128(10), pp.1249–55.

Chauhan, B.C. & Johnson, C.A., 1999. Test-retest variability of frequency-doubling perimetry and conventional perimetry in glaucoma patients and normal subjects. *Investigative Ophthalmology & Visual Science*, 40(3), pp.648–56.

Chen, C.W., 1983. Enhanced intraocular pressure controlling effectiveness of trabeculectomy by local application of mitomycin-C. *Asia-Pacific Academy of*

Ophthalmology, 9, p.172.

Chen, H. & Weber, A.J., 2001. BDNF enhances retinal ganglion cell survival in cats with optic nerve damage. *Investigative Ophthalmology & Visual Science*, 42(5), pp.966–74.

Chen, W. *et al.*, 2013. Comparison of Macular and Retinal Nerve Fiber Layer Thickness in Untreated and Treated Binocular Amblyopia. *Current Eye Research*, 38(12), pp.1248–1254.

Choi, D.W., 1988. Glutamate neurotoxicity and diseases of the nervous system. *Neuron*, 1(8), pp.623–34.

Chrysostomou, V. *et al.*, 2013. Oxidative stress and mitochondrial dysfunction in glaucoma. *Current Opinion in Pharmacology*, 13(1), pp.12–15.

Chrysostomou, V., Troncone, I.A. & Crowston, J.G., 2010. Mechanisms of Retinal Ganglion Cell Injury in Aging and Glaucoma. *Ophthalmic Research*, 44(3), pp.173–178.

Clavagnier, S., Dumoulin, S.O. & Hess, R.F., 2015. Is the Cortical Deficit in Amblyopia Due to Reduced Cortical Magnification, Loss of Neural Resolution, or Neural Disorganization? *Journal of Neuroscience*, 35(44), pp.14740–14755.

Conway, B.R., 2001. Spatial structure of cone inputs to color cells in alert macaque primary visual cortex (V-1). *Journal of Neuroscience*, 21(8), pp.2768–83.

Conway, B.R. & Livingstone, M.S., 2006. Spatial and Temporal Properties of Cone Signals in Alert Macaque Primary Visual Cortex. *Journal of Neuroscience*, 26(42), pp.10826–10846.

Cornsweet, T., 1962. The Staircase-Method in Psychophysics. *American Journal of Psychology*, 75(3), pp.485–491.

- Cox, J.F., Suh, S. & Leguire, L.E., 1996. Vernier acuity in amblyopic and nonamblyopic children. *Journal of Pediatric Ophthalmology and Strabismus*, 33(1), pp.39–46.
- Cursiefen, C. *et al.*, 2000. Migraine and tension headache in high-pressure and normal-pressure glaucoma. *American Journal of Ophthalmology*, 129(1), pp.102–4.
- Dacey, D.M., 1994. Physiology, morphology and spatial densities of identified ganglion cell types in primate retina. *Ciba Foundation Symposium*, 184, pp.12-28-34, 63–70.
- Dacey, D.M. & Lee, B.B., 1994. The “blue-on” opponent pathway in primate retina originates from a distinct bistratified ganglion cell type. *Nature*, 367(6465), pp.731–5.
- Dacey, D.M. & Petersen, M.R., 1992. Dendritic field size and morphology of midget and parasol ganglion cells of the human retina. *Proceedings of the National Academy of Sciences of the United States of America*, 89(20), pp.9666–70.
- Dalimier, E. & Dainty, C., 2010. Role of ocular aberrations in photopic spatial summation in the fovea. *Optics Letters*, 35(4), pp.589–91.
- Dandona, L., Hendrickson, A. & Quigley, H.A., 1991. Selective effects of experimental glaucoma on axonal transport by retinal ganglion cells to the dorsal lateral geniculate nucleus. *Investigative Ophthalmology & Visual Science*, 32(5), pp.1593–9.
- Davila, K.D. & Geisler, W.S., 1991. The relative contributions of pre-neural and neural factors to areal summation in the fovea. *Vision Research*, 31(7–8), pp.1369–80.
- Davis, B.M. *et al.*, 2016. Automatic quantitative analysis of experimental primary and secondary retinal neurodegeneration: implications for optic neuropathies. *Cell*

Death Discovery, 2, p.16031.

Derick, R.J. *et al.*, 1994. A clinical study of peripapillary crescents of the optic disc in chronic experimental glaucoma in monkey eyes. *Archives of Ophthalmology*, 112(6), pp.846–50.

Derrington, A.M. & Hawken, M.J., 1981. Spatial and temporal properties of cat geniculate neurones after prolonged deprivation. *Journal of Physiology*, 314, pp.107–20.

DiProspero, N.A. *et al.*, 2004. Early changes in Huntington's disease patient brains involve alterations in cytoskeletal and synaptic elements. *Journal of Neurocytology*, 33(5), pp.517–33.

Donovan, H.C., Weale, R.A. & Wheeler, C., 1978. The perimeter as a monitor of glaucomatous changes. *British Journal of Ophthalmology*, 62(10), pp.705–8.

Doughty, M.J. & Zaman, M.L., 2000. Human corneal thickness and its impact on intraocular pressure measures: a review and meta-analysis approach. *Survey of Ophthalmology*, 44(5), pp.367–408.

Downs, J.C., 2015. Optic nerve head biomechanics in aging and disease. *Experimental Eye Research*, 133, pp.19–29.

Drasdo, N. & Fowler, C.W., 1974. Non-linear projection of the retinal image in a wide-angle schematic eye. *The British Journal of Ophthalmology*, 58(8), pp.709–14.

Dreyer, E.B. *et al.*, 1994. Greater sensitivity of larger retinal ganglion cells to NMDA-mediated cell death. *Neuroreport*, 5(5), pp.629–31.

Egrilmez, S. *et al.*, 2004. Surgically induced corneal refractive change following glaucoma surgery: nonpenetrating trabecular surgeries versus trabeculectomy. *Journal of Cataract and Refractive Surgery*, 30(6), pp.1232–9.

- Ersan, I. *et al.*, 2012. Evaluation of Retinal Nerve Fiber Layer Thickness in Patients With Anisometropic and Strabismic Amblyopia Using Optical Coherence Tomography. *Journal of Pediatric Ophthalmology & Strabismus*, 50(2), pp.113–7.
- Fellman, R.L., Lynn, J.R. & Starita, R.J., 1989. Clinical importance of spatial summation in glaucoma. *Perimetry Update 1988/1989*, p.Msterdam: Kugler & Gedini.
- Fischer, B., 1973. Overlap of receptive field centers and representation of the visual field in the cat's optic tract. *Vision Research*, 13(11), pp.2113–20.
- Flammer, J., Drance, S.M. & Zulauf, M., 1984. Differential light threshold. Short- and long-term fluctuation in patients with glaucoma, normal controls, and patients with suspected glaucoma. *Archives of Ophthalmology*, 102(5), pp.704–6.
- Flynn, J.T., 1967. Spatial Summation in Amblyopia. *Archives of Ophthalmology*, 78(4), pp.470–474.
- Foster, P.J. *et al.*, 1996. Glaucoma in Mongolia. A population-based survey in Hövsgöl province, northern Mongolia. *Archives of Ophthalmology*, 114(10), pp.1235–41.
- Foster, P.J. *et al.*, 2000. The prevalence of glaucoma in Chinese residents of Singapore: a cross-sectional population survey of the Tanjong Pagar district. *Archives of Ophthalmology*, 118(8), pp.1105–11.
- Foster, P.J. *et al.*, 2002. The definition and classification of glaucoma in prevalence surveys. *British Journal of Ophthalmology*, 86(2), pp.238–42.
- Freeman, R.D. & Bradley, A., 1980. Monocularly deprived humans: nondeprived eye has supernormal vernier acuity. *Journal of Neurophysiology*, 43(6), pp.1645–53.
- Fujimoto, N. *et al.*, 2002. Learning effect for frequency doubling perimetry in patients with glaucoma. *American Journal of Ophthalmology*, 133(2), pp.269-70

- Fukuoka, S. *et al.*, 2011. Effect of trabeculectomy on ocular and corneal higher order aberrations. *Japanese Journal of Ophthalmology*, 55(5), pp.460–466.
- Gardiner, S.K., Fortune, B. & Demirel, S., 2013. Signal-to-Noise Ratios for Structural and Functional Tests in Glaucoma. *Translational Vision Science & Technology*, 2(6), p.3.
- Garway-Heath, D.F. *et al.*, 2002. Relationship between electrophysiological, psychophysical, and anatomical measurements in glaucoma. *Investigative Ophthalmology & Visual Science*, 43(7), pp.2213–20.
- Garway-Heath, D.F. *et al.*, 1998. Vertical cup/disc ratio in relation to optic disc size: its value in the assessment of the glaucoma suspect. *British Journal of Ophthalmology*, 82(10), pp.1118–1124.
- Ghodrati, M., Morris, A.P. & Price, N.S.C., 2015. The (un)suitability of modern liquid crystal displays (LCDs) for vision research. *Frontiers in Psychology*, 6, p.303.
- Gilbert, C.D. & Wiesel, T.N., 1992. Receptive field dynamics in adult primary visual cortex. *Nature*, 356(6365), pp.150–2.
- Glezer, V.D., 1965. The receptive fields of the retina. *Vision Research*, 5(9), pp.497–525.
- Glovinsky, Y., Quigley, H.A. & Dunkelberger, G.R., 1991. Retinal ganglion cell loss is size dependent in experimental glaucoma. *Investigative Ophthalmology & Visual Science*, 32(3), pp.484–91.
- Glovinsky, Y., Quigley, H.A. & Pease, M.E., 1993. Foveal ganglion cell loss is size dependent in experimental glaucoma. *Investigative Ophthalmology & Visual Science*, 34(2), pp.395–400.
- Goodyear, B.G., Nicolle, D.A. & Menon, R.S., 2002. High resolution fMRI of ocular

- dominance columns within the visual cortex of human amblyopes. *Strabismus*, 10(2), pp.129–36.
- Guidelines, E., 2017. European Glaucoma Society Terminology and Guidelines for Glaucoma, 4th Edition - Part 1. *British Journal of Ophthalmology*, 101(5), p.73 LP-127.
- Gustafsson, J. *et al.*, 2001. Peripheral astigmatism in emmetropic eyes. *Ophthalmic and Physiological Optics*, 21(5), pp.393–400.
- Hagemans, K. & van der Wildt, G., 1979. The influence of the stimulus width on the contrast sensitivity function in amblyopia. *Investigative Ophthalmology & Visual Science*, 18(8), pp.842–847.
- Harwerth, R.S. *et al.*, 1999. Ganglion cell losses underlying visual field defects from experimental glaucoma. *Investigative Ophthalmology & Visual Science*, 40(10), pp.2242–50.
- Harwerth, R.S., Wheat, J.L. & Rangaswamy, N. V., 2008. Age-Related Losses of Retinal Ganglion Cells and Axons. *Investigative Ophthalmology & Visual Science*, 49(10), p.4437.
- Havvas, I. *et al.*, 2013. Comparison of SWAP and SAP on the point of glaucoma conversion. *Clinical Ophthalmology*, 7, pp.1805–10.
- Heijl, A. *et al.*, 2003. Measuring visual field progression in the Early Manifest Glaucoma Trial. *Acta Ophthalmologica*, 81(3), pp.286–93.
- Heijl, A. *et al.*, 2013. Rates of visual field progression in clinical glaucoma care. *Acta Ophthalmologica*, 91(5), pp.406–12.
- Heijl, A. *et al.*, 2002. Reduction of intraocular pressure and glaucoma progression: results from the Early Manifest Glaucoma Trial. *Archives of Ophthalmology*,

120(10), pp.1268–79.

Heijl, A., Lindgren, A. & Lindgren, G., 1989. Test-retest variability in glaucomatous visual fields. *American Journal of Ophthalmology*, 108(2), pp.130–5.

Hendrickson, A. *et al.*, 1987. Effects of early unilateral blur on the macaque's visual system. II. Anatomical observations. *Journal of Neuroscience*, 7(5), pp.1327–1339.

Henson, D.B. *et al.*, 2000. Response variability in the visual field: comparison of optic neuritis, glaucoma, ocular hypertension, and normal eyes. *Investigative Ophthalmology & Visual Science*, 41(2), pp.417–21.

Heron, G., Adams, A.J. & Husted, R., 1987. Foveal and non-foveal measures of short wavelength sensitive pathways in glaucoma and ocular hypertension. *Ophthalmic & Physiological Optics*, 7(4), pp.403–4.

Hitchings, R.A., 1978. The optic disc in glaucoma, III: diffuse optic disc pallor with raised intraocular pressure. *British Journal of Ophthalmology*, 62(10), pp.670–5.

Holder, G.E., 1987. Significance of abnormal pattern electroretinography in anterior visual pathway dysfunction. *British Journal of Ophthalmology*, 71(3), pp.166–71.

Hollingworth, P. *et al.*, 2011. Common variants at ABCA7, MS4A6A/MS4A4E, EPHA1, CD33 and CD2AP are associated with Alzheimer's disease. *Nature Genetics*, 43(5), pp.429–35.

Hollows, F.C. & Graham, P.A., 1966. Intra-ocular pressure, glaucoma, and glaucoma suspects in a defined population. *The British Journal of Ophthalmology*, 50(10), pp.570–86.

Hong, Y.J. *et al.*, 1998. The effect of mitomycin-C on postoperative corneal astigmatism in trabeculectomy and a triple procedure. *Ophthalmic surgery and lasers*, 29(6), pp.484–9.

- Hubel, D.H. & Wiesel, T.N., 1968. Receptive fields and functional architecture of monkey striate cortex. *The Journal of Physiology*, 195(1), pp.215–43.
- Hubel, D.H., Wiesel, T.N. & LeVay, S., 1977. Plasticity of ocular dominance columns in monkey striate cortex. *Philosophical Transactions of the Royal Society of London*, 278(961), pp.377–409.
- Husain, R. *et al.*, 2013. Longitudinal changes in anterior chamber depth and axial length in Asian subjects after trabeculectomy surgery. *British Journal of Ophthalmology*, 97(7), pp.852–856.
- Iester, M. *et al.*, 2000. Learning effect, short-term fluctuation, and long-term fluctuation in frequency doubling technique. *American Journal of Ophthalmology*, 130(2), pp.160–164.
- Investigators, A., 2000. The Advanced Glaucoma Intervention Study (AGIS): 7. The relationship between control of intraocular pressure and visual field deterioration. The AGIS Investigators. *American journal of ophthalmology*, 130(4), pp.429–40.
- Johnson, C.A. *et al.*, 1993. Blue-on-yellow perimetry can predict the development of glaucomatous visual field loss. *Archives of Ophthalmology*, 111(5), pp.645–50.
- Johnson, C.A., 1994. Selective versus nonselective losses in glaucoma. *Journal of Glaucoma*, 3 Suppl 1, pp.S32-44.
- Johnson, C.A. & Samuels, S.J., 1997. Screening for glaucomatous visual field loss with frequency-doubling perimetry. *Investigative Ophthalmology & Visual Science*, 38(2), pp.413–25.
- Johnson, E.C. *et al.*, 2000. Chronology of optic nerve head and retinal responses to elevated intraocular pressure. *Investigative Ophthalmology & Visual Science*,

41(2), pp.431–42.

- Johnson, J.E. *et al.*, 1986. Brain-derived neurotrophic factor supports the survival of cultured rat retinal ganglion cells. *The Journal of Neuroscience*, 6(10), pp.3031–8.
- Johnson, T. V & Tomarev, S.I., 2010. Rodent models of glaucoma. *Brain research bulletin*, 81(2–3), pp.349–58.
- Jonas, J.B., Gusek, G.C. & Naumann, G.O., 1988a. Optic disc, cup and neuroretinal rim size, configuration and correlations in normal eyes. *Investigative Ophthalmology & Visual Science*, 29(7), pp.1151–8.
- Jonas, J.B., Gusek, G.C. & Naumann, G.O., 1988b. Optic disk morphometry in high myopia. *Graefe's Archive for Clinical and Experimental Ophthalmology*, 226(6), pp.587–90.
- Jones, K.R., Kalil, R.E. & Spear, P.D., 1984. Effects of strabismus on responsivity, spatial resolution, and contrast sensitivity of cat lateral geniculate neurons. *Journal of Neurophysiology*, 52(3), pp.538–52.
- Kamal, D.S. *et al.*, 1999. Detection of optic disc change with the Heidelberg retina tomograph before confirmed visual field change in ocular hypertensives converting to early glaucoma. *The British Journal of Ophthalmology*, 83(3), pp.290–4.
- Kamal, D.S. *et al.*, 2000. Use of sequential Heidelberg retina tomograph images to identify changes at the optic disc in ocular hypertensive patients at risk of developing glaucoma. *The British Journal of Ophthalmology*, 84(9), pp.993–8.
- Kass, M.A. *et al.*, 2002. The Ocular Hypertension Treatment Study: a randomized trial determines that topical ocular hypotensive medication delays or prevents the onset of primary open-angle glaucoma. *Archives of Ophthalmology*, 120(6), pp.701-13-30.

- Katz, L.M., Levi, D.M. & Bedell, H.E., 1984. Central and peripheral contrast sensitivity in amblyopia with varying field size. *Documenta Ophthalmologica*, 58(4), pp.351–73.
- Kelly, D.H., 1966. Frequency Doubling in Visual Responses. *Journal of the Optical Society of America*, 56(11), p.1628.
- Keltner, J.L. *et al.*, 2006. The association between glaucomatous visual fields and optic nerve head features in the Ocular Hypertension Treatment Study. *Ophthalmology*, 113(9), pp.1603–12.
- Kerrigan-Baumrind, L.A. *et al.*, 2000. Number of ganglion cells in glaucoma eyes compared with threshold visual field tests in the same persons. *Investigative Ophthalmology & Visual Science*, 41(3), pp.741–8.
- Khuu, S.K. & Kalloniatis, M., 2015. Spatial summation across the central visual field: implications for visual field testing. *Journal of Vision*, 15(1), p.15.1.6.
- King-Smith, P.E. *et al.*, 1994. Efficient and unbiased modifications of the QUEST threshold method: theory, simulations, experimental evaluation and practical implementation. *Vision Research*, 34(7), pp.885–912.
- King-Smith, P.E., Lubow, M. & Benes, S.C., 1984. Selective damage to chromatic mechanisms in neuro-ophthalmic diseases I. Review of published evidence. *Documenta Ophthalmologica*, 58(3), pp.241–50.
- King, W.M. *et al.*, 2006. Expansion of visual receptive fields in experimental glaucoma. *Visual Neuroscience*, 23(1), pp.137–42.
- Kiorpes, L. *et al.*, 1998. Neuronal correlates of amblyopia in the visual cortex of macaque monkeys with experimental strabismus and anisometropia. *Journal of Neuroscience*, 18(16), pp.6411–24.

- Klein, B.E. *et al.*, 1992. Prevalence of glaucoma. The Beaver Dam Eye Study. *Ophthalmology*, 99(10), pp.1499–504.
- Kleitman, N. & H, P. r., 1929. Contribution à l'étude des facteurs régissant le taux de summation des impressions lumineuses de surface inégale. *L'année psychologique*, 29, pp.57–91.
- Kook, M.S., Kim, H.B. & Lee, S.U., 2001. Short-term effect of mitomycin-C augmented trabeculectomy on axial length and corneal astigmatism. *Journal of Cataract & Refractive Surgery*, 27(4), pp.518–523.
- Kratz, K.E. *et al.*, 1979. Retinal X- and Y-cells in monocularly lid-sutured cats: normality of spatial and temporal properties. *Brain Research*, 172(3), pp.545–51.
- Kulze, J.C., Stewart, W.C. & Sutherland, S.E., 1990. Factors associated with a learning effect in glaucoma patients using automated perimetry. *Acta Ophthalmologica*, 68(6), pp.681–6.
- Lascaratos, G. *et al.*, 2012. Mitochondrial dysfunction in glaucoma: understanding genetic influences. *Mitochondrion*, 12(2), pp.202–12.
- Latham, K., Whitaker, D. & Wild, J.M., 1994. Spatial summation of the differential light threshold as a function of visual field location and age. *Ophthalmic & Physiological Optics*, 14(1), pp.71–8.
- Lee, S. *et al.*, 2011. Mitochondrial dysfunction in glaucoma and emerging bioenergetic therapies. *Experimental Eye Research*, 93(2), pp.204–12.
- Leeprechanon, N. *et al.*, 2007. Frequency-doubling perimetry: comparison with standard automated perimetry to detect glaucoma. *American Journal of Ophthalmology*, 143(2), pp.263–271.
- Leguire, L.E. *et al.*, 1990. SKILL card results in amblyopic children. *Journal of*

Pediatric Ophthalmology and Strabismus, 31(4), pp.256–61.

Lelkens, A.M. & Zuidema, P., 1983. Increment thresholds with various low background intensities at different locations in the peripheral retina. *Journal of the Optical Society of America*, 73(10), pp.1372–8.

Leske, M.C. *et al.*, 2003. Factors for glaucoma progression and the effect of treatment: the early manifest glaucoma trial. *Archives of Ophthalmology*, 121(1), pp.48–56.

Leventhal, A.G., Rodieck, R.W. & Dreher, B., 1981. Retinal ganglion cell classes in the Old World monkey: morphology and central projections. *Science*, 213(4512), pp.1139–42.

Levi, D.M. & Klein, S.A., 1985. Vernier acuity, crowding and amblyopia. *Vision Research*, 25(7), pp.979–91.

Levitt, H., 1971. Transformed up-down methods in psychoacoustics. *The Journal of the Acoustical Society of America*, 49(2), Suppl 2:467+.

Levitt, J.B. *et al.*, 2001. Visual response properties of neurons in the LGN of normally reared and visually deprived macaque monkeys. *Journal of Neurophysiology*, 85(5), pp.2111–29.

Lie, I., 1980. Visual detection and resolution as a function of retinal locus. *Vision Research*, 20(11), pp.967–74.

Linden, R. & Perry, V.H., 1982. Ganglion cell death within the developing retina: a regulatory role for retinal dendrites? *Neuroscience*, 7(11), pp.2813–27.

Lucas, D.R. & Newhouse, J.P., 1957. The toxic effect of sodium L-glutamate on the inner layers of the retina. *Archives of Ophthalmology*, 58(2), pp.193–201.

Maddess, G.H.H., 1992. Performance of nonlinear visual units in ocular hypertension and glaucoma. *Clinical Vision Science*, 7(5), pp.371–383.

- Man, X. *et al.*, 2015. Anatomical effects of clear lens extraction by phacoemulsification versus trabeculectomy on anterior chamber drainage angle in primary angle-closure glaucoma (PACG) patients. *Graefe's Archive for Clinical and Experimental Ophthalmology*, 253(5), pp.773–778.
- McKee, S.P., Levi, D.M. & Movshon, J.A., 2003. The pattern of visual deficits in amblyopia. *Journal of Vision*, 3(5), pp.380–405.
- Medeiros, F.A. *et al.*, 2012. Estimating the rate of retinal ganglion cell loss in glaucoma. *American Journal of Ophthalmology*, 154(5), p.814–824.e1.
- Medeiros, F.A., Sample, P.A. & Weinreb, R.N., 2004. Frequency doubling technology perimetry abnormalities as predictors of glaucomatous visual field loss. *American Journal of Ophthalmology*, 137(5), pp.863–71.
- Merigan, W.H. & Maunsell, J.H., 1993. How parallel are the primate visual pathways? *Annual Review of Neuroscience*, 16, pp.369–402.
- Metha, A.B., Vingrys, A.J. & Badcock, D.R., 1993. Calibration of a color monitor for visual psychophysics. *Behavior Research Methods, Instruments, & Computers*, 25(3), pp.371–383.
- Mikelberg, F.S. *et al.*, 1989. The normal human optic nerve. Axon count and axon diameter distribution. *Ophthalmology*, 96(9), pp.1325–8.
- Millodot, M., 1981. Effect of ametropia on peripheral refraction. *American Journal of Optometry and Physiological Optics*, 58(9), pp.691–5.
- Morgan, J.E., 2012. Retina ganglion cell degeneration in glaucoma: an opportunity missed? A review. *Clinical & Experimental Ophthalmology*, 40(4), pp.364–8.
- Morgan, J.E. *et al.*, 2006. Retinal ganglion cell remodelling in experimental glaucoma. *Advances in Experimental Medicine and Biology*, 572, pp.397–402.

- Morgan, J.E., 2002. Retinal ganglion cell shrinkage in glaucoma. *Journal of Glaucoma*, 11(4), pp.365–70.
- Morgan, J.E., 1994. Selective cell death in glaucoma: does it really occur? *British Journal of Ophthalmology*, 78(11), pp.875-9-80.
- Morgan, J.E., Uchida, H. & Caprioli, J., 2000. Retinal ganglion cell death in experimental glaucoma. *British Journal of Ophthalmology*, 84(3), pp.303–10.
- Morrison, J.C., Johnson, E. & Cepurna, W.O., 2008. Rat models for glaucoma research. In *Progress in Brain Research*. pp. 285–301.
- Movshon, J.A. *et al.*, 1987. Effects of early unilateral blur on the macaque's visual system. III. Physiological observations. *Journal of Neuroscience*, 7(5), pp.1340–51.
- Mozaffarieh, M. & Flammer, J., 2013. New insights in the pathogenesis and treatment of normal tension glaucoma. *Current Opinion in Pharmacology*, 13(1), pp.43–49.
- Mulholland, P.J. *et al.*, 2015. Estimating the critical duration for temporal summation of standard achromatic perimetric stimuli. *Investigative Ophthalmology & Visual Science*, 56(1), pp.431–7.
- Mutti, D.O. *et al.*, 2000. Peripheral refraction and ocular shape in children. *Investigative Ophthalmology & Visual Science*, 41(5), pp.1022–30.
- Nesher, R. *et al.*, 1990. Steady-state pattern electroretinogram following long term unilateral administration of timolol to ocular hypertensive subjects. *Documenta Ophthalmologica*, 75(2), pp.101–9.
- Neufeld, A.H., Hernandez, M.R. & Gonzalez, M., 1997. Nitric oxide synthase in the human glaucomatous optic nerve head. *Archives of Ophthalmology*, 115(4), pp.497–503.

- Neufeld, A.H., Sawada, A. & Becker, B., 1999. Inhibition of nitric-oxide synthase 2 by aminoguanidine provides neuroprotection of retinal ganglion cells in a rat model of chronic glaucoma. *Proceedings of the National Academy of Sciences of the United States of America*, 96(17), pp.9944–8.
- Nickells, R.W., 1999. Apoptosis of retinal ganglion cells in glaucoma: an update of the molecular pathways involved in cell death. *Survey of Ophthalmology*, 43 Suppl 1, pp.S151-61.
- von Noorden, G.K., 1970. Experimental Amblyopia in Monkeys. *Archives of Ophthalmology*, 84(2), p.206.
- North, R. V *et al.*, 2010. Electrophysiological evidence of early functional damage in glaucoma and ocular hypertension. *Investigative Ophthalmology & Visual Science*, 51(2), pp.1216–22.
- O’Leary, N., Chauhan, B.C. & Artes, P.H., 2012. Visual Field Progression in Glaucoma: Estimating the Overall Significance of Deterioration with Permutation Analyses of Pointwise Linear Regression (PoPLR). *Investigative Ophthalmology & Visual Science*, 53(11), p.6776.
- Okeke, C.O. *et al.*, 2009. Adherence with topical glaucoma medication monitored electronically the Travatan Dosing Aid study. *Ophthalmology*, 116(2), pp.191–9.
- Osborne, N.N., 2010. Mitochondria: Their role in ganglion cell death and survival in primary open angle glaucoma. *Experimental Eye Research*, 90(6), pp.750–757.
- Pakravan, M. *et al.*, 2015. Intraocular lens power changes after mitomycin trabeculectomy. *European Journal of Ophthalmology*, 25(6), pp.478–482.
- Pan, F. & Swanson, W.H., 2006. A cortical pooling model of spatial summation for perimetric stimuli. *Journal of Vision*, 6(11), pp.1159–71.

- Papastathopoulos, K.I., Jonas, J.B. & Panda-Jonas, S., 1995. Large optic discs in large eyes, small optic discs in small eyes. *Experimental Eye Research*, 60(4), pp.459–61.
- Pease, M.E. *et al.*, 2000. Obstructed axonal transport of BDNF and its receptor TrkB in experimental glaucoma. *Investigative Ophthalmology & Visual Science*, 41(3), pp.764–74.
- Pelli, D.G., 1997. Pixel independence: measuring spatial interactions on a CRT display. *Spatial Vision*, 10(4), pp.443–6.
- Perry, V.H., Oehler, R. & Cowey, A., 1984. Retinal ganglion cells that project to the dorsal lateral geniculate nucleus in the macaque monkey. *Neuroscience*, 12(4), pp.1101–23.
- Phu, J., Kalloniatis, M. & Khuu, S.K., 2016. The Effect of Attentional Cueing and Spatial Uncertainty in Visual Field Testing B. Thompson, ed. *PLOS ONE*, 11(3), p.e0150922.
- Piper, H., 1903. N Über die Abhängigkeit des Reizwertes leuchtender Objekte von ihre Flächen-bezw. Winkelgrasseo Title. *Zeitschrift für Psychologie und Physiologie der Sinnesorgane*, 32, pp.98–112.
- Di Polo, A. *et al.*, 1998. Prolonged delivery of brain-derived neurotrophic factor by adenovirus-infected Müller cells temporarily rescues injured retinal ganglion cells. *Proceedings of the National Academy of Sciences of the United States of America*, 95(7), pp.3978–83.
- Porciatti, V. & Ventura, L.M., 2004. Normative data for a user-friendly paradigm for pattern electroretinogram recording. *Ophthalmology*, 111(1), pp.161–8.
- Porciatti, V. & Ventura, L.M., 2009. Physiologic significance of steady-state pattern

- electroretinogram losses in glaucoma: clues from simulation of abnormalities in normal subjects. *Journal of Glaucoma*, 18(7), pp.535–42.
- Porciatti, V. & Ventura, L.M., 2012. Retinal ganglion cell functional plasticity and optic neuropathy: a comprehensive model. *Journal of Neuro-ophthalmology*, 32(4), pp.354–8.
- Quigley, H.A. *et al.*, 1987. Chronic glaucoma selectively damages large optic nerve fibers. *Investigative Ophthalmology & Visual Science*, 28(6), pp.913–20.
- Quigley, H.A., 1995. Ganglion cell death in glaucoma: pathology recapitulates ontogeny. *Australian and New Zealand Journal of Ophthalmology*, 23(2), pp.85–91.
- Quigley, H.A., 2011. Glaucoma. *Lancet*, 377(9774), pp.1367–1377.
- Quigley, H.A., 2005. Glaucoma: macrocosm to microcosm the Friedenwald lecture. *Investigative Ophthalmology & Visual Science*, 46(8), pp.2662–70.
- Quigley, H.A. *et al.*, 1983. Morphologic changes in the lamina cribrosa correlated with neural loss in open-angle glaucoma. *American Journal of Ophthalmology*, 95(5), pp.673–91.
- Quigley, H.A., 1999. Neuronal death in glaucoma. *Progress in Retinal and Eye Research*, 18(1), pp.39–57.
- Quigley, H.A. *et al.*, 2001. The prevalence of glaucoma in a population-based study of Hispanic subjects: Proyecto VER. *Archives of Ophthalmology*, 119(12), pp.1819–26.
- Quigley, H.A. & Addicks, E.M., 1981. Regional differences in the structure of the lamina cribrosa and their relation to glaucomatous optic nerve damage. *Archives of Ophthalmology*, 99(1), pp.137–43.

- Quigley, H.A., Addicks, E.M. & Green, W.R., 1982. Optic nerve damage in human glaucoma. III. Quantitative correlation of nerve fiber loss and visual field defect in glaucoma, ischemic neuropathy, papilledema, and toxic neuropathy. *Archives of Ophthalmology*, 100(1), pp.135–46.
- Quigley, H.A., Davis, E.B. & Anderson, D.R., 1977. Descending optic nerve degeneration in primates. *Investigative Ophthalmology & Visual Science*, 16(9), pp.841–9.
- Quigley, H.A., Dunkelberger, G.R. & Green, W.R., 1988. Chronic human glaucoma causing selectively greater loss of large optic nerve fibers. *Ophthalmology*, 95(3), pp.357–63.
- Quigley, H.A. & Vitale, S., 1997. Models of open-angle glaucoma prevalence and incidence in the United States. *Investigative Ophthalmology & Visual Science*, 38(1), pp.83–91.
- Rabacchi, S.A. *et al.*, 1994. Nerve growth factor reduces apoptosis of axotomized retinal ganglion cells in the neonatal rat. *Neuroscience*, 63(4), pp.969–73.
- Racette, L. *et al.*, 2003. Primary open-angle glaucoma in blacks: a review. *Survey of Ophthalmology*, 48(3), pp.295–313.
- Ransom-Hogg, A. & Spillmann, L., 1980. Perceptive field size in fovea and periphery of the light- and dark-adapted retina. *Vision Research*, 20(3), pp.221–8.
- Redmond, T. *et al.*, 2013. Changes in Ricco's area with background luminance in the S-cone pathway. *Optometry and Vision Science*, 90(1), pp.66–74.
- Redmond, T. *et al.*, 2010a. Sensitivity loss in early glaucoma can be mapped to an enlargement of the area of complete spatial summation. *Investigative Ophthalmology & Visual Science*, 51(12), pp.6540–8.

- Redmond, T. *et al.*, 2010b. The effect of age on the area of complete spatial summation for chromatic and achromatic stimuli. *Investigative Ophthalmology & Visual Science*, 51(12), pp.6533–9.
- Reed, M.J. *et al.*, 1996. Contrast letter thresholds in the non-affected eye of strabismic and unilateral eye enucleated subjects. *Vision Research*, 36(18), pp.3011–8.
- Rempt, F., Hoogerheide, J. & Hoogenboom, W.P., 1971. Peripheral retinoscopy and the skiagram. *Ophthalmologica*, 162(1), pp.1–10.
- Ricco, A., 1877. Relazione fra il minimo angolo visuale e l'intensità luminosa. *Memorie della Regia Accademia di Scienze, lettere ed arti in Modena*, 17, pp.47–160.
- Richards, W., 1967. Apparent modifiability of receptive fields during accommodation and convergence and a model for size constancy. *Neuropsychologia*, 5(1), pp.63–72.
- Rodieck, R.W., Binmoeller, K.F. & Dineen, J., 1985. Parasol and midget ganglion cells of the human retina. *Journal of Comparative Neurology*, 233(1), pp.115–32.
- Rossetti, L. *et al.*, 2006. Learning effect of short-wavelength automated perimetry in patients with ocular hypertension. *Journal of Glaucoma*, 15(5), pp.399–404.
- Rountree, L. *et al.*, 2018. Optimising the glaucoma signal/noise ratio by mapping changes in spatial summation with area-modulated perimetric stimuli. *Scientific Report*, 8(1):2172.
- Sample, P.A. *et al.*, 1993. Short-wavelength color visual fields in glaucoma suspects at risk. *American Journal of Ophthalmology*, 115(2), pp.225–33.
- Sample, P.A., Bosworth, C.F. & Weinreb, R.N., 1997. Short-wavelength automated perimetry and motion automated perimetry in patients with glaucoma. *Archives of Ophthalmology*, 115(9), pp.1129–33.

- Sample, P.A., Boynton, R.M. & Weinreb, R.N., 1988. Isolating the color vision loss in primary open-angle glaucoma. *American Journal of Ophthalmology*, 106(6), pp.686–91.
- Sample, P.A., Madrid, M.E. & Weinreb, R.N., 1994. Evidence for a variety of functional defects in glaucoma-suspect eyes. *Journal of Glaucoma*, 3 Suppl 1, pp.S5-18.
- Sample, P.A. & Weinreb, R.N., 1992. Progressive color visual field loss in glaucoma. *Investigative Ophthalmology & Visual Science*, 33(6), pp.2068–71.
- Schefrin, B.E. *et al.*, 1998. The area of complete scotopic spatial summation enlarges with age. *Journal of the Optical Society of America*, 15(2), pp.340–8.
- van der Schoot, J. *et al.*, 2010. The ability of short-wavelength automated perimetry to predict conversion to glaucoma. *Ophthalmology*, 117(1), pp.30–4.
- Sehi, M. *et al.*, 2010. Reversal of retinal ganglion cell dysfunction after surgical reduction of intraocular pressure. *Ophthalmology*, 117(12), pp.2329–36.
- Sehi, M. *et al.*, 2011. The impact of intraocular pressure reduction on retinal ganglion cell function measured using pattern electroretinogram in eyes receiving latanoprost 0.005% versus placebo. *Vision Research*, 51(2), pp.235–42.
- Seidemann, A. *et al.*, 2002. Peripheral refractive errors in myopic, emmetropic, and hyperopic young subjects. *Journal of the Optical Society of America*, 19(12), pp.2363–73.
- Shapley, R. & Hawken, M.J., 2011. Color in the cortex: single- and double-opponent cells. *Vision Research*, 51(7), pp.701–17.
- Sharma, B.D. & Chaturvedi, R.P., 1982. Disc-cup asymmetry in normal and chronic simple glaucoma. *Indian Journal of Ophthalmology*, 30(3), pp.133–4.

- Sherman, S.M. & Stone, J., 1973. Physiological normality of the retina in visually deprived cats. *Brain Research*, 60(1), pp.224–30.
- Shou, T. *et al.*, 2003. Differential dendritic shrinkage of alpha and beta retinal ganglion cells in cats with chronic glaucoma. *Investigative Ophthalmology & Visual Science*, 44(7), pp.3005–10.
- Siliprandi, R. *et al.*, 1992. N-methyl-D-aspartate-induced neurotoxicity in the adult rat retina. *Visual Neuroscience*, 8(6), pp.567–73.
- Simmers, A.J. *et al.*, 2003. Deficits to global motion processing in human amblyopia. *Vision Research*, 43(6), pp.729–738.
- Sommer, A. *et al.*, 1991. Relationship between intraocular pressure and primary open angle glaucoma among white and black Americans. The Baltimore Eye Survey. *Archives of Ophthalmology*, 109(8), pp.1090–5.
- Spear, P.D. & Hou, V., 1990. Retinal ganglion-cell densities and soma sizes are unaffected by long-term monocular deprivation in the cat. *Brain Research*, 522(2), pp.354–358.
- Spearman, C., 1908. The method of “right and wrong cases” (‘constant stimuli’) without gauss’s formulae. *British Journal of Psychology*, 2(3), pp.227–242.
- Spry, P.G. *et al.*, 2001. Variability components of standard automated perimetry and frequency-doubling technology perimetry. *Investigative Ophthalmology & Visual Science*, 42(6), pp.1404–10.
- Susanna, R., 1983. The lamina cribrosa and visual field defects in open-angle glaucoma. *Canadian Journal of Ophthalmology*, 18(3), pp.124–6.
- Swanson, W.H. *et al.*, 2011. Responses of primate retinal ganglion cells to perimetric stimuli. *Investigative Ophthalmology & Visual Science*, 52(2), pp.764–71.

- Swanson, W.H., Feliuss, J. & Pan, F., 2004. Perimetric defects and ganglion cell damage: interpreting linear relations using a two-stage neural model. *Investigative Ophthalmology & Visual Science*, 45(2), pp.466–72.
- Tabernero, J. & Schaeffel, F., 2009. Fast scanning photoretinoscope for measuring peripheral refraction as a function of accommodation. *Journal of the Optical Society of America*, 26(10), pp.2206–10.
- Tafreshi, A. *et al.*, 2009. Visual Function-Specific Perimetry to Identify Glaucomatous Visual Loss Using Three Different Definitions of Visual Field Abnormality. *Investigative Ophthalmology & Visual Science*, 50(3), p.1234.
- Taylor, M.M., 1967. PEST: Efficient Estimates on Probability Functions. *Journal of the Acoustical Society of America*, 41(4A), p.782.
- Tham, Y.C. *et al.*, 2014. Global prevalence of glaucoma and projections of glaucoma burden through 2040: a systematic review and meta-analysis. *Ophthalmology*, 121(11), pp.2081–90.
- Thibos, L.N. *et al.*, 2002. Standards for reporting the optical aberrations of eyes. *Journal of Refractive Surgery*, 18(5), pp.S652-60.
- Thompson, B. *et al.*, 2011. Impaired spatial and binocular summation for motion direction discrimination in strabismic amblyopia. *Vision Research*, 51(6), pp.577–84.
- Treutwein, B., 1995. Adaptive psychophysical procedures. *Vision Research*, 35(17), pp.2503–22.
- Turpin, A. *et al.*, 2002. Development of efficient threshold strategies for frequency doubling technology perimetry using computer simulation. *Investigative Ophthalmology & Visual Science*, 43(2), pp.322–31.

- Turpin, A. *et al.*, 2003. Properties of perimetric threshold estimates from full threshold, ZEST, and SITA-like strategies, as determined by computer simulation. *Investigative Ophthalmology & Visual Science*, 44(11), pp.4787–95.
- Turpin, A., Artes, P.H. & McKendrick, A.M., 2012. The Open Perimetry Interface: an enabling tool for clinical visual psychophysics. *Journal of Vision*, 12(11), p.22-.
- Turpin, A., Jankovic, D. & McKendrick, A.M., 2007. Retesting visual fields: utilizing prior information to decrease test-retest variability in glaucoma. *Investigative Ophthalmology & Visual Science*, 48(4), pp.1627–34.
- Vajaranant, T.S. *et al.*, 2010. Gender and glaucoma: what we know and what we need to know. *Current Opinion in Ophthalmology*, 21(2), pp.91–9.
- Varma, R., Steinmann, W.C. & Scott, I.U., 1992. Expert agreement in evaluating the optic disc for glaucoma. *Ophthalmology*, 99(2), pp.215–21.
- Vassilev, A. *et al.*, 2005. Human S-cone vision: relationship between perceptive field and ganglion cell dendritic field. *Journal of Vision*, 5(10), pp.823–33.
- Vassilev, A. *et al.*, 2000. Spatial summation of blue-on-yellow light increments and decrements in human vision. *Vision research*, 40(8), pp.989–1000.
- Vassilev, A. *et al.*, 2003. Spatial summation of S-cone ON and OFF signals: effects of retinal eccentricity. *Vision research*, 43(27), pp.2875–84.
- Ventura, L.M. *et al.*, 2013. Pattern electroretinogram progression in glaucoma suspects. *Journal of Glaucoma*, 22(3), pp.219–25.
- Ventura, L.M. *et al.*, 2006. The relationship between retinal ganglion cell function and retinal nerve fiber thickness in early glaucoma. *Investigative Ophthalmology & Visual Science*, 47(9), pp.3904–11.
- Ventura, L.M., Feuer, W.J. & Porciatti, V., 2012. Progressive loss of retinal ganglion

cell function is hindered with IOP-lowering treatment in early glaucoma.

Investigative Ophthalmology & Visual Science, 53(2), pp.659–63.

Ventura, L.M. & Porciatti, V., 2005. Restoration of retinal ganglion cell function in early glaucoma after intraocular pressure reduction: a pilot study. *Ophthalmology*, 112(1), pp.20–7.

Vianna, J.R. & Chauhan, B.C., 2015. How to detect progression in glaucoma. In *Progress in Brain Research*. pp. 135–158.

Viswanathan, S., Frishman, L.J. & Robson, J.G., 2000. The uniform field and pattern ERG in macaques with experimental glaucoma: removal of spiking activity. *Investigative Ophthalmology & Visual Science*, 41(9), pp.2797–810.

Volbrecht, V.J. *et al.*, 2000. Spatial summation in human cone mechanisms from 0 degrees to 20 degrees in the superior retina. *Journal of the Optical Society of America*, 17(3), pp.641–50.

Walker, R.A. *et al.*, 2011. Macular and peripapillary retinal nerve fibre layer thickness in adults with amblyopia. *Canadian Journal of Ophthalmology*, 46(5), pp.425–427.

Wall, M. *et al.*, 2009. Repeatability of automated perimetry: a comparison between standard automated perimetry with stimulus size III and V, matrix, and motion perimetry. *Investigative Ophthalmology & Visual Science*, 50(2), pp.974–9.

Walsh, P., Kane, N. & Butler, S., 2005. The clinical role of evoked potentials. *Journal of Neurology, Neurosurgery, and Psychiatry*, 76 Suppl 2(suppl_2), p.ii16-22.

Wang, J.J., Mitchell, P. & Smith, W., 1997. Is there an association between migraine headache and open-angle glaucoma? Findings from the Blue Mountains Eye Study. *Ophthalmology*, 104(10), pp.1714–9.

Wang, L. *et al.*, 2003. Optical aberrations of the human anterior cornea. *Journal of*

- Cataract & Refractive Surgery*, 29(8), pp.1514–21.
- Wässle, H. & Boycott, B.B., 1991. Functional architecture of the mammalian retina. *Physiological Reviews*, 71(2), pp.447–80.
- Watson, A.B. & Fitzhugh, A., 1990. The method of constant stimuli is inefficient. *Perception and Psychophysics*, 47(1), pp.87-91.
- Watson, A.B. & Pelli, D.G., 1983. QUEST: a Bayesian adaptive psychometric method. *Perception & Psychophysics*, 33(2), pp.113–20.
- Weber, A.J. et al., 2000. Experimental glaucoma and cell size, density, and number in the primate lateral geniculate nucleus. *Investigative Ophthalmology & Visual Science*, 41(6), pp.1370–9.
- Weber, A.J. & Harman, C.D., 2008. BDNF Preserves the Dendritic Morphology of α and β Ganglion Cells in the Cat Retina after Optic Nerve Injury. *Investigative Ophthalmology & Visual Science*, 49(6), p.2456.
- Weber, A.J., Kaufman, P.L. & Hubbard, W.C., 1998. Morphology of single ganglion cells in the glaucomatous primate retina. *Investigative Ophthalmology & Visual Science*, 39(12), pp.2304–20.
- Werner, E.B., Saheb, N. & Thomas, D., 1982. Variability of static visual threshold responses in patients with elevated IOPs. *Archives of Ophthalmology*, 100(10), pp.1627–31.
- White, A.J.R. et al., 2002. An examination of physiological mechanisms underlying the frequency-doubling illusion. *Investigative Ophthalmology & Visual Science*, 43(11), pp.3590–9.
- Wiesel, T.N. & Hubel, D.H., 1966. Spatial and chromatic interactions in the lateral geniculate body of the rhesus monkey. *Journal of Neurophysiology*, 29(6),

pp.1115–56.

- Wild, J.M. *et al.*, 2006. Evidence for a learning effect in short-wavelength automated perimetry. *Ophthalmology*, 113(2), pp.206–15.
- Wild, J.M. *et al.*, 1989. The influence of the learning effect on automated perimetry in patients with suspected glaucoma. *Acta Ophthalmologica*, 67(5), pp.537–45.
- Williams, C. *et al.*, 2008. Prevalence and risk factors for common vision problems in children: data from the ALSPAC study. *British Journal of Ophthalmology*, 92(7), pp.959–64.
- Wilson, M.E., 1970. Invariant features of spatial summation with changing locus in the visual field. *Journal of Physiology*, 207(3), pp.611–22.
- Wilson, M.E., 1967. Spatial and temporal summation in impaired regions of the visual field. *The Journal of Physiology*, 189(2), pp.189–208.
- Xu, J. *et al.*, 2013. Retinal nerve fibre layer thickness and macular thickness in patients with esotropic amblyopia. *Clinical and Experimental Optometry*, 96(3), pp.267–271.
- Yang, A. & Swanson, W.H., 2007. A new pattern electroretinogram paradigm evaluated in terms of user friendliness and agreement with perimetry. *Ophthalmology*, 114(4), pp.671–9.
- Yang, G. & Masland, R.H., 1994. Receptive fields and dendritic structure of directionally selective retinal ganglion cells. *The Journal of Neuroscience*, 14(9), pp.5267–80.
- Zaja-Milatovic, S. *et al.*, 2005. Dendritic degeneration in neostriatal medium spiny neurons in Parkinson disease. *Neurology*, 64(3), pp.545–7.
- Zeile, A.J. *et al.*, 2006. Disclosing disease mechanisms with a spatio-temporal

summation paradigm. *Graefe's Archive for Clinical and Experimental Ophthalmology*, 244(4), pp.425–32.

Zhang, X., Cheng, M. & Chintala, S.K., 2004. Kainic Acid–Mediated Upregulation of Matrix Metalloproteinase-9 Promotes Retinal Degeneration. *Investigative Ophthalmology & Visual Science*, 45(7), p.2374.